Analysis of a hybrid renewable energy system in the optimal management of water resources in arid islands

MARIA MARGARITA BERTSIOU

PhD Thesis

March 2023

Analysis of a hybrid renewable energy system in the optimal management of water resources in arid islands

PhD Thesis

Maria Margarita Bertsiou

National Technical University of Athens
School of Civil Engineering
Department of Water Resources and Environmental Engineering
Laboratory of Hydrology and Water Resources Development

Athens, March 2023

Author: Maria Margarita Bertsiou

Title: Analysis of a hybrid renewable energy system in the optimal management of water resources in arid islands

PhD Thesis

March 2023

Supervisor:

Professor Evangelos Baltas, NTUA

Advisory board:

Professor Evangelos Baltas, NTUA

Professor Sotirios Karellas, NTUA

Associate Professor Nikolaos Mamassis, NTUA

Examination board:

Professor Evangelos Baltas, NTUA

Professor Sotirios Karellas, NTUA

Associate Professor Nikolaos Mamassis, NTUA

Associate Professor Dimitrios Karpouzos, AUTh

Professor Vassilios Tsihrintzis, NTUA

Professor Andreas Anayiotos, CUT

Professor Elpida-Kleanthi Kolokytha, AUTh

National Technical University of Athens

School of Civil Engineering

Department of Water Resources and Environmental Engineering

Laboratory of Hydrology and Water Resources Development

To Dimitris

«... ο δρόμος για την επιβίωση δεν περνάει από τα σουπερμάρκετ και τις κούτες με τα εβαπορέ, αλλά είναι κάτι εντελώς διαφορετικό. Ο δρόμος για την επιβίωση περνάει από τις εναλλακτικές προτάσεις που χωρίς να έχουν μυωπία απέναντι στην κοινωνική ταξικότητα αρνούνται την καταναλωτική χυδαιότητα και διακρίνονται από ένα σεβασμό στα ενεργειακά αποθέματα του πλανήτη.»

Μέρες «Τσέρνομπιλ»

Ανδρέας Ι. Κασσέτας, "Το φάντασμα του Λεονάρντο"

M. Bertsiou, E. Baltas, Power to hydrogen and power to water using wind energy, Wind, 2(2), 305-324, 2022, https://doi.org/10.3390/wind2020017

M. Bertsiou, E. Baltas, Energy, economic and environmental analysis of a hybrid power plant for electrification and drinking and irrigation water supply, Environmental Processes, 9(2), 1-28, 2022, https://doi.org/10.1007/s40710-022-00575-x

M. Bertsiou, E. Baltas, Management of energy and water resources by minimizing the rejected renewable energy, Sustainable Energy Technologies and Assessments, Volume 52, 102002, 2022, https://doi.org/10.1016/j.seta.2022.102002M

M. Bertsiou, A.P. Theochari, E. Baltas, Multi-criteria analysis and GIS methods for wind turbine siting in a North Aegean island, Energy Science & Engineering, Volume 9, January 2021, Pages 4-18, https://doi:10.1002/ese3.809

M. Bertsiou, E. Feloni, D. Karpouzos, E. Baltas, Water management and electricity output of a Hybrid Renewable Energy System (HRES) in Fournoi island in Aegean Sea, Renewable Energy, Volume 118, April 2018, Pages 790–798, https://doi:10.1016/j.renene.2017.11.078

Contents

Renewable energy sources (RES) are the main priority for the European Union (EU), as evidenced by the institutional framework introduced over the past few decades leading to the increasing penetration of RES in the energy balance worldwide. Renewable energy sources are becoming increasingly popular as the world looks to transition away from fossil fuels and reduce greenhouse gas emissions (GHG). Also, the necessity for carbon-free technology, such as RES applications, to meet the world's electricity needs, is driven by climate change. The renewable energy target for 2030 was set at a minimum of 32% of gross final consumption, 32.5% for energy efficiency, and a minimum of 40% reduction in GHG under the Renewable Energy Directive 2018/2001/EU (RED II). The transition to renewable energy sources offers several benefits, including reducing GHG, reducing energy costs and increasing energy security by relying on local, sustainable sources of power. The increasing penetration of RES in the power mix has led to new challenges in balancing supply and demand. Wind and solar energy are intermittent and dependent on various climatic factors, making it challenging to forecast energy availability and meet immediate electricity demand. The solution to this problem is to use hybrid renewable energy systems (HRES), which combine at least one form of RES and at least one form of energy storage technology to store surplus renewable energy that cannot be utilized immediately.

This research aims to develop a comprehensive approach for the integration of renewable energy sources in meeting energy and water needs in remote islands, by exploiting both their wind and solar potential, as well as different storage technologies for the storage of surplus renewable energy. The study area is Fournoi Korseon, an island in the North Aegean Sea. A methodology for the evaluation of eligible sites for the installation of wind turbines is developed, using a combination of Multi-Criteria Decision-Making (MCDM) and Geographic Information Systems (GIS) and considering various technical, environmental, and legal criteria for the design of a wind farm. Afterwards, energy management strategies are described based on single or hybrid storage methods, depending on the storage technologies of seven different scenarios, resulting in the reliability analysis of each HRES and the estimation of economic and environmental indices. Finally, the methodology for calculating the rejected energy during the operation of an HRES is presented.

1.1   Renewable energy sources

Renewable energy sources (RES) are the main priority for the European Union (EU), as evidenced by the institutional framework introduced over the past few decades leading to the increasing penetration of RES in the energy balance worldwide (Dalala et al., 2022; I. Khan et al., 2022). Renewable energy sources are becoming increasingly popular as the world looks to transition away from fossil fuels and reduce greenhouse gas emissions (GHG). The environmental impact of RES is generally negligible when compared to conventional energy sources (Dhar et al., 2020). Also, the necessity for carbon-free technology, such as RES applications, to meet the world's electricity needs, is driven by climate change (Potashnikov et al., 2022). These sources of energy are sustainable and can be replenished naturally over time, making them a more environmentally friendly and long-term solution for energy needs. The balance between emissions and removals by 2050 is the ultimate objective. The renewable energy target for 2030 was set at a minimum of 32% of gross final consumption, 32.5% for energy efficiency, and a minimum of 40% reduction in GHG under the Renewable Energy Directive 2018/2001/EU (RED II) (Directive (EU) 2018/2001, 2018).

Wind Energy is generated by wind turbines. Wind turbines are tall, slender towers with large blades that spin in the wind. The spinning blades generate electricity, which can be used for electricity demands. Wind energy is a clean and renewable source of energy, and it is also becoming more affordable as technology advances. Wind turbines can be installed on land or in the ocean, and they have a relatively small footprint, making them a good option for areas with limited space. One of the most appealing RES for distant areas' load demands is the use of wind turbines, not only because of their low initial costs but also because of the variety of industrial and domestic systems they can supply (Farh et al., 2022). Also, compared to solar panels, wind turbines require less land space, and compared to hydroelectric energy cause less transformation (Ioannidis & Koutsoyiannis, 2020). Wind energy displays a declining trend of the Levelized Cost of Energy (LCOE) (Canbulat et al., 2021), and in 2019 it had a global energy production capacity of 650.8 GW (Finnegan et al., 2021). By 2030, this capacity is predicted to increase to 1000 GW (Subramanian et al., 2021). However, it is also crucial to take into account how wind turbines affect landscapes' visibility (Bilgili & Alphan, 2021). Also, blades, the most significant and expensive component of a wind turbine, increase the operation and maintenance cost, particularly in offshore turbines which coincide with the migratory routes of birds as a result of global warming (Celik et al., 2022).

Solar energy is also one of the most popular renewable energy sources. Solar panels can be installed on rooftops, in fields, and on the sides of buildings (Jouttijärvi et al., 2022) to exploit solar irradiance and convert it into electricity. Solar panels operate in silent mode, have low transport costs and & zero maintenance and operation costs (Nirmal Mukundan et al., 2020), however, they also have a high initial cost, require relatively large surfaces for installation (Giamalaki & Tsoutsos, 2019), due to the low power density of solar radiation, and need periodic cleaning to avoid reduction of efficiency due to pollution (Kazem et al., 2020).

Hydroelectric energy is generated by harnessing the natural flow of moving water to generate electricity. Dams are built across rivers to create reservoirs, and the water is then released through turbines to generate electricity. Hydroelectric energy is a clean, more efficient and reliable (Wang et al., 2023) renewable source of energy. Additionally, hydroelectric energy can be stored in reservoirs, which means that it can be used when needed. However, the construction of a reservoir can be expensive, and it is anticipated to have negative environmental effects, including a significant impact on biodiversity and land use (Dorber et al., 2020; Swanson & Bohlman, 2021). On the other hand, besides the benefits of power generation, if they are well-designed, these projects have the potential to mitigate various negative effects and advance ecotourism in the area, providing positive socioeconomic effects and promoting sustainable growth. Examples of such typical situations are found in Karditsa, in Greece, the Plastira Lake (Sargentis et al., 2021) and in China, on the Yangtze River, the Three Gorges Dam (Xia et al., 2018).

Biomass energy is generated from organic materials, such as wood, agricultural waste, and municipal solid waste. These materials are burned to generate electricity or heat. Biomass energy is a renewable source of energy, and it can help reduce waste by using materials that would otherwise be discarded. However, the use of biomass is associated with disadvantages such as broad distribution, low energy density, and an imbalanced seasonal supply (Yang et al., 2019). Geothermal energy is accumulated in the earth's crust. Direct use of this energy is possible for space heating. This kind of power plant often emits incredibly low pollution (Bravi & Basosi, 2014). Geothermal energy has seen an increase in direct use in recent years of 8%, with the majority of this energy going toward space heating and only a few locations on earth are eligible to extract it (Rahman et al., 2022). Oceans are also significant fossil fuel substitutes because they store energy in a variety of ways, including thermal energy by exploiting the temperature difference between warmer surface water and cooler bottom water, kinetic energy from the waves and tides, chemical energy by chemicals from the ocean and biological energy from ocean biomass (M. Z. A. Khan et al., 2022). These are relatively new technologies and are still in the early stages of development but have the potential to play a significant role in the global energy mix. Osmotic power plants, a comparatively recent type of RES with significant potential, harvest renewable energy by using two independent water columns with different salinities that are separated by a semipermeable membrane (Rahman et al., 2022).

The EU and individual states both suggest new regulations for the use of renewable energy sources. The Green Paper "Energy for the Future" from the European Commission (Energy for the Future, 1997) for environmental protection is credited as marking its commencement in 1997. According to Directive 2009/28/EC (Directive 2009/28/EC,2009), the National Action Plan for reaching a 20% contribution of renewable energy in total energy consumption by 2020 has been released. It contains estimations for the growth of the energy industry and the adoption of RES technologies by 2020. The 20-20-20 EU Climate and Energy Package's three main targets are a 20% reduction in GHG, a 20% increase in the share of renewable energy sources in final energy consumption, and a 20% improvement in energy efficiency, all by the year 2020. The 20-20-20 targets are the response to the growing concern about the impact of climate change and the need to reduce GHG. The 20% reduction target for GHG is based on 1990 levels and applied to the EU as a whole. To achieve this target, the EU put in place a number of measures, including the EU Emissions Trading System (ETS), which is first launched in 2005 (Sato et al., 2022) and places a cap on emissions from the energy and industrial sectors and allows companies to trade emissions allowances. On 14 July 2021, it was proposed by the European Commission (EC) the extension of the scope of ETS in order for GHG from the maritime sector to also be included (Lagouvardou & Psaraftis, 2022). The 20% target for renewable energy sources aims to increase the use of renewable energy sources in the energy mix and reduce dependence on fossil fuels. To achieve this target, member states are required to develop national renewable energy action plans and to increase the share of renewable energy sources in electricity, heating, and transport. The 20% improvement target in energy efficiency refers to the improvement of energy efficiency in buildings, industry, and transport. This target aims to reduce energy consumption and the associated GHG, while also promoting cost savings and increased energy security. The 20-20-20 targets have a significant impact on the energy and climate policies of the EU and its member states. It encourages investment in renewable energy sources (Turan & Uyar, 2022) and energy efficiency measures, and it helps to drive innovation in the energy sector. One of the main challenges of the 20-20-20 targets is ensuring that all member states are able to meet their targets. While some member states can achieve their targets in advance of the 2020 deadline, others face significant challenges, particularly in meeting the renewable energy target (Brodny & Tutak, 2023). Some member states face a lack of suitable renewable resources or a lack of funding for renewable energy projects (Madaleno et al., 2022). According to EEA (European Environment Agency, 2021), by 2020, the EU has reduced its GHG by 31%, exceeds its target for renewable energy sources with a 21.3% share in the final energy consumption, and achieves a 17.5% improvement in energy efficiency. Greece, being a member of the EU, takes part in the EU's overarching initiative to enhance the share of renewable energy sources in the energy balance. According to Law 3851/2010, Greece's 2020 goals include increasing the share of RES in the final consumption of energy by 20% and in electricity consumption by 40%.

The Paris Agreement on Climate Change (Paris Agreement, 2016) is a landmark agreement that was adopted by the United Nations Framework Convention on Climate Change (UNFCCC) at the 21st Conference of Parties (COP21) in Paris on December 12, 2015. The agreement sets out a framework for action to limit global warming to well below 2°C above pre-industrial levels and pursue efforts to limit the temperature increase to 1.5°C. The Paris Agreement builds on the previous UNFCCC agreements, including the Kyoto Protocol, and is the culmination of years of negotiations and efforts by the international community to address the issue of climate change. It has been signed by 196 countries and ratified by 189, making it the most widely supported international agreement in history. The key objectives of the Paris Agreement are to strengthen the ability of countries to deal with the impacts of climate change, increase the resilience of ecosystems, and facilitate the transition to low-carbon economies. The agreement recognizes that the actions of each country to reduce GHG will be critical in achieving the overarching goal of limiting global warming. To achieve this goal, the Paris Agreement sets out a range of provisions and mechanisms that aim to promote international cooperation and collaboration. These include the Nationally Determined Contributions (NDCs), each country's own national climate plans that are required to be submitted. These outline their efforts to reduce GHG and adapt to the impacts of climate change. These plans are reviewed and updated every five years. The Paris Agreement establishes also a system of transparency and accountability to ensure that countries are fulfilling their commitments and reporting their progress. This includes regular reporting on emissions and adaptation efforts, as well as a review process to assess progress toward the long-term goals of the agreement. Moreover, the Paris Agreement recognizes that developing countries may require support in developing their own low-carbon technologies and implementing their NDCs. The agreement, therefore, provides for technology transfer and capacity-building to help support these efforts. At last, developed countries are required to provide financial support to developing countries to help them implement their NDCs and adapt to the impacts of climate change.

Over the period 2005-2018, European countries more than doubled their RES capacity from 180 GW to 465 GW (Eionet Report - ETC/CME 2019/8. European Topic Centre on Climate Change Mitigation and Energy, 2019). In Figure 1-1 the renewable energy's share (hydropower, solar, wind, geothermal, wave and tidal) in the energy mix is presented. In 2019, around 11% of global primary energy came from renewable technologies (Ritchie et al., 2022).

The transition to renewable energy sources is a critical step in reducing GHG and mitigating the effects of climate change (Chien et al., 2021). RES-based projects are environmentally friendly solutions against the climate crisis, the rise of global temperature and environmental pollution (Dehghani et al., 2017; Nazir et al., 2019), protecting at the same time the biodiversity and the forests (Nunez et al., 2019). The advantages of renewable energy sources make this shift beneficial despite the difficulties that appear, such as updating infrastructure and adjusting to variable energy sources

(Nik et al., 2021). Prioritizing investment, legislative changes, and public support are crucial as countries and industries around the world work for the transition to renewable energy sources in order to assure a sustainable, low-carbon future (Heffron et al., 2021).

Share of primary energy from renewable sources, 2021
Renewable energy sources include hydropower, solar, wind, geothermal, bioenergy, wave, and tidal. They don't include traditional biofuels, which can be a key energy source, especially in lower-income settings.

Our World in Data

No data 0%   1%   2%   5%   10%   20%   50%   100%
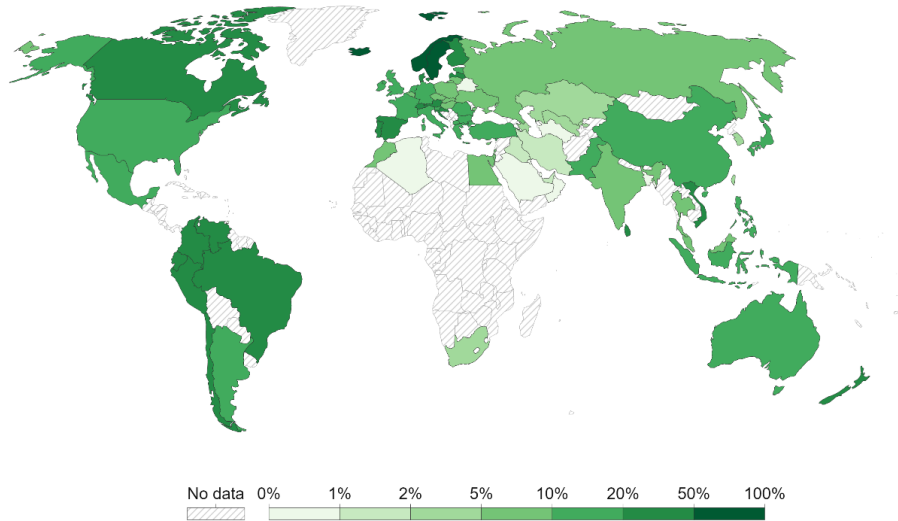
Source: Our World in Data based on BP Statistical Review of World Energy (2022)   OurWorldInData.org/energy • CC BY
Note: Primary energy is calculated using the 'substitution method', which accounts for the energy production inefficiencies of fossil fuels.

Figure 1-1 Share of primary energy from renewable sources for year 2021 (Ritchie et al., 2022)

One of the primary benefits of transitioning to renewable energy sources is reducing GHG (He et al., 2022; Sacchi et al., 2022). Fossil fuels, such as oil, coal, and gas, release large amounts of carbon dioxide, contributing to climate change and having negative impacts on human health and the environment (Olabi & Abdelkareem, 2022). By using renewable energy sources, these emissions are reduced and the negative impacts of climate change are limited. In addition to reducing emissions, renewable energy sources can also help reduce energy costs (Ainou et al., 2022) and increase energy security (Cergibozan, 2022; Nasir et al., 2022) by relying on local, sustainable sources of power. Finally, transitioning to renewable energy sources can also create jobs and boost economic growth (Liu et al., 2022). According to the International Renewable Energy Agency (IRENA), the renewable energy sector employed over 11 million people globally in 2018. This number is expected to continue growing as countries invest in renewable energy infrastructure and technologies. In Figure 1-2, the total energy supply by different sources is presented for Greece from 1990 to 2021. In Figure 1-3 the renewable energy supply (wind, solar and hydro) is depicted for Greece from 1990 to 2021. According

to International Energy Agency (IEA), for the year 2021 in Greece, the energy supply from wind is 10,483.0 GWh, from solar is 5,106.0 GWh and from hydropower is 5,967.0 GWh.

Total energy supply (TES) by source, Greece 1990-2021
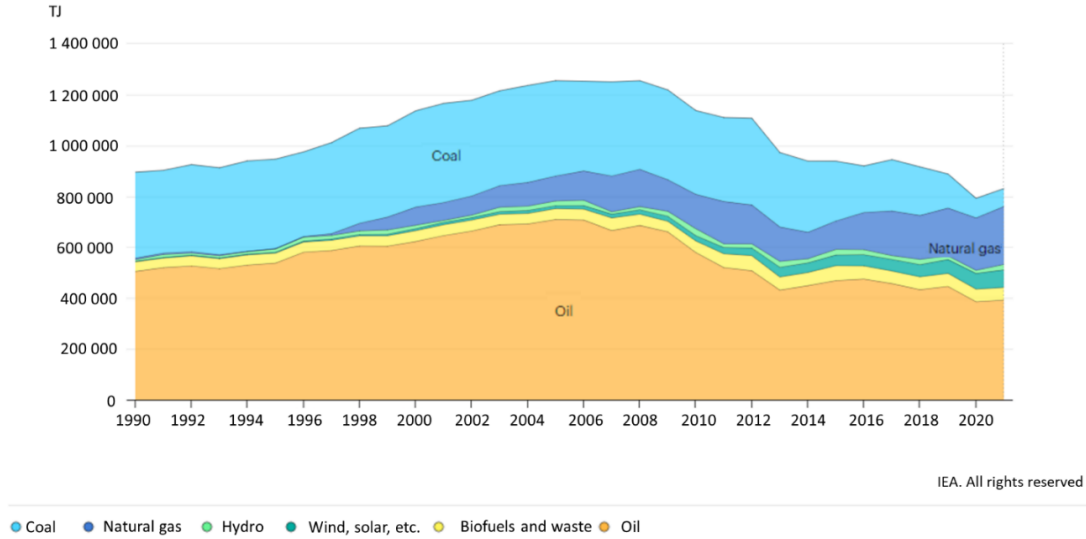
Figure 1-2 Total energy supply by source, Greece 1990-2021 (International Energy Agency, 2021)

Besides the benefits of renewable energy sources, there are also significant challenges that come with the transition. One of the main challenges is technical and operational problems (Al-Shetwi, 2022), by adapting infrastructure to accommodate new sources of power. Many power grids are designed to handle large, centralized power plants, making it difficult to integrate smaller, decentralized sources of renewable energy (López González & Garcia Rendon, 2022), leading to problems in stability and power quality. Updating the infrastructure to support renewable energy sources will require significant investment and planning (Aleluia et al., 2022). Another challenge is the intermittent nature of renewable energy sources (Janota et al., 2022), particularly solar and wind power. Unlike traditional power plants that can generate a consistent amount of energy, renewable energy sources rely on weather conditions to generate power. This intermittent behavior makes it difficult to predict and manage energy supply, requiring new approaches to energy management and storage (M. Bertsiou et al., 2018; Sánchez et al., 2022). Finally, transitioning to renewable energy sources will require significant government, financial and social support (Krupnik et al., 2022). Many countries and industries are still heavily reliant on fossil fuels, and the transition to renewable energy will require significant policy changes, investment, and public support (Leonhardt et al., 2022).

Renewable electricity generation by source, Greece 1990-2021
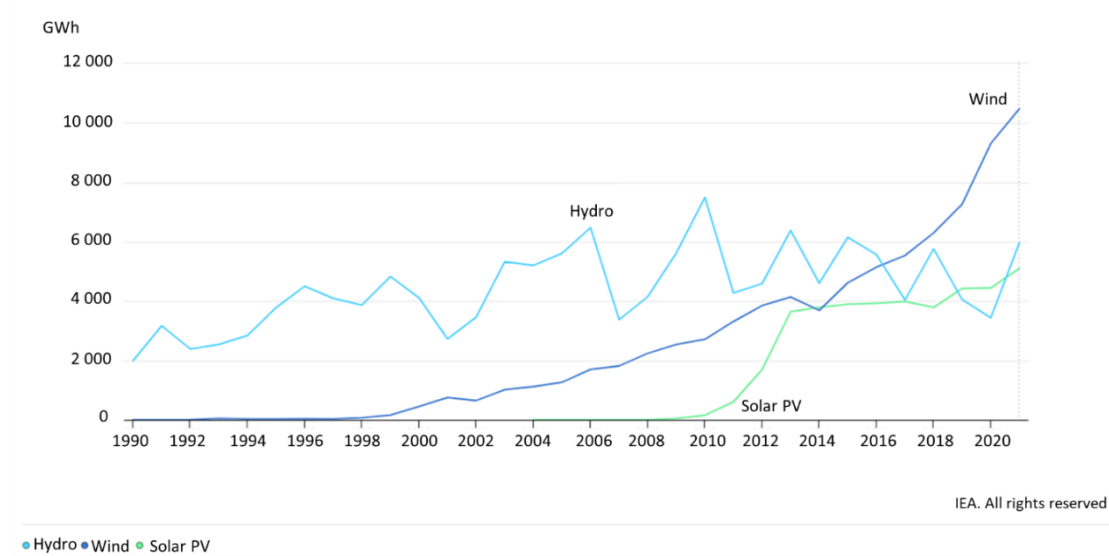
GWh

• Hydro • Wind • Solar PV

Figure 1-3 Renewable energy supply by source, Greece 1990-2021 (International Energy Agency, 2021)

The COVID-19 pandemic has caused significant disruption to economies, industries and the energy sector worldwide. The measures implemented to slow the spread of the virus, such as lockdowns, travel restrictions, and social distancing, have resulted in reduced energy demand across all sectors. The largest appears in transport and services and the smaller in industry, while household consumption increased (Rokicki et al., 2022). The increase in remote working and online learning has resulted in a shift in energy demand from commercial buildings to residential buildings. The COVID-19 pandemic has also had a significant impact on the energy supply, with disruptions to production, transportation, and storage (Dong et al., 2022). The decline in energy demand has resulted in an oversupply of energy, leading to a drop in prices and reduced investment in new energy projects. At the same time, the pandemic has also accelerated the energy transition and raised questions about the resilience of energy systems to crises (Zakeri et al., 2022), highlighting the need for diversified and flexible energy sources and systems. To accelerate the energy transition in the post-COVID-19 stage, (Tian et al., 2022) propose a road map that includes expanding green funding options, promoting global collaboration, and improving green stimulus programs. The COVID-19 pandemic has prompted governments and industry players to take measures to mitigate the impact of the crisis and support the energy transition.

The Recovery and Resilience Facility (RRF) is a fund set up by the EU to support member states in their recovery from the economic and social impacts of the COVID-19 pandemic. Greece is one of the countries that has been allocated funding from the RRF, and a significant portion of the funding is

dedicated to the country's energy sector. The RRF funding for Greece's energy sector is intended to support the country's transition to a low-carbon economy, as well as to improve energy efficiency and security. The funding is expected to support a range of projects, including RES projects, energy efficiency measures for improving energy efficiency in buildings and infrastructure, modernization of Greece's energy infrastructure, including the development of smart grids and the upgrading of energy transmission and distribution networks and support for the development of green hydrogen production in Greece.

Ukraine is a significant energy producer and transit country and the war in Ukraine has had a profound impact on the country's energy sector, affecting both the production and distribution of energy (Allam et al., 2022). Some of the major impacts of Europe's energy sector are the damage to energy infrastructure, disruptions to coal supplies, dependence on Russian gas and reduced electricity exports.

1.2 Hybrid renewable energy systems and storage technologies

New challenges between the supply and demand of renewable energy arise from the RES's increasing penetration in the power mix. Due to the intermittent nature of wind and solar energy potential and their dependence on various climatic factors, forecasting wind and solar energy is very challenging (Olabi et al., 2021). Also, the stochastic nature of RES makes it challenging to meet immediate electricity demand (Brenna et al., 2020; Ciupageanu et al., 2019; Khalili et al., 2020). For all the above, it is necessary to use wind turbines and photovoltaic modules as part of a hybrid renewable energy system (HRES).

HRESs combine at least one form of RES and at least one form of energy storage technology, as it is shown in Figure 1-1, for storing the surplus renewable energy that cannot be utilized immediately, due to lower energy demand compared to energy generation. Thus, contribute to the reduction of GHG, due to the reduced operation of local production stations (LPS), and to energy independence.

Regarding Greece, the first HRES operating is in Ikaria. Its construction started in 2011 and it is operating since 2019. It consists of a wind park on Stravokountoura hill, with three wind turbines of 900 kW each. The micro hydroelectric station of Proespera, with a 1.05 MW hydro turbine, utilizes only the excess water of the Pezi Dam reservoir after the obligations for water supply, ecological supply and irrigation are first covered. The micro hydroelectric station of Kato Proespera, with two hydro turbines with a total power of 3.1 MW, utilizes both the excess water of the reservoir and the water that comes from pumped storage. Two water reservoirs with a capacity of 80,000 m^3 each in the areas of Proespera and Kato Proespera, which will serve the needs of pumped storage for the absorption of wind energy and a water reservoir with a total volume of approximately 910,000 m^3 in Pezi. The Kato Proespera pumping station, with 12 pumps with a nominal power of 250 kW each and

the Energy Control and Load Distribution Centers of Naera and Ikaria, which will be installed in a space within the LPSS in Agios Kyrikos, ensuring both the communication between the individual parts of the Project as well as the energy security of the island and its reliability electrical system (PPC Renewables, 2023). During winter the water surplus is exploited in the upper PHS and in refilling water losses from the two new reservoirs during the previous summer. During the summer the water of the upper reservoir is used for the water irrigation demands, while the n two new reservoirs are used for the operation of the PHS system. in a conventional cycle of the PHS plant (Katsaprakakis et al., 2022). The project contributes to the reduction of 13,800 tons of emitted CO_2 pollutants per year, from the minimized use of the LPS. It strengthens the island's energy sufficiency, during most of the year, and limits its dependence on conventional fuels. The environmental impacts from the construction of the project are reversed by implementing environmental restoration measures, such as tree planting). Finally, this project is upgrading Ikaria in the field of tourism, as it is expected to become a pole of attraction for students, scientists and environmentally aware citizens, due to the innovations and the "green" nature of the project (PPC Renewables, 2023).
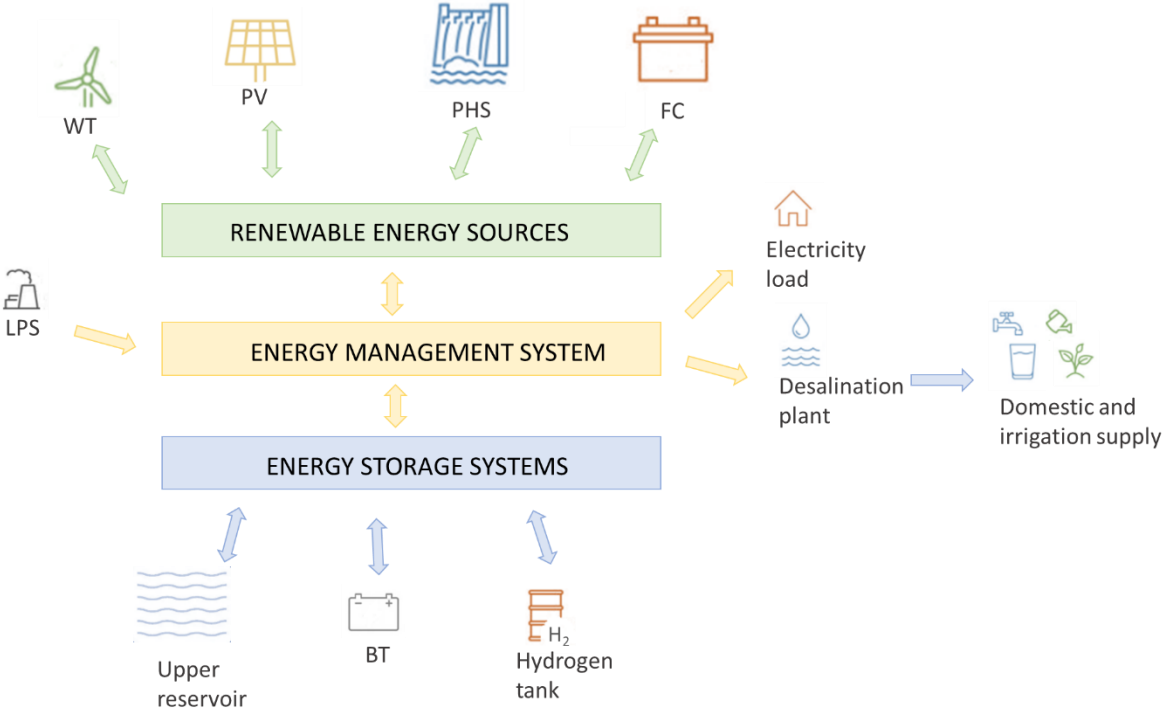
Figure 1-4 Hybrid Renewable Energy Systems

The second HRES is in Tilos Island, which is installed in 2017. TILOS project consist of a WT of 800 kW, a 160 kWp PV station and an 800 kW battery storage system. Also, it has been installed an EV charger at the TILOS info-kiosk in Livadia with 4.93 kWp of PVs on the roof of the kiosk for charging needs (Kaldellis, 2021; Kaldellis & Zafirakis, 2020). The development of this project, which will be

implemented in four more Greek islands, Anafi, Donousa, Leros and Fournoi Korseon, is contributing to the reduction of carbon dioxide emissions, to the protection of the environment by the increased integration of RES in the energy mix of the islands and to the reduction of energy costs. Simultaneously it ensures the substantial detachment of the islands from conventional fuels and improves their energy security (EUNICE, 2023). Finally, an HRES in Astypalaia will be ready for use by the end of 2023, which will include 3MW of PVs photovoltaics and a 7MWh battery storage system, to cover up to 50% of the island's total energy demand and 100% of electric vehicle charging needs. By the end of 2026, the expansion of the project is planned with the addition of WTs that aim to cover more than 80% of the total energy demand of the island (Smart & Sustainable Island, 2023).

The integration of RES plants and energy storage systems, not only solves the problems that arise from the stochastic nature of natural resources, but also enhances the grid's reliability and efficiency, providing power quality services (Krishan & Suhag, 2019). Simultaneously the high-cost electricity generation can be decreased, especially in non-interconnected islands (NNIs) which are supplied by LPS, comprising conventional fuels (Gkiokas et al., 2022). Storing energy during periods of low demand and/or high energy generation, while utilizing the stored energy when the demand is high and/or the energy production is low, leads to the satisfaction of unmet demand. The subject of stand-alone HRES becomes more attractive in the context of autonomous networks, such as non-interconnected islands (NNIs). The use of HRESs provides a significant supply of the required electrical demand, avoiding simultaneously general or partial blackouts in NNIs during periods of high demand. The integration of pumped hydro storage (PHS), batteries (BT) and hydrogen production storage (FC) with wind turbines (WTs) and photovoltaic modules (PVs) to handle the intermittent nature of RES is a competitive and rapidly expanding field of research.

PHS is one of the most widely used energy storage technologies, an environmentally friendly method, which can be easily installed, where it is permitted by topography (Ökten & Kurşun, 2022) and water resources availability (Hunt et al., 2020). This technology involves pumping water from a lower reservoir to a higher reservoir when there is a surplus RES. When there is deficit of energy the water flows back down to the lower reservoir through a hydro turbine. About 96% of the world's total energy storage capacity is comprised of PHS (Baldinelli et al., 2020; Blakers et al., 2021). According to (IRENA, 2020), the installed hydropower capacity reached 1310 GW. PHS can achieve energy efficiencies of up to 85% for large-scale systems (Alkhalidi et al., 2022), making it one of the most efficient energy storage technologies available. Also, PHS excels because of its long lifetime, the swift response time, and is suitable for long-term storage, since the only losses occur due to seepage and evaporation (Hoffstaedt et al., 2022). It has been rated as the most sustainable storage technology, according to (Ren & Ren, 2018). However, PHS requires a high capital cost (Arabkoohsar & Namib, 2021). Building the infrastructure required for pumped hydro storage, such as reservoirs and

turbines, can be expensive. In addition, PHS requires a significant amount of space and access to suitable terrain.

Previous research works have already studied the integration of PHS to RES-based projects. Nassar et al. (2021) propose a method for optimal sizing of a PV/WT/PHS for sustainable electricity supply to an urban community in Libya. The optimization problem is constrained by operating conditions and output uncertainty of renewable energy systems. Different operating scenarios are considered for optimal sizing of the HRES. Using climate conditions and load consumptions, energy production is estimated by the System Advisory Model software. The optimal power capacity ratio of the PV array to the wind turbine farm is found to be 1:5 based on LCOE. PHS contributes to 15% of the annual load energy, demonstrating that the RESs coupled with PHS is a cost-competitive and reliable alternative for urban areas with high potential for RES. A simulation tool that models the operation of a PV/WT/PHS plant, considering the variability of solar and wind sources and modeling each subsystem with variable efficiency depending on the operating regime is presented by Notton et al. (2017). The tool considers the variability of solar and wind sources and models each subsystem with variable efficiency depending on the operating regime. An optimization of the PHS operation is developed using four reversible pumps in parallel to replace costly and polluting combustible turbines. The tool considers all electrical productions, including renewables, fuel, and imported energy. The simulation shows that the HRES can cover up to 80% of the peak demand on an annual basis. The impact of the HRES's characteristics on performance is studied and different hybrid system configurations are also highlighted. Xu et al. (2020) investigate a WT/PV/PHS system in Xiaojin, Sichuan, China as a case study. The techno-economic index is used to design the HRES and a trade-off analysis is done between maximum power supply reliability and minimum investment cost using Multi-Objective Particle Swarm Optimization (MOPSO) based on Pareto optimality theory. The analysis also considers the curtailment rate (CR) of wind and solar power due to policy requirements. The results show that the WT/PV/PHS configuration has a lower levelized cost of energy (LCOE) than the PV/PHS and the WT/PHS and equal to 0.091 $/kWh for LPSP of 5%. Particle Swarm Optimization (PSO) performs better than other methods in finding the least LCOE. The policy of CR leads to higher investment costs, and both MOPSO and the weighted sum approach (WSA) perform well in finding the Pareto fronts. Syafii et al. (2021) conduct a techno-economic and environmental analysis of a PV/WT/PHS/Diesel (DG) system for a rural microgrid system. The analysis between eight feasible configurations finds that the optimal system configuration is the PV/DG/PHS. The net present cost (NPC) and payback period (PBP) are in accordance with economic feasibility analysis criteria. However, the cost of energy is greater than the electrical utility tariff, but the system is still feasible for remote island areas. Eisapour et al. (2021) propose a resilient smart hybrid renewable energy system to meet the electricity and heat demand of Eram Campus, Shiraz University. Simulations, optimizations, and sensitivity analyses were performed to explore the feasibility of the suggested energy system, which consists of a micro gas

turbine, thermal boilers, converters, PVs, PHS units, and a predictive controller. The levelized cost of electricity is 0.09$/kWh. The energy system reduces the annual carbon dioxide production of the Campus by 8000 megatons compared to using the national energy grid. Lopes et al. (2020) propose a new approach to designing WPSS using Particle Swarm Optimization, which takes into account the technical and economic feasibility and uncertainty of design parameters. The model found that wind energy availability has the most impact on the Net Present Value (NPV) of the project and increasing Capital Expenditure (CAPEX) uncertainty by 50% with a reduced project lifetime can lead to a negative NPV. The potential benefits of installing a WT/PHS in the insular power system of Samos, in Greece, are discussed in (Bouzounierakis et al., 2019). The research uses real hourly data for a year to assess the economic viability of the project under different billing scenarios and the impact on the insular power system operation for various PHS sizes. It suggests that such installations could significantly improve the operation of isolated power systems with high wind and solar potential, such as many Greek islands, by compensating for imbalances between power generation and load demand. Kapsali and Anagnostopoulos (2017) investigate the economic viability of large-scale wind energy production and local energy storage in interconnecting Lesbos Island with the mainland grid. The Levelized Cost of Energy (LCOE) is calculated for two scenarios: the island's interconnection with or without local energy storage and the results show that combining the island's interconnection WT/PHS system is economically attractive. Maisanam et al. (2021) discuss the integration of socio-environmental factors with techno-economic factors in designing and sizing a PV/PHS/Biogas (BG) system for the electrification of a remote Indian town, and a GOA-based meta-heuristic optimizer is developed for solving the optimization problem. Results show that the contribution of socio-environmental factors in the present case is 6% of the total net present cost (TNPC) compared to 94% for techno-economic factors. The optimal HRES size is obtained as 57.5 kW of PVs, 8 kW of BG plant, 378.4 kWh of energy storage, and 33 kW of converter size.

Batteries are another widely used energy storage technology, particularly for small-scale applications. Batteries store energy in chemical form and release it as electrical energy when it is needed. There is a range of battery technologies available, including lead-acid, lithium-ion, and flow batteries. One of the key advantages of batteries is their flexibility. Batteries can be used for a wide range of applications, from small-scale applications such as providing energy for household consumption, to large-scale applications such as providing energy storage for power grids. Especially, flow batteries have gained considerable recognition for large-scale applications due to their simple design and operation, long operational life and quick response (Esan et al., 2020). Generally, batteries have a fast response time and thus they are effective for peak-demand periods (Zhang et al., 2018). In addition, batteries can be easily scaled to meet the needs of different applications, making them a particularly effective energy storage technology for HRESs. Moreover, batteries have a long lifespan, and especially Lithium-ion batteries (Qi et al., 2022) and can be recharged and discharged repeatedly

without significant degradation, making them a reliable and cost-effective energy storage technology. On the other hand, the production of batteries requires a significant amount of energy and resources and their disposal at the end of their life is combined with environmental impacts (Dehghani-Sanij et al., 2019).

Many studies of HRES coupling with batteries have been conducted. Hamanah et al. (2020) propose a methodology to optimize the configuration of a WT/PV/BT/DG system. The objective is to minimize annual cost while considering energy not served and renewable energy fraction constraints. The lightning search algorithm is used to obtain the best cost value, and simulation results show the optimal variables for the system components. The proposed approach is found to be effective in achieving the cheapest renewable energy generation. El-houari et al. (2021) evaluate the energy, economic, and environmental aspects of an autonomous PV/WT/BT. The HOMER Pro software was used for optimization and economic evaluation, and simulations were carried out for 24 cities in different climatic regions, in Morocco. The results show that the HRES can save up to 128.21 tons of CO_2 release in the city of Eddakhala, with the lowest levelized cost of energy predicted for this city. The study suggests that these projects can promote socioeconomic development in remote and isolated areas and can be widespread in the African continent due to decreasing costs of renewable energy equipment. Kazem et al. (2017) design and evaluate a hybrid PV/WT/BT/DG system searching for the best configuration for the lowest cost of energy and the minimization of GHG. The simulations and analysis are conducted using HOMER software to meet the electrical load demand for Masirah Island in Oman. A hybrid PV/WT/BT system for the generation of electricity for a typical house in a remote village in southeastern Iraq is proposed in (Al-Shammari et al., 2021). The optimal sizing for each component was determined using techno-economic feasibility analysis, and the proposed hybrid system resulted in better, cleaner, economical, and more reliable electricity compared to a single source. The renewable factor of the system was 100%, and the cost of energy was 0.566 US$/KWh. Katsivelakis et al. (2021) examine the feasibility and viability of HRESs in Donoussa island, Greece, for supplying electricity in remote areas. The study uses HOMER Pro software to conduct a techno-economic analysis for three scenarios with different adoption rates and configurations of PV, WT, BT and DG. Based on the lowest Net Present Cost (NPC), the smallest proportion of excess electricity, and LCOE, the best system design is chosen using the HOMER Pro software. The simulation's findings may provide some operational guidelines for a workable hybrid system on Donoussa island. The simulation results confirm the use of a hybrid system with negligible excess electricity, acceptable NPC and LCOE, and a respectable level of RES integration. In their research, Fiorentzis et al. (2020) discuss the importance of transitioning to sustainable energy sources and implementing energy-efficient development. The study focuses on the Greek island of Astypalaia as a case study for the full-scale implementation of the WT/BT system Results show that the use of an

HRES can increase RES penetration and reduce fuel costs, while the fast response of the batteries can enhance system's stability during disturbances.

The development of hydrogen storage solutions in HRESs has received more attention in recent years. Hydrogen can be produced using excess energy from RES to electrolyze desalinated water and stored for later use. When the stored hydrogen is needed, it can be used to produce energy through a fuel cell. There are also several different types of hydrogen storage technology being developed, including compressed gaseous hydrogen, liquid hydrogen and material-based hydrogen storage. Currently, these are the three primary storage methods (Yanxing et al., 2019). Each of these technologies has its own advantages and disadvantages, and the choice of technology will depend on the specific application and requirements of the hybrid renewable system (Izadi et al., 2022). Compressed hydrogen storage is one of the most common methods of hydrogen storage and involves compressing hydrogen gas into high-pressure tanks. This technology is well-established and is currently used in a variety of applications, including fuel cell vehicles (Alves et al., 2022) and stationary power generation. Liquid hydrogen storage is another method of hydrogen storage that involves cooling hydrogen gas to a liquid state, which allows for higher storage density. This technology is currently used in some applications, such as rocket fuel, but is not as widely used as compressed hydrogen storage due to its higher cost and complexity (Schrotenboer et al., 2022). Solid-state hydrogen storage is an emerging technology that involves storing hydrogen in a solid-state material, such as metal hydrides or carbon nanotubes (Simanullang & Prost, 2022). This technology has the potential to provide higher storage density and improved safety compared to other hydrogen storage methods but is still in the early stages of development and has not yet been widely commercialized. Hydrogen can be produced locally, increasing the independence of the energy supply (Yue et al., 2021). One of the key advantages of hydrogen production is its high power density (Sürer & Arat, 2022). In addition, hydrogen can be easily transported and stored for as long as it is required, making it a flexible energy storage technology (Escamilla et al., 2022). Compared to PHS, installing a hydrogen production unit requires much less space, and no specific topographic parameters are necessary. Moreover, its production has the potential for zero emissions, however, when it is produced by conventional fuels a large amount of CO_2 is generated, meaning that hydrogen is not an environmentally friendly solution anymore (Yu et al., 2021). When hydrogen is produced using only RES, meaning exploiting RES for the electrolysis of the water too, this leads to the decarbonization of hydrogen, producing green hydrogen (Kakoulaki et al., 2021). When hydrogen is produced using only RES, it can be a completely clean and sustainable energy storage technology (Ishaq et al., 2022). Surplus energy from RESs can be utilized for the production and storage of green hydrogen for use when RES production is less than the load demand (Elberry et al., 2021). In addition, hydrogen can be used to power fuel cell vehicles and other applications, providing a versatile energy source for a wide range of

applications, including fuel cells, heating, and transportation. However, one of the main issues about hydrogen production and storage is its safety (San Marchi et al., 2017).

Many studies have been published, in which hydrogen storage solutions for HRESs are implemented. Hinokuma et al. (2021) propose a PV/WT/FC system using a fuzzy logic control algorithm to reduce building load demand in Japan. The proposed system is simulated using MATLAB-Simulink and validated experimentally. A techno-economic analysis is conducted, revealing potential surplus power generation and lower LCOE using the proposed system, with potentially significant savings of 2.17 million yen per year. The operation of a PV/hydrogen system is examined in (Ceran et al., 2021) analyzing the aging effects on the HRES in terms of energy production decrease and demand for additional hydrogen storage during 10 years of the system operation. The study suggests that the system performance decline is non-linear and depends on the load profile and PV module types. Rezaei et al. (Rezaei, Naghdi-Khozani, et al., 2020) analyze the economic viability of harnessing wind energy for hydrogen production in Afghanistan. The levelized cost of wind-generated electricity is projected for all 34 capital cities, and the energy efficiency of the hydrogen production system, the Levelized Cost of Hydrogen (LCOH), and the payback period are investigated for the city with the least LCOE. Ghenai et al. (2020) design an off-grid hybrid PV/FC system using modeling, simulation, and optimization techniques to meet the energy demand of a residential community in a desert region by increasing the RES penetration. The simulation results show that the system has a 40.2% renewable fraction, is economically viable with an LCOE of 0.14 €/kWh and is environmentally friendly with zero carbon dioxide emissions during electricity generation. Sultan et al. (2021) present a novel metaheuristic optimization technique, called Improved Artificial Ecosystem Optimization (IAEO), for designing an optimal grid-dependent and off-grid HRES consisting of three different configurations PV/FC, WT/FC and PV/WT/FC. The minimum value of COE is 0.370 €/kWh for the PV/FC configuration in the integrated system and 0.420 €/kWh for the PV/WT/FC model in the isolated system.

All the above storage solutions can be used to provide energy storage for a wide range of applications, from small-scale to large-scale. In addition, batteries and hydrogen can be used to power fuel cell vehicles and other applications, providing a versatile energy source for a wide range of applications. A combination of energy storage technologies is needed to ensure that RES can provide reliable energy on demand. Pumped hydro storage, batteries, and hydrogen production are all promising energy storage technologies for hybrid renewable systems. The choice of energy storage technology will depend on a range of factors, including the specific application, energy storage requirements, and the local energy infrastructure. As RES continue to play an increasingly important role in meeting our energy needs, the development and deployment of effective energy storage technologies will be critical for ensuring sustainable and reliable energy.

Many research studies that compare different storage technologies coupling with HRES have been published in recent years. The potential of wind energy to meet the electricity needs of remote island communities, as well as the challenges associated with high wind energy penetration in existing electrical grids and the solution of integrated hybrid energy systems, including energy storage technologies and mathematical models for sizing and simulation, are presented in (Kaldellis, 2020). Hybrid energy solutions are evaluated on a financial basis, considering environmental impacts and finally examples of wind-based hybrid energy applications from around the world are provided. Pujari and Rudramoorthy (2021) conduct the design and pre-feasibility techno-economic analysis of an HRES for rural electrification in a village, in India. Six different hybrid system configurations are considered, and the PV/DG/BT is found to be the least costly and most optimal, providing a reliable power supply to the village's energy requirements and achieving a significant reduction in carbon emissions compared to diesel generators. Das et al. (2021) present a review of HRESs coupling with PHS systems analyzing the technical details, cost-effectiveness, and environmental indicators. The study identifies PHS-based systems as offering significant cost and environmental benefits over battery storage technologies. The design and optimization of a WT/PV/Biomass/PHS energy system for the minimization of the cost of energy while considering technical, economic, and environmental parameters is presented in (Alturki & Awwad, 2021). Three optimization algorithms are used to compare the proposed system with a system that uses battery storage. The results show that the proposed system is both economically and environmentally feasible, and the pumped-hydro storage hybrid system is more cost-effective than the battery storage hybrid system. Islam et al. (2021) compare a PV/WT/PHS energy system with battery-based systems and diesel-only systems in Newfoundland, Canada. The study investigates the effects of uncertainty on sizing the hybrid system. Results show that the proposed hybrid system can supply electricity to the community at a significantly lower cost compared to diesel-only systems and that it can save a substantial amount of diesel and CO_2 emissions. Additionally, the pumped hydro storage-based system is more cost-effective than battery-based systems, and the integration of hydro into the PV/Wind/PHS option reduces the cost of energy by 58%. Katsaprakakis et al. (2019) examine the optimal electricity storage technologies for small, insular, autonomous electrical grids integrated with RES. Three Greek islands are studied as case studies and PHS and electrochemical storage with lead-acid or lithium-ion batteries are investigated as potential storage options. The study finds that PHS is a competitive alternative for larger islands, while BT systems can achieve 80-90% RES penetration. The economic feasibility is ensured with electricity selling prices between 200 and 350 €/kWh, and the payback periods for investments are estimated between 6 and 10 years.

The produced RES that cannot be utilized simultaneously and neither can be stored during the operation of a single storage HRES, subject to available storage capacity, ends up in a dump. Surplus energy can be further exploited by being stored in a second storage technology in a hybrid

storage HRES Many studies on hybrid storage HRESs have been published. The optimal design of an off-grid WT/PV/BT/FC hybrid system is proposed in (Marocco et al., 2022), where both LCOE and CO2 emissions are considered simultaneously. The proposed methodology is applied to the Froan islands, in Norway and results show that energy storage devices, especially hydrogen storage systems, are key components to reducing the dependency on fossil fuels and enhancing renewable energy penetration. The cheapest configuration, which includes both batteries and hydrogen, has an LCOE of 0.41 €/kWh, which is around 35% lower than the LCOE of the system coupled only with batteries as energy storage. Javed et al. (2019) simulate a domestic PV/BT/supercapacitor hybrid system. A Fuzzy Logic Control Strategy (FHCS) is implemented to control the power flow of the hybrid energy storage system components, improving the system efficiency and enhancing battery lifespan while reducing maintenance costs. Simulation studies validate the proposed system's effectiveness and potential to electrify more underserved communities. In (M. M. Bertsiou & Baltas, 2022c) the authors investigate two models of surplus energy storage systems for islands that use wind power. The first model uses a PHS system, and the second model uses a hybrid pumped hydrogen storage system consisting of a PHS and a hydrogen storage system. The goal of the study is to compare the two systems in fulfilling the energy requirements of the island's electricity load and desalination demands. The results show that the hybrid system has a higher cost of energy but a lower loss of load probability than the single storage system. Ferrario et al. (2021) evaluate the optimal sizing of a WT/PV/BT/FC system for a real hybrid renewable microgrid in Huelva, Spain. Four storage configurations are assessed, and results show that a hybridized energy storage capacity is beneficial for energy security and efficiency but can represent a substantial additional cost. Increasing battery capacity is more beneficial for the abatement of loss of load, while increasing FC capacity is more useful to absorb excess energy. In (Akter et al., 2022), the examination of Bangladesh's energy situation and the design of a 100% RES-based off-grid power system for St. Martin's Island is proposed. The mixed-integer linear programming optimization technique is used to demonstrate the efficacy of the suggested PV/BT/FC system and four cases are explored to show the system's cost-effectiveness and profit-maximizing potential. Kefif et al. (2022) propose a WT/PHS/BT system for Algeria's Yesser valley. The study aims to determine the optimal design size for the system using batteries to increase reliability. Homer Pro software is used to model and analyze the system's economic feasibility based on variable water flow and wind speeds. Results show that the hybrid system is capable of meeting the load demand in different areas of the valley, and the financial cost of the system is inversely proportional to wind and flow rate speed. Canales et al. (2021) present a mathematical model for the size and performance optimization of a WT/PV/PHS/BT system. The study focuses on Ometepe Island in Nicaragua and evaluates how different capital costs and LPSP affect the system's optimal sizing and cost of energy. The COE ranges from €0.047/kWh to €0.095/kWh. In (Lata-García et al., 2018), a techno-economic analysis of a PV/PHS/FC/BT system is presented for the electrical supply of isolated

loads. The optimal location of the turbine is determined to maximize the hydroelectric generator's performance, and the techno-economic study of all components of the hybrid system is carried out. The results show that the hybrid system provides the required power, optimizes hydroelectric and solar photovoltaic generation, and maintains the battery storage subsystem loading status to avoid deep discharges. Dambone Sessa et al. (2018), propose an HRES consisting of flywheels and batteries to support primary frequency regulation in the electrical network. The study investigates the benefits of flywheels in mitigating the accelerating aging that Li-ion batteries suffer during grid frequency regulation operation through experimental aging tests and simulations. The results suggest that proper power control between the batteries and flywheels can effectively counteract Li-ion battery aging. Phan and Lai (2019) present a WT/PV/BT/FC system. The study focuses on optimal sizing, maximum power point tracking (MPPT) control, and energy management system development. The result of COE is 0.660 €/kWh. In (Dawood et al., 2020), three case scenarios of an HRES are examined for a hypothetical remote community in Western Australia. PV is the primary RES, while the battery, the hydrogen and the battery-hydrogen are the alternative energy storages. Using the HOMER Pro software, the simulation results show that the hybrid energy storage system is the most cost-effective scenario for electrifying remote communities with low energy generation costs and reducing their carbon footprint. Guezgouz et al. (2019) propose a new energy management strategy to coordinate a hybrid energy storage system based on pumped hydro storage with batteries. The optimal size of the system was determined using a multi-objective optimization approach, and the results showed that the hybrid storage system provides higher reliability at a lower cost and reduces the curtailment of renewable generation. However, sensitivity analysis revealed that the optimal hybrid storage configuration is less resilient to potential changes in renewable energy availability, and special actions must be taken to avoid lower performance. Seedahmed et al. (2022) examine the use of HRES for the electrification of remote areas with a focus on the Al-Shumaisi cluster in Saudi Arabia. Two hybrid configurations, a WT/FC/BT/DG and a WT/FC/BT system, are proposed and compared to a configuration using only DG units. The results show that the WT/FC/BT/DG configuration is the most economic and eco-friendly solution with a reduction in NPC and a decrease in pollutants, compared to DG-based units.

1.3 Desalination technologies

Water shortage has negative effects on the Greek islands, and there is poor transportation connectivity to the mainland. The use of bottled water is rising in response to the need for drinking water, which increases living costs. Transporting potable water to the islands from the mainland costs between 7 and 12 euros per cubic meter (Bardis et al., 2020; Myronidis & Nikolaos, 2021). Based on the various social features of the customers, variations in the water demand as a result of climatic change also appear (Fiorillo et al., 2021)). Climate change has an impact on evapotranspiration as

well, which affects irrigation water requirements and has an impact on water management and agricultural productivity ((Maqsood et al., 2022)). Moreover, issues with groundwater quantity and quality arise as a result of the numerous, unregistered private wells drilled for irrigation purposes. A key component of water demand is irrigation. At the same time, there is an endless supply of seawater surrounding the Greek islands. In order to support the transition to RES and mitigate the effects of climate change, an HRES and a desalination unit can be combined to provide significant domestic water supplies for locals and visitors, as well as water for agricultural and industrial uses. This partnership increases water and energy efficiency (Panagopoulos, 2021). Desalination requires a significant amount of energy, and the use of fossil fuels to power desalination plants can contribute to GHG. Combining desalination with renewable energy systems can help reduce the carbon footprint of desalination and make it more sustainable. Especially in the case of Greek islands, HRES coupling with a desalination plant can use wind and solar energy, as well as the seawater surrounding each island, to solve both energy shortages (Spiller et al., 2022) and water scarcity (Kakoulas et al., 2022; Vourdoubas, 2022; Zafeirakou et al., 2022). Seawater desalination can guarantee the supply of water to islands with limited water resources (Herrera-León et al., 2018). In addition, the use of RES-based technologies for household and agricultural applications improves the security of the water supply and the independence from fossil fuels, while also providing the chance to improve the Water-Energy nexus (Simão & Ramos, 2020). The Water-Energy nexus (WEN), the interdependency between water and energy, is a well-known subject that has drawn more interest from the research and policy sectors (Wichelns, 2017). In addition to providing for water demands, the availability of water resources allows for the concurrent exploitation of RES to provide for energy needs as well. The availability of water resources may have an impact on the capacity to generate electricity to meet energy needs (Nouri et al., 2019). The combination of RES and water resources will decrease the use of fossil fuels, provide the islands with the necessary amounts of energy, lessen blackouts caused by system overload, and lastly, through the desalination process, contribute to issues with water shortages. The usage of both energy and water resources simultaneously is required by everything spoken above. Water is finite, whereas energy is renewable. This is a key distinction. Although desalination of saltwater could be a solution to the limited nature of water supplies, oceans are the only sources of water that are practically unbounded (Kalogirou, 2018). Large amounts of energy are needed to remove salt from seawater, and the environmentally favorable energy sources for the desalination process are renewables (Bundschuh et al., 2021).

Desalination is the process of removing salt and other minerals from seawater or brackish water to make it suitable for human consumption or agricultural use. There are two main methods of desalination: thermal and membrane-based (Figure 1-5). Thermal desalination involves heating seawater to produce steam, which is then condensed to produce fresh water. The most common form of thermal desalination is Multi-Stage Flash distillation, which uses multiple stages of heating

and cooling to separate salt and other minerals from the water. Another form of thermal desalination is Multi-Effect Evaporation, which uses a series of evaporators to produce steam and condensers to produce fresh water.
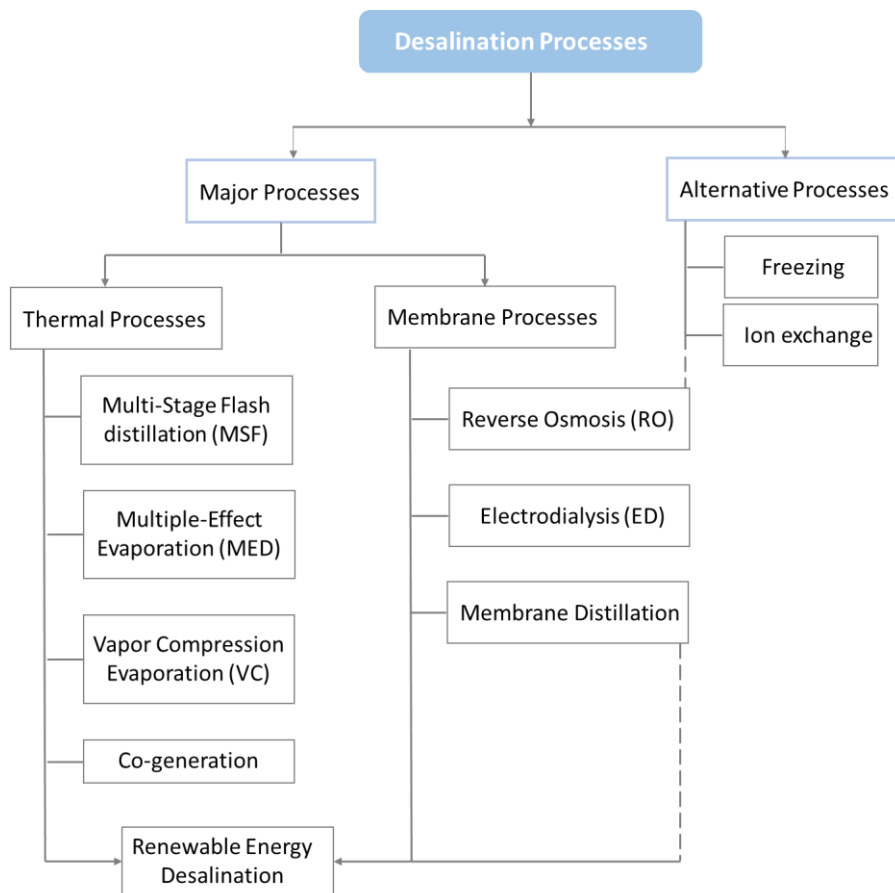

Figure 1-5 Desalination methods (Thimmaraju et al., 2018)

Membrane-based desalination involves forcing seawater through a semi-permeable membrane that separates salt and other minerals from the water. The most common form of membrane-based desalination is Reverse Osmosis (RO), which uses high pressure to force seawater through a membrane and into a collection tank. Another form of membrane-based desalination is electrodialysis, which uses an electric current to remove salt and other minerals from the water (Thimmaraju et al., 2018). Membrane-based desalination units have been erected during the past 20 years and currently compensate for around 70% of all plants. Nowadays, 63% of the desalination market is accounted for by reverse osmosis (RO) desalination (Gude, 2016). Also, compared to thermal-based desalination technologies, RO plants have a capital cost that is around 25% lower (Alkaisi et al., 2017). Desalination units can be used to supply desalinated water for electrolysis to produce green hydrogen from RES. The need for desalinated irrigation water is also anticipated to meet the region's irrigation needs in addition to the demand for household water.

Among all desalination technologies that can be used in conjunction with RES, RO is the main desalination technique because it uses little energy and has low associated costs (Esmaeilion, 2020) and this can be also seen in Figure 1-6, where RO corresponds to 51% of the total use of RES-based desalination technologies. The energy consumption for a RO system varies from 3.7 and 8 kWh/m^3 (Fornarelli et al., 2018; D. Xu et al., 2019) and is influenced by both the water's quality and the size of the desalination unit. Higher power consumption is caused by increasing water salinity and smaller desalination plant sizes (Navarro Barrio et al., 2021). In Figure 1-7 the use of freshwater globally is depicted, according to (Pugsley et al., 2018).
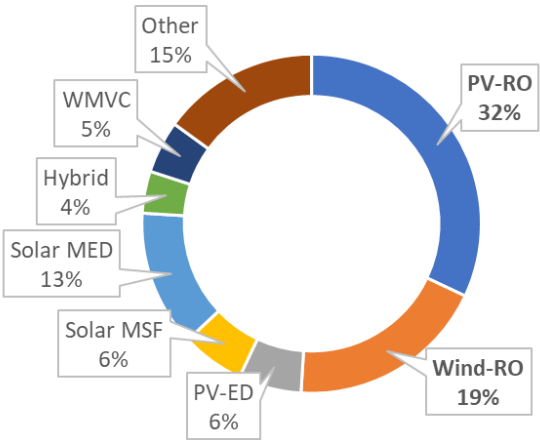

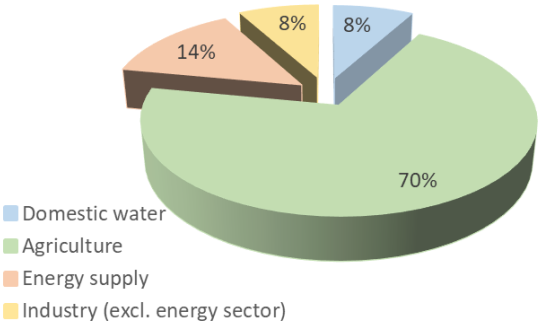Figure 1-6 RES-based desalination technologies (Dhonde et al., 2022)

Figure 1-7 Use of fresh water globally (Pugsley et al., 2018)

The association of HRES with a desalination unit for domestic and agricultural purposes has acquired great interest recently. Rezaei et al. (2020) investigate e the use of wind turbines and photovoltaic systems for water desalination and hydrogen production and provides valuable insights for developing nations on using RES to solve water and energy shortage issues. Bertsiou et al. (2018) describe the design of an HRES, which utilizes wind and hydropower for electricity generation and

desalination of seawater to cover domestic and agricultural water demands. The system's performance is evaluated in three scenarios, and the study shows the potential of the project in fulfilling the island's electricity and water needs, while in (Bertsiou M et al., 2017) a cost-benefit analysis has been conducted for the proposed HRES. In (Stoyanov et al., 2021) a methodology for sizing a hybrid renewable energy system with wind and PV generation and water tank storage for agricultural applications in off-grid areas, is presented. The methodology is applied to sites in Bulgaria with specific crops and meteorological data. The combinations of PV and wind generators and water tank capacities are compared based on investment cost, crop requirements, and system oversizing. The results show trends in hybrid system sizing and the potential to apply the methodology to various sites, generators, and crops. In (Ajiwiguna et al., 2021)], the optimization of a photovoltaic-powered reverse osmosis system with a seasonal water storage tank to achieve low water cost and stable water supply, is proposed. Results show that the optimum combinations of component capacity are achieved at a designed operating time of 8 to 9 hours per day, and the water costs are competitive, 2.46 €/m3, making this system a promising concept for a stand-alone system. Das et al. (2022), optimize a PV/WT/DG/BT system to supply reliable electricity and fresh water to a community on an island in Bangladesh. The generated excess energy is utilized to run a RO process for desalination. Results show a cost of energy of 0.234 $/kWh, 1.64 jobs, and 24,038 kWh/yr excess energy. The excess energy is utilized to achieve a maximum reduction of 11.8% and 9.3% in overall system cost and electricity cost, respectively, while job creation increases by 6%. Sarris et al. (2019) implement a WT/PHS system coupling with a desalination unit to address the lack of fresh water and energy in remote areas. The simulation model operates with hourly data for the period 2007-2017 and investigates the optimum distribution of the produced wind energy. The study presents the results of the HRES simulation in covering the water and electricity demands of Patmos island. Skroufouta and Baltas (2021) investigate a PV/WT/PHS system with a desalination unit in Karpathos, Greece, where 40-year synthetic time series are used for meteorological and demand data, drinking and irrigation water demands, and wind and solar radiation. The system can cover the entire drinking water needs of the island, 89.75% of irrigation and 50.63% of energy needs. The IRR of various selling prices of desalinated water and energy ranges from 10% to 17%, rendering the investment viable and even profitable. Borge-Diez et al. (2021) investigate the economic viability of desalination plants powered by RES. Results show that the projects can be economically profitable under certain conditions of grants and investors' expected benefits, but sales of water and energy can be a limiting factor. In (Triantafyllou et al., 2021) the evaluation of the energy needs and water resources of Nisyros Island, which currently relies on costly water transportation from the mainland, is conducted. The study proposes a PV-based configuration to sustainably power the island's desalination units, with a focus on economic benefits. In (Kotsifakis et al., 2020) examine and compare three different scenarios, for meeting domestic water demand on Lipsi island. Life-cycle cost analysis is performed

to evaluate each scenario from an economic point of view. Kourtis et al. (2019) examine five different water resource management scenarios on eight dry islands of the Aegean Sea in Greece, comparing the current practice of water hauling via ship against alternative water supply schemes for meeting water demand. The optimal solution for each island is proposed based on a life cycle cost analysis and assessed under six climate change scenarios in terms of renewable energy requirements for reliability. The scenarios show decreasing performance in terms of reliability under climate change. Eltamaly et al. (2021) propose the use of a PV/WT/BT system to provide fresh water to Arar City in Saudi Arabia using RO desalination. Results show that the use of RES is superior and cost-effective compared to conventional power sources, with a cost of $0.745/m3 for freshwater production. Nikas-Nasioulis et al. (2022) implement an HRES that utilizes wind energy to meet the energy, water, and electromobility demands of Kos Island. Two different scenarios are studied, using hourly meteorological and demand data from 2016-2020, analyzing CO_2 emissions, and performing a cost-benefit analysis. The HRES makes the island autonomous and self-sufficient, reduces pollution, and improves the quality of life. Elmaadawy et al. (2020) propose a WT/PV/DG/BT system to power a desalination plant and asses the techno-economic and environmental feasibility of different off-grid power systems. Results show that the proposed HRES outperforms other alternatives and a potential reduction of up to 81.5% in carbon dioxide emissions compared to existing diesel systems is achieved. Papapostolou et al. (2020) explore the challenges of small islands in terms of water and energy resources, under the WEN. The paper suggests a comprehensive strategy to deal with these issues by implementing alternatives that combine sustainable energy and water supplies. Using Anafi Island as a case study, the suggested framework is illustrated, and a linear programming model is created to demonstrate that electricity and water supply from RES are possible at a reasonable cost while minimizing GHGs.

1.4 Thesis contribution

The contribution of this research consists of the development of an integrated methodological framework for the siting of wind turbines, of the energy management strategies of HRESs coupling with different storage technologies, single or hybrid, with the simultaneous fulfillment of energy and water demands and of the methodological framework for the estimation of the rejected renewable energy from an HRES. The major research points of this thesis can be summarized in the following points.

A. A specific methodology is presented in order to evaluate potential sites for the installation of wind turbines, using different scenarios and performing a sensitivity analysis. It considers both the parameter of the environmental constraints and the current legislation framework for the siting of a wind farm. Scenarios of installing a wind farm with the lowest possible energy losses due to power transmission via cables are also being investigated. Results show how installation

locations are affected based on specific siting criteria (technical, economic and cultural scenario), as well as how changes in specific criteria affect the final installation locations. The methodology and the results are analyzed in Chapter 3, while the conclusions are presented in section 7.1.

B. An assessment of HRESs using wind turbines and photovoltaic modules and coupling with a desalination unit and different storage technologies for the storage of surplus renewable energy is presented. This research focuses on the comparison of different storage systems, providing the corresponding detailed energy management strategies for single or hybrid storage with the simultaneous energy supply for household consumption and for the required desalinated water for domestic and irrigation demands, based on an energy, economic and environmental analysis. The methodology uses geographical, meteorological, population and demand (water, energy) data, leading to conclusions about the functioning and the reliability of such projects. The study tries to answer which configuration is more efficient in the fulfillment of energy and water demands, leading to the avoidance of the startup of polluting local power stations. How each configuration affects the cost of energy, the cost of desalinated water, the loss of load probability, the payback period and the reduction of the CO_2 emissions? How are changes in meteorological, demographical and installation factors affecting the results?

C. The methodological framework for the estimation and minimization of the rejected renewable energy through an HRES by the upper reservoir, the pumping station and the direct penetration of wind energy to the grid is provided. The amount of rejected energy is attempted to be calculated based on the percentage of direct penetration of wind energy to the system and on the percentage of energy set for desalination versus pumping. This will make the grid system more reliable and sustainable. It will, also, result in the promotion of RES, which has been a priority globally, to the reduction of the consumption of fossil fuels and to energy and water independence. Also, the units of energy needed for storing excess energy versus the energy produced by a pumped hydro storage system are investigated. Based on the results of rejected energy from an HRES, the optimal direct percentage of renewable energy to the system is determined afterward. The methodology and the results are analyzed in Chapter 6, while the conclusions are presented in section 7.3.

1.5   Thesis structure

In Section 1 of the thesis, a presentation of renewable energy sources and the prevailing institutional framework in Greece, as well as the EU's policy on RES is presented. In addition, an analysis of hybrid renewable energy systems is presented. Importance is given to the various energy storage methods, like pumped hydro storage, batteries and hydrogen production. Also, the water desalination process is demonstrated with a particular reference to the reverse osmosis method, which is the most

widespread and is examined in the context of this work. Finally, the aim, motivation, structure and contribution of this research are presented.

In Section 2, the study area and the data processing are presented. Fournoi Korseon in the North Aegean is used as the case study for all the scenarios and the application of the methodology. Data about population, demand, as well as meteorological data of the island is displayed from 2013 until 2019. Also, monthly wind speed, solar radiation and temperature for the reference year 2019 are displayed. The estimation of the optimal angle of the PVs is presented for each month and the mathematical background for the calculation of the total radiation on the tilted plane is presented. Finally, the area protection regime is depicted and the legislation framework for wind turbine sitting is provided.

Section 3 presents a combined use of Multi-Criteria Decision-Making (MCDM) and Geographic Information Systems (GIS) methodology for the evaluation of eligible sites for wind turbine sitting for three scenarios with different combinations of criteria is presented. An extra constraint is examined, the minimum distance from the main settlement of the island. This leads to the lowest possible energy losses through the cables during the power transmission. Finally, a sensitivity analysis is performed, to determine the impact of each criterion on the suitability maps of an area.

Section 4 presents the methodology that is created and followed in this thesis. The methodology initially concerns the modeling of each component of the HRES. Also, the various configurations, based on the combination of the various components that have been analyzed initially, are presented. Energy management strategies are described based on single or hybrid storage methods, depending on the storage technologies of each scenario. Subsequently, the methodology for the economic and environmental analysis that will be conducted, as well as the indicators that will be calculated to make the comparison between the scenarios, are presented.

In Section 5 the results are presented for each examined configuration according to the methodology. Daily and monthly results about coverage of energy and water demands by the HRES, share of energy from different energy sources, consumed and produced energy of the HRES and the charging and discharging procedure for each storage method are displayed. Also, reliability analysis of each HRES, as well as economic and environmental indices are estimated, like the cost of energy (COE), cost of water (COW), loss of load probability (LOLP), payback period (PBP) and eliminated CO_2 quantities.

In Section 6, the methodology for calculating the rejected energy from an HRES is presented. This rejected energy depends on three different factors, the direct penetration of renewable energy into the network, the capacity of the pumping station and the volume of the upper reservoir. Based on the results of rejected energy from an HRES, the optimal direct percentage of renewable energy to the system is determined afterward.

In Section 7, the conclusions about the 'behavior' of each storage method in the context of an HRES are presented. Also, key findings about the minimization of the rejected renewable energy of an HRES and the scenario with the optimal hierarchy of criteria, which combine both low cost and a larger surface for installation are demonstrated. Furthermore, thoughts and considerations for future research are provided.

Subsequently, the Acknowledgments and the References; list are available. At the end of this thesis, the appendices are presented. In Appendix A – Abbreviations the Abbreviations are listed, in Appendix B – List of Figures and Appendix C – List of Tables the list of Figures and Tables are presented respectively, in Appendix D – Extended Summary in Greek (Εκτεταμένη περίληψη) the extended summary in Greek is provided and in Appendix E – Complete List of Publications the complete list of publications by the author, associated with this thesis, is demonstrated.

2.1   Fournoi Korseon

Fournoi Korseon or Fournoi Ikarias or Fournoi is a cluster of islands, islets and rocky islets of the Aegean Sea, in Greece. Their location is southwestern of island Samos and eastern of island Ikaria. The main ones are Thymena, Thymenaki (or Thymenonisi), Alatonisi (or Alafonisi, or Alatsonisi) in the west, Fournoi, Kisiria (or Diapori) in the center, Strongylo, Platy (or Plaka), Makronisi (or Markri) in the south and Anthropofas (or Anthro), Little Anthropofas, Kedro (or Little Anthropofas), Agridio (or Prasonisi), Agios Minas, Little Agios Minas, and Plakaki to the east. The main inhabited areas are Fournoi, Thymena and Agios Minas. Fournoi Korseon is the largest island of the cluster with an area of 30.5 km^2 and the capital settlement with 1400 inhabitants. The characteristic of the islets of Fournoi is the very large coastline of 120 km, which exceeds in length that of Samos, which is comparatively much larger in size. Thymaina is the second-largest island of the complex with an area of 10.071 km^2 and its population is 151 inhabitants living in the two settlements of the island, Thymaina with 140 inhabitants and Keramidou with 11 inhabitants. Agios Minas has an area of 2.1 km^2 and only 3 inhabitants. The highest point of the island is 470 m.

Fournoi Korseon belongs to the Municipality of Fourni Korseon, Prefecture of Samos, North Aegean region. The municipality initially operated according to the Kapodistrias Plan as one of the eight municipalities of the prefecture of Samos from 1999 to 2010 based in the settlement of Fournoi. With the administrative division of 2011 (Kallikratis Plan), the administrative boundaries and the headquarters of the municipality did not change. Fournoi is located between the two large islands of the prefecture, Samos and Ikaria. Its area is 44 sq. km. All the settlements of the municipality are located on the largest island of Fournoi apart from Thymaina and Keramidou which are located on the island of Thymaina. In Figure 2-1 the island and its settlements are shown. The digital elevation model is obtained by the National Cadastre & Mapping Agency SA of Greece. The pixel size is 5 × 5 m, the geometric accuracy RMSE is z ≤ 2.00 m and the absolute accuracy is about 3.92 m with a 95% confidence level.

The climate in Fournoi Korseon, due to the geographical location and the influence of the sea, is characterized as the Mediterranean with mild winters and prolonged dry and hot summers, low annual rainfall and great sunshine all year round. Frost is rare in these areas, and even more rarely hail or snow. The average annual temperature is 18.4 °C. The average monthly minimum is 10 °C in February, and the average monthly maximum is 28.4°C in July. The prevailing winds are mainly westerly and northerly with intensities above 6 B. The relative humidity has an average value of 72.5

% in winter and 47.5 % in summer. The dry season lasts from April to October. The days of frost are 1.2 per year, snow 1.5 and hail 3.3. The sunshine reaches 2915 hours per year with a maximum price of 398 hours in July, one of the highest in Greece.
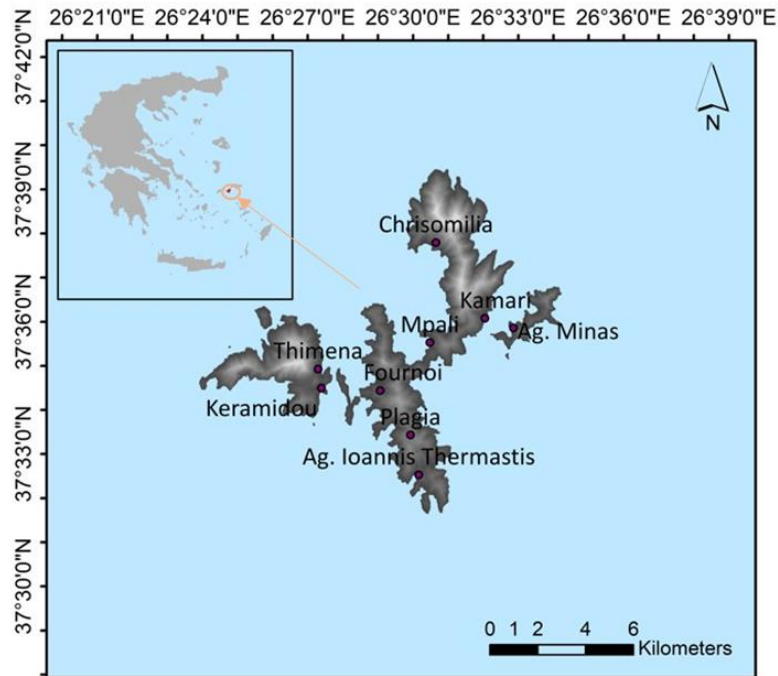

Figure 2-1 Study area – Fournoi Korseon island

The island has an underground landfill. In 2011 a static study of biological treatment was prepared for the settlement of Fournoi, but the construction has not been done until today. The road network of the island connects Chora (port) with almost all the settlements. The permanent population uses mainly cars for their transportation, while in summer the visitors of the island are served by a small bus and some boats for the transfer to beaches, such as in Thymaina and Keramidou. The island has a gas station. The ferry connection is served by the port in Chora with ferries from the ports of Piraeus, Ikaria and Samos. There is a network of Hellenic Telecommunications Organisation S.A. which reaches almost all settlements. Mobile telephony is served by all networks and there are three antennas installed, two by Cosmote, near the settlement of Fournoi and on the Varela hill, and the third, by Vodafone, near the settlement of Plagia. In the settlement of Fournoi, the service of the municipality of Fournoi Korseon operates together with the technical service of the municipality. Also, the settlement has a Citizen Service Center (and the second one in Thymaina), a police station, a port station, a health center, a Hellenic Post office, a high school and two primary schools (and a third primary school in the settlement of Chrysomilia).

Most of the area of the island and specifically 76%, is covered by hardwood vegetation. They are followed by a much smaller proportion the natural pastures (14.5%), areas with sparse vegetation (2.0%), land covered mainly by agriculture with significant areas of natural vegetation (1.2%), intermittent urban construction (1.1%), transitional wooded shrubs (1.1%) and indefinite coverage (4%).

☐ Wind Farms - Under Evaluation
▲ Wind turbines of wind and hybrid power plants - production license
☐ Hybrid power plants - production license
☐ Hybrid power plants - rejection decisions

Figure 2-2 RAE Geoportal Map of Regulatory Authority for Energy (RAE) - https://geo.rae.gr/

There is no extended production of agricultural products on the island, except for a few olives and vineyards for private use. It is the island of fishermen and beekeepers, as the main areas of activity of the inhabitants are fishing and beekeeping. The traditional products of the island are summarized in thyme honey, royal jelly, pollen, propolis, jams and desserts, herbs and natural wax. The excellent natural landscape of Fournoi, the typical residential environment of the settlements, the beaches and especially the calm rhythm of life are the strong elements that attract visitors. Today there are 27 companies registered either as rooms for rent or as hotels. The restaurant lists 10 businesses that offer food, coffee and drinks. The tourist activity belongs to the residents. The peak of the tourist season is located in August when most visitors are mainly Greeks and European foreigners. In recent years there has been a significant extension of the tourist season, as it starts in May and gradually

increases until September. At the beginning and end of the summer season the visitors are German naturalists and walkers who come either individually or in small groups.

Chrysomilia since 2008 is connected to a water supply network and to a desalination plant with a capacity of 100 m^3/day. The desalinated water is available to the residents through a desalination reservoir. The desalination system is supplied on a daily basis with 11 m^3/hr of sea water 45% of which is desalinated produced water and 65% returns to the sea with the salt. The water is deionized and enriched with various trace elements to be potable. The chemicals used are controlled by various electronic indicators and frequently a sample is sent to the State General Chemistry Laboratory for inspection. The desalination plant is not autonomous and is supplied with electricity produced by conventional fuels. In Thymaina the water is drilled from a natural spring of 94 m depth. Purification of water is accomplished by the method of reverse osmosis. The reverse osmosis filter was installed in 2009. The water after drilling is transported to a large reservoir of 3,000 m^3 and after filtration is transported through pipes to a smaller tank of 400 m^3, which can meet the needs of the island for 3 to 4 days. In the settlement of Fournoi, where most of the permanent population lives, there is no water supply. For their domestic water needs, the residents use rainwater harvesting systems and potable water is available in a public tap in the central square of the village. The alternative is the use of bottled water which increases the cost of the water and at the same time burden the environment. There is no municipal water supply available for agricultural use. Private wells are used for irrigation needs, which leads to the salinization of the aquifers and lowering of the groundwater table. However, there is no large agricultural production and agricultural products are available for private use.

The island is submarine-connected with the nearby island of Samos in order to fulfill its energy demands. This results sometimes in extended blackouts. The situation worsens during the summer months when demand increases due to tourism. Although, the island's wind and solar potential are very high, however, they are unexploited yet. As shown in Figure 2-2 possible locations for the installation of wind farms (Geoportal Map of Regulatory Authority for Energy (RAE) , 2022) are under evaluation (yellow polygons), while a hybrid project in the east of the island has production a license from RAE and the operating license is pending (green color). This is a project similar to the Tilos project from Eunice Energy Group. Finally, in the south of the island, an application for a hybrid project has been rejected.

The whole island belongs to the Natura habitat, according to Filotis, the database of the Greek Nature (Filotis, Database for the Natural Environment of Greece, 2022). Many monuments of the island prove the long history of the island. The main of them are the Akropoli, the Ancient Settlement of Kamari, the Ancient Quarry in Petrokopio and Sarkofagos. Akropoli is a huge cyclopean wall of a prehistoric castle with hewn stones on the hill of Agios Georgios above the village. On the foundations of the

ancient castle a classical era castle is built which constitutes the Akropolis of Fournoi. There is also a temple in the castle. The Ancient Quarry in Petrokopio is found at the mouth of a small cove in Petrokopio. In many parts of the hill, the traces of ancient quarrying are clear, while the entire slope from the quarry of Petrokopio to the coast is covered with lapis and large pieces of marble. The archaeologists confirm that ancient Miletos is built from these marbles. A second ancient quarry also exists in the Tsiganario area. Ancient Settlement of Kamari is located on the western side of the island and owes its name to a ruined semi-cylindrical dome. A settlement of late antiquity has been identified in this area. Remains of buildings extend from the slopes of the low hill to the sea and continue into it. Rectangular rooms and the outline of a pithos can be seen in the shallow water. The walls are built with stones. On the hill, in the precinct of the church of Taxiarches, there are fluted columns of granite, porolite and rectangular marble slabs. The traces of clandestine digging of graves are evident among the thick bushes that cover the slope. Sarkofagos was found on a plot of land in the main settlement of Fournoi and today it stands in the village square in a perfect parallelepiped shape with embossed decorations and an inscription. This monument is similar to two others found in the Kampos Collection of Ikaria, in ancient Oinoi. Since during the excavation the Sarkofagos was found resting on rectangular supports it is assumed that it must have been found in its original position and that a Roman cemetery must be located in the vicinity. The entire system is installed so as not to be visible from the island's archeological monuments due to restrictions imposed by legislation and spatial criteria (Baltas & Dervos, 2012).

2.2   Data collection and processing

2.2.1   Population data

The permanent population of the island is provided by the Technical Service of the island, and it is 1400 residents. However, it is worth noting that the population of the island fluctuates significantly depending on the time of year, as Fournoi is a popular tourist destination in the Aegean Sea, and its population can swell during the summer months. According to the Technical Service of the island, the population reaches 4000 during summer and especially in August, which is the month with the most tourist traffic in the Greek islands. In Table 2-1 the data on the population and its monthly fluctuations throughout the year are presented.

Table 2-1 Monthly population data

Month	Population	Month	Population
January	1,400	July	3,000
February	1,400	August	4,000
March	1,400	September	1,700
April	1,400	October	1,400
May	1,700	November	1,400
June	2,600	December	1,400

2.2.2 Demand data

Domestic water requirements are provided by the Technical Service of the island and are equal to about 91,500 m^3 per year. Monthly demands range from 5,000 m^3, from October to April, to 16,000 m^3 in August, the most demanding month due to tourism. In Figure 2-3 the daily consumption profile used is presented for a day in August.

For the estimation of irrigation water requirements, data about the crops and the corresponding areas cultivated on the island are used. These data have been obtained by (Hellenic Statistical Authority, 2022) and are presented in Table 2-2.
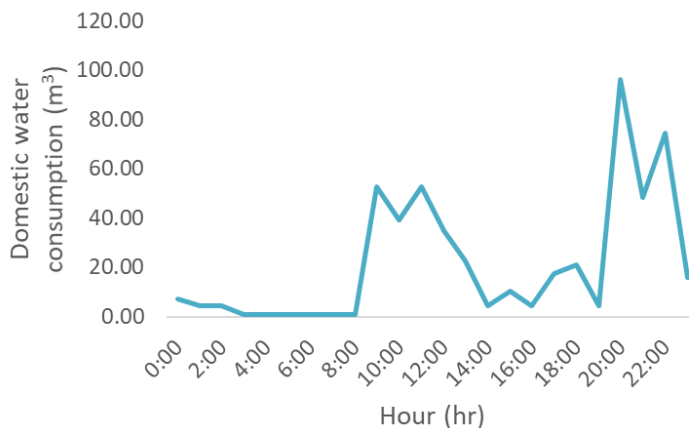
Figure 2-3 Hourly domestic water consumption for 15th of August

According to the Hellenic Statistical Authority, the 76% of the island is covered by scrub vegetation, the 14.5% is grazing land, areas with sparse vegetation are about 2.0%, intermittent civil construction covers the 1.1% of the total area, transitional wooded scrublands are 1.1%, indeterminate coverage is 4% and land covered by agricultural and natural vegetation is 1.2%. Using the Blaney-Criddle method (Blaney HF & Criddle WD, 1962) the evapotranspiration is calculated and is construed as irrigation water. Blaney and Criddle developed an empirical relationship between evaporation, average air temperature, and average daylight hours. Evapotranspiration is directly dependent on

the sum of the products of the average monthly air temperatures and the percentage of daylight hours of the month, in an actively growing crop with sufficient soil moisture according to Equation 2-1.

$$ET = kF = k\frac{(1.8T + 32)p}{3.94}$$

where ET is the monthly potential evaporation in mm, k is an empirical crop coefficient referring to the specific crop, T is the average monthly air temperature in °C and p is the percentage of daylight hours of the month and is given by Equation 2-2.

$$p = 100\frac{N \cdot \mu}{365 \cdot 12}$$

where N is the average astronomical length of the day in hr and μ is the number of days in that month.

k values have been determined by Blaney and Criddle for various crops. The method was originally developed to calculate the seasonal needs that refer to the germination period of each crop. The values of the monthly crop coefficients of irrigated crops and the seasonal crop coefficient of each crop have significant differences. This is due to the different development of the root system and the aboveground part of the crop depending on the stage of development in which it is located. Therefore, to calculate the monthly water needs of the crops, it is necessary to use the monthly crop coefficients.

Table 2-2 Crop's area

Crops	Area (m^2)
Cereals	14,800.00
Vegetables	7,075.00
Citrus fruits	41,650.00
Fruit trees	122,225.00
TOTAL	185,750.00

The irrigation season extends from April to September and desalination for irrigation purposes is calculated only for these months. Total irrigation water requirements are equal to about 102,000 m^3 per year, while the minimum monthly demand is 1,000 m^3 in April and the maximum is 30,000 m^3 in July.

The demand for desalinated water is increased in summer due to both tourism and the irrigation season. The monthly demands for desalinated water for both domestic and irrigation purposes are presented in Table 2-3.

Table 2-3 Monthly domestic and irrigation water requirements

Month	Domestic water (m³)	Irrigation water (m³)
January	5,400	0
February	5,400	0
March	5,400	0
April	5,400	988
May	7,200	20,033
June	10,200	25,842
July	12,000	29,114
August	15,600	26,299
September	7,200	10,391
October	5,400	0
November	5,400	0
December	5,400	0
TOTAL	90,000	112,667

Irrigation is performed at night as this prevents excessive evaporation, which can waste a large amount of water. Also, during the night the demand for domestic water and energy consumption is reduced, so any RES production can more easily be given directly for desalination of irrigation water and achieve more demand coverage.

The desalination of seawater is performed by the reverse osmosis method. The energy consumption for desalination is estimated equal to 5.85 kWh/m³ (Fornarelli et al., 2018; D. Xu et al., 2019). In Table 2-4 the monthly energy requirements for domestic and irrigation water desalination, as well as the energy requirements for the household consumption (electric load) are presented. During winter the maximum demand for household consumption is observed, while in July and in August the maximum consumption is for the desalination process.

Data about electric load are provided by the Public Power Corporation (PPC) and the monthly variation is given, also, in Table 2-4. The demand increases in winter due to energy-consuming habits, like water and building heating. It, also, increases in the summer due to tourism. The consumption ranges from 162,840 kWh in September to 665,446 kWh from December to March. Electricity data are provided monthly and their aggregation into an hourly step is based on the consumption profile for Athens by (Psiloglou et al., 2009). In Figure 2-4 the daily consumption profile used is presented for a day in August.

Table 2-4 Monthly electricity requirements for desalination and household consumption

Month	Domestic water (kWh)	Irrigation water (kWh)	Household consumption (kWh)	Total consumption (kWh)
January	31,590	0	665,446	697,036
February	31,590	0	601,048	632,638
March	31,590	0	665,446	697,036
April	31,590	5,778	495,990	533,358
May	42,120	117,192	296,050	455,362
June	59,670	151,177	286,500	497,347
July	70,200	170,315	434,000	674,515
August	91,260	153,850	504,835	749,945
September	42,120	60,788	162,840	265,748
October	31,590	0	168,268	199,858
November	31,590	0	325,680	357,270
December	31,590	0	665,446	697,036
TOTAL	**526,500**	**659,100**	**5,271,549**	**6,457,149**
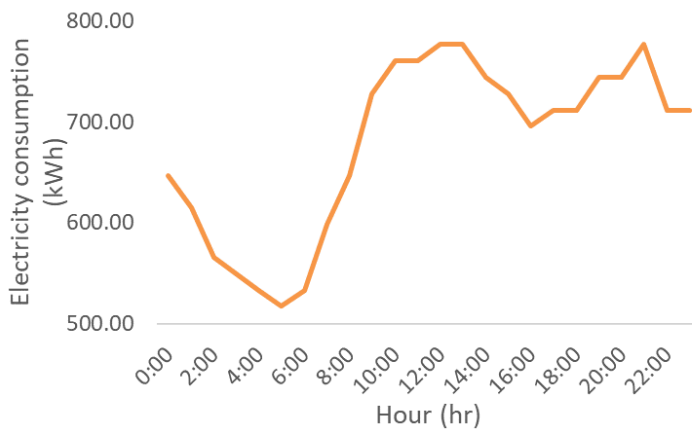
Figure 2-4 Hourly electricity consumption for 15th of August

2.2.3 Meteorological data

The island has high wind and solar potential. In Figure 2-5 the wind potential is depicted according to annual wind speed data at a height of 40 m. The layer of these data is obtained by Geodata (GEODATA, Open Data Accessible to Everyone, 2019), which they have been calculated by the Centre for Renewable Energy Sources and Saving (CRES) based on an extensive program of in situ measurements and application of a mathematical model.
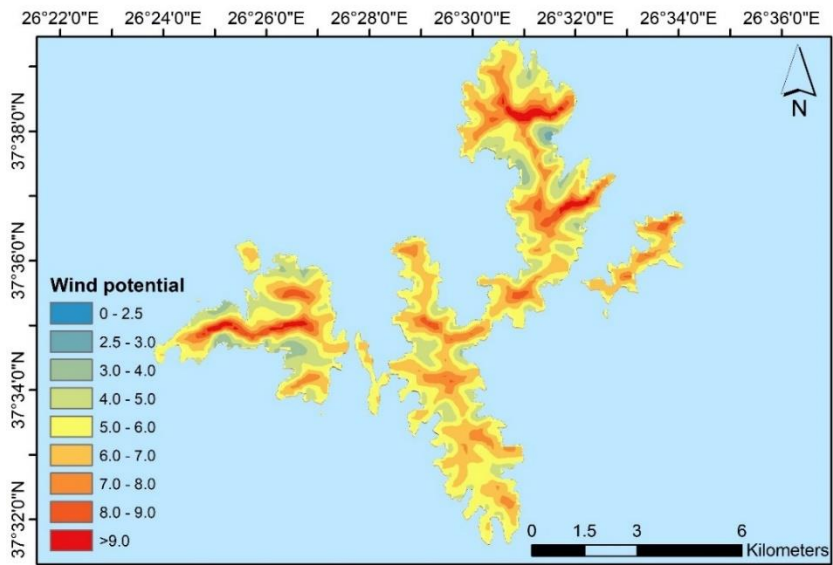
Figure 2-5 Wind potential of Fournoi Korseon island
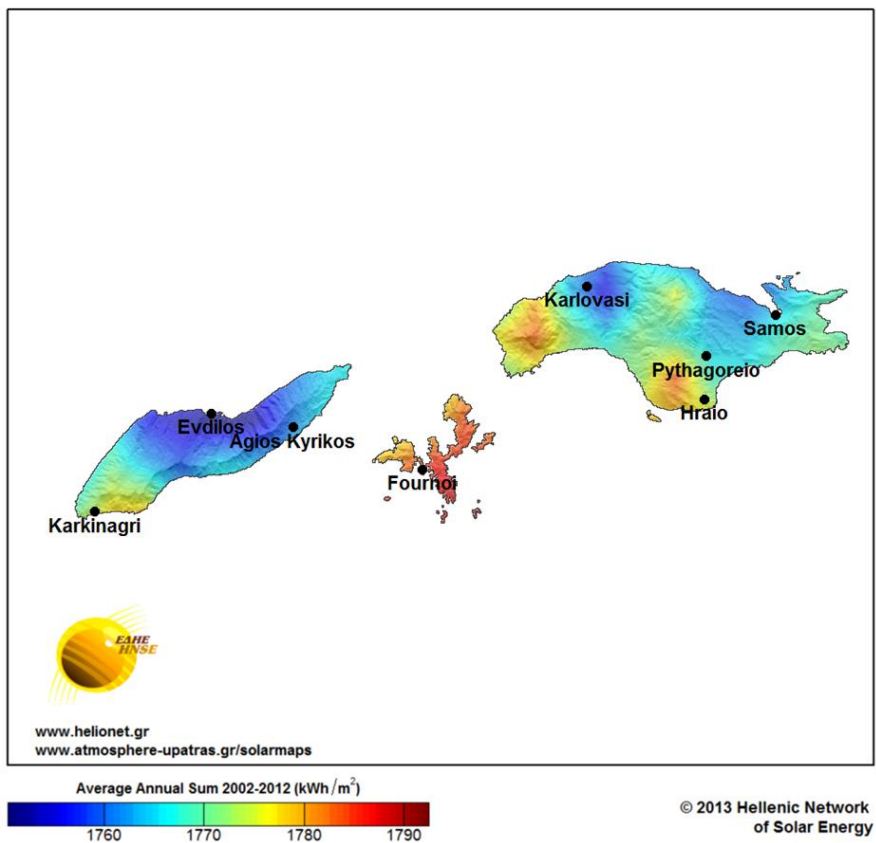
Figure 2-6 Solar potential in Fournoi Korseon and the nearby islands, Samos and Ikaria (Source: Hellenic Network of Solar Energy)

Figure 2-6 presents the map of Global Horizontal Irradiation (GHI) in kWh/m^2 for Fournoi (the island in the center) from the Hellenic Network of Solar Energy (Nikitidou et al., 2015). In the west is Ikaria and in the east is Samos. It is observed that Fournoi has a particularly high solar potential. Hellenic Network of Solar Energy has implemented an integrated system for real-time monitoring of the available solar potential in Greece by producing solar energy maps in detailed spatial and temporal analysis and providing a forecast of solar energy levels. The system is supported by an updated climatic study of solar energy for the period 2002-2012. The project combines for the first time for Greece solar energy measurements from a well-organized network of stations, with satellite images of the cloud cover, satellite data of atmospheric suspensions and calculations with models leading to the production of maps (and data) of solar energy from Greece in a very detailed time and space scale, as well as in the daily short-term forecast of solar energy levels (Hellenic Network of Solar Energy 2002-2012, 2022).

(a)

(b)

(c)

(d)
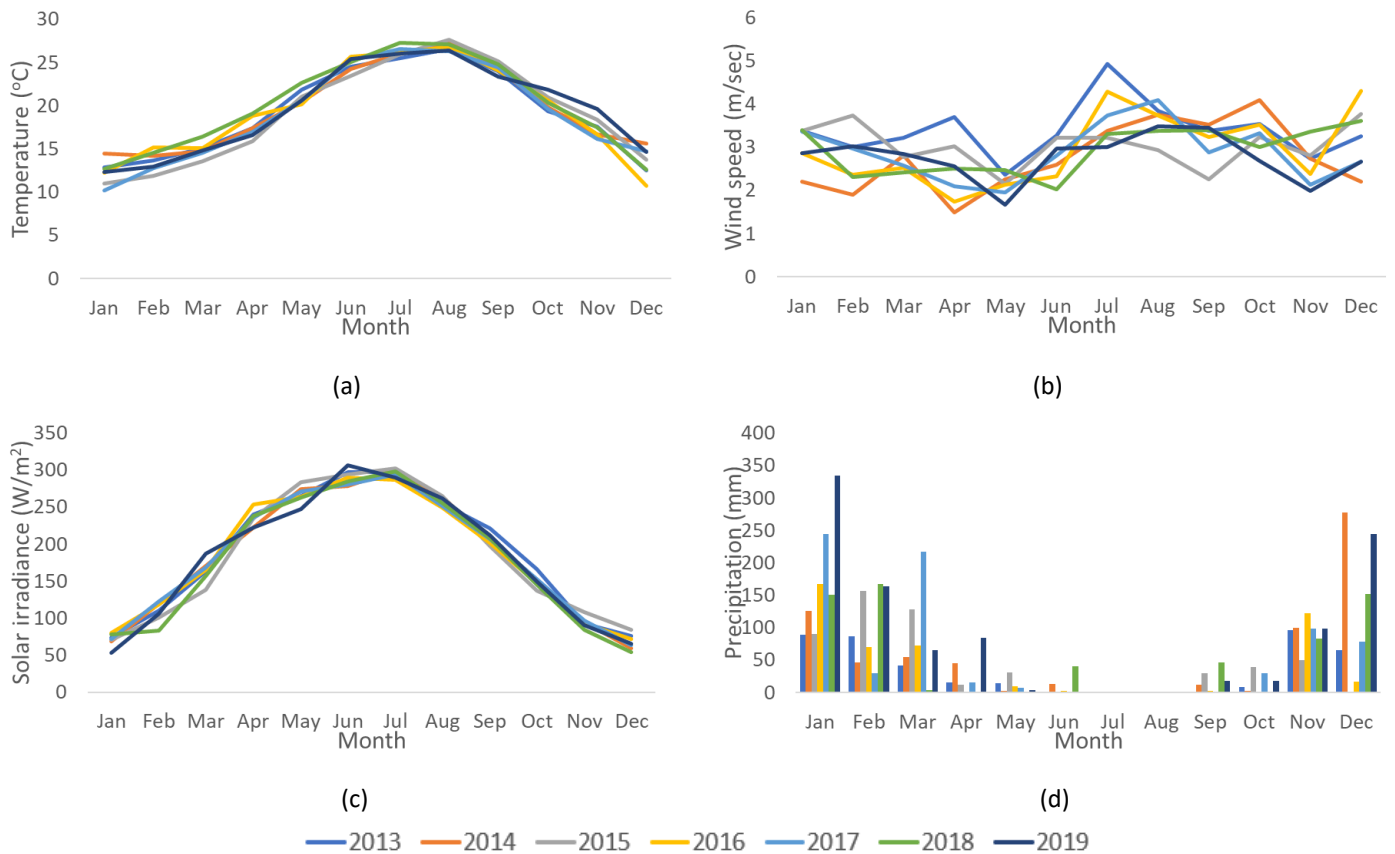
Figure 2-7 Monthly data for years 2013-2019 (a) temperature, (b) wind speed, (c) solar irradiance, (d) precipitation

Data about wind speed, temperature and precipitation are obtained from the weather station of Fournoi Korseon of the National Observatory of Athens Automatic Network-NOANN (Lagouvardos et

al., 2017). Also, data about solar irradiance are obtained from the weather station of Samos Island, as in the station of Fournoi there are no measurements of solar irradiance. In Figure 2-7 the monthly data for the years 2013-2019 are shown about (a) temperature, (b) wind speed, (c) solar irradiance and (d) precipitation. Also, in Figure 2-8 the monthly wind speed, solar radiation and temperature for the reference year 2019 are depicted.

For the calculation of the energy from the PV, the irradiance on the tilted plane is used, where the tilted plane is the inclination of the PV frame. This angle must be optimal for every month in order to make the best use of the solar potential and the PVs for energy production. To find the optimal angle for the study area, the radiation is calculated for each month on the tilted plane and Figure 2-9 shows the values of the radiation for a series of angles. Each month the PV is considered to have the optimal angle.
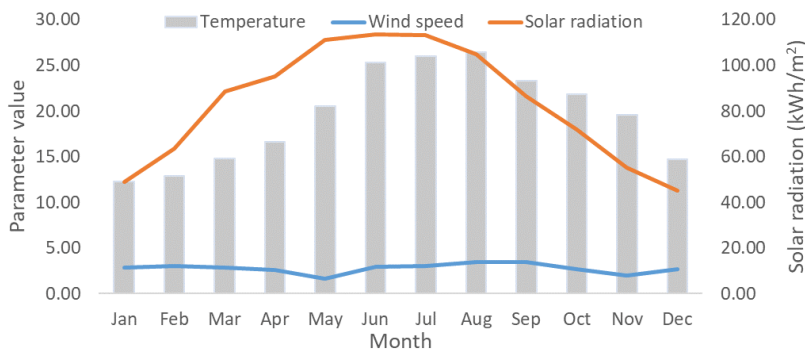
Figure 2-8 Monthly wind speed, solar radiation and temperature for the reference year 2019
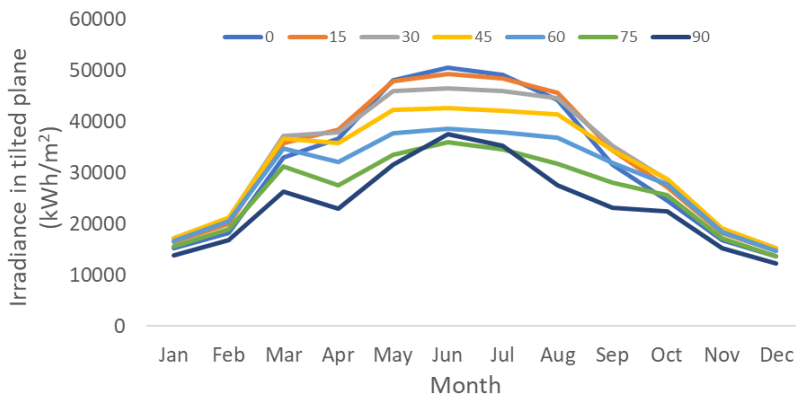
Figure 2-9 Total irradiance in tilted plane for different for different inclination of PV

To calculate the irradiance on the tilted plane, the solar deviation δ from Equation 2-3 is estimated.

$$\delta = 23.45 \cdot sin \left(360 \cdot \frac{D+284}{365} \right)$$
<div align="right">Equation 2-3</div>

where D is the number of days in the year.

The hourly sunset angle ω_{ss} is then calculated according to Equation 2-4.

$$\omega_{ss} = \begin{cases} \beta = 0, \quad \gamma = 0, \quad cos^{-1}(-tan\varphi \cdot tan\delta) \\ \gamma = 0, \quad \beta \neq 0, \quad min[cos^{-1}(-tan\varphi \cdot tan\delta), \quad cos^{-1}(-tan(\varphi - \beta) \cdot tan\delta)] \end{cases}$$

Equation 2-4

where β is the slope of the reference surface in degrees. Also, γ is the azimuth surface angle in degrees and is equal to 0 for the south orientation and φ is the latitude, also in degrees, which for Fournoi Korseon is equal to 37.58º.

The geometric factor for the average day of the month, R_b, is calculated according to Equation 2-5.

$$R_b = \frac{\left[cos(\varphi - \beta) \cdot cos\delta \cdot sin\omega_{ss} + \left(\frac{\pi}{180}\right) \cdot \omega_{ss} \cdot sin(\varphi - \beta) \cdot sin\delta\right]}{\left[cos\varphi \cdot cos\delta \cdot sin\omega_{ss} + \left(\frac{\pi}{180}\right) \cdot \omega_{ss} \cdot sin\varphi \cdot sin\delta\right]}$$

Equation 2-5

The average monthly clearness index k_t is calculated, which is defined as the quotient of the average monthly total solar radiation on the ground to the corresponding value in the atmosphere. The calculation is based on the linear relationships that have been extracted, using available data on the average monthly values of the clearness index in various regions of Greece by (Vazaios, 1987) and using the latitude for the region of interest (Balaras et al., 2006). Table 2-5 shows the monthly values of the clearness index k_t for Fournoi Korseon.

Table 2-5 Monthly clearness index k_t for Fournoi Korseon

Month	k_t
January	0.4211
February	0.4535
March	0.4919
April	0.5356
May	0.5819
June	0.5966
July	0.6039
August	0.6025
September	0.5817
October	0.5226
November	0.4757
December	0.4235

The ratio of the mean diffuse radiation to the corresponding mean total radiation in a horizontal plane is calculated according to Equation 2-6 by (Collares-Pereira & Rabl, 1979).

$$\frac{H_d}{H} = 0.775 + 0.00653 \cdot (\omega_{ss} - 90) - [0.505 + 0.0455 \cdot (\omega_{ss} - 90)]$$
$$\cdot cos(115 \cdot k_t - 103)$$

<div align="right">Equation 2-6</div>

Finally, the total radiation is calculated on the tilted plane from Equation 2-7.

$$\frac{H_T}{H} = \left(1 - \frac{H_d}{H}\right) \cdot R_b + 0.5 \cdot \left(\frac{H_d}{H}\right) \cdot (1 + cos\beta) + 0.5 \cdot \rho \cdot (1 - cos\beta)$$

<div align="right">Equation 2-7</div>

where ρ is the reflectivity of the surface.

2.3 Area Protection Regime

The important habitats are distinguished for the presence in them of endangered species of the Greek flora and fauna. Endangered species are species that are in immediate danger of extinction (endangered), those who may be in danger (vulnerable) and those who are vulnerable because they have small populations (rare). The condition of the habitats, the species of flora and fauna and in general the ecological wealth of the Greek nature still remains very good in comparison with the other European countries. The area of Fournoi Korseon, according to the database for the Greek nature Filotis (Filotis, Database for the Natural Environment of Greece, 2022) is a Corine and Natura habitat. Figure 2-10 (a) shows the area covered by the Corine habitat with the code name "Fournoi Islands of Ikaria - A00010082", (b) the Natura habitat GR4120004 'Ikaria - Fournoi and Coastal Zone' and (c) the Natura habitat GR4120006 'Island Fournoi and Islets Thymaina, Alatsonisi, Thymainaki, Strongylo, Plaka, Makronisi, Mikros and Megalos Anthropofagos, Agios Minas'.

| (a) | (b) | (c) |

Figure 2-10 Filotis database (a) Corine habitat A00010082 "Fournoi Islands of Ikaria", (b) Natura habitat GR4120004 'Ikaria - Fournoi and Coastal Zone', (c) Natura habitat GR4120006 'Island Fournoi and Islets Thymaina, Alatsonisi, Thymainaki, Strongylo, Plaka, Makronisi, Mikros and Megalos Anthropofagos, Agios Minas'.

The total area of the habitat is 4507.02 ha, the land area is 6100.00 ha, the total perimeter is 129.0 km and the maximum altitude is 514.0 m. There is sparse shrub vegetation, many sea cliffs, bays and smaller coastal rocks. The condition of the place is degraded and requires maintenance. It is an area with seabirds, as well as an important passage for birds. The Mediterranean Seal was common, but the current situation is unknown. Illegal fishing is a threat to the area. Remarkable plants, mammals and birds appear in the area, the list of which can be found in Filotis. The total area of the habitat GR4120004 is 12909.00 ha, the rough area is 9467.81 ha, the total perimeter is 182.0 km and the maximum altitude is 1000.0 m. The site is characterized by high biodiversity and the abundance of endemic and local endemic plants and invertebrates appearing in the area. The high altitudes of the island, the geographical location of the nearby island of Ikaria and the plenty of biotopes are responsible for the high endemism. The main threats to the habitat derive from human activities and especially the fires that are caused by humans. Also, grazing is an additional threat to the habitat, as well as the reforestation of species that do not belong to the natural ecosystem of the area. A major threat to marine species, plants and animals, is uncontrolled fishing. Also, the increase in tourism is a potential threat to the coasts and, also, for the vegetation due to free camping and the uncontrolled waste with all that entails. Remarkable plants, mammals and amphibians/reptiles appear in the area, the list of which can be found in Filotis. The total area of the habitat GR4120006 is 4587.16 ha, the land area is 4587.16 ha, the total perimeter is 137.7 km and the maximum altitude is 488.0 m. Coasts are characterized by most typical Aegean cliffs, reefs and cavities. The vegetations which are dominated are phrygana and maquis, olive groves and cereal fields. Breeding seabirds and typical Mediterranean scrub species appear here. Remarkable birds appear in the area, the list of which can be found in Filotis.

2.4 Legislation framework for wind turbine sitting

A number of laws and regulations govern the legal framework for wind turbine sitting in Greece. According to them there are building and operating licenses. A building license must be obtained from the local authorities before a wind turbine can be set up. Additionally, the Regulatory Authority for Energy (RAE) must be contacted to obtain an operating license. This license can be used up to 25 years. Also, wind turbines with a capacity of more than 3 MW require an environmental impact assessment (EIA). The potential effects of the wind turbines on the community and surrounding environment must be considered in the EIA. In accordance with the guidelines established by the Hellenic Electricity Transmission System Operator (ADMIE), wind turbines must be connected to the grid. Additionally, developers must ensure that their wind turbines comply with ADMIE's grid code requirements. The local authorities' planning and zoning regulations must be followed by wind turbines. The proposed locations of wind turbines must be in areas designated for renewable energy projects, which developers must ensure. Furthermore, health and safety regulations must be

followed when designing and sitting wind turbines. In addition, developers must conduct risk assessments and implement appropriate safety measures. It is essential to keep in mind that the requirements might differ depending on the capacity and location of the proposed wind turbine.

According to (Official Gazette 2464, 2008) about the Renewable Energy Sources and their environmental impact, Greece is divided into four main categories as far as the installation of wind turbines is concerned, based on the wind potential that can be exploited and the spatial and the environmental characteristics of Greece.

a. The mainland, including, also, Euboea.

b. Attica, which is considered separately from the rest of the mainland, due to its metropolitan nature.

c. Crete and all the inhabited islands of the Ionian and the Aegean Sea. In this category belongs this case study of Fournoi Korseon as one of the islands of southern Aegean Sea.

d. Offshore marine space and uninhabited islets.

Areas of incompatibility and exclusion zones, where the installation of wind turbines is prohibited are summarizes in the following categories.

a. Declared World Heritage Sites, monuments of major importance, delimited archaeological sites.

b. Areas of absolute nature protection.

c. The Ramsar Wetlands (boundaries of Wetlands of international importance).

d. The cores of national farms and the delimited monuments of nature and aesthetic forests.

e. Priority Areas in the territory of Greece that belong to NATURE 2000 network in accordance with Directive 2006/613/EC of the European Parliament. It should be noted that according to (Official Gazette 85, 2010) the installation of RES stations is allowed as a means of climate protection, provided that the terms and conditions determined in the context of the environmental impact studies of the stations, ensure the preservation of the protected areas.

f. Within town plans and settlement boundaries before 1923 or below 2000 inhabitants.

g. Areas of organized development of productive activities in the tertiary sector.

h. Informally designed, within the context of off-plan construction, tourist and residential areas.

i. The bathing shores included in the bathing water quality monitoring program coordinated by the commanding ministry.

j. The parts of the quarry areas and the mining zones.

k. Other areas or zones that are currently subject to a special land use scheme, which does not permit the location of wind farms.

This chapter is based on the publication "M. Bertsiou, A.P. Theochari, E. Baltas, Multi-criteria analysis and GIS methods for wind turbine siting in a North Aegean island, Energy Science & Engineering, Volume 9, January 2021, Pages 4-18, https://doi:10.1002/ese3.809"

3.1   MCDM and GIS methodology for wind farm design

In this section a methodology for the evaluation of eligible sites for the installation of WT is presented and it is based to (M. M. Bertsiou et al., 2021). It is a combination of Multi-Criteria Decision-Making (MCDM) and Geographic Information Systems (GIS) for the design of a wind farm in the study area. It is based on geomorphological, technical and spatial criteria, according to the current legislation framework, as it has been presented in section 2.4. The concept behind this strategy is to offer a versatile decision-making structure that presents various scenarios, allowing the decision-maker, which could be the manufacturer, local community, or ministry, to select the order of importance of the criteria that suits their specific region and priorities. The goal is to provide a personalized approach that meets the unique needs of each stakeholder. Criteria weights are estimated by the implementation of the Analytic Hierarchy Process (AHP) to illustrate their impact on the final design. AHP is based on a framework by (Saaty, 1977). The criteria that are selected to be evaluated are presented below. Some of the criteria mentioned in the legislation framework have been not taken into account, like wetlands, Ramsar, monasteries, as all the above do not exist in the island.

- The first criterion is the wind potential, C_{wind}. For maximizing the produced energy from the wind turbines, the wind potential should have maximum possible value.
- The second criterion is the altitude in which the wind turbines are installed, C_{alt}. Wind potential tends to be more intense at higher altitudes, so it is considered that high altitudes are required to increase wind energy production.
- The third criterion is the distance from the settlements, C_{setl}. According to the framework legislation, there is an exclusion zone within 500 m of the settlements where the installation of the wind turbines is prohibited. On the other hand, the closer a wind turbine can be installed to the settlement that supplies electricity, there are less amounts of lost energy through the cables and thus more demands are covered.
- Next criterion is the distance from the road network, C_{road}. According to the framework legislation, the installation of the wind turbines is not prohibited up to 10,000 km from the road network. As Fournoi Korseon is a small island, this restriction is satisfied in advance. It

is preferable to install the wind turbines in places close to the road network in order to avoid the construction of accompanying projects, i.e., road excavation etc.

- The next criterion is the distance from mobile telephony antennas, C_{tele}. Like the criterion about the distance from the road network, it is preferable to install the wind turbines in places close to mobile telephony antennas in order to avoid the construction of accompanying works and instead take advantage of the accompanying projects constructed for the mobile telephony antennas. Also, according to the framework legislation, there must be an exclusion zone from telecommunications stations, designated in the context of the environmental impact assessments. In this study, this zone is assumed equal to 200 m.

- The sixth and last criterion is the distance from the archaeological sites, C_{arch}. According to the legislation is prohibited to install wind turbines within 500 meters from the archaeological sites and it is preferable the installation to be far away for the cultural heritage protection. Construction of technical projects are avoided near monuments, due to visibility restrictions from them.

The methodology followed factor standardization and constraint enforcement is depicted in Table 3-1.

Table 3-1 Criteria for wind turbine sitting

Criteria	Standardization	Constraints
C_{wind}	Equation 3-6	Wind speeds > 2 m/sec
C_{alt}	Equation 3-6	High altitudes meet high wind potential
C_{setl}	Equation 3-7	Distance from their boundaries > 500m
C_{road}	Equation 3-7	Distance < 10,000 m
C_{tele}	Equation 3-7	Distance > 200 m
C_{arch}	Equation 3-6	Distance > 500 m

The National Cadastre & Mapping Agency S.A. of Greece provides the digital elevation model for the study area, with a pixel size of 5x5 meters, a geometric accuracy RMSE of z ≤ 2.00 meters, and an absolute accuracy of approximately 3.92 meters for a 95% confidence level. Wind potential is measured by CRES (Centre for Renewable Energy Sources and Saving), using an extensive program of in situ measurements and mathematical models and the corresponding layer is obtained by Geodata (GEODATA. Open Data Accessible to Everyone). Settlements are obtained by CORINE Land Cover 2018 (CORINE Land Cover 2018. Land Cover Dataset for 2018), by choosing continuous urban construction and intermittent urban construction categories. In this database, the main settlement of Fournoi accessed, making necessary to manual digitize the remaining settlements using the basemap from ArcGIS Online. Road network' layer is obtained by Geofabrik OpenStreetMap Data(Geofabrik. OpenStreetMap Data, 2019). The layer of mobile telephony antennas is manually digitized according

to data from the Antenna Construction Information Portal (Antenna Construction Information Portal, 2019) of the National Committee of Telecommunications & Postals. The layer of archaeological sites is also manually digitized based on Official Gazettes (Official Gazette 15, 1991; Official Gazette 25, 1993; Official Gazette 1031, 1996) about the characterization of certain areas as archaeological sites. The digital elevation model and consequently the layer of the altitude, are raster data, while the layers of the remaining five criteria are vector layers with no spatial resolution. Both raster and vectors layers are linked to tabular databases storing attribute information about the locations delineated by the grid cells, the nodes and the polygons and they have a common Projected Coordinate System. The GIS-MCDM model for the wind turbine sitting is presented in Figure 3-1.
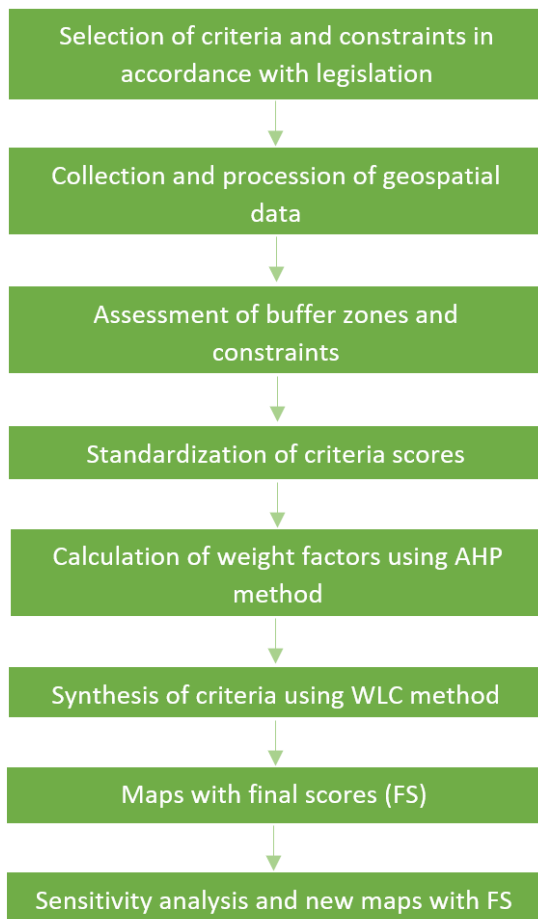
Figure 3-1 GIS-MCDM model for wind turbine sitting

First, the selection of the criteria and the corresponding constraints according to the legislation framework is made. All the data are collected and using ArcMap all the layers are entered, defining the buffer zones for each criterion, where the installation of wind turbines is forbidden. For the remaining area of the island, a final score, FS, is estimated based the weight of each criterion.

Four methods are used for the estimation of the weights:

- the ranking, which is the simplest method and the classification of the criteria is made by the decision makers according to their preferences. In this method,
- the rating, where there is a predetermined scale for the estimation of the weights,
- the trade-off method, where direct assessments between alternative pairs are made,
- the pairwise comparison, which involves creating a ratio matrix by comparing pairs of alternatives. This is the method used in this study, as its advantage is that it provides a structured approach for group discussions and helps to identify areas of agreement and disagreement when the weights of the criteria are set (Drobne & Lisec, 2009). The whole technique is developed by (Saaty, 1977) and it is known as AHP. The method used for the combination of the decision criteria and their weights into a final score is the Weighted Linear Combination (WLC) producing a suitability map.

The final score (FS), which depicts the suitability index is estimated by Equation 2-1 (Malczewski, 1999).

$$FS = \sum_{j=1}^{n} w_{ij} a_{ij}$$

Equation 3-1

w: weighting parameter

a: value parameter

i: the selected scenario

j: the selected criterion

n: total number of the criteria

When constraints must be applied, the FS is multiplied with the product of these constraints (Saaty, 1977) and the new FS is estimated by Equation 3-2.

$$FS = \sum_{j=1}^{n} w_{ij} a_{ij} \cdot \prod c_j$$

Equation 3-2

c_j: the score of Boolean constraints

The optimal sites for wind turbine sitting are determined by the final score. Each weight is calculated by AHP method. The AHP assumes that the final decision depends on available data as well as the experience and knowledge of the decision maker. The decision makers in this case are wind turbine designers who use a MCDM analysis to develop standardized procedures for solving problems like site selection. This involves combining different factors like geomorphological, technical, and spatial

criteria, and transforming geographic data into a resulting decision. The relationship between input and output maps is clearly defined through this procedure. The GIS organizes data into distinct thematic maps known as layers. This strategy aims to give decision-makers the ability to select the criteria hierarchy that best suits their particular area and priorities while also providing a flexible decision framework for a variety of scenarios. Both MCDM's ability to combine geographical data and the preferences of the decision maker into a one-dimensional value of alternative decisions and GIS's data acquisition, storage, retrieval, manipulation, and analysis capabilities are crucial to the methodology (Malczewski, 2004). The first step of the analysis is identifying the general problem and the individual objective. The current legislation framework in Geece guides the designers to the selection of the criteria. The various possible scenarios that represent the various purposes of decision-makers are investigated. As can be seen in Table 3-2, after collecting and analyzing the geospatial data, the determination of any imposed constraints and the standardization of the criteria scores is followed. After that, the results are produced by determining the criteria's composition and the appropriate weights. The idea behind AHP is that the data that is available and the knowledge and the experience of the decision maker are similarly important. This approach has been used in a number of studies (Ali et al., 2018; Al-Shabeeb et al., 2016; Rehman & Khan, 2017). The current approach is based on building a hierarchical model to solve the problem. This model allows for pairwise comparisons based on a fundamental comparison scale developed by (Saaty, 1977) as shown in Table 3-2. The comparisons are based on how important the two factors in determining suitability are in relation to one another. The ability to capture both subjective and objective aspects of a decision is the main feature of this method (Malczewski, 2006). The AHP method's output, are linearly combined to arrive at the final score and select the best locations for the wind farms.

Table 3-2 Scale and description of importance

Numerical value	Importance
1	Equal
3	Weak importance of one over another
5	Essential or strong importance
7	Demonstrated importance
9	Absolute importance
2, 4, 6, 8	Intermediate values between the two adjacent judgments

The last step of AHP method is the estimation of the consistency ratio (CR). The CR is estimated for each scenario by comparing the consistency index of the matrix CI and the consistency index of a random matrix RI. This relationship is described by Equation 3-3. It specifies the likelihood that the ratings in the matrix will be generated at random.

$$CR = \frac{CI}{RI}$$

The CR values should be up to 10% guaranteeing the acceptance of the hierarchy and the calculated weights, otherwise, the re-evaluation is needed. The analysis of the matrix should provide information about where the inconsistencies occur.

The CI is estimated by Equation 3-4.

$$CI = (\lambda_{max} - n)/(n - 1)$$

Where n indicates the total number of the criteria

The λ_{max} is estimated by Equation 3-5.

$$\lambda_{max} = \sum_{j=1}^{n} \frac{\sum_{j=1}^{n} w_{ij} a_{ij}}{w_{ij}}$$

The consistency index of a random matrix RI is provided in Table 3-3 and it depends on the number of the criteria.

In order to categorize the selected criteria in a common scale of comparison, they are standardized using GIS environment and specifically ArcMap program. The common scale of comparison is necessary in order the FS can be comparable. There are many standardization methods (Voogd, 1983), however the simplest is the linear transformation (Drobne & Lisec, 2009) and it uses the minimum and the maximum values of each criterion as a scaling measure. For standardized range, SR, between 0 and 1, the transformation is conducted by Equation 3-6, if the optimum value is the maximum value of the criterion and by Equation 3-7 if the optimum value is the minimum value of the criterion.

Table 3-3 Random matrix in AHP method

n	RI	n	RI
1	0	7	1.32
2	0	8	1.41
3	0.58	9	1.45
4	0.90	10	1.49
5	1.12	11	1.51
6	1.24	12	1.58

$$x_i = \frac{(FV_i - FV_{min})}{(FV_{max} - FV_{min})} \cdot SR$$

$$x_i = 1 - \frac{(FV_i - FV_{min})}{(FV_{max} - FV_{min})} \cdot SR$$

FV_{min}: minimum value of the factor

FV_{max}: maximum value of the factor

FV_i: value of each raster cell

Finally, by Equation 3-2and through Map Algebra Toolset of ArcMap, the final map is developed, presenting the FS for each site of the island. Sites with the higher values of FS are more suitable for wind farm sitting. Three scenarios are implemented for different hierarchy of the selected criteria and the hierarchy of each scenario is shown in Table 3-4 Scenarios and hierarchy of criteria for wind turbine sitting.

Table 3-4 Scenarios and hierarchy of criteria for wind turbine sitting

	Scenario 1	Scenario 2	Scenario 3
C1	C_{wind}	C_{wind}	C_{wind}
C2	C_{alt}	C_{alt}	C_{road}
C3	C_{setl}	C_{arch}	C_{setl}
C4	C_{road}	C_{road}	C_{tele}
C5	C_{tele}	C_{setl}	C_{alt}
C6	C_{arch}	C_{tele}	C_{arch}

The study considers three different scenarios, each focusing on different criteria that will result in the best outcome for the wind farm project, considering wind potential as a priority in all scenarios. The technical scenario (Scenario 1) prioritizes criteria that will result on the best performance of the wind turbine siting planning. These criteria are wind potential and criteria related to settlements and roads to ensure that power transmission via cables is not affected. The second is the cultural scenario (Scenario 2), which gives a higher weight to the distance from archaeological sites. Finally, in the economic scenario (Scenario 3), the focus is on the lowest cost of the project, which results in the avoidance of high altitudes, although the priority is still the high wind potential, and preference for locations near road networks or existing telecommunications stations, in order further projects, like road excavation to be avoided.

Three additional suitability maps are generated adding a constraint on the proximity to the main settlement of Fournoi Korseon, which has the most residents and the highest energy demands. The main settlement is inhabited by 1400 people compared to Aghios Minas with 3 inhabitants and Thimena with 151 inhabitants. Considering the criteria of the distance from the main settlement and

by installing the wind turbines near this area with increased energy needs, leads to the reduction of energy losses during the transmission through remote areas

To evaluate the sensitivity of the results, a sensitivity analysis is performed on the weights of the criteria, specifically C_{wind} and C_{arch} of S1. The analysis examines the effects of ±5% and ±10% changes in the proposed values for these criteria. Finally, new suitability maps and final scores are produced based on the updated weights.

3.2   Suitability maps

The results obtained from GIS and MCDM methods for analyzing wind turbine WT siting are heavily influenced by various factors. These factors include the selection of criteria for analysis, the data provided, the method used to standardize data, and the weighting and analytical method used to calculate the Final Suitability (FS) score. Table 3-1 Criteria for wind turbine sitting displays the criteria used in this analysis, which include wind potential, altitude, distance from settlements, road network, telecommunication sites, and archaeological sites. Wind potential is given priority in all scenarios since it is essential for maximizing energy generated by the turbines. The study implements three scenarios based on the hierarchy of criteria. Pairwise comparison is performed, and weights are determined for each criterion using the AHP method. The WLC method is used to combine the decision criteria and their weights into an FS score that is used to create a suitability map. The hierarchy of criteria for each scenario is displayed in Table 3-4 Scenarios and hierarchy of criteria for wind turbine sitting. To ensure the same basis of comparison, five classes/zones are created based on FS scores, which have values between zero and one. The first class (Zone A) is the zero zone and corresponds to areas where turbines are not permitted to be installed and is represented in grey color. This zone covers 27.9% of the island's total area and remains the same for each scenario, as it shows the excluded areas of the island for the installation of wind turbines according to the current legislation. The remaining four classes (Zone B, C, D and E) are classified based on FS scores up to 0.25, 0.50, 0.75, and the maximum value that each FS can reach. These classes are displayed in the legend of each figure.

3.2.1   Technical scenario

Table 3-5 displays the results of the pairwise comparison for the first scenario, with corresponding weights and consistency ratio (CR) of 0.089, which is less than 0.1. This scenario is mainly focused on technical aspects, prioritizing wind potential in the study area. In contrast, the distance from archaeological sites is assigned the lowest weight.

Table 3-5 Weights and pairwise comparison for Scenario 1

Scenario 1							
	C_{wind}	C_{alt}	C_{setl}	C_{road}	C_{tele}	C_{arch}	Weights
C_{wind}	1	3	5	5	9	9	0.444
C_{alt}	1/3	1	3	3	7	7	0.235
C_{setl}	1/5	1/3	1	3	5	5	0.144
C_{road}	1/5	1/3	1/3	1	5	5	0.106
C_{tele}	1/9	1/7	1/5	1/5	1	3	0.043
C_{arch}	1/9	1/7	1/5	1/5	1/3	1	0.028

The suitability site map for S1 is illustrated in Figure 3-2, where the total area of the island is divided into different zones based on the classification criteria. The grey zone A represents 27.9% of the island's total area, while the other zones - B, C, D, and E - show areas that are suitable for wind turbine installation according to the classification criteria. Zone C is the largest zone and covers about 41% of the island, followed by zone D with a percentage of 26.9%. The best zone for installation is zone E, which covers 1.7% of the island's area and has a maximum FS value of approximately 0.91.
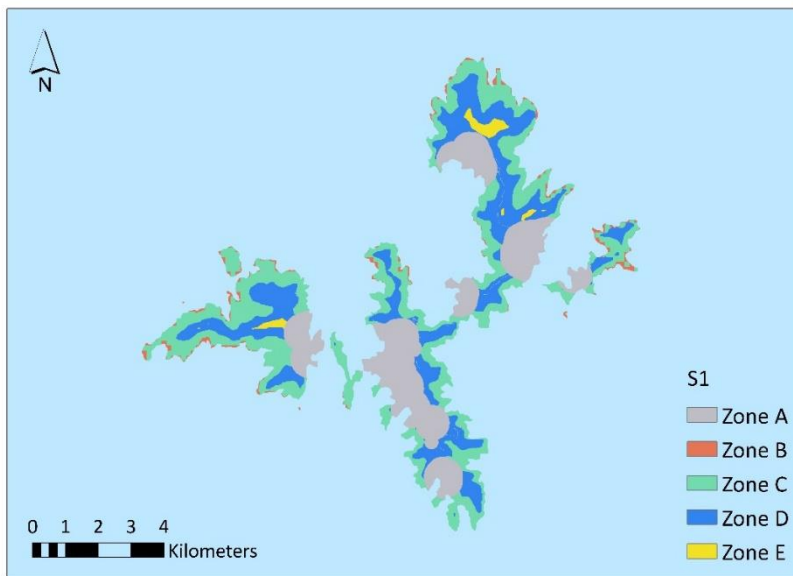
Figure 3-2 Suitability map for Scenario 1

3.2.2 Cultural scenario

The weights and the pairwise comparison for the second scenario are displayed in Table 3-6. The corresponding CR is estimated about 0.066. This cultural-oriented scenario prioritizes the distance from archaeological sites and attributes greater significance to it, besides the wind potential, which is always a priority in all cases examined. In contrast, the distance from telecommunication sites has the least weight in the decision-making process.

Table 3-6 Weights and pairwise comparison for Scenario 2

Scenario 2							
	C_{wind}	C_{alt}	C_{setl}	C_{road}	C_{tele}	C_{arch}	Weights
C_{wind}	1	3	9	5	9	3	0.410
C_{alt}	1/3	1	7	5	9	3	0.274
C_{setl}	1/9	1/7	1	1/3	3	1/5	0.043
C_{road}	1/5	1/5	3	1	5	1/3	0.086
C_{tele}	1/9	1/9	1/3	1/5	1	1/7	0.025
C_{arch}	1/3	1/3	5	3	7	1	0.162

The suitability site map for the second scenario is presented in Figure 3-3, which shows that zone B corresponds to 7.9% of the island area, while zone C covers 51.4% of the island. Zone D corresponds to 12.5% of the total island area, and zone E has the lowest coverage of only 0.3%, which is the most favorable class for installation. The maximum value of FS for this scenario is about 0.84, which is lower than the corresponding value of the first scenario, indicating that cultural restrictions have a negative impact on the FS for this island.
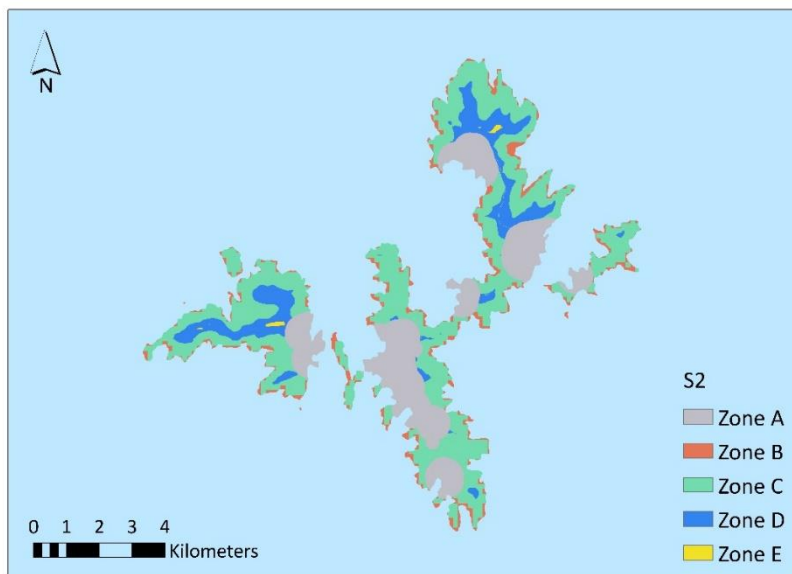
Figure 3-3 Suitability map for Scenario 2

3.2.3   Economic scenario

The weights for the third scenario, based on pairwise comparison, are given in Table 3-7, and the CR is less than 0.1 and equal to 0.081. This scenario is more focused on economics and aims to minimize the project's cost. Wind potential is still the priority; however, high-altitude areas are avoided, focusing on the reduction of the initial cost of the installation. Additionally, to avoid additional infrastructure project that may be needed when installing a wind farm, such as road excavation, the preferred locations are those that are close to existing telecommunications stations or the road network. The factor with the lowest weight is the distance from the archaeological sites.

Table 3-7 Weights and pairwise comparison for Scenario 3

Scenario 3							
	C_{wind}	C_{alt}	C_{setl}	C_{road}	C_{tele}	C_{arch}	Weights
C_{wind}	1	7	5	3	7	9	0.442
C_{alt}	1/7	1	1/5	1/7	1/3	3	0.046
C_{setl}	1/5	5	1	1/3	3	7	0.146
C_{road}	1/3	7	3	1	5	9	0.260
C_{tele}	1/7	3	1/3	1/5	1	5	0.081
C_{arch}	1/9	1/3	1/7	1/9	1/5	1	0.025
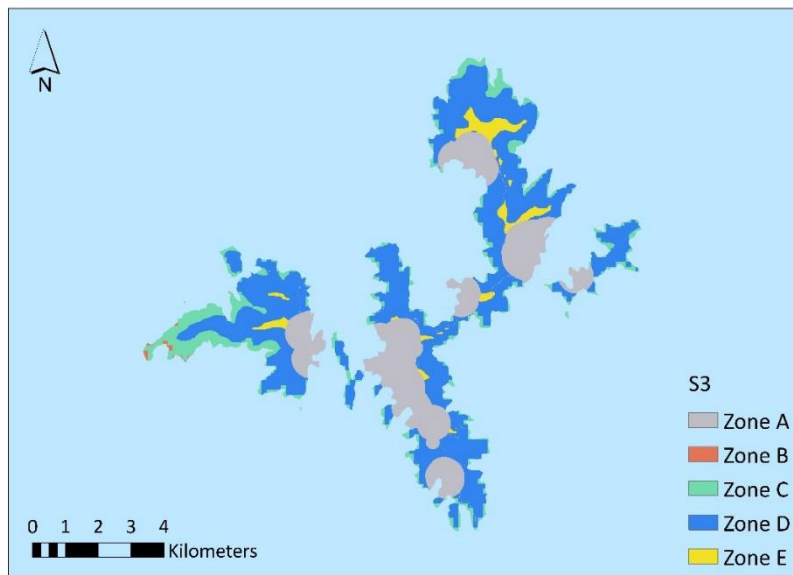
Figure 3-4 Suitability map for Scenario 3

The suitability site map of this scenario is shown in Figure 3-4. Zone B is covering only 0.2%, zone C is covering 13.8%, zone D is covering 54.1%, and zone E is covering 4% of the total island area. The highest value of FS is 0.93, which is higher than the corresponding values of the first and the second

scenarios. S3 has the highest percentage of zone D compared to S1 and S2, which have their highest values in zone C. Furthermore, this scenario has the highest percentage of zones D and E, which occupy nearly 60% of the island. This suggests that locations with high wind potential can be combined with lower altitudes, creating even more possibilities for installation in the last zone, E.

3.2.4   Proximity to the main settlement

The study also includes three additional suitability maps, considering the constraint of the proximity to the main settlement of Fournoi. The wind farm installation is preferred to be located near the area with the most residents and the highest energy requirements. By limiting the distance from the main settlement, energy losses due to transmission from remote areas are reduced. In this scenario, the percentage of Zone A remains the same as in the previously examined scenarios and covers 27.9% of the total island area. However, the additional suitability maps have only three zones, with zone B having FS values of up to 0.25, zone C up to 0.5, and zone D up to the highest possible FS values that can be reached.

The suitability maps for S1, S2, and S3 are shown in Figure 3-5 (a), (b), (c), respectively. Zone A is shown in grey, covering 27.9% of the total island area, which is the same with S1, S2 and S3 scenarios. However, in these three additional scenarios, only four zones are depicted as the FS value does not exceed 0.744, which is lower than the corresponding value for the initial scenarios, where FS is up to 0.929. This happens due to the introduction of an additional constraint, resulting in lower FS values. For the first scenario, over 69% of the island area is divided between zones B and C, while for S2 and S3, the corresponding percentages are 71% and 61%, respectively. Zone D accounts for 1.81% in the first scenario, 0.19% for the second, and 10.48% the third.
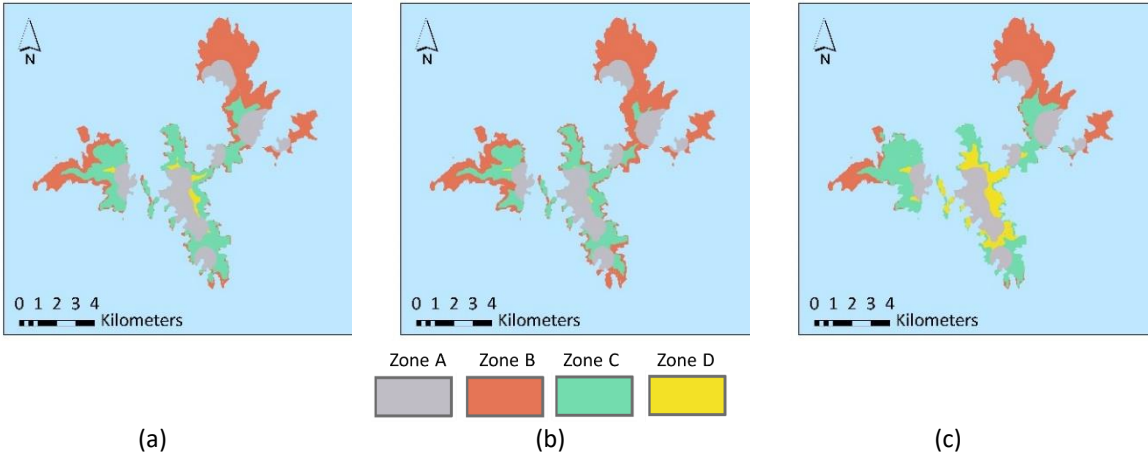
Figure 3-5 Suitability map concerning the proximity to the main settlement (a) Scenario 1, (b) Scenario 2 and (c) Scenario 3

3.2.5 Sensitivity analysis for wind turbine sitting

In this research work, the factors C_{wind} and C_{arch} for the first scenario are selected to conduct a sensitivity analysis. The former is considered the most significant criterion for the installation of the wind farms, while the latter has the least weight. The sensitivity analysis aims to assess the impact of a change in these two criteria, the most and the least important on the results. Figure 3-6 (a), (b), (c) and (d) represents the suitability maps of the first scenario, by changing C_{wind} by -10%, -5%, +5% and +10% respectively. Zone D varies from 28.48% for a 10% reduction of the weight of wind potential to 25.41% for a 10% increase, while the initial area is 26.87%. Similarly, Zone E varies from 1.63% for a 10% reduction of the weight of wind potential to 1.75% for a 10% increase, while the initial area is 1.68%. It is evident that increasing the weight of C_{wind}, may lead to a decrease in the number of positions in Zone D and a corresponding increase in Zone E. This is to be expected because locations with higher wind potential are more suitable for wind turbine sitting. For each change in C_{wind}, the maximum value of FS is between 0.90 and 0.92.

(a) (b) (c) (d)
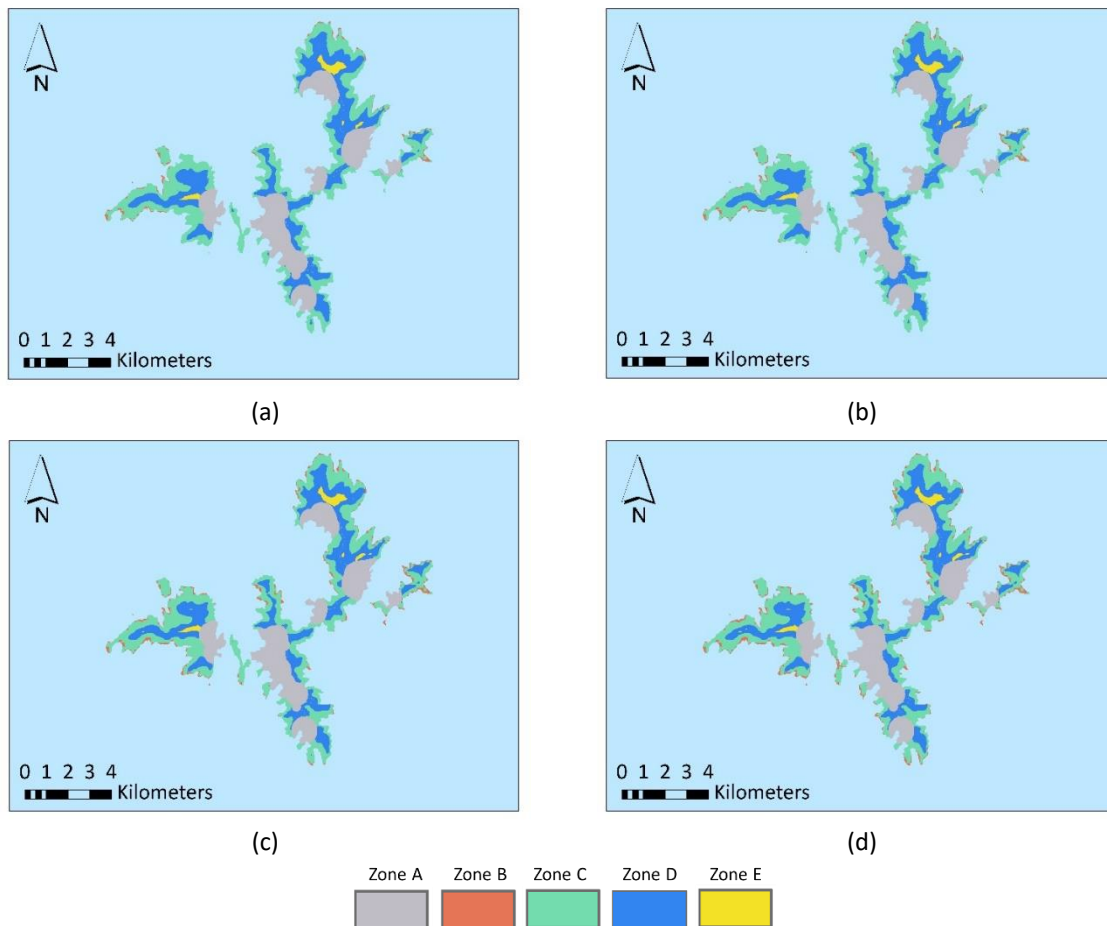
Figure 3-6 Suitability map of Scenario 1 based on sensitivity analysis of C_{wind} (a) -10%, (b) -5%, (c) +5%, (d) +10%

The suitability maps of the first scenario for changing C_{arch} by -10%, -5%, +5%, and +10% are depicted in Figure 3-7 (a), (b), (c), and (d), respectively. Zone D ranges from 27.09% for a 10% decrease of the C_{arch} weight to 26.64% for a 10% increase, with the initial area being 26.87%. Similarly, Zone E ranges from 1.72% for a 10% reduction of the C_{arch} weight to 1.64% for a 10% increase, with the initial area being 1.68%. The maximum FS value is about 0.91 for all changes in C_{arch}. Because the island's monuments are dispersed throughout the region, giving more importance to the distance from them leads to a decrease in the optimal locations. As a result, it is evident that increasing the weight of C_{arch} reduces the optimal locations in both Zone D and E.

(a)

(b)

(c)

(d)

| Zone A | Zone B | Zone C | Zone D | Zone E |
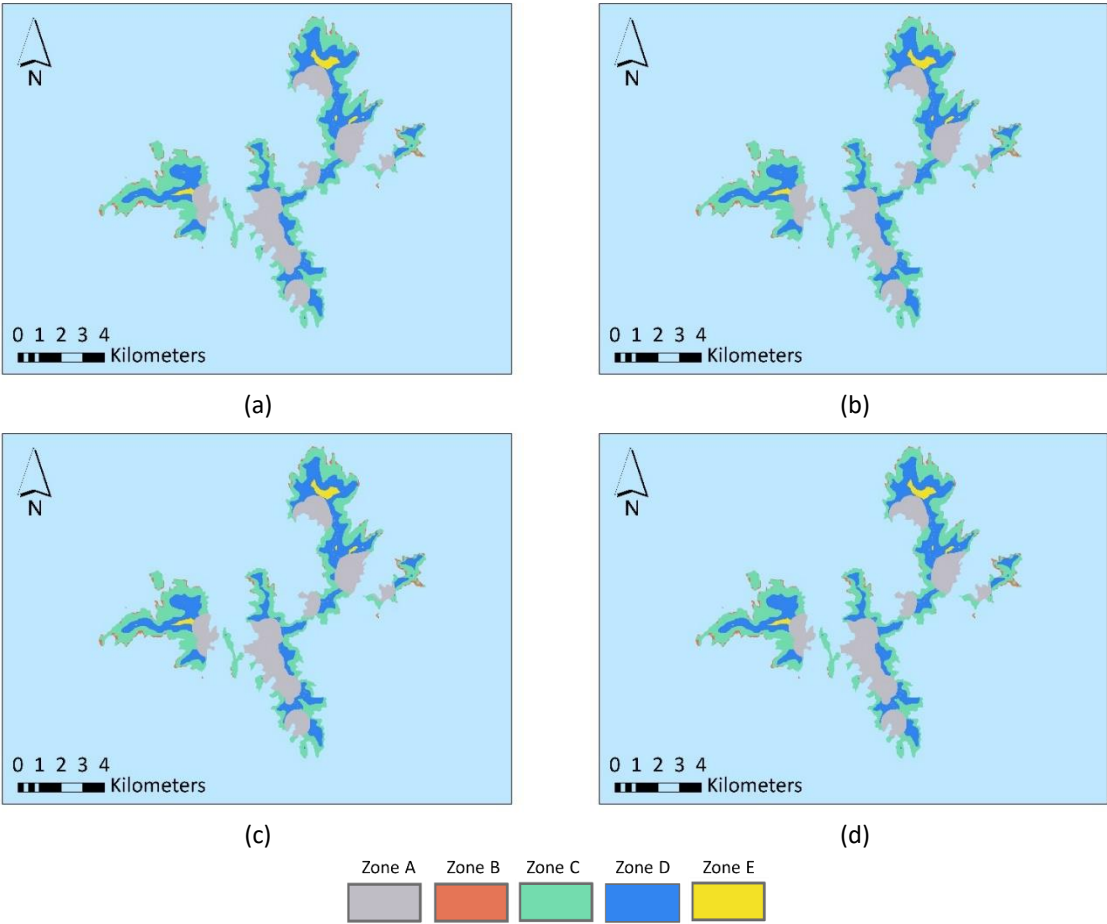
Figure 3-7 Suitability map of Scenario 1 based on sensitivity analysis of C_{arch} (a) -10%, (b) -5%, (c) +5%, (d) +10%

4 Energy Management Strategies and Economic and Environmental Analysis

4.1 Modelling of resource component

In this study, evaluation and comparison of the results of different scenarios of HRES coupling with different RES and different storage technologies are presented. In the different scenarios of HRESs one or more RES are coupled while, depending on the examined scenario, single or hybrid storage is integrated for the excess energy. Below the different RES and storage technologies that are used in the different scenarios, are presented.

4.1.1 Wind turbine (WT)

The estimation of the produced energy from a wind turbine is based on its power curve, given by the manufacturer. The power curve shows the correlation between the power output of the WT and the wind speed at hub height, considering the power coefficient. Every WT has four parts of operation (M. M. Bertsiou & Baltas, 2022a)according to Equation 4-1.

$$\begin{cases} \qquad\qquad \text{if } u(t) < u_{cut-in} \text{ then } P_{WT}(t) = 0 \\ \text{if } u_{cut-in} < u(t) < u_{rated} \ \text{ then } P_{WT}(t) = \text{according to the wind speed and the power curve} \\ \qquad \text{if } u_{rated} \leq u(t) < u_{cut-out} \text{ then } P_{WT}(t) = P_{WT}^{max} \\ \qquad\qquad \text{if } u(t) \geq u_{cut-out}(t) \text{ then } P_{WT}(t) = 0 \end{cases} \qquad \text{Equation 4-1}$$

If $u(t) < u_{cut-in}$ the power output is equal to zero. u_{cut-in} (m/sec) indicates the wind speed at which the wind turbine starts to operate and produce power P_{WT} (kW), according to the wind speed and the power curve. Rated speed u_{rated} (m/sec) indicates the wind speed where the wind turbine starts to produce the maximum power P_{WT}^{max} (kW), until an upper limit of $u_{cut-out}$ (m/sec), up to which the wind turbine stops its operation for safety reasons, In order to protect against possible damage due to very high winds speeds.

Enercon E-44's 900 Kw power curve is employed in this study. Figure 4-1 shows the power curve as well as a description of the various operating parts. The manufacturer provides the power coefficient for this model, which ranges from 0.00 to 0.50 depending on the wind speed at the hub height (ENERCON Product Overview, 2022). The nominal power P P_{WT}^{max} of the wind turbine and the wind speed u determine its output, P_{WT}. For this model u_{cut-in} is equal to 2 m/sec, u_{rated} is equal to 17 m/sec and $u_{cut-out}$ is equal to 25 m/sec. For $25 \leq u < 2$ the power output is equal to zero. For $17 \leq u < 25$ the power output has its maximum value equal to 900 kW and for $2 < u < 17$ the power output is calculated according to the power curve. Equation 4-2 provides the 5th degree

polynomial trendline with an R-squared value greater than 0.99 that was derived by the power curve for estimating power production (y) based on wind speed (x).

$$y = 0.0188x^5 - 0.9387x^4 + 16.679x^3 - 124.97x^2 + 436.34x - 563.22$$
<div align="right">Equation 4-2</div>
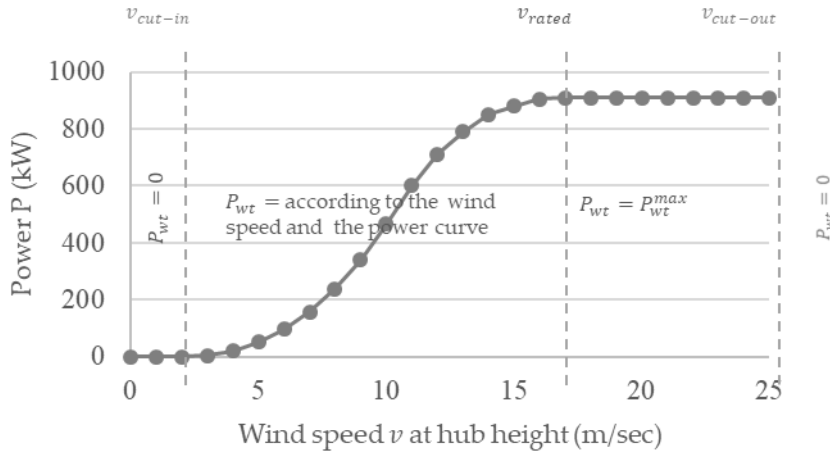
Figure 4-1 The power curve of Enercon E-900 wind turbine.

The data for the operation of the WTs used in this study are shown in Table 4-1.

Table 4-1 Data for WT operation

Parameter	Value
Cut-in speed, u_{cut-in} [m/s]	3
Rated speed, u_{rated} [m/s]	17
Cut-out speed, $u_{cut-out}$ [m/s]	25
Hub height [m]	50

Data of wind speed, v_s, are obtained at the altitude at which the weather station is installed, h_s. To obtain the wind speed, v_{wt}, at the hub height of the wind turbine, h_{wt}, Equation 4-3 is used (Van Sark et al., 2019), where h_{ref} is the roughness length parameter and it depends on the ground surface of the installed wind turbines.

$$v_{wt} = v_s \cdot \left[\frac{ln\left(\frac{h_{wt}}{h_{ref}}\right)}{ln\left(\frac{h_s}{h_{ref}}\right)} \right]$$
<div align="right">Equation 4-3</div>

According to (M. M. Bertsiou et al., 2021), the placement of wind turbines is designed to obtain advantage of high wind potential and to take into account their proximity to Fournoi's main

settlement in order to minimize power loss through the transmission cables. In Chapter 3, the approach followed and results for WT siting are explained in depth.

4.1.2 Photovoltaic module (PV)

PVs compared to other RES are superior due to their ability for direct electricity production, their silent mode operation and the fact that they can gradually implemented to an RES system. Also, they produce zero CO_2 emissions, they require minimum maintenance cost, they have a long lifetime and their installation is more aesthetic acceptable compared to other RES and especially to WTs.

A PV directly produces energy from solar irradiance. The output of a PV in direct current (DC) is estimated according to Equation 4-4 (Lin et al., 2020):

$$P_{PV}(t) = P_{STC} \cdot \frac{G_t(t)}{G_{STC}} \cdot PR_{PV} \cdot PR_{inv} \cdot PR_{grid} \cdot PR_T(t) \qquad \text{Equation 4-4}$$

P_{STC}: the peak capacity of the PV at Standard Test Conditions (STC) (W/m²)

$G_t(t)$: the solar irradiance on the tilted plane (W/m²)

PR_{PV}: efficiency of the PV (%)

PR_{inv}: efficiency of the inverter (%)

PR_{grid}: efficiency of the grid connection (%)

$PR_T(t)$: efficiency of the PV cell (%)

In the industry they use STC standards in order to test the efficiency of the PVs under common conditions of of solar energy exploitation. STC index refers to 1000 W/m² solar irradiance (G_{STC}), 25° C cell temperature ($T_{C,STC}$) and mass of the air equal to 1.5.

The efficiency of the PV cell $PR_T(t)$ is based on the difference between the cell temperature, $T_C(t)$ (°C), and the temperature at STS, $T_{C,STC}$ (°C). This efficiency is estimated for each time step according to Equation 4-5 (Mavromatakis et al., 2010):

$$PR_T(t) = 1 - \gamma \cdot \left[T_C(t) - T_{C,STC} \right] \qquad \text{Equation 4-5}$$

γ: the maximum thermal coefficient of power (/°C)

The cell temperature $T_C(t)$ is estimated by Equation 4-6 (Bouabdallah et al., 2015):

$$T_C(t) = T_{amb}(t) + (NOCT - T_{NOCT}) \cdot \frac{G_t(t)}{G_{NOCT}} \qquad \text{Equation 4-6}$$

$T_{amb}(t)$: the ambient temperature (°C)

$NOCT$: the Normal Operating Cell Temperature ($^{\circ}$C)

T_{NOCT}: the temperature in NOCT equal to 20 $^{\circ}$C

G_{NOCT}: the solar irradiance in NOCT equal to 800 W/m^2

Also, in NOCT the wind speed is considered equal to 1 m/sec.

Table 4-2 shows the data used in this study for the PV operation. It is assumed that twin-shift tracking stents are coupled with the series-parallel connected PVs helping to the rotation of the PVs and ensuring the perpendicular incidence of the solar irradiance. By this way, the utilization of the maximum solar energy is achieved (Li & Qiu, 2016). The conversion of direct current, produced by the PV, to alternative current (AC) is performed through the connection with an inverter. The maximum output of the PVs is obtained when the load intersects the current voltage at the Maximum Power Point (MMP), according to the voltage current curve (I-V) of the PV. In real time operation the load mismatch and the variation of the solar irradiance and the temperature prevent this intersection (Cotfas & Cotfas, 2019). To surmount this and to consistently maximize the PVs' output in accordance with the temperature and the solar irradiation, it is assumed that PVs are connected to the inverter through the Maximum Power Point Tracking control (MPPT) (Karami et al., 2017). This means that the produced power output of the PVs is supposed to be at every time step equal to the maximum power (Notton et al., 2010).

Table 4-2 Data for PV operation

Parameter	Value
Nominal operating cell Temperature (NOCT) [$^{\circ}$C]	45
Solar irradiance (STC) [W/m^2]	1000
Cell temperature (STC) [$^{\circ}$C]	25
Thermal coefficient of power, γ [/$^{\circ}$C]	0.004
PV efficiency [%]	88.5
Inverter efficiency [%]	97
Grid connection efficiency [%]	99

4.1.3 Pumped hydro storage (PHS)

The pumped hydro storage system uses the surplus energy from the WTs and/or PVs for pumping seawater to a reservoir in a high altitude, through the pumping station. The volume of the pumped water, V_p (in m^3), is given by Equation 4-7 (Simão & Ramos, 2020).

$$V_p = \frac{E_{sur} \cdot PR_p}{\rho \cdot g \cdot H}$$

Equation 4-7

ρ: water density (kg/m^3)

g: gravity acceleration (m/sec²)

H: the net head (m)

PR_p: efficiency of the pump station (%)

E_{sur}: energy surplus (kWh)

When more energy is required than the produced from the WTs and/or the PVs, then the hydro turbine operates producing energy by releasing water from the upper reservoir to a reservoir at the height of the turbine. The produced hydro energy, E_{def} (in kWh), is estimated by Equation 4-8 (Simão & Ramos, 2020).

$$E_{def} = \rho \cdot g \cdot H \cdot V_h \cdot PR_t \qquad \text{Equation 4-8}$$

V_h: released water from the upper reservoir to the hydro turbine (m³)

PR_t: efficiency of the hydro turbine (%)

Restrictions to the upper and lower limit of the upper reservoir are applied according to Equation 4-9 and Equation 4-10. It is assumed that the lower limit cannot be less than 10% of the total capacity due to safety reasons.

$$RV_{PHS}^{min} \leq RV_{PHS} \leq RV_{PHS}^{max} \qquad \text{Equation 4-9}$$

$$RV_{PHS}^{min} = 0.1 \cdot RV_{PHS}^{max} \qquad \text{Equation 4-10}$$

RV_{PHS}^{min}: minimum storage capacity of the upper reservoir (m³)

RV_{PHS}^{max}: minimum storage capacity of the upper reservoir (m³)

RV_{PHS}: capacity of the upper reservoir according to the days of autonomy (m³)

The PHS system consists of an upper reservoir, a pumping station and a hydro turbine. The technical characteristics shown of the PHS operation in shown in Table 4-3.

Table 4-3 Data for PHS operation

Parameter	Value
Net head [m]	192
Days of autonomy	2
Pumping station efficiency [%]	78
Hydro turbine efficiency [%]	90

The hydroelectric plant works by pumping water from one reservoir at sea level to another at a higher height when the demand for electricity is low. Water from the upper reservoir is released when demand for electricity is higher, and as it flows toward the lower reservoir, where it is stored once more for future use, it generates electricity for the island's electricity grid through the hydroelectric

plant. The second reservoir's altitude and the water volume available have a direct relationship with the amount of energy produced. The second reservoir's altitude and the amount of water that is available, both affect how much energy is produced. The stored water volume in the higher reservoir from the previous time step is increased by the water volume that is stored there in the next time step. The benefit of this operation is the potential to store surplus energy and use it during high demand hours of the day or low wind and solar potential hours, even if more energy is needed to pump the water to the higher altitudes than is generated through the hydro turbine.

4.1.4 Desalination unit (DU)

A desalination unit is coupled in all scenarios for the desalination of seawater in order to cover domestic and irrigation demands. Also, the desalination unit is necessary in the scenarios where energy is stored through the production of hydrogen. In these cases, the generation of green hydrogen presupposes the electrolysis of pure desalinated water. Energy consumption for reverse osmosis (RO) desalination ranges between 3.7 and 8 kWh/m^3 (Al-Karaghouli & Kazmerski, 2013; Fornarelli et al., 2018; D. Xu et al., 2019) and in this study is assumed equal to 5.85 kWh/m^3.

4.1.5 Battery (BT)

The storage capacity of the battery, C_{bat} (in kWh) is estimated by Equation 4-11 (El-houari et al., 2021).

$$C_{bat} = \frac{P_L \cdot d_A}{PR_{bat} \cdot PR_{inv} \cdot DOD}$$

Equation 4-11

P_L: average daily consumption (kWh/day)

d_A: number of autonomy days

PR_{bat}: efficiency of the battery (%)

PR_{inv}: efficiency of the inverter (%)

DOD: depth of discharge of the battery (%)

The storage capacity of the battery, C_{Ah} (in Ah) is estimated by Equation 4-12

$$C_{Ah} = \frac{C_{bat} \cdot 1000}{V_{bat}}$$

Equation 4-12

V_{bat}: nominal voltage of the battery (V)

The technical characteristics of the battery used in this study are given in Table 4-4.

When there is surplus energy and the battery is charging, the state of charge (SOC) at each time step is estimated according to Equation 4-13.

$$SOC(t) = SOC(t-1) \cdot (1 - \sigma) + E_{sur} \cdot PR_{bat}$$

<div align="right">Equation 4-13</div>

$SOC(t)$: state of charge at time t (kWh)

$SOC(t-1)$: state of charge at time t-1 (kWh)

σ: self-discharge rate (%)

When there is energy deficit and the battery is discharging, the state of charge (SOC) at each time step is estimated according to Equation 4-14.

$$SOC(t) = SOC(t-1) \cdot (1 - \sigma) - E_{def} \cdot PR_{bat}$$

<div align="right">Equation 4-14</div>

Restrictions to the minimum and the maximum state of charge of the battery are applied according to Equation 4-15 and Equation 4-16

$$SOC_{min} \leq C_{bat} \leq SOC_{max}$$

<div align="right">Equation 4-15</div>

$$SOC_{min} = (1 - DOD) \cdot C_{bat}$$

<div align="right">Equation 4-16</div>

SOC_{min}: minimum state of charge of the battery (kWh)

SOC_{max}: maximum state of charge of the battery (kWh)

The technical characteristics of the battery in this study are given in Table 4-4.

Table 4-4 Data for battery storage

Parameter	Value
Battery efficiency [%]	82
Inverter efficiency [%]	82
Days of autonomy	2
Depth of discharge, DOD [%]	80
Self-discharge, σ [%]	2

4.1.6   Hydrogen exploitation (FC)

Hydrogen can be produced by the electrolyzer, which converts the excess energy into hydrogen. This is performed through the electrolysis of water. The production of 1 kg of hydrogen requires 9 kg of desalinated water (Hausmann et al., 2021; Rievaj et al., 2019). In standard conditions the heating value of the hydrogen is equal to 3.4 kWh/m^3, its density is 0.09 kg/m^3 and finally, 1 kg of hydrogen produces 37.8 kWh/gr (Abdelshafy et al., 2018). When there is surplus energy, it is used for hydrogen production by the electrolyzer, H_2 (in kg), which is estimated by Equation 4-17 (Abdelshafy et al., 2018)

$$H_2 = E_{sur} \cdot PR_{el} \; / \; 37.8$$

<div align="right">Equation 4-17</div>

PR_{el}: efficiency of the electrolyzer

When there is energy deficit the fuel cell converts the stored hydrogen into energy. 1 kg of hydrogen can produce energy, E_{FC} (in kWh), estimated by Equation 4-18 (Abdelshafy et al., 2018).

$$E_{FC} = H_2 \cdot PR_{FC} \cdot 37.8$$

Equation 4-18

PR_{FC}: efficiency of the fuel cell

Fuel cells are categorized based on the electrolyte they use and the temperature at which they operate (Martínez-Huerta & Lázaro, 2017). Due to its maturity, quick reaction to varying loads, and short start-up time, the proton exchange membrane fuel cell (PEMFC) is anticipated to be the fuel cell type chosen for this study. (Dawood et al., 2020; Robinius et al., 2018).

Restrictions to the upper and lower limit of the hydrogen tank are applied according to Equation 4-19 and Equation 4-20.

$$TANK_{H_2}^{min} \leq TANK_{H_2} \leq TANK_{H_2}^{max}$$

Equation 4-19

$$TANK_{H_2}^{min} = 0.1 \cdot TANK_{H_2}^{max}$$

Equation 4-20

$TANK_{H_2}^{min}$: minimum storage capacity of the hydrogen tank (kg)

$TANK_{H_2}^{max}$: maximum storage capacity of the hydrogen tank (kg)

$TANK_{H_2}$: total capacity of the hydrogen tank (kg)

The technical characteristics of the electrolyzer and the fuel cell used in this study are given in Table 4-5.

Table 4-5 Data for hydrogen production

Parameter	Value
Electrolyzer efficiency [%]	90
Fuel cell efficiency [%]	50

4.2 Configurations and Energy Management Strategies

In this section, the configurations that will be examined, based on the combination of the RES and the storage methods that have been analyzed in the previous section, are presented. A storage system is coupled in all configurations, as the stochastic nature of the RES (wind and solar) potential prevents the simultaneous satisfaction of demand in correspondence with renewable energy production. Based on the configuration examined, a PHS, a BT and an HT are used for the storage of excess energy. Also, two configurations with hybrid storage technologies are evaluated, a hybrid pumped hydrogen storage system (HPHS), consisting of a PHS and a hydrogen storage system, and a

hybrid pumped battery storage system (HPBS), consisting of a PHS and a battery storage system. Also, in almost all the configurations a desalination unit is coupled for the satisfaction of drinking and irrigation water supply.

According to (Kaldellis et al., 2001), the nominal capacity of the installed WTs is selected based on the meteorological data as well as the island's demand for energy and desalinated water. The sizing of the storage systems (upper reservoir, batteries, hydrogen tank) is based on the number of autonomy days for the HRES. This number is the days that the storage system of the HRES provides the required energy for the demands of the island, even if the wind and solar potential are low and no energy can be produced by the WTs and the PVs. Energy storage systems typically consider two days of autonomy (Bhandari et al., 2015). Also, it is assumed that at the start of the simulation, the upper reservoir is half full and the batteries and the hydrogen tank are up to their minimum level. By using the extra energy generated by WTs and PVs, seawater is pumped into the higher reservoir. It must be noted that this reservoir does not supply the island's desalination plant. The latter is supplied with seawater and adds fresh water to the desalination reservoir. An energy surplus is required for the pumps to operate, and if there isn't enough to start the pumping station, no water is stored in the upper reservoir. The same applies to determining the hydro turbine's rated power. It must be ensured that in the case of low wind potential, it can handle the maximum load. The pumping system's estimated nominal power is calculated using (Kaldellis et al., 2001). A reaction turbine, specifically a Francis model, is the turbine that is proposed to be employed in this study (Ferreira & Camacho, 2017). For the sizing of the fuel cell and the electrolyzer, it is considered that the first should be able to handle any electrical load that cannot be met by other RES or storage systems (Ceran et al., 2021), depending on the configuration under examination, and the second can convert any surplus energy into hydrogen at each time step. Load demand that is not covered by the WTs, the PVs, the hydro turbine, the batteries, or the fuel cell, depending on the examined configuration, is covered by the grid, meaning the startup of the local power station. To control the response of the HRES and its reliability in covering the required demand for electricity and drinking and irrigation water supply, the simulations are performed with hourly data inputs. In Table 4-6, the configurations that are examined in this study are presented.

Table 4-6 Configurations of RES systems examined

Configuration	1	2	3	4	5	6	7
WT	✓	✓	✓	✓	✓	✓	✓
PV			✓	✓	✓	✓	✓
DU		✓	✓	✓	✓	✓	✓
PHS	✓	✓	✓			✓	✓
BT				✓		✓	
FC					✓		✓

In the first configuration (WT/PHS) the HRES consists of a wind park and a PHS storage system. The excess energy from the WTs is used only for pumping and storing water in order to exploit hydropower to meet electricity needs. It is the only configuration where there is no desalination unit and no drinking and irrigation water demand is fulfilled. The second configuration (WT/DU/PHS) has the same RES and storage unit; however, a desalination unit is coupled in this HRES providing fresh water for drinking and irrigation demand. In the third configuration (WT/PV/DU/PHS), PVs are added, compared to the previous configuration, in order to examine the reliability of the system if the use of RES is not limited to the utilization of wind potential but also solar potential at the same time. In Configuration 4 (WT/PV/DU/BT). the storage technology the storage method involves the use of batteries, instead of the PHS system of Configuration 3. In the fifth configuration (WT/PV/DU/FC), the battery has been replaced with a hydrogen production and utilization system. In configuration 6 (WT/PV/DU/HPBS) a hybrid pumped battery storage system, consisting of a PHS and a battery storage system is used as a storage technology and in the seventh configuration (WT/PV/DU/HPHS) the hybrid storage system consists of a PHS and a hydrogen storage system. The detailed presentation of the seven configurations, as well as the energy management strategies of each one, are presented in the following sections. The three RES (wind, solar, and hydro) and the performance of various storage systems (PHS, battery, hydrogen) are the foundations for the proposed energy management strategies for single or hybrid storage, which compare the effectiveness of these energy storage technologies in meeting social needs like electricity and water.
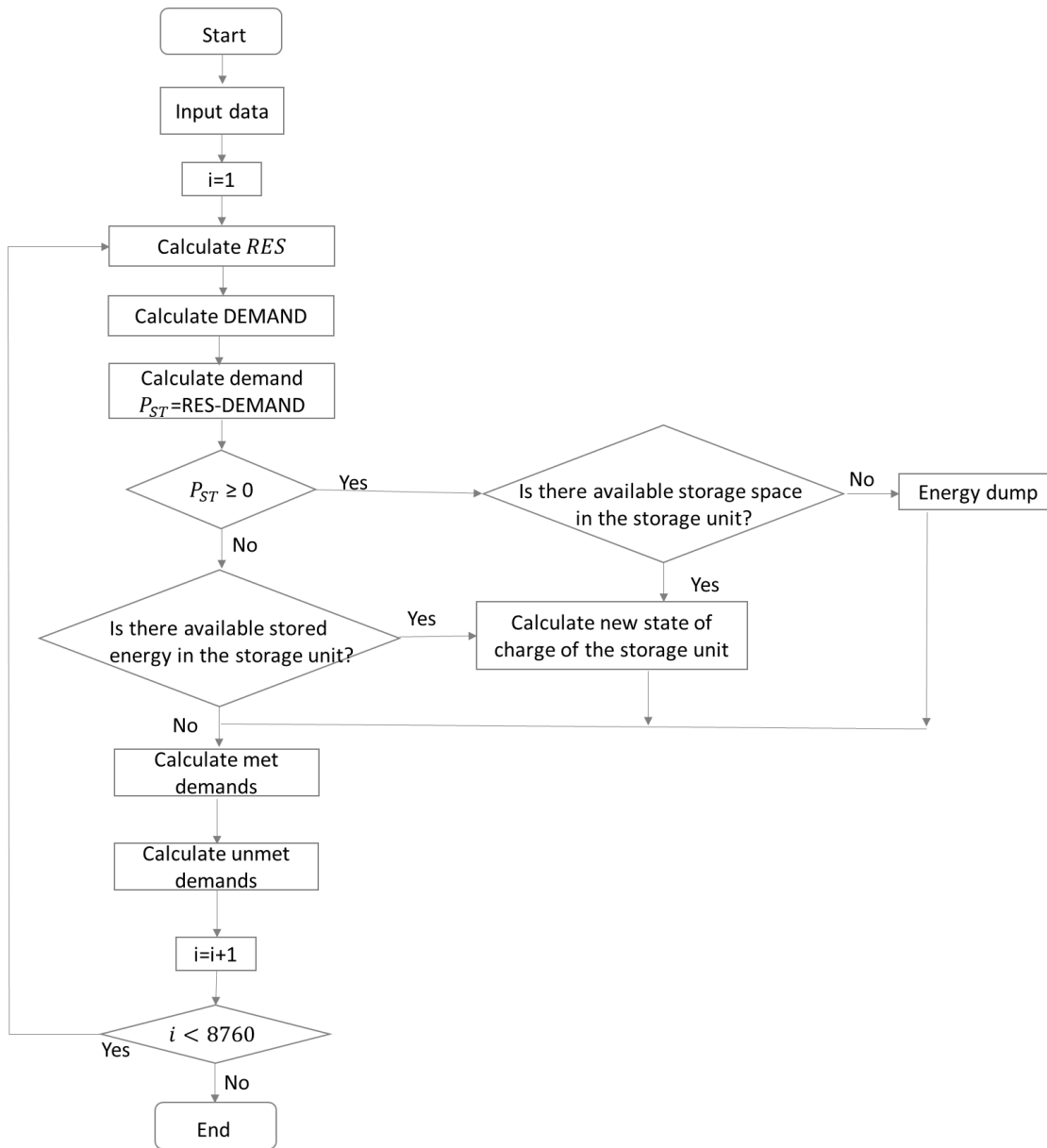
Figure 4-2 Basic energy management strategy for single storage HRES

The first five configurations of the HRESs are considered to have simple storage, i.e. a single storage unit for the excess energy. The storage strategy followed is shown in Figure 4-2. The step is hourly, to guarantee the highest possible reliability of the results and the procedure is performed for one year of data (i=8760). The input data are entered, meteorological data and the demand data of the island. The energy produced by the WTs and/or PVs is calculated according to the under-consideration configuration. In every configuration, priority is given to the domestic water, after to the irrigation water and at last to the energy for electricity demand. The renewable energy produced

is calculated (RES) for each step and each demand is checked if it can be fulfilled, according to the aforementioned priority. In the first configuration, where water demand is now included, all the produced RES energy covers exclusively the electrical needs. Once the check for each of the three demands is made, it is then checked if there is excess energy P_{ST}. If there is excess energy, then it is checked if there is available storage space in the storage unit. If not, then unfortunately the excess energy is rejected, if yes then the new state of charge of the storage unit is calculated, always checking that the maximum state of charge level of the storage unit is not exceeded and the met and unmet demands for one hour are estimated, before approaching the next step.

In case there is no excess energy, P_{ST}, but there is still demand that has not been fulfilled, it is checked if there is available stored energy in the storage unit. If there is available stored energy then the new state of charge is calculated and at the end, the met and unmet demands for one hour are estimated again.

In the last two configurations, there is hybrid storage, i.e. a combination of two different storage methods. The storage strategy followed is shown in Figure 4-3. The step is again hourly and the procedure is performed for one year of data (i=8760). Again, as in the simple storage method, the data is entered and the process is no different until the control of excess energy P_{ST}. After this step, the way of controlling and utilizing the excess energy differs.

As it is shown in the flowchart, if there is excess energy, it is checked if there is available storage space in the first storage unit. If yes, then the new state of charge of the first storage unit is calculated. If not or if there is still excess energy, it is checked if there is available storage space in the second storage unit. If yes, then the new state of charge of the second storage unit is calculated. If no, or if there is still excess energy after the charging of the second storage unit until its maximum state of charge level, then unfortunately the excess energy is rejected. In both storage units, it is always checked that the maximum state of charge level is not exceeded when they are in charging mode.
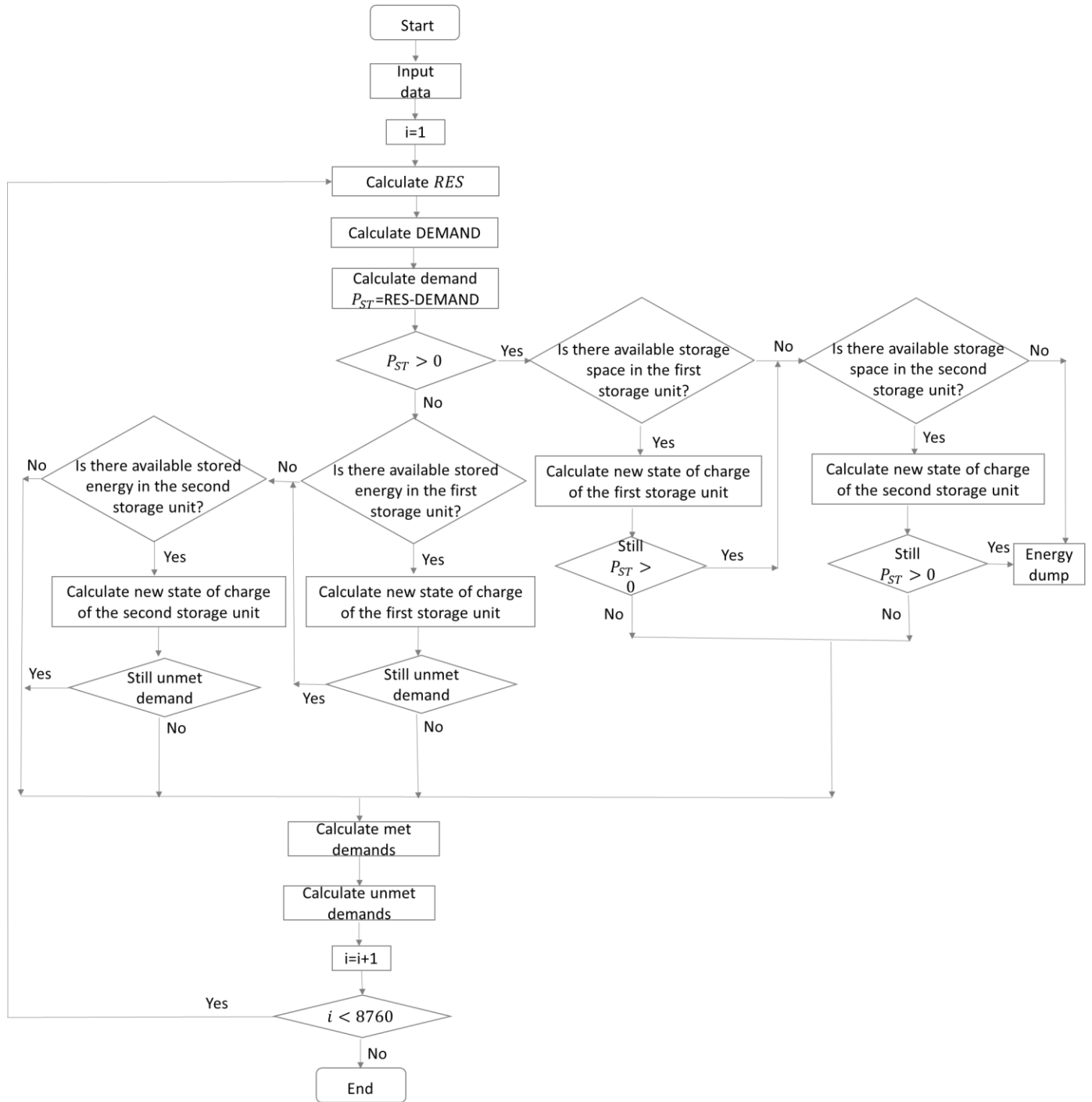
Figure 4-3 Basic energy management strategy for hybrid storage HRES

If there is no excess energy but there is still demand that has not been fulfilled, it is checked if there is available stored energy in the first storage unit. If there is available stored energy then the new state of charge is calculated. If no, or if there is still unmet demand, it is checked if there is available

stored energy in the second storage unit. If there is available stored energy then the new state of charge is calculated and, in any case, it is checked if there is still unmet demand and both met and unmet demand is estimated for each step.

4.2.1 WT/PHS

In the first configuration, the HRES combines wind energy and hydro energy from PHS. The schematic representation of the HRES and the installed capacity of all components appear in Figure 4-4 and Table 4-7 respectively. This configuration is tested to meet exclusively the electricity demand on the island and all the generated energy is used only for the electricity needs, without giving energy for the desalination of seawater to fulfill domestic or irrigation water.
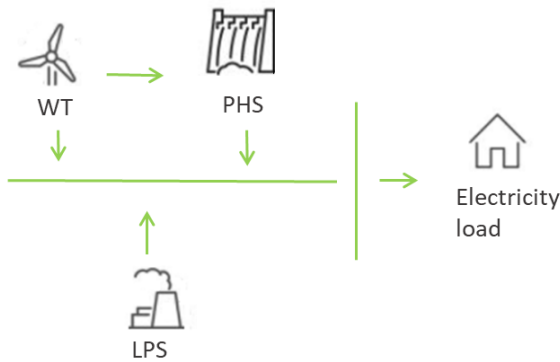
Figure 4-4 Schematic representation of WT/PHS

In this configuration, PHS is used as a storage system and is considered to be charging and discharging according to the procedure described below. The energy management for the estimation of the reliability of the system to cover the electrical demands of the island is presented in Figure 4-5. Energy from the wind turbines is given for electrical needs, while if there is excess energy, P_{ST}, it is used for pumping seawater and storing it in the upper reservoir if there is available storage space. If the upper reservoir is full there is an energy dump, otherwise, the reservoir is charging, according to Equation 4-7. The volume of water that could be stored in the upper reservoir, according to P_{ST}, depends on its capacity RV_{PHS}, and on the water that is stored in the previous time step ($t - 1$). If there is an energy deficit, then the stored water is converted to energy by the hydro turbine, and it is ready for use when the energy produced by the WTs is not sufficient to cover the electrical demands of the island. The reservoir is discharging, according to Equation 4-8. At any time, the upper reservoir is

subject to restrictions regarding the upper and lower limit, according to Equation 4-9 and Equation 4-10. When both wind and hydro energy cannot cover the demand, then LPS covers the deficit.

Table 4-7 Specification data of the installed components of WT/PHS

Component	Installed Capacity
WT [MW]	3.6
Upper reservoir [m^3]	61,343
Pumps [MW]	2.6
Hydro turbine [MW]	1.0
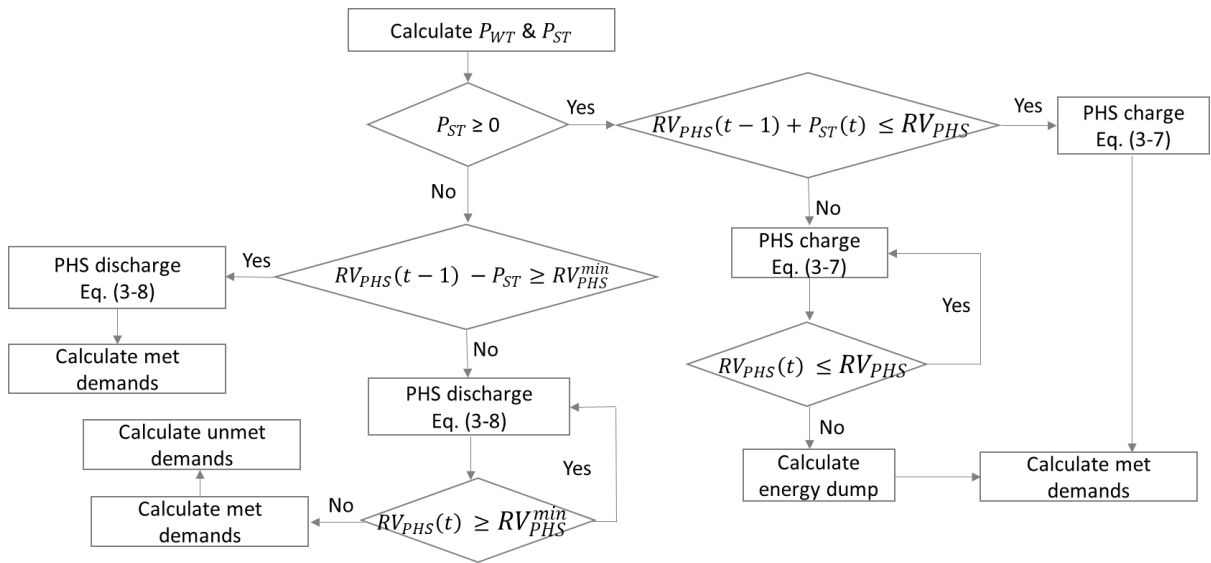
Figure 4-5 Energy management for WT/PHS

4.2.2   WT/DU/PHS

The second configuration differs from the first only in the addition of a desalination system in order to desalinate seawater to meet the domestic and irrigation water needs of the island. HRES combines wind energy from four wind turbines and hydro energy from PHS, which is the storage system. The schematic representation of the HRES and the installed capacity of all components appear in Figure 4-6 and Table 4-8 respectively. This configuration is tested to meet electricity and water demands on the island. The energy management strategy is the same as the energy management of configuration 1, however in this case P_{ST} is calculated concerning both electrical and water needs.
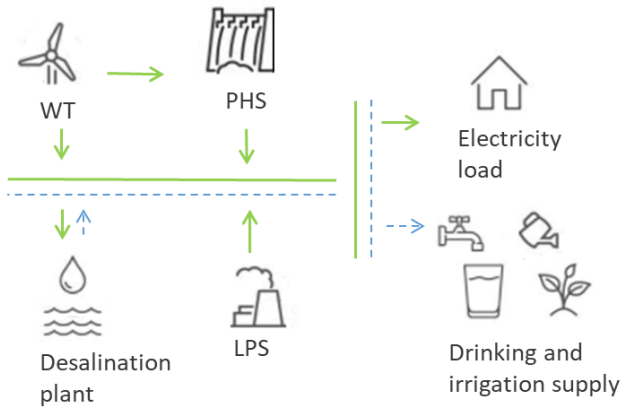
Figure 4-6 Schematic representation of WT/DU/PHS

Priority at each step is given to domestic water. It is determined if the wind energy generated is adequate to supply the energy requirements for desalinating the required volume of domestic water for the corresponding time step. The remaining energy related to the desalination of irrigation water is determined in a similar way, and finally the same procedure is applied for the electric load. In this configuration, also PHS is used as a storage system. Energy from the wind turbines is calculated and is given for domestic water, irrigation water and electrical needs, while, if there is extra energy left after satisfying the three demands, P_{ST}, it is used for pumping seawater and storing it in the upper reservoir if there is available storage space. If the upper reservoir is full there is an energy dump, otherwise, the reservoir is charging, according to Equation 4-7. The volume of water that could be stored in the upper reservoir, according to P_{ST}, depends on its capacity RV_{PHS}, and on the water that is stored in the previous time step ($t - 1$). If there is an energy deficit, then the stored water is converted to energy by the hydro turbine, and it is ready for use when the energy produced by the WTs is not sufficient to cover the water and electricity demands of the island. The reservoir is discharging, according to Equation 4-8. At any time, the upper reservoir is subject to restrictions regarding the upper and lower limit, according to Equation 4-9 and Equation 4-10. When both wind and hydro energy cannot cover the demand, then LPS covers the deficit.

Table 4-8 Specification data of the installed components of WT/DU/PHS

Component	Installed Capacity
WT [MW]	3.6
Upper reservoir [m³]	75,243
Pumps [kW]	2.6
Hydro turbine [MW]	1.2
Desalination unit (m³/day)	1,230

4.2.3 WT/PV/DU/PHS
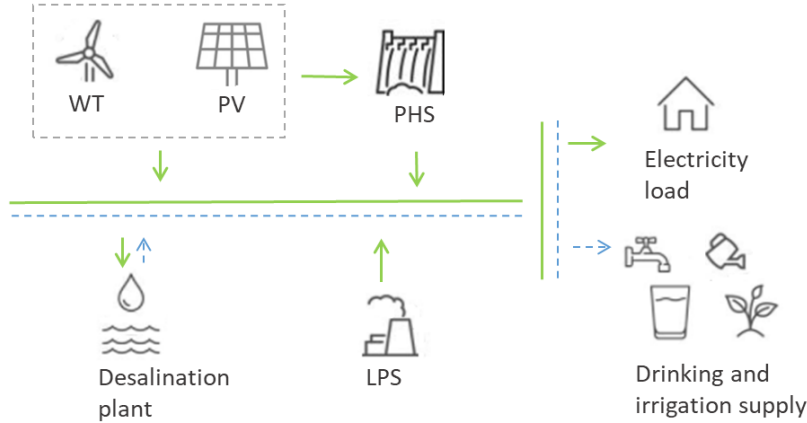
Figure 4-7 Schematic representation of WT/PV/DU/PHS

In this configuration, HRES combines wind energy from 1.8 MW of installed wind turbines and solar energy from solar panels 2.0 MW. HRES is coupled with a desalination unit for domestic and irrigation water. PHS is used as the storage system. The schematic representation of the HRES and the installed capacity of all components appear in Figure 4-7 and Table 4-9 respectively. This configuration is tested to meet electricity and water demands on the island. The energy management strategy is the same as the energy management of configuration 2, however in this case renewable energy is provided by both wind turbines and solar panels. The energy management for the estimation of the reliability of the system to cover the electrical demands of the island is presented in Figure 4-8. P_{ST} is calculated concerning both electrical and water needs.

Table 4-9 Specification data of the installed components of WT/PV/DU/PHS

Component	Installed Capacity
WT [MW]	1.8
PV [MW]	2.0
Upper reservoir [m^3]	75,243
Pumps [kW]	2.6
Hydro turbine [MW]	1.2
Desalination unit [m^3/day]	1,309
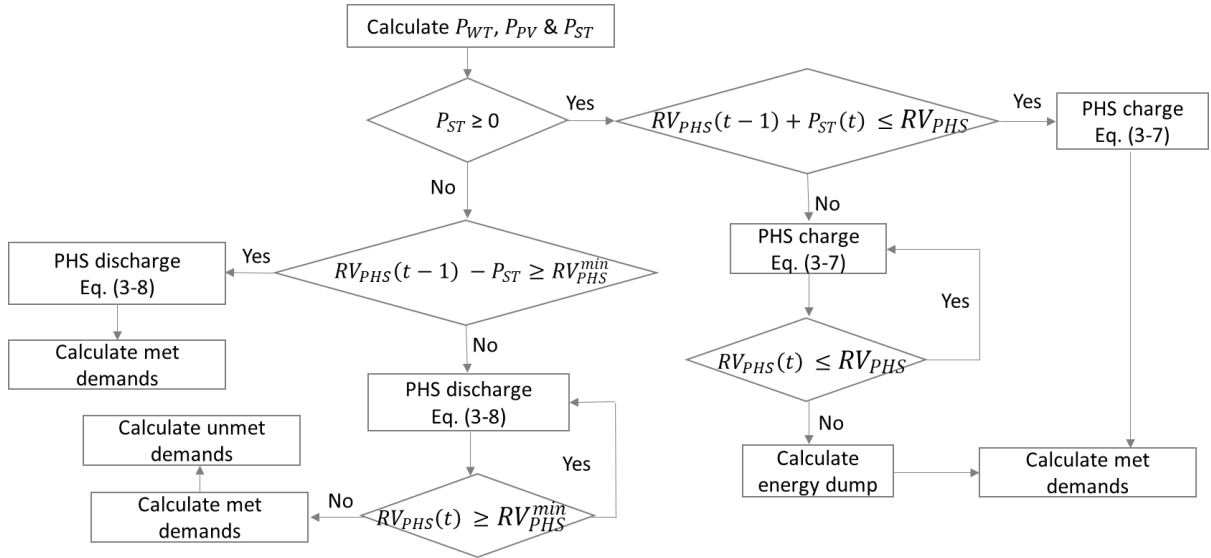
Figure 4-8 Energy management for WT/PV/DU/PHS

Priority at each step is given to domestic water. It is determined if the wind and solar energy generated is adequate to supply the energy requirements for desalinating the required volume of domestic water for the corresponding time step. The remaining energy related to the desalination of irrigation water is determined in a similar way, and finally the same procedure is applied for the electric load. If there is extra energy left after satisfying the three demands, P_{ST}, it is used for pumping seawater and storing it in the upper reservoir if there is available storage space. If the upper reservoir is full there is an energy dump, otherwise, the reservoir is charging, according to Equation 4-7. The volume of water that could be stored in the upper reservoir, according to P_{ST}, depends on its capacity RV_{PHS}, and on the water that is stored in the previous time step ($t-1$). If there is an energy deficit, then the stored water is converted to energy by the hydro turbine, and it is ready for use when the energy produced by the WTs and PVs is not sufficient to cover the water and electricity demands of the island. The reservoir is discharging, according to Equation 4-8. The upper reservoir is always limited by restrictions on the higher and lower limits, together with the pumping and releasing operations of the pumps and the hydro turbine, according to Equation 4-9 and Equation 4-10. When both wind and hydro energy cannot cover the demand, then LPS covers the deficit.

4.2.4 WT/PV/DU/BT

This configuration differs from the previous one only in the storage technology. Excess energy is stored in batteries. Renewable energy also is provided by WTs and PVs and there is also a desalination unit to cover water needs. Here, also, priority is given to domestic water, then to irrigation water and

then to the electrical load. The schematic representation of the HRES and the installed capacity of all components appear in Figure 4-9 and Table 4-10 respectively. The sizing of the batteries is also based on two days of autonomy and batteries are calculated equal to 59,420 kWh.
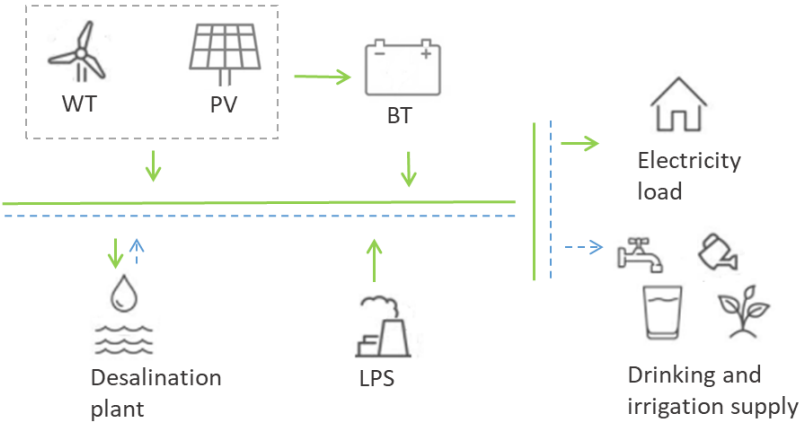
Figure 4-9 Schematic representation of WT/PV/DU/BT

The energy management of this configuration is presented in Figure 4-10. If P_{ST} energy is greater than zero , then the extra energy is stored in the batteries. It is checked the battery bank has the required capacity and then, it is charged. The new state of charge is calculated according to Equation 4-13. If there is an energy deficit (P_{ST}<0) and the battery bank has the required capacity, then the battery bank is discharged and the new state of charge is calculated according to Equation 4-14. At any time, the state of charge of the battery is subject to the constraints of Equation 4-15 and Equation 4-16, concerning SOC_{min} and SOC_{max}.

Table 4-10 Specification data of the installed components of WT/PV/DU/BT

Component	Installed Capacity
WT [MW]	1.8
PV [MW]	2.0
Battery storage capacity [kWh]	60,000
Desalination unit [m^3/day]	1,320
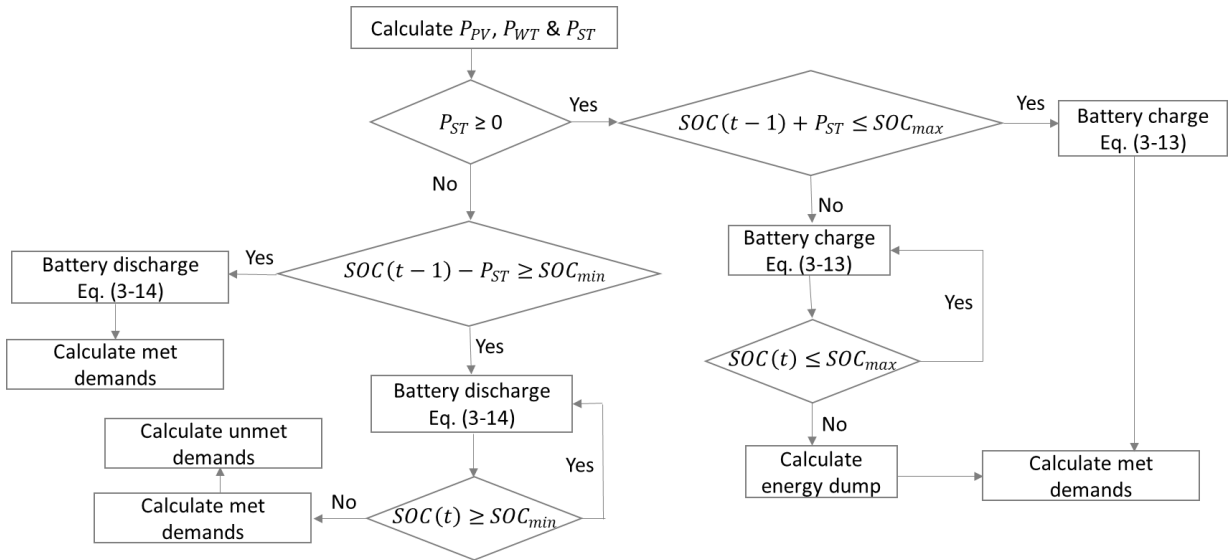
Figure 4-10 Energy management for WT/PV/DU/BT

4.2.5 WT/PV/DU/FC

This scenario differs from the previous two in storage τtechnology. Excess energy is stored in a hydrogen tank. Renewable energy also is provided by WTs and PVs and there is also a desalination unit to cover water needs. Here, also, priority is given to domestic water, then to irrigation water and then to the electrical load. The schematic representation of the HRES and the installed capacity of all components appear in Figure 4-11 and Table 4-11 respectively. The sizing of the hydrogen tank is also based on two days of autonomy and is calculated equal to 1,860 kg.
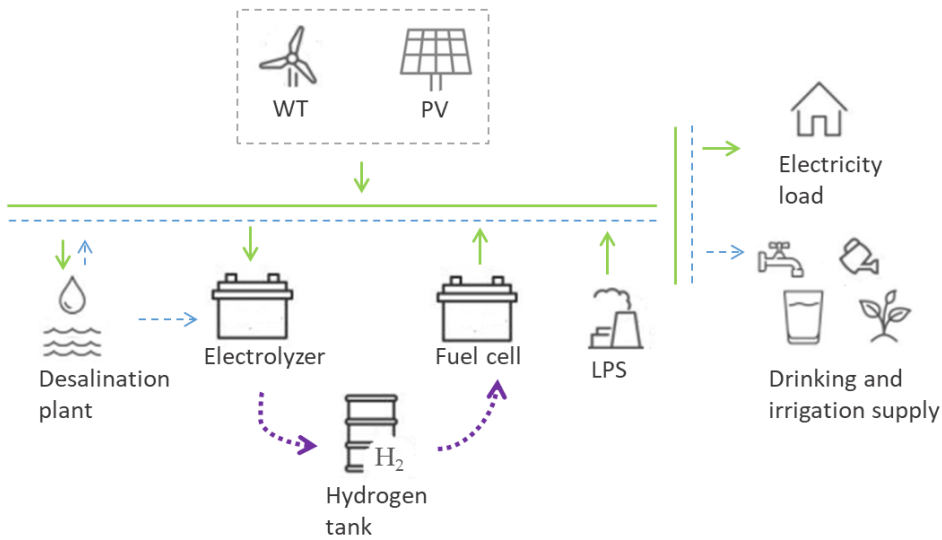
Figure 4-11 Schematic representation of WT/PV/DU/FC

Table 4-11 Specification data of the installed components of WT/PV/DU/FC

Component	Installed Capacity
WT [MW]	1.8
PV [MW]	2.0
Electrolyzer [MW]	2.8
Fuel cell [MW]	1.9
Hydrogen tank [kg]	1,876
Desalination unit [m³/day]	1,200

The energy management of this configuration is presented in Figure 4-12. If P_{ST} energy is greater than zero , then the extra energy is used by the electrolyzer to convert it to hydrogen. Energy is also required for the desalination of the necessary amount of water that is needed for hydrogen production. The amount of produced hydrogen, in kg, is calculated according to Equation 4-17. In the case of an energy deficit, the stored hydrogen is converted into energy through the fuel cell, according to Equation 4-18. The hydrogen tank is subject to storage restrictions according to Equation 4-19 and Equation 4-20, concerning $TANK_{H_2}^{min}$ and $TANK_{H_2}^{max}$.
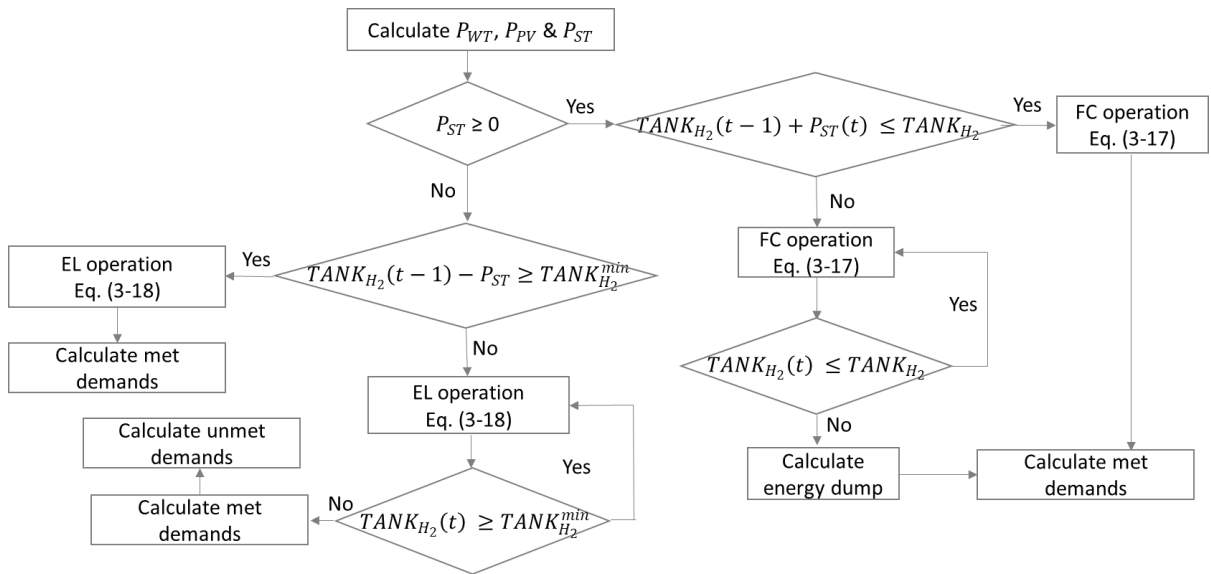
Figure 4-12 Energy management for WT/PV/DU/FC

4.2.6   WT/PV/DU/HPBS

In this configuration hybrid storage technology, including PHS and batteries, is installed. The RES comes from WTs and PVs and the coverage priorities apply as in the previous scenarios. In this configuration, it is considered that each storage technology has been dimensioned for one day of

autonomy so that a total of two days of autonomy can be covered. If there is an excess of energy, it is initially stored in the PHS. If, however, there is an amount that cannot be stored in the tank or if there is excess energy that could not be used by the pumping station, then this additional energy is led to the batteries. The schematic representation of the HRES and the installed capacity of all components are presented in Figure 4-13 and Table 4-12 respectively. The sizing of the upper reservoir and the battery capacity is based on one day of autonomy each and is calculated as equal to 37,246 m^3 and 29,700 kWh respectively.
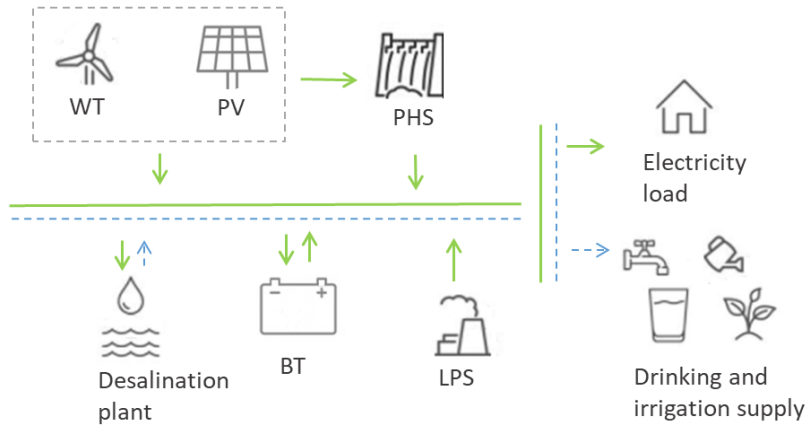
Figure 4-13 Schematic representation of WT/PV/DU/HPBS

The energy management of this configuration is presented in. Energy from WTs and PVs is used for the fulfillment of domestic water. It is checked whether the produced wind and solar energy are sufficient to meet the electrical needs for the desalination of the required quantity of domestic water for the corresponding step. This procedure is followed for the remaining energy concerning the fulfillment of irrigation water and at last for the fulfillment of electrical load. The surplus energy is calculated. This energy is firstly used for pumping water to the upper reservoir according to Equation 4-7. If the upper reservoir is full or if there is remaining energy that is not sufficient for the operation of the pumps, is stored in batteries. This unexploited energy that is sent to the batteries is estimated according to the methodology by Bertsiou and Baltas (2022b) and it is presented in section 6. For the storage of excess energy in batteries, it is checked the battery bank has the required capacity and then, it is charged. The new state of charge is calculated according to Equation 4-13. If there is an energy deficit and the battery bank has the required capacity, then the battery bank is discharged and the new state of charge is calculated according to Equation 4-14. At any time, the state of charge of the battery is subject to the constraints of Equation 4-15 and Equation 4-16, concerning SOC_{min} and SOC_{max}. Load demand that is not covered by the wind turbines, the hydro turbine, nor the batteries, is covered by the grid, meaning the startup of the LPS.

Table 4-12 Specification data of the installed components of WT/PV/DU/HPBS

Component	Installed Capacity
WT [MW]	1.8
PV [MW]	2.0
Upper reservoir [m^3]	37,621
Pumps [kW]	1.25
Hydro turbine [MW]	0.85
Battery storage capacity [kWh]	30,000
Desalination unit [m^3/day]	1,300
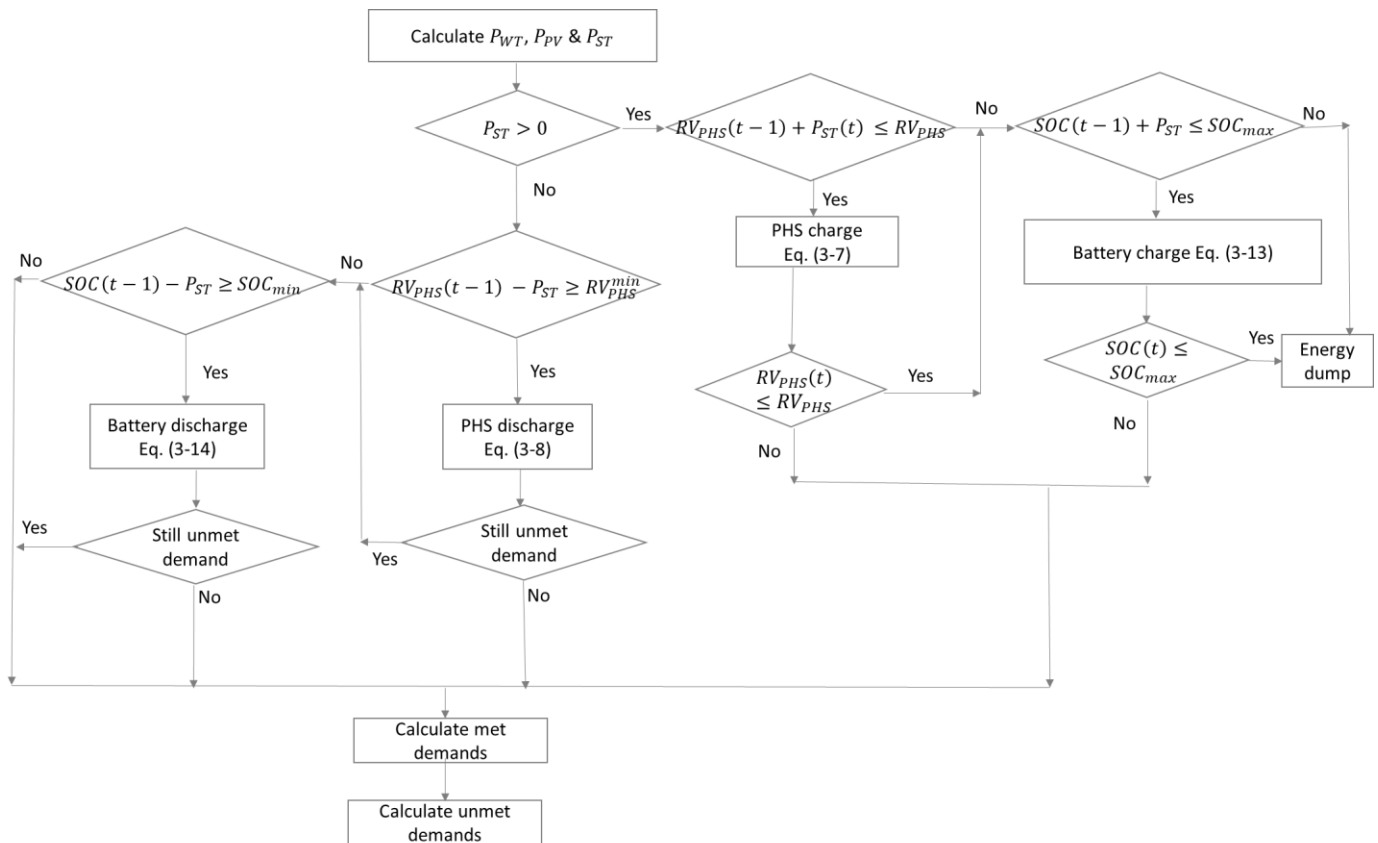
Figure 4-14 Energy management for WT/PV/DU/HPBS

4.2.7　WT/PV/DU/HPHS

In this configuration, the hybrid storage consists of PHS and a hydrogen storage system. The schematic representation of the HRES and the installed capacity of all components are presented in Figure 4-15 and

Table 4-13 respectively. The sizing of the upper reservoir and hydrogen tank is based in one day of autonomy each and is calculated equal to 37,246 m^3 and 1,860 kg respectively.

The energy management of this configuration is presented in Figure 4-16. Energy from WTs and PVs is used for the fulfillment of domestic water. It is checked whether the produced wind and solar energy are sufficient to meet the electrical needs for the desalination of the required quantity of domestic water for the corresponding step. This procedure is followed for the remaining energy concerning the fulfillment of irrigation water and at last for the fulfillment of electrical load. The surplus energy is calculated. This energy is firstly used for pumping water to the upper reservoir according to Equation 4-7. However, in this case, there is a hydrogen storage system as a supplementary system to the whole HRES. The energy that cannot be stored through the pumped hydro storage system, because either the upper reservoir is full or the remaining energy is not sufficient for the operation of the pumps, is stored in the form of hydrogen in the hydrogen tank. This unexploited energy that is sent to the electrolyzer is estimated according to the methodology by Bertsiou and Baltas (2022b) and it is presented in section 6.
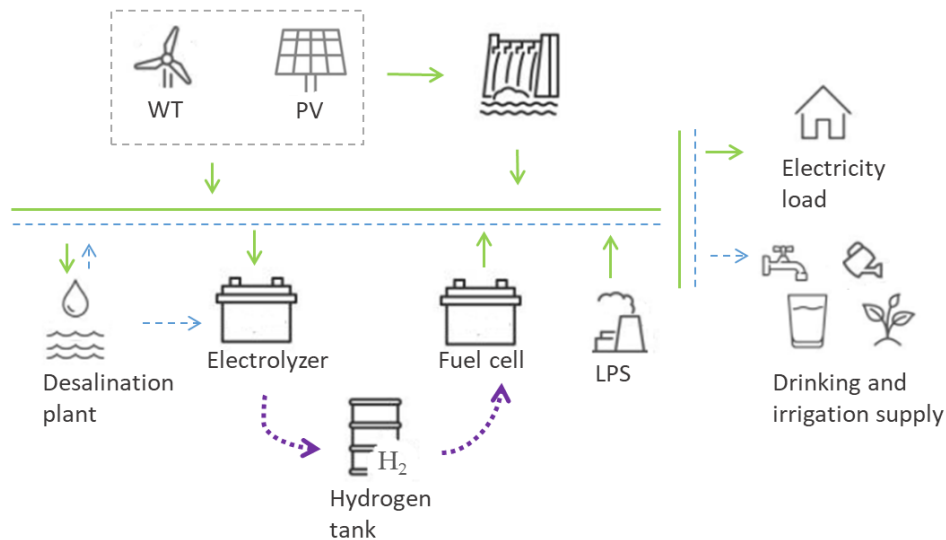
Figure 4-15 Schematic representation of WT/PV/DU/HPHS

Table 4-13 Specification data of the installed components of WT/PV/DU/HPHS

Component	Installed Capacity
WT [MW]	1.8
PV [MW]	2.0
Upper reservoir [m^3]	37,621
Pumps [kW]	1.25
Hydro turbine [MW]	0.85
Electrolyzer [MW]	2.6
Fuel cell [MW]	1.9
Hydrogen tank [kg]	938
Desalination unit [m^3/day]	1,300
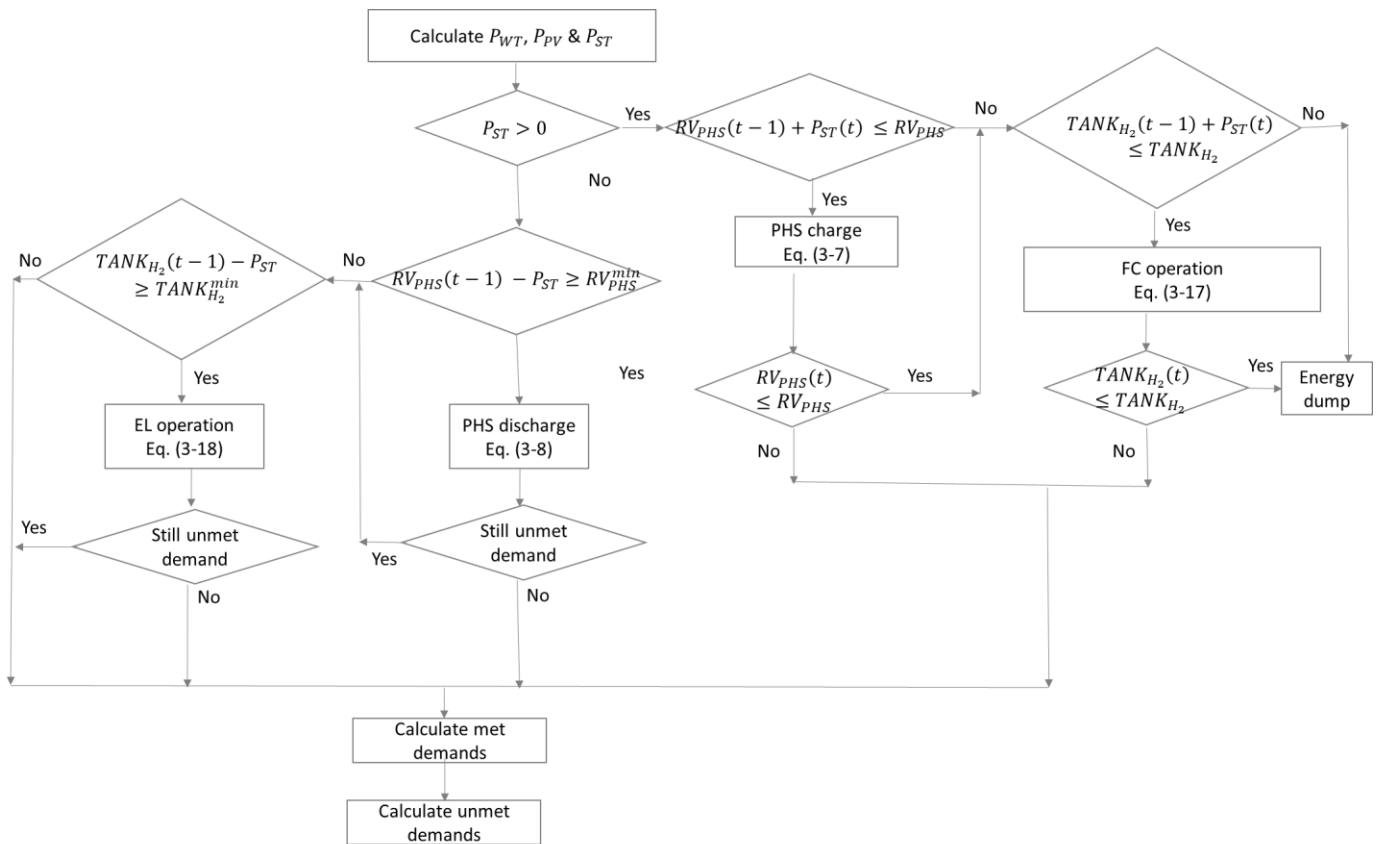
Figure 4-16 Energy management for WT/PV/DU/HPHS

By electrolyzing desalinated water, the electrolyzer transforms this energy into hydrogen. This means that it is necessary to make sure that there is enough energy available to desalinate the water used

for electrolysis and to produce hydrogen. Equation 4-17 is used to get the amount of hydrogen produced in kg. When neither the WTs nor the PVs are able to meet the demand, PHS is used. When neither of these sources of energy can meet the demand, the required amount of hydrogen converts into energy by the fuel cell and is sent to the grid. The stored hydrogen is converted into energy through the fuel cell, according to Equation 4-18. The hydrogen tank is subject to storage restrictions according to Equation 4-19 and Equation 4-20, concerning $TANK_{H_2}^{min}$ and $TANK_{H_2}^{max}$. The grid, which entails the startup of the LPS, supplies any load demand that is not fulfilled by the wind turbines, the solar panels, the hydro turbine, or the fuel cell.

4.3 Economic and environmental analysis

Cost of Water (COW), Loss of Load Probability (LOLP), and Cost of Energy (COE) are also evaluated for the HRES. Equation 4-21 estimates COE (Hausmann et al., 2021; Ma & Javed, 2019).

$$COE = \frac{CAPEX + OPEX + C_{rpl} - C_{slv}}{E_{hres}}$$ Equation 4-21

where $CAPEX$ is the total HRES's initial investment cost (in €), $OPEX$ is the cost of operating and maintaining each component (in €), C_{rpl} is the replacement cost over the project's lifetime (in €), C_{slv} is the salvage cost, which is the value of each HRES component at the end of the project's lifetime (in €), and E_{hres} is the energy produced by the HRES (in kWh). Salvage cost is estimated separately for each component by Equation 4-22.

$$C_{slv} = C_{rpl} \cdot \left\{ \frac{LF_{comp} - \left[LF_{hres} - \left(LF_{comp} \cdot integer \left(\frac{LF_{hres}}{LF_{comp}} \right) \right) \right]}{LF_{comp}} \right\} \cdot \left[\frac{1}{(1+i)^{LF_{hres}}} \right]$$ Equation 4-22

where LF_{comp} is the lifetime of each component and LF_{hres} is the lifetime of the HRES.

COW (€/m³) is estimated by Equation 4-23.

$$COW = COE \cdot E_{des}$$ Equation 4-23

where E_{des} is the energy required for the desalination of seawater (kWh/m³). The economic parameters applied in this analysis are shown in Table 4-14.

The evaluation of the reliability of the HRES is estimated LOLP, which is calculated by Equation 4-24 (Ma & Javed, 2019).

$$LOLP\ [\%] = \frac{\sum_1^n E_{loss}}{\sum_1^n E_{load}}$$ Equation 4-24

where n is the number of hrs in a year of simulations, E_{load} is the annual load demand, and E_{loss} is the unmet demand. There are four separate LOLPs that are calculated: the energy demand for

domestic water desalination $LOLP_d$, the energy demand for irrigation water desalination $LOLP_{ir}$, the energy demand for the household consumption $LOLP_{el}$, and the sum of the three demands $LOLP_{hres}$.

Table 4-14 Economic Parameters

Component	Parameter	Value
Wind turbine	Initial cost (€/kW)	906
(Baruah et al., 2021)	Operation and maintenance cost (€/kW)	136
	Lifetime (years)	25
Photovoltaic module	Initial cost (€/kW)	800
(Javed et al., 2021)	Operation and maintenance cost (€/kW)	11.2
	Lifetime (years)	25
Desalination unit	Initial cost (€/m³/day)	484
(Abdelshafy et al., 2018)	Operation and maintenance cost (€/m³/day)	0.32
Reservoir	Initial cost (€/m³)	154
(He et al., 2021)	Operation and maintenance cost (€/m³)	3.1
	Lifetime (years)	35
Hydro turbine	Initial cost (€/kW)	910
(He et al., 2021)	Operation and maintenance cost (€/kW)	18
	Lifetime (years)	10
Pumping station	Initial cost (€/kW)	217
(He et al., 2021)	Operation and maintenance cost (€/kW)	4.35
	Lifetime (years)	20
Battery	Initial cost (€/kWh)	200
(Jurasz et al., 2020)	Operation and maintenance cost (€/kWh)	4
	Replacement cost (€/kWh)	150
	Lifetime (years)	15
Hydrogen tank	Initial cost (€/kg)	1182
(Abdelshafy et al., 2018)	Operation and maintenance cost (€/kg)	13.6
	Replacement cost (€/kg)	1092
	Lifetime (years)	20
Electrolyzer	Initial cost (€/Ah)	606
(Abdelshafy et al., 2018)	Operation and maintenance cost (€/Ah)	1.8
	Replacement cost (€/Ah)	455
	Lifetime (years)	5
Fuel cell	Initial cost (€/kW)	910
(Abdelshafy et al., 2018)	Replacement cost (€/Ah)	774
	Operation and maintenance cost (€/kW)	0.02
	Lifetime (years)	5

In order to recover the full cost of the investment, the PBP determines the project's required years of operation. It is based on the total investment cost and the net yearly savings (AS). Equation 4-25 provides a mathematical description of it.

$$PBP = \frac{Initial\ Costs + \sum_{n=1}^{N} O\&M\ Costs}{AS}$$

The initial costs represent the initial investment, installing and replacement costs of the system, including the cost of each unit, depending on the configuration examined. Initial cost does not include any subsidies from the national or local government policies. The operation & maintenance costs refer to the corresponding costs for the total life, 25 years of an HRES. The net annual savings contains the net revenue it is expected to earn each year by using the HRES instead of other energy sources. PBP is determined using the current kWh pricing and the cost per cubic meter of desalinated water. According to the PPC, the price of a kWh is the average tariff for various consumptions (daytime or nighttime consumption), and it is equal to 0.22833 €. (Public Power Corporation, 2023). However, such projects can be more competitive by a reduction of the selling price gap. This can be achieved on case of an increase in energy prices. The price of water for the islands ranges from 7 to 12 €/m^3 (Bardis et al., 2020; Myronidis & Nikolaos, 2021), and in this study is considered equal to 10 €/m^3. It's important to note that the PBP calculation evaluate the financial viability of a project, without considering other factors that may impact the return on investment, such as inflation, tax benefits, or changes in energy prices over time.

Equation 4-26 is used to calculate the amounts of CO$_2$ that the HRES system eliminates, EM_{CO_2} (tn/year), when 1 kWh supplied by the HRES replaces 1 kWh provided by the LPS:

$$EM_{CO_2} = \frac{[E_{PV} \cdot (F_{grid} - F_{PV}) + E_{WT} \cdot (F_{grid} - F_{WT})]}{10^6}$$

where E_{WT} and E_{PV} represent the energy (kWh) generated by WT and PV systems, respectively; F_{WT} and F_{PV} represent the emission factors of wind and solar technologies, which are about 13.7 g CO2/kWh for wind and 50 g CO2/kWh for solar, respectively (El-houari et al., 2021). F_{grid} represents the emission factor of each country's grid. According to the country datasheet, the GHG intensity of electricity production for Greece in 2020 is about 479.2 g CO2/kWh (European Environment Agency, 2020). The price of one ton of CO$_2$ is calculated based on the price of ton in the market on December 08, 2022 (Ember, Daily Carbon Prices, 2022). Note that its price displays an average daily increasing trend of 0.6%.

5.1   Scenarios/Configurations

Initially, the results for the first configuration are presented, concerning the use of WTs and PHS to cover electrical loads without the integration of a desalination unit. The average rate of reliability for a whole year (12 months) is presented in Figure 5-1. It is shown that the average coverage of electricity demand (subscript "el") and, subsequently, the reliability of the entire HRES (subscript "hres") is over 80%.

Figure 5-1 Reliability analysis of WT/PHS

In Figure 5-2, the share of energy of three different sources is presented. These sources are the wind turbines, the use of the PHS and the use of the LPS (GRID) when demand can be covered neither by the WTs nor by the PHS. The results refer to the coverage of electrical demand and the subscript 'el' is used. Wind turbines, and subsequently the hydro turbine, are used to first supply the energy. Unmet demands are treated by the island's local network. It is observed that during July, September and October, the LPS does not operate, while in August its contribution is the minimum. This result is particularly important considering that July and August are referred to as the tourist season. However, as it has been analyzed in section 2.2 and in Table 2-4, the household consumption during the summer is reduced, compared to the winter months, possibly due to the fact that the devices used in the winter for the supply of hot water and for heating are more energy-intensive. So, during these months, the demands and the produced RES are in balance and HRES is completely autonomous.

In addition, the amount of wind energy used changes every month and is based on the demands and the current wind potential. On the contrary, the hydro energy generated is dependent on the excess energy and the water that has been pumped and stored according to Equation 4-7.

The results regarding the annual contribution of each energy source to meet the electrical load of the island are presented in Figure 5-3. The contribution of WTs is the maximum at 57%, while the use of PHS and GRID is almost the same and circa 21%.
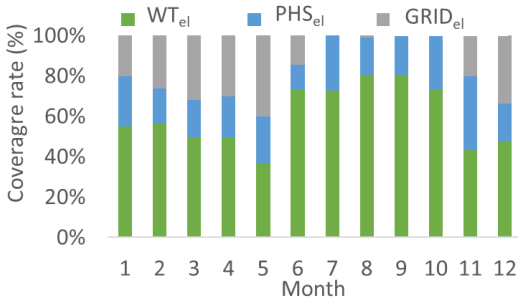
Figure 5-2 Share of energy of WT/PHS by WT, PHS and GRID for electrical load
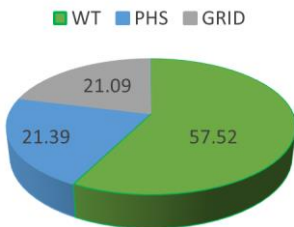
Figure 5-3 Satisfied consumption by different energy sources of WT/PHS
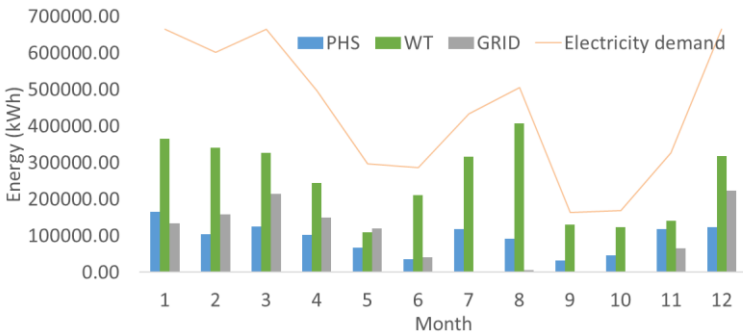
Figure 5-4 Energy balance and demand of WT/PHS

In Figure 5-4 the monthly contribution of the WTs, the PHS and the GRID are presented, as well as the monthly electricity demand. The autonomy of the HRES is also presented here from July to October. Due to tourism, the demand for electricity is high in August, however, the peak occurs in the winter. Although there is a high demand in August, there is also a higher wind potential during that month. As a result, the use of the LPS varies from zero to very low values. Especially during August, the wind potential has its maximum value.

The share of energy of the WT/PHS configuration is depicted in Figure 5-5. Results for August are presented in (a) and for December in (b). The demand is demonstrated in negative values, to compare demand and offer. The selection of these months is based on the demands. December presents the higher demand in electricity, while August is the month with the highest arrival of tourists. PHS operates smoother during August compared to December and more use of the LPS is observed in December, compared to August, since more energy demands arise.

(a)   (b)
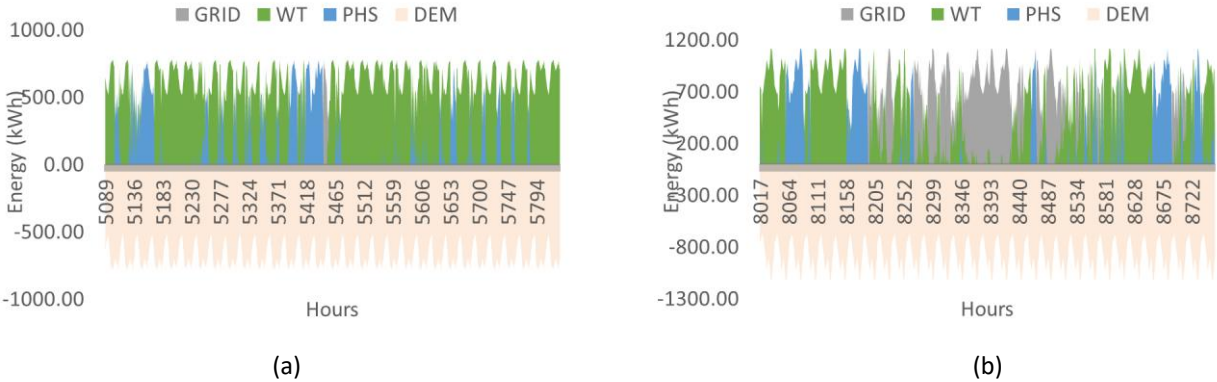
Figure 5-5 Share of energy of WT/PHS for electricity demands in (a) August; (b) December

Figure 5-6 presents the hourly storage level of the upper reservoir over a year. A comparison between Figure 5-5 and Figure 5-6 shows that the pattern of charging and discharging of the upper reservoir is similar to the pattern of the GRID. Every time the upper reservoir is not fully discharged, GRID does not operate and HRES is autonomous. On the other hand, every time the upper reservoir is fully discharged, HRES is based on the local power station to cover all electrical demands.
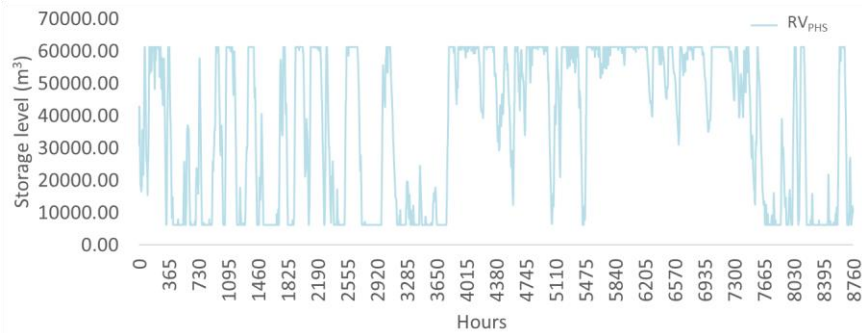
Figure 5-6 Storage level of upper reservoir in WT/PHS

Finally, the surplus energy that is given for pumping during the operation of the HRES, as well as the energy that is given by the operation of the hydro turbine, are shown in Figure 5-7, in an hourly step. It seems that the energy for pumping is higher that the produced hydro energy. First, this occurs because the use of the hydro turbine is not constantly required to cover electrical needs, as most of them have already been satisfied by the direct use of wind energy by the WTs. However, it must be emphasized that even when the hydro turbine is used, the energy that produces is less than the

energy consumed in the pumping station and this process is used for the storage of excess energy and in order to meet the demand that does not coincide with the production of wind energy.
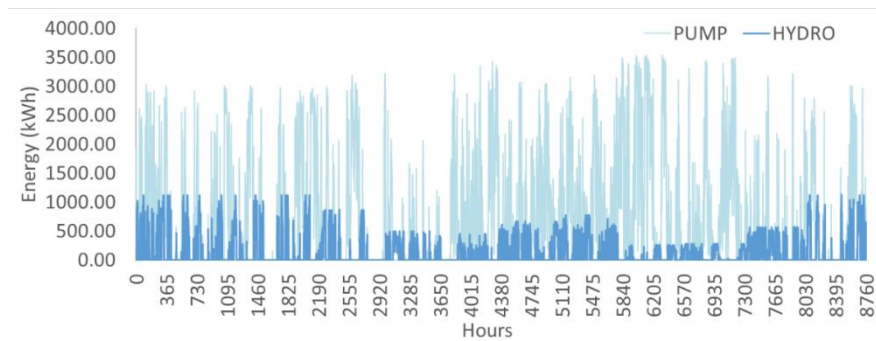
Figure 5-7 Energy for pumping and energy by hydro turbine in WT/PHS

Table 5-1 presents results about the initial cost, the operation and maintenance cost, the cost of energy, the loss of load probability of the HRES, the eliminated CO_2 quantities and the CO_2 price. The initial cost for the WT/PHS configuration is 13,1882,955 €, while the $O\&M$ cost is 691,526 €. The COE is 0.281 €/kWh, higher that the price from PPC, which applies today to energy tariffs. PBP has not been calculated since HRES price is higher than today energy price. However, for this scenario, the benefits of reducing emissions, which amount to 1,936 tn/year, must also be considered. This price is also translated into the penalty from the Emissions Trading System and for this HRES it IS calculated at €172,200. LOLP for the HRES is 21.09%, meaning that about 80% HRES can provide the required energy for the fulfillment of the electrical load of the island.

Table 5-1 Economic, environmental and reliability analysis for WT/PHS

Key Parameter	Value
$Initial\ cost$ [€]	13,882,955
$O\&M\ cost$ [€]	691,526
COE [€/kWh]	0.281
$LOLP_{hres}$ [%]	21.09
EM_{CO_2} [tn/year]	1,936.36
$EM_{CO_2}\ price$ [€]	172,200.88

The rest of the configurations concern HRESs that simultaneously aim to cover energy and water demands, to make the comparisons in the final price of energy and water, when water desalination is also involved. In each of the following figures, the rest of configurations (a)-(f), according to the description of each caption.

The average reliability rate for a full year (12 months) is shown in Figure 5-8. For each of the demands—electricity, domestic water and irrigation water—that are indicated by the subscripts of

the legend, "el," "d," and "ir," respectively, generated outputs are estimated. Furthermore, an overall average for the reliability of the whole HRES (subscript "hres") is retrieved. It is shown that the average coverage of each demand is consistently over 80% for each month and for each configuration. Fulfillment of domestic water demands is always higher and between 80% and 90%, as domestic water is a priority in every configuration. Configurations that include PVs, (b)-(f), show better results, concluding that the division of the production of renewable energy between WTs and PVs leads to better satisfaction of the demands, by exploiting both wind and solar potential during the day. Also, hybrid storage technologies, (e)- (f), provide better results for each demand separately, as the energy that would otherwise be utilized, in these two cases is exploited by an additional storage system, batteries for (e) and hydrogen storage system for (f).

In Figure 5-9 the share of energy by the different energy sources for each demand (domestic water 'd', irrigation water 'ir', electrical load 'el') and of each configuration is presented. Depending on the configuration there are wind turbines (WT), photovoltaic modules (PV), the pumped hydro storage system (PHS), batteries (BT), the hydrogen storage system (FC), and the operation of the LPS (GRID). In all configurations, the energy is initially supplied by the wind turbines and then from photovoltaic modules when they are applied. The third energy source is the storage technology of each configuration. Initially, increased monthly use of LPS is observed in WT/DU/PHS compared to the other scenarios, which proves that the integration of PVs into the energy mix leads to optimal results, as both wind and solar potential can be exploited during the day, giving more satisfactory results. The monthly WT and PV contribution is common per demand across all configurations, since as originally analyzed it is used to fulfill as much demand as possible before the excess is diverted to storage. Also, as demonstrated in chapter 2.2.3, the amount of wind and solar energy that is utilized varies for each month and is dependent on both the needs and the current wind and solar potential. On the other hand, the produced hydro energy (conf. b), the energy from the batteries (conf. c), or the energy from the fuel cell (conf. d) depends on the excess energy, but the energy generated by the fuel cells (conf. g) and batteries (conf. e) for the hybrid storage systems, is dependent on the hydro turbine's unexploited energy, due to the limitations of the upper reservoir or the pumping station capacity. In each configuration, it is observed that in September and October for either of the demands and for either of the storage systems, GRID is not used. Demands and generation of RES are in balance during these months, and HRES is fully autonomous. However, WT/PV/DU/PHS and WT/PV/DU/BT can almost fully cover domestic demand during June and July and in August the use of the LPS is limited. On the contrary, in WT/PV/DU/FC, it is observed a reduced coverage in these months, perhaps since in the hydrogen storage system, enough energy is also required for the desalination of the water that is led to the electrolyzer.
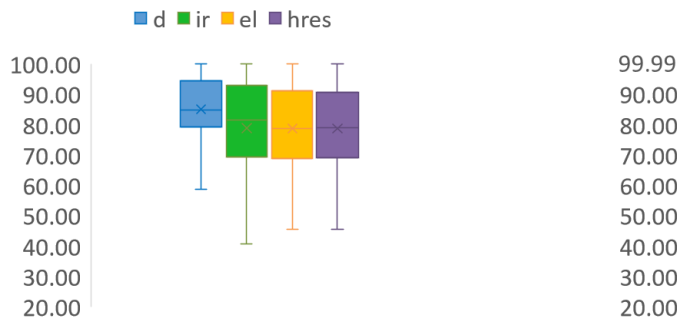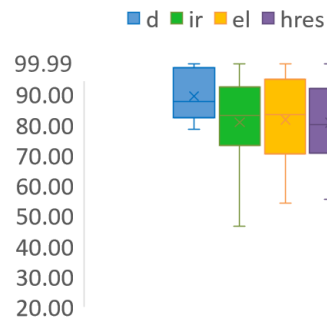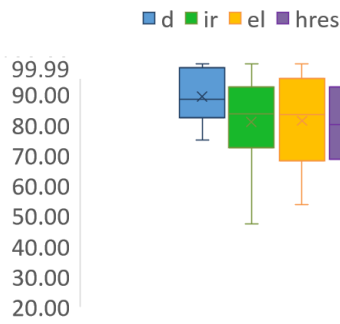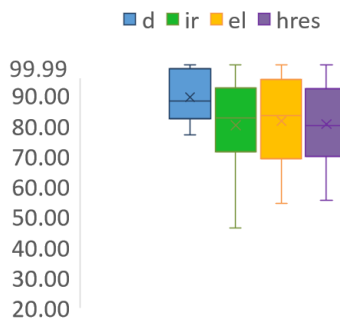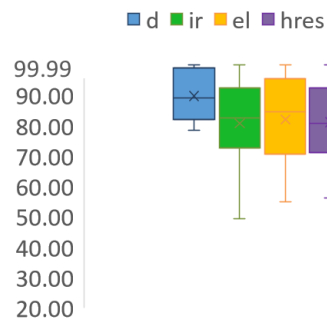
Figure 5-8 Reliability analysis: (a) WT/DU/PHS; (b) WT/PV/DU/PHS; (c) WT/PV/DU/BT; (d) WT/PV/DU/FC; (e) WT/PV/DU/HPBS; (f) WT/PV/DU/HPHS
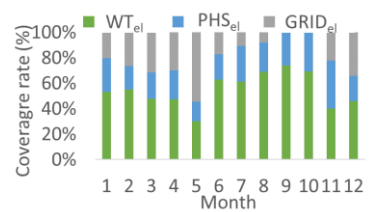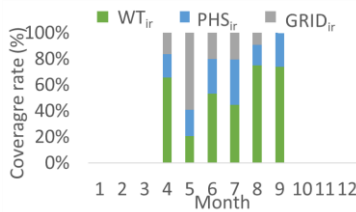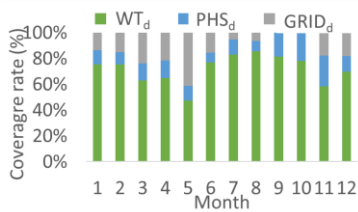
(a)
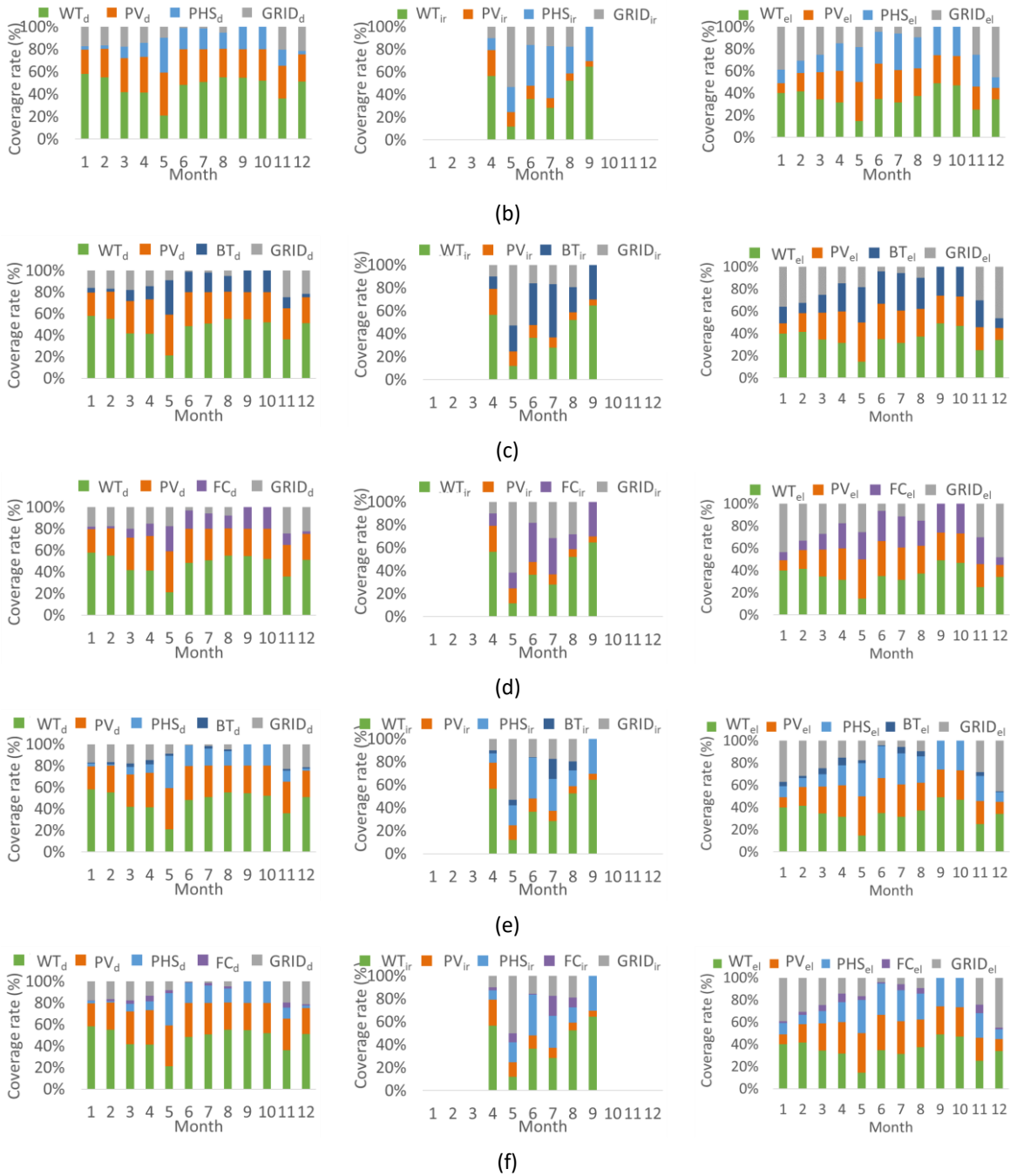
Figure 5-9 Share of energy for domestic water, irrigation water and electrical load: (a) WT/DU/PHS; (b) WT/PV/DU/PHS; (c) WT/PV/DU/BT; (d) WT/PV/DU/FC; (e) WT/PV/DU/HPBS; (f) WT/PV/DU/HPHS

Equally satisfactory results in terms of domestic water supply are also given by HRESs where they have a hybrid storage system, i.e., in WT/PV/DU/HPBS and WT/PV/DU/HPHS. During the irrigation season, beginning in May, the need for irrigation increases and there is a greater use of the LPS for irrigation reasons. As a result, there is greater use of the LPS for electricity too, the third demand to

meet. The greater demand for irrigation water has also an impact on how domestic water is covered during the irrigation season, lowering the coverage rate from the HRES, compared to other months of the year when no irrigation water needs to be desalinated. Between the systems with simple and hybrid storage a monthly reduced use of LPS is observed, as in these systems the energy is further exploited by wind turbines and photovoltaic modules, while otherwise, in single storage configurations, more energy would be rejected. For (a)-(d) uncovered needs are covered by the local network of the island, while in (e)-(f) the storage of unexploited energy through the batteries and the fuel cell, respectively, is utilized before the use of the grid.

In Figure 5-10, the different energy sources that participate yearly in the energy mix of the island are presented. In WT/DU/PHS, the total contribution from WTs is smaller than in the rest configurations where the energy mix includes energy from PVs. The contribution of WTs and PVs is the same in the rest configurations, (b)-(f), as expected since the selection of the storage technology does not affect the penetration of the renewable energy sources in the hybrid renewable energy system, while the contribution of the storage system and LPS present a significant difference. The configuration with the minimum use of GRID is WT/PV/DU/HPHS, which means initially that hybrid storage surpasses the final results and that the use of hydrogen as a second storage unit, compared to batteries, results in reduced use of conventional fuels. This is impressive, even though the production of hydrogen requires the consumption of more energy for the desalination of the water to the electrolyzer. Fluctuation is observed in the contribution of pumped hydro storage and battery compared to the hydrogen storage system. Although all three storage systems have been dimensioned according to two days of autonomy, the PHS and the BT satisfy about 21% of the total demand, while FC satisfies 17% of the total demand, indicating that the FC participates less in the energy balance and increase the use of the LPS. Subsequently, among the configurations with simple storage, pumped storage gives better results about the use of GRID at 21.77%, while the maximum use of GRID is observed in the single storage with a hydrogen system. In WT/PV/DU/FC, this energy consumption for water desalination becomes apparent, depriving it of the fulfillment of the island's energy needs, whether it is energy needs for domestic and irrigation water desalination or energy needs for household consumption. Also, the use of GRID is similar in both simple battery storage and hybrid battery storage, so the comparison should be made below with the resulting final energy and water prices.
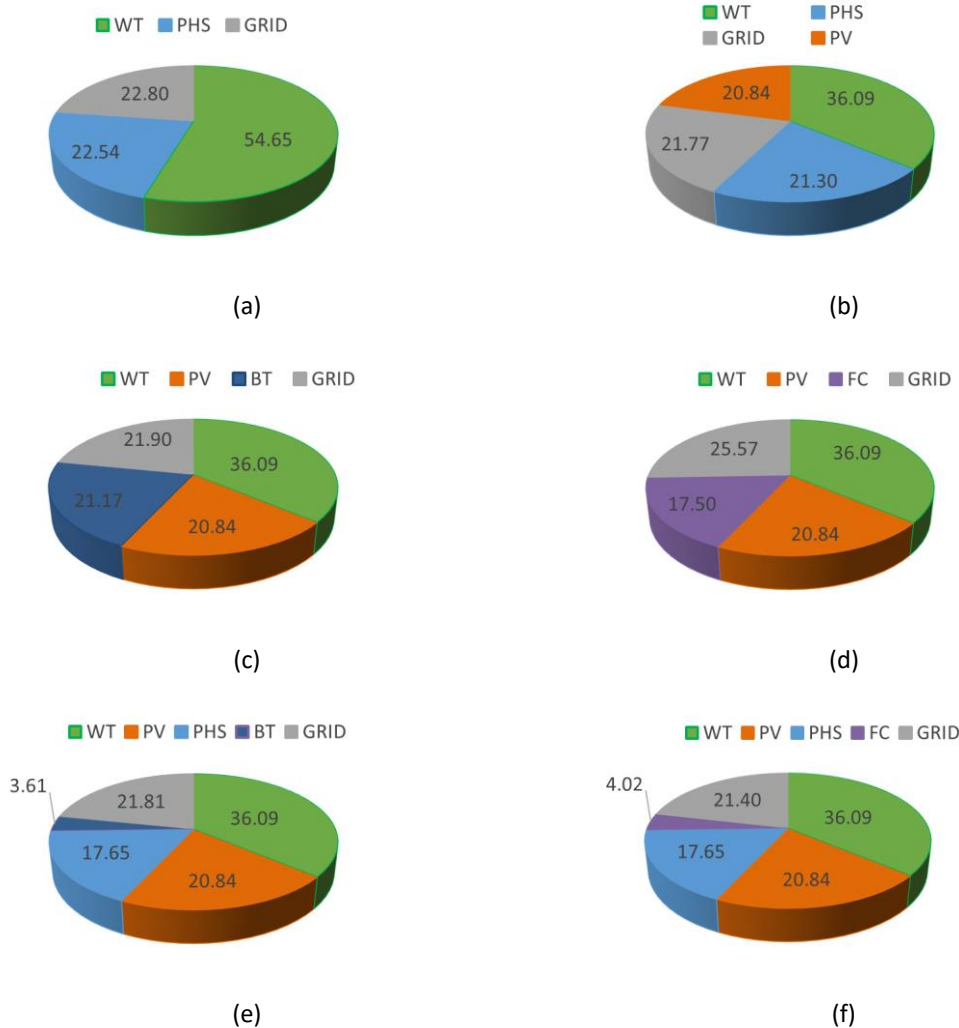
Figure 5-10 Satisfied consumption by different energy sources: (a) WT/DU/PHS; (b) WT/PV/DU/PHS; (c) WT/PV/DU/BT; (d) WT/PV/DU/FC; (e) WT/PV/DU/HPBS; (f) WT/PV/DU/HPHS

More specifically, the monthly contribution from each energy source compared with the monthly electricity household consumption, as well as energy for desalination needs (domestic and irrigation water), are shown in Figure 5-11. In all single storage configurations, (a)- (d), HRES is completely autonomous in September and October, while in hybrid storage configurations, (e) and (f), this autonomy extends to June. The irrigation season lasts from April to September, and in July, when temperature rises and the likelihood of rain is quite low, the highest request for irrigation water is observed. Due to tourism, August is the month with the maximum demand for water supplies. Finally, although demand for energy is high in August because of tourism, it peaks in the winter, maybe as a result of the increased usage of lightbulbs throughout the day and the high use of heating equipment. The use of the LPS ranges from zero to very low values, for both storage systems, in August, because an increased wind and solar potential is observed despite the fact that there are high demands at this same time.
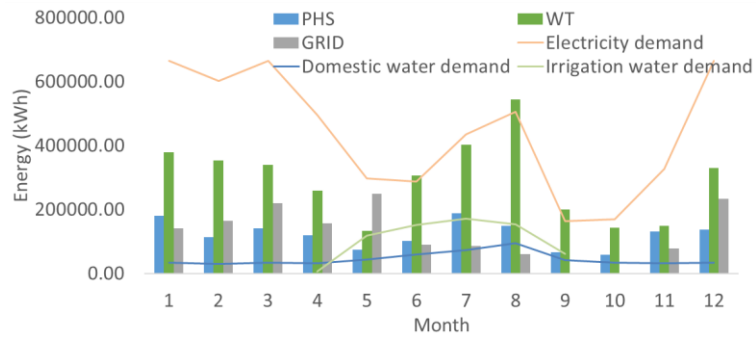
(a)
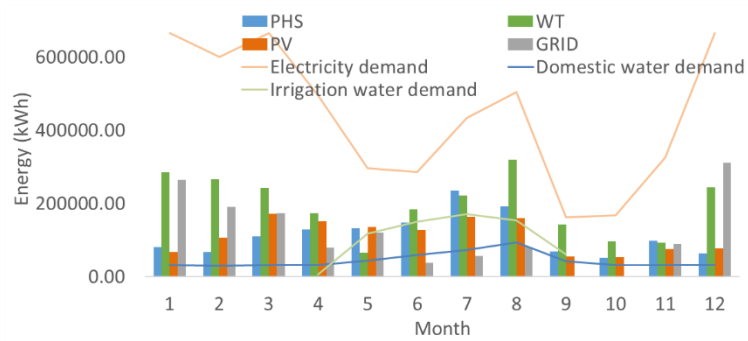
(b)
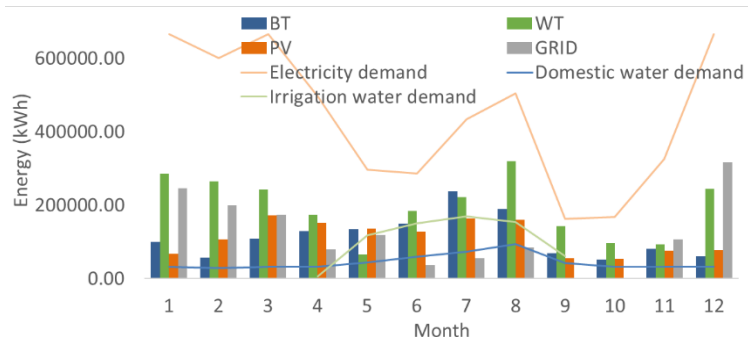
(c)
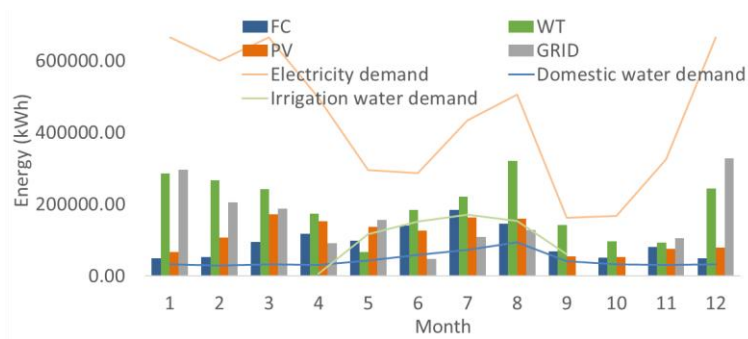
(d)
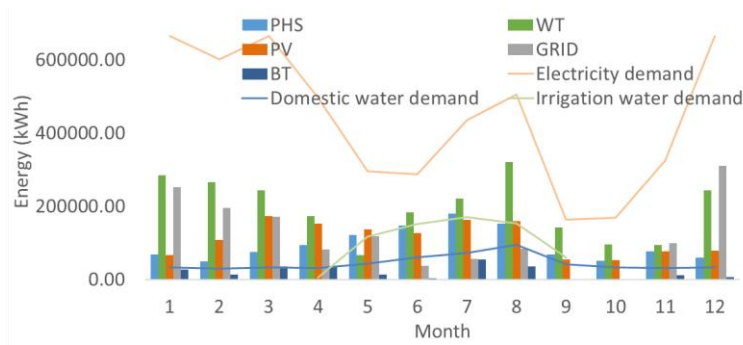
(e)
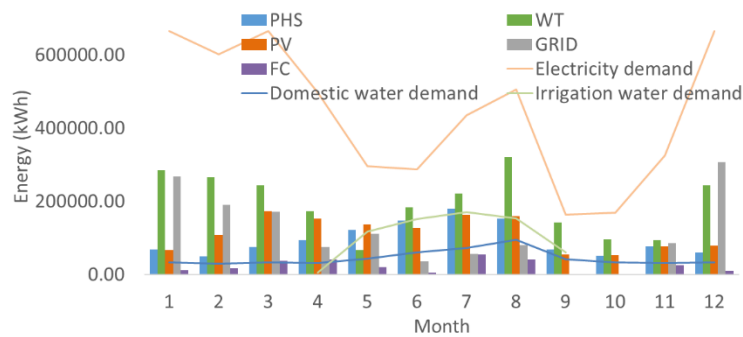
(f)

Figure 5-11 Energy balance and demand: (a) WT/DU/PHS; (b) WT/PV/DU/PHS; (c) WT/PV/DU/BT; (d) WT/PV/DU/FC; (e) WT/PV/DU/HPBS; (f) WT/PV/DU/HPHS

The hourly share of energy, compared to the total energy demand, for August (5089 h-5832 h) and December (8017 h-8760 h) is presented in Figure 5-12. To make the comparison clear, the demand (DEM) is shown with negative pricing. The demand determines the months that are chosen. The highest demand for energy is in December, whereas the highest demand for desalinated water for residential and agricultural usage is in August. Irrigation is expected to be performed after sunset, and the pattern of rising values that appears in August is caused by this irrigation water required after midnight. Other demands, such as domestic water and energy for household consumption, are substantially lower at night. The comparison of the configurations shows that there are periods during both months when the grid would normally be in operation that is now taken over by the operation of the fuel cells and batteries. Also, compared to single storage, hybrid storage systems provide additional days of autonomy. Also, compared to August, in December the second storage seems to be more active. This could be related to the fact that even though the overall required energy needs are increased in December, in comparison to August, simultaneously the higher wind potential results in more excess energy being delivered and exploited by the electrolyzer. And while in August there is an increased solar potential, as can be noticed by Figure 5-10, WTs have a greater participation in the energy mix throughout the year. And while in August there is an increased solar potential, as it is depicted in Figure 4-10 WTs have a greater participation

in the energy mix. Moreover, since there are larger energy demands in December compared to August, the grid is used more frequently. Additionally, as previously explained, the demand for irrigation water is moved independently to the nighttime, where demand for domestic water and electricity is minimized, giving the HRES the opportunity to fulfill separately these irrigation demands and supply more energy during the rest of the day depending on the solar and wind potential.

(a)

(b)

(c)

(d)

(e)

(f)
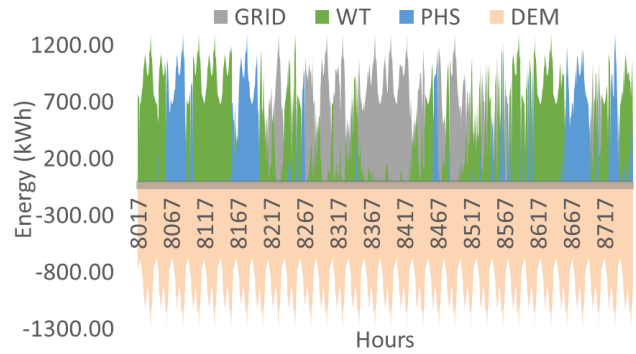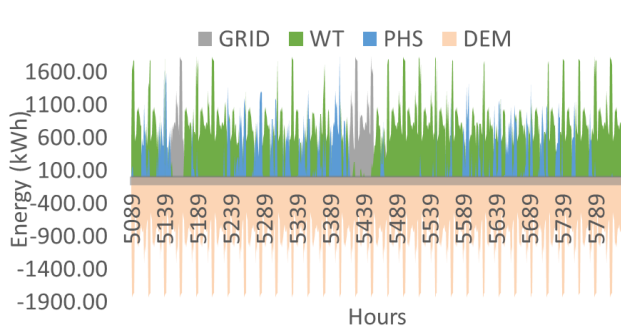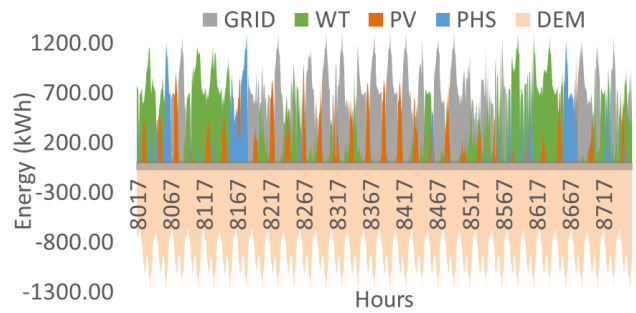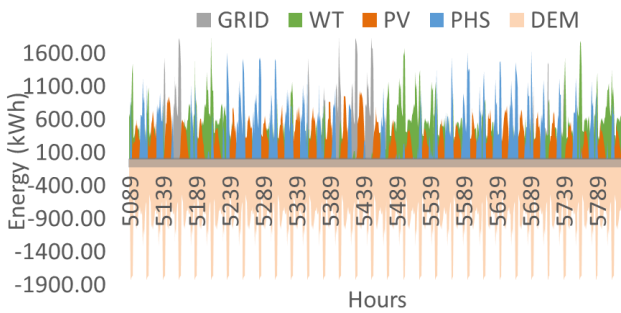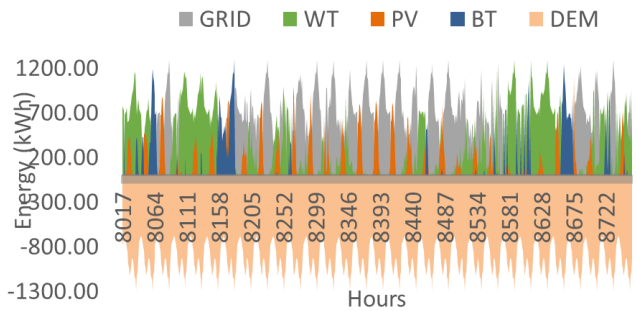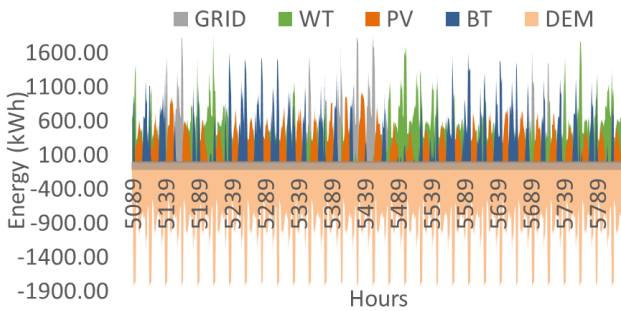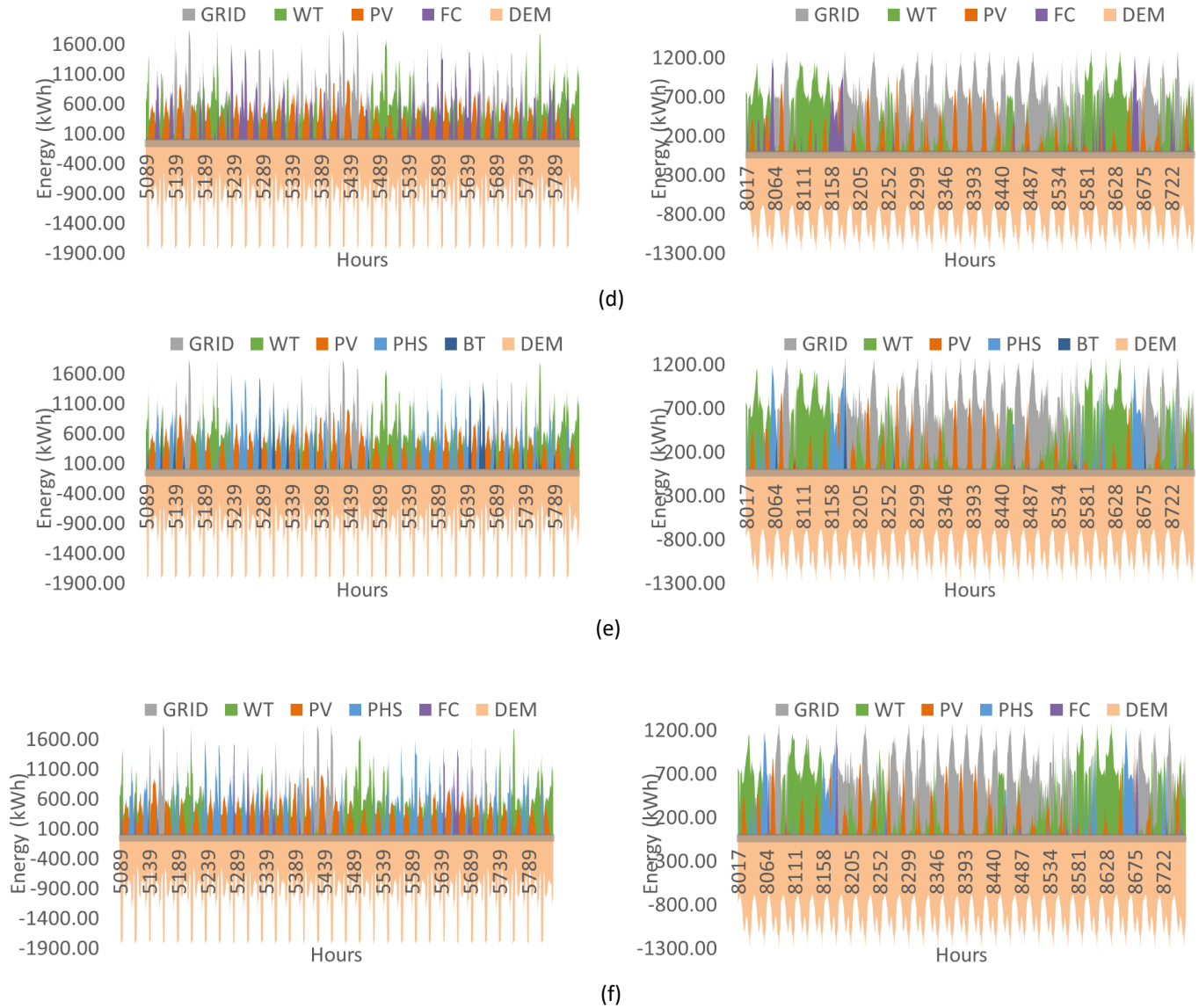
Figure 5-12 Share of energy in August (5089-5832) and December (8017-8760): (a) WT/DU/PHS; (b) WT/PV/DU/PHS; (c) WT/PV/DU/BT; (d) WT/PV/DU/FC; (e) WT/PV/DU/HPBS; (f) WT/PV/DU/HPHS

The monthly demands, as well as the monthly amounts of domestic and irrigation water that are satisfied and unsatisfied, are shown in Figure 5-13. Although water desalination is a priority and it is covered by the direct use of RES before the excess energy is stored for future use, the results are better in the configurations with hybrid storage technology. Between the single storage technologies, PHS results in higher fulfillment of both domestic and irrigation water. And in this category of demand, it seems that the combination of wind and solar parks provides better coverage results, due to the simultaneous exploitation of wind and solar potential. On a monthly basis, the fulfillment of water supply is up to 87% for configurations that combine WTs and PVs, while this percentage

declines for irrigation water, as expected, given that irrigation water is the last demand in the hierarchy of importance. In all configurations, there is full coverage autonomy for October, while the autonomy extends for the domestic water supply to June and July for WT/PV/DU/PHS, WT/PV/DU/BT, WT/PV/DU/HPBS, WT/PV/DU/HPHS. Only the WT/PV/DU/FC scenario shows losses of load during July in the domestic water supply.
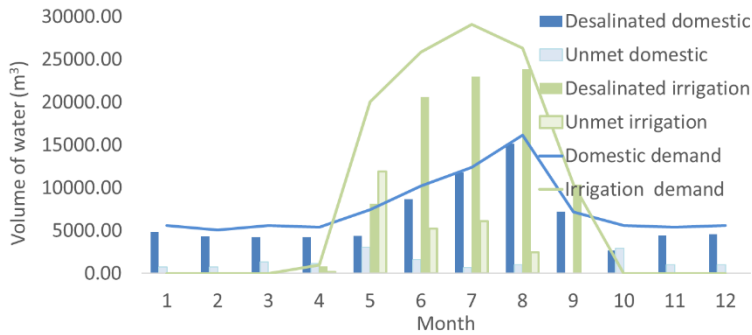

(a)
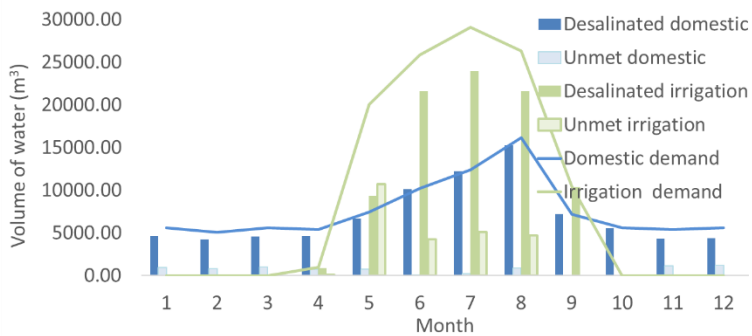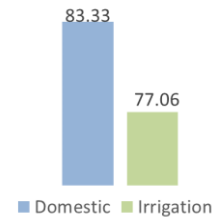
(b)
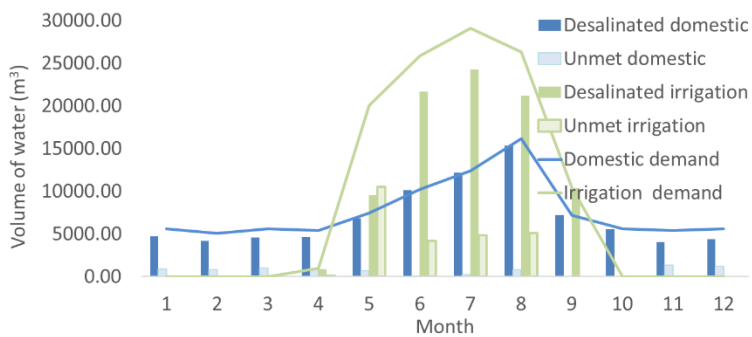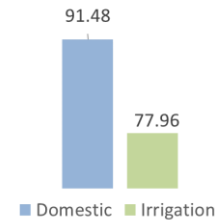
(c)
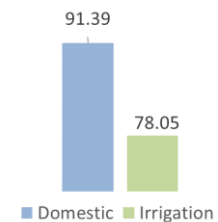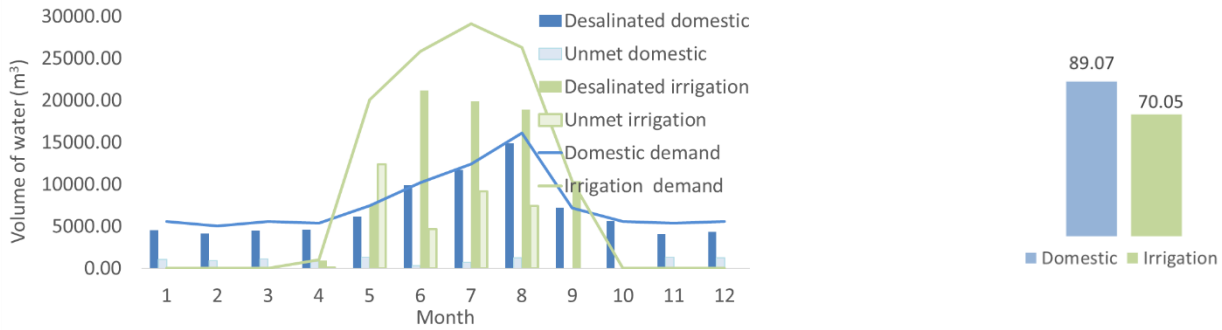
(d)
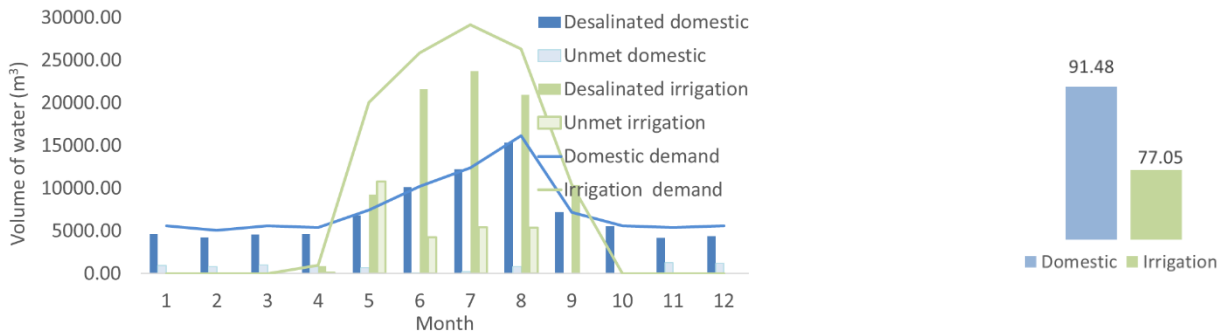
(e)
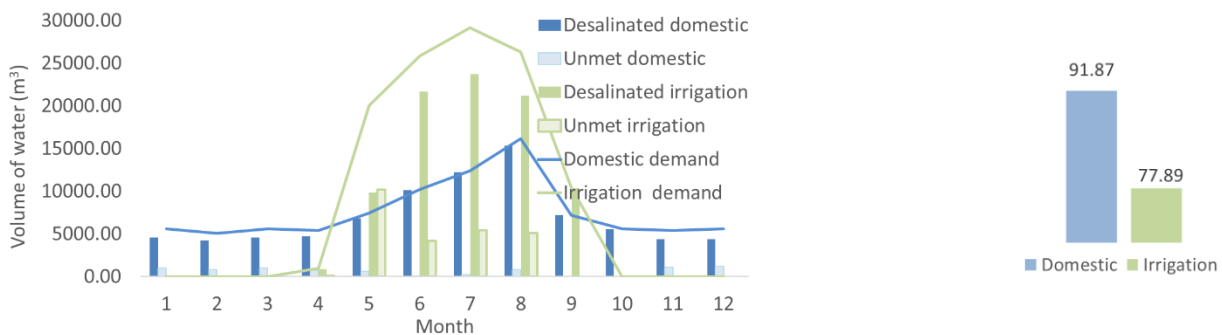
(f)

Figure 5-13 Satisfied and unsatisfied consumption and demand of domestic and irrigation water: (a) WT/DU/PHS; (b) WT/PV/DU/PHS; (c) WT/PV/DU/BT; (d) WT/PV/DU/FC; (e) WT/PV/DU/HPBS; (f) WT/PV/DU/HPHS

Figure 5-14 presents the hourly storage level of each storage technology over a year. For single storage configurations, it shows how each storage technology, the upper reservoir, the batteries and the hydrogen tank charge and discharge. Similarly, for hybrid storage technologies the charging and discharging of both storage media simultaneously is presented. It is demonstrated that in both WT/PV/DU/HPBS and WT/PV/DU/HPHS configurations, the batteries and hydrogen tank, respectively, start to discharge whenever the upper reservoir reaches its lowest level, delivering energy for the satisfaction of the unmet needs. The level of the batteries and the hydrogen tank

remains unchanged at times when the upper reservoir never reaches its lowest level. The operation of the LPS means that there are demands that have not been covered by the HRES and the upper reservoir, the batteries, or the hydrogen tank simultaneously has reached their minimum level. A comparison between Figure 4-12 (e) and (f) and Figure 4-14 (e) and (f) shows that LPS starts to operate every time both the upper reservoir and batteries or hydrogen tank are at their minimum level of charge. Days that none of them reach their minimum level means that no use of LPS is observed, no conventional fuels are used and the island is fully autonomous.
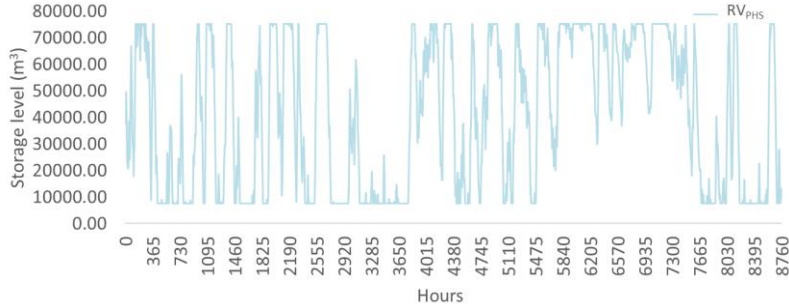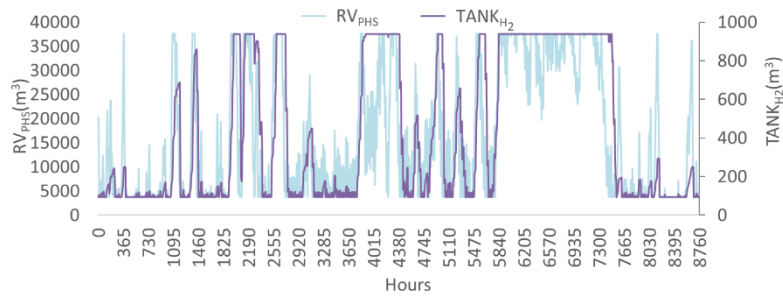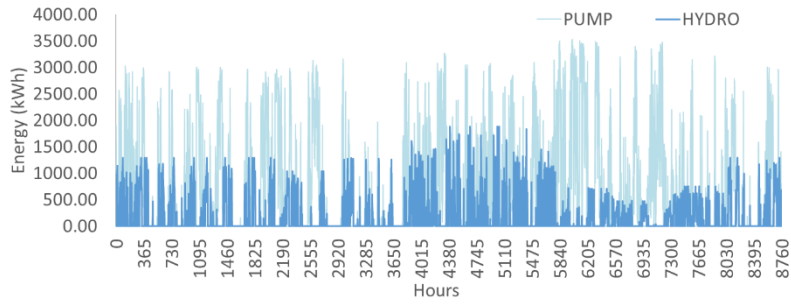

(a)
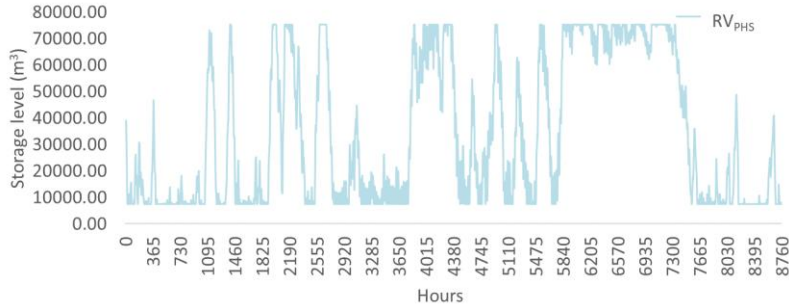
(b)
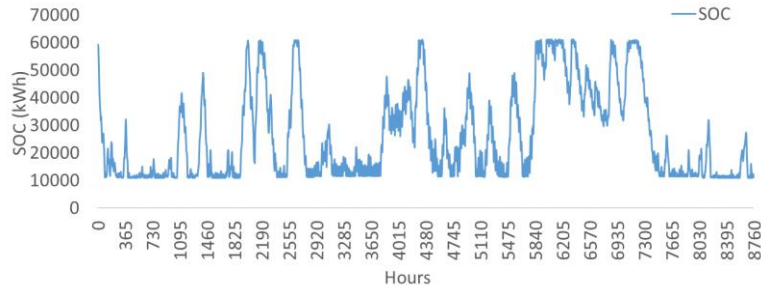
(c)
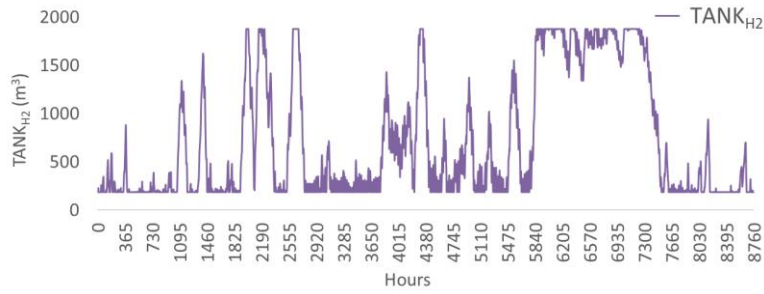
(d)
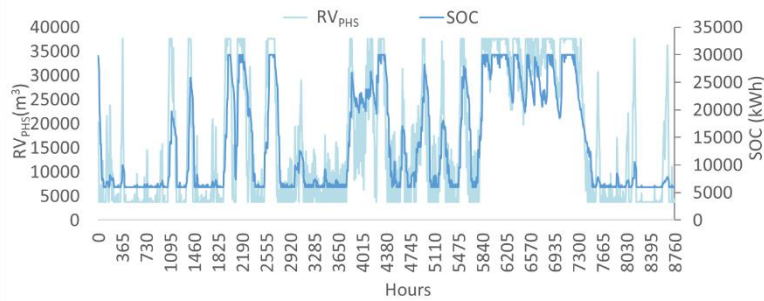
(e)

(f)

Figure 5-14 Storage level: (a) WT/DU/PHS; (b) WT/PV/DU/PHS; (c) WT/PV/DU/BT; (d) WT/PV/DU/FC; (e) WT/PV/DU/HPBS; (f) WT/PV/DU/HPHS

This study examines HRES coupled to various storage systems, including PHS, a battery, a hydrogen tank, or a combination among them. The energy used to desalinate water in order to meet domestic and agricultural needs is included in the HRESs under examination. The energy used in the pump station for the pumping and storing of water in the upper reservoir is another factor in HRESs with a PHS storage system. These hourly consumptions are depicted in Figure 5-15 (a), (b), (e), and (f) over the period of a year (legend PUMP). The hydro turbine's hourly energy output is displayed concurrently (legend HYDRO). Additionally, after pumping, there is energy that is not used, either because the pumps are unable to utilize it or because the upper reservoir is full and cannot store any more water. The batteries (legend SOC) in WT/PV/DU/HPBS and the electrolyzer (legend EL) in WT/PV/DU/HPHS receive the unexploited energy and use it to produce hydrogen. This energy is also

used for the amount of energy that is required to desalinate seawater so that it can be utilized for electrolysis in the WT/PV/DU/HPHS configuration. In configurations (e) and (f) with the hybrid storage, the lines of SOC and EL show the energy used by the batteries and electrolyzer, respectively, and also represent the energy that cannot be utilized in the single storage HRESs. In the case of an energy deficit, the lines of BT and FC represent the energy generated by the batteries and fuel cells, respectively. SOC, BT, EL and FC in Figure 5-15 (c) and Figure 5-15 (d) have a similar mode of operation with the only difference that here all the excess energy from the WTs and the PVs is sent to the batteries and the electrolyzer after the initial coverage of the demands.

The energy generated by the three different storage technologies, PHS, BT, and FC, follows a similar pattern in the systems' attempt to fulfill the energy requirements, as illustrated in Figure 5-15 (b), (c), and (d). Additionally, it is demonstrated that the energy generated by the PHS, BT, and FC systems is typically lower than the energy needed to operate the pumps, charge the batteries, and operate the electrolyzer (EL) to produce hydrogen. Even so, the idea behind an HRES is to store generated energy from RES that cannot be utilized immediately and use it at high demand periods where the startup of the LPS and subsequently the consumption of fossil fuels is the alternative solution. The different behavior of PHS, BT, and FC storage technologies, as shown in Figure 5-10, can be explained by the fact that the energy needed by the electrolyzer for hydrogen production also includes the energy needed for the desalination of the water being used. For FC storage configuration, LPS's contribution is increased throughout the year. The energy used to pump and charge the batteries seems to be more than the energy consumed during desalination in WT/PV/DU/FC. However, in the comparison between the two configurations with hybrid storage, it is observed a greater contribution of FC compared to BT, and therefore a reduced use of LPS in the case of hydrogen compared to batteries. A possible explanation is that in hybrid storage there is less and less frequent use of the secondary storage technology, FC or BT, so the time the battery is idle leads to more energy loss due to battery discharge and depends on the self-discharge rate, σ, of the battery.

Results about the initial cost, the operation and maintenance cost, the cost of energy and water, the payback period, the loss of load probability of each demand and the whole HRES, the eliminated CO_2 quantities and CO_2 price are presented in Table 5-2 for single storage technology and in Table 5-3 for hybrid storage technology. The future increase in the price of kWh does not affect COE, as COE is affected only by initial cost, operation and maintenance costs and salvage cost, and also by the energy that is produced by the HRES. However, an increase in the price of energy will make such projects more competitive, by reducing the selling price gap.
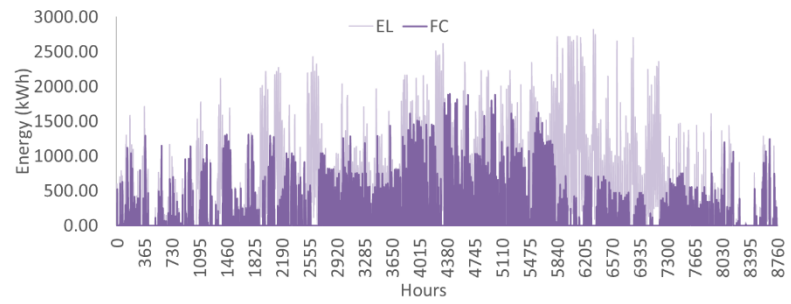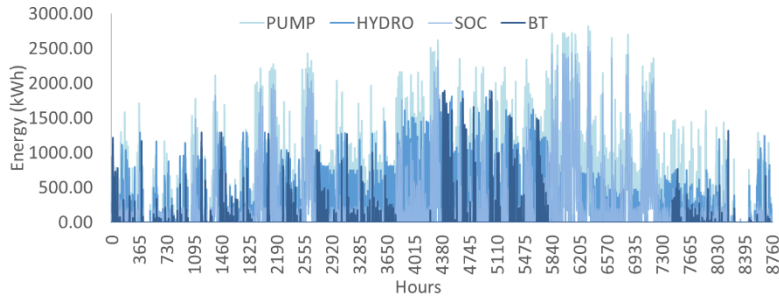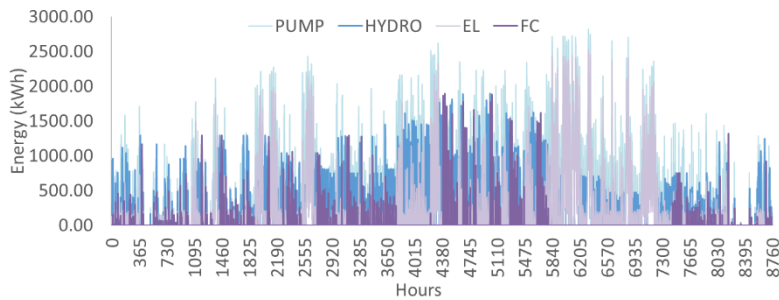
(a)
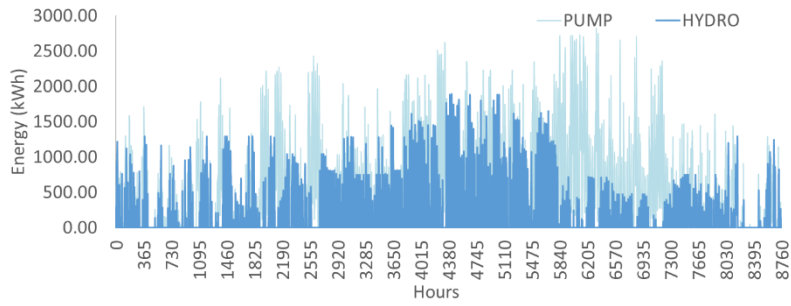
(b)
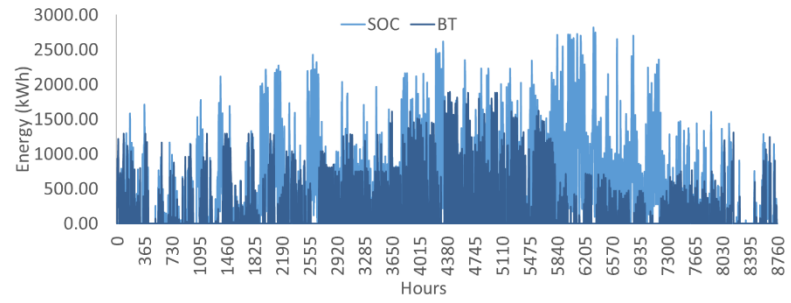
(c)

(d)

(e)

(f)

Figure 5-15 Consumed and produced energy: (a) WT/DU/PHS; (b) WT/PV/DU/PHS; (c) WT/PV/DU/BT; (d) WT/PV/DU/FC; (e) WT/PV/DU/HPBS; (f) WT/PV/DU/HPHS

Comparisons between single storage technologies, Table 5-2, show that PHS configurations have a lower initial cost, however, O&M costs are reduced in the case of hydrogen storage. Also, between WT/DU/PHS and WT/PV/DU/PHS, the second configuration has lower O&M costs. So, it is observed that with the introduction of PV over WT, the cost is considerably reduced, which means that further WT replacement can also lead to lower energy and water prices. So, the comparison also depends on the LOLP of each HRES. Also, the highest initial cost is seen in the case of the battery storage system. All of the above are factored into the final COE and COW values. The lowest value is observed in the WT/PV/DU/PHS, followed by the WT/PV/DU/FC, WT/DU/PHS and finally the WT/PV/DU/BT. Consequently, the same sequence is followed for PBP. However, the lowest LOLP values are observed in WT/PV/DU/PHS and the maximum in WT/PV/DU/FC, concluding that in simple storage the WT/PV/DU/PHS configuration is overall superior. The configuration, which consists only of WTs gives better results in terms of CO_2 quantities and the penalty from the Emissions Trading System, even though the emission factor of solar technologies is higher compared to wind technologies. This happens because the contribution of the respective storage technology is also important in the final energy mix.

Table 5-2 Economic, environmental and reliability analysis for single storage configurations

Key Parameter	WT/DU/PHS	WT/PV/DU/PHS	WT/PV/DU/BT	WT/PV/DU/FC
$Initial\ cost$ [€]	16,652,335	16,690,685	24,937,252	22,510,192
$O\&M\ cost$ [€]	735,035	513,534	508,261	299,102
COE [€/kWh]	0.262	0.215	0.281	0.241
COW [€/m^3]	1.532	1.257	1.643	1.408
$LOLP_{hres}$ [%]	22.79	21.74	21.90	25.57
$LOLP_{el}$ [%]	23.73	23.08	23.25	26.51
$LOLP_d$ [%]	13.49	8.47	8.61	10.93
$LOLP_{ir}$ [%]	22.80	21.81	21.95	20.95
PBP [years]	13.59	11.18	14.26	12.05
EM_{CO_2} [tn/year]	2,323.56	2,286.37	2,282.54	2.175.48
$EM_{CO_2}\ price$ [€]	206,634.42	203,326.79	202,986.69	193.465.41

Table 5-3 Economic, environmental and reliability analysis for hybrid storage configurations

Key Parameter	WT/PV/DU/HPBS	WT/PV/DU/HPHS
$Initial\ cost$ [€]	23,083,058	28,378,818
$O\&M\ cost$ [€]	525,898	423,220
COE [€/kWh]	0.267	0.292
COW [€/m^3]	1.561	1.705
$LOLP_{hres}$ [%]	21.74	21.33
$LOLP_{el}$ [%]	23.02	22.66
$LOLP_d$ [%]	8.50	8.11
$LOLP_{ir}$ [%]	22.32	21.47
PBP [years]	13.77	10.87
EM_{CO_2} [tn/year]	2,285.26	2,297.24
$EM_{CO_2}\ price$ [€]	203,227.94	204,293.25

Comparisons between hybrid storage technologies, Table 5-3, show lower initial costs in WT/PV/DU/HPBS, but lower maintenance costs in WT/PV/DU/HPHS. Finally, concerning COE and COW, the lowest values are achieved when batteries are combined with PHS. However, as the choice must be made in conjunction with the LOLP values, lower LOLP values but also a shorter PBP are observed in the hybrid configuration consisting of PHS and hydrogen storage technology. In terms of CO_2 quantities and the penalty from the Emissions Trading System, WT/PV/DU/HPHS presents better results. Between simple and hybrid storage, lower LOLP values are given by the hybrid storage, however, energy and water prices are comparatively higher than in the single storage options.
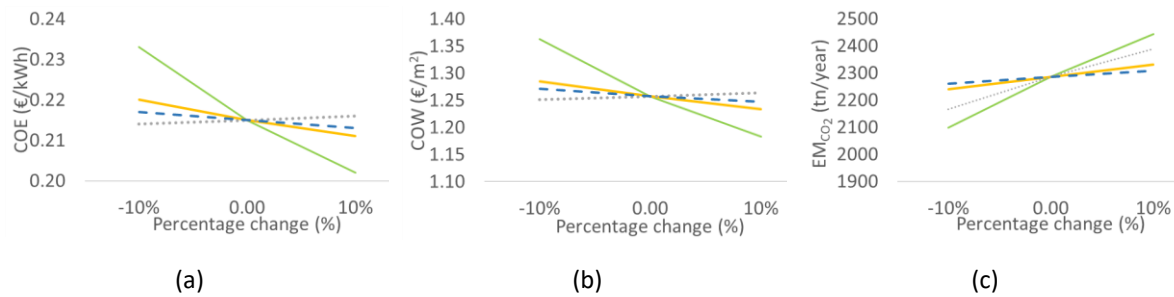
5.2 Sensitivity analysis

5.2.1 Between single storage technologies

A sensitivity analysis is conducted between two single storage configurations, WT/PV/DU/PHS and WT/PV/DU/FC based on certain key parameters. The comparison between these two configurations shows how each of them is affected by each key parameter. Key parameters refer to the installation height of the WTs, meteorological data such as wind speed and solar radiation, and the population of the island. Every parameter is examined in the context of an increase and a decrease of 10% in order to show the relationship between the change in the key parameter's value and the six energy, economic and environmental indices that are calculated, COE, COW, EM_{CO_2}, PBP, use of the storage technology (PHS or FC) and LOLP$_{hres}$. Table 5-4 and

Table 5-5 present results for PHS and FC storage technologies respectively. Also, in Figure 5-17 the corresponding graphical results are depicted.

Table 5-4 Sensitivity analysis results for WT/PV/DU/PHS

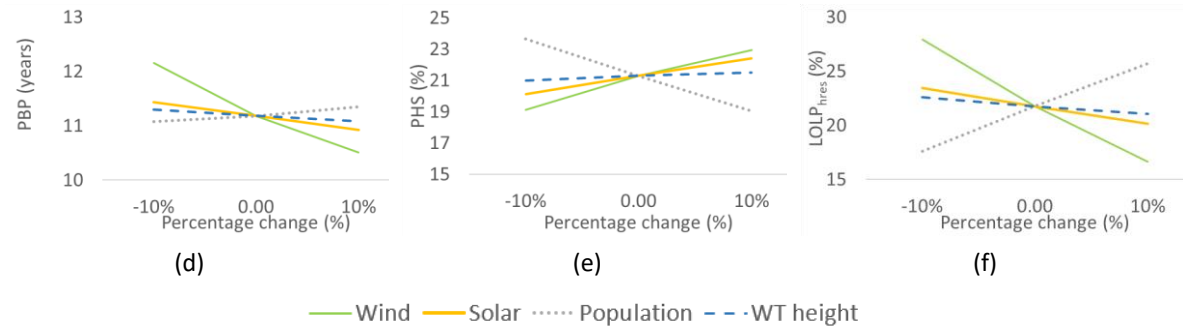| Key parameter [WT/PV/DU/PHS]	COE [€/kWh]	COE [€/m²]	EM_{CO_2} [tn/year]	PBP [years]	PHS [%]	$LOLP_{hres}$ [%]
Wind [-10%]	0.233	1.363	2097.16	12.50	19.13	27.93
Wind [+10%]	0.202	1.183	2443.10	10.80	22.94	16.65
Solar [-10%]	0.220	1.285	2239.07	11.75	20.12	23.47
Solar [+10%]	0.211	1.233	2330.27	11.18	22.42	20.14
Population [-10%]	0.214	1.251	2166.56	11.18	23.64	17.62
Population [+10%]	0.216	1.264	2387.57	11.79	19.04	25.69
WT height [-10%]	0.217	1.271	2260.44	11.62	20.98	22.59
WT height [+10%]	0.213	1.247	2307.49	11.39	21.49	21.06

(a)   (b)   (c)

Figure 5-16 Sensitivity analysis graphical results for WT/PV/DU/PHS

Table 5-5 Sensitivity analysis results for WT/PV/DU/FC

| Key parameter [WT/PV/DU/FC]	COE [€/kWh]	COE [€/m²]	EM_{CO_2} [tn/year]	PBP [years]	FC [%]	$LOLP_{hres}$ [%]
Wind [-10%]	0.260	1.519	1986.66	13.19	15.33	31.75
Wind [+10%]	0.226	1.321	2331.15	11.28	19.12	20.19
Solar [-10%]	0.243	1.423	2132.62	12.21	16.48	27.13
Solar [+10%]	0.239	1.396	2212.50	11.94	18.38	24.21
Population [-10%]	0.244	1.429	2063.39	12.17	19.71	21.57
Population [+10%]	0.239	1.400	2267.95	12.07	15.31	29.45
WT height [-10%]	0.243	1.422	2149.67	12.19	17.18	26.41
WT height [+10%]	0.239	1.396	2197.71	11.95	17.73	24.84
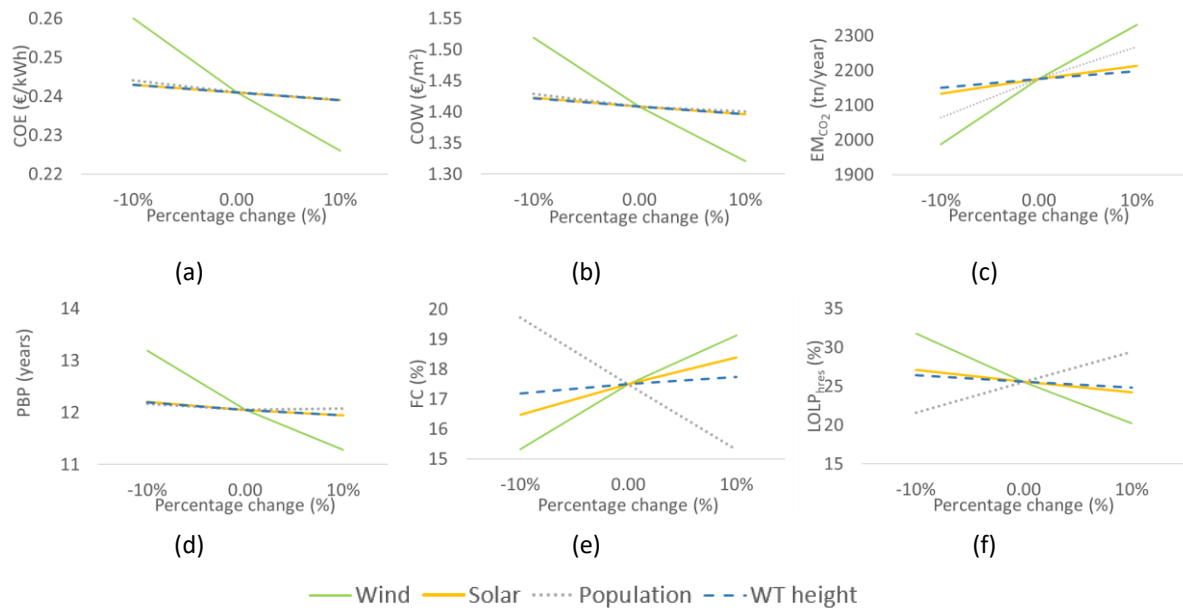
Figure 5-17 Sensitivity analysis graphical results for WT/PV/DU/FC

For both configurations, COE is affected more by the changes in the wind potential. This is explained by the fact that COE depends on annual renewable energy production. Although the installed capacity of WTs is lower than this of PVs, WTs have a higher share in the energy production than PVs possibly because of the higher wind potential of the island. Also, the increase in wind potential influences less intensively compared to its decrease. This occurs possibly because the increase in wind potential does not mean the production of more energy. Every WT has a $u_{cut-out}$ and if the wind velocity exceeds $u_{cut-out}$, the WT stops operating for security reasons. Moreover, COE is affected more intensely in WT/PV/DU/FC by the variation in the population, compared to the WT/PV/DU/PHS. It is noteworthy that COE is more influenced by the variation in population in the WT/PV/DU/FC. This is possibly related to the months of autonomy of each system. As WT/PV/DU/PHS gives more days of autonomy, any variation in the population will have a higher impact on the WT/PV/DU/FC configuration, which does not show the same reliability in autonomy. However, the population affects more the PBP in WT/PV/DU/PHS. Changes in population mean changes in demand, in the dimensioning of the upper reservoir, the hydro turbine and in the desalination unit and finally in changes in the initial and operation and maintenance costs. The wind potential has a greater impact on EM_{CO_2}. Although the emission factor of WT is lower, as explained above, WTs have a higher share in energy production and that makes EM_{CO_2} to be more affected by wind speed fluctuations. Also, wind potential affects more intensely WT/PV/DU/FC, as far as EM_{CO_2} is concerned. Furthermore, it can be observed that in both configurations the increase in population increases EM_{CO_2}. This may be explained by the fact that in this methodology framework, RES is given directly to the system to meet water energy demands before storing excess energy. A portion of this percentage is discarded when there is no storage space available. When the population, and therefore the demands increase, then this rejected energy decreases and more RES is utilized by the HRES. Therefore, the eliminated CO_2 quantities increase. It is also remarkable that the slope of the wind potential and the population is steeper for the contribution of the FC in the WT/PV/DU/FC configuration than for the contribution of the PHS in the WT/PV/DU/PHS configuration. This may be explained by the fact that the pumps maybe cannot handle all the excess energy, due to their installed capacity, in contrast with WT/PV/DU/FC where the variation in the wind potential and the population has a better response according to the hydrogen tank capacity. Also, in WT/PV/DU/PHS, the LPS is operating less than in WT/PV/DU/FC, where enough energy is consumed in the desalination of the water that is required for the electrolysis. The same is depicted for the LOLP$_{hres}$, which is affected more in the WT/PV/DU/FC. This is expected since the same behavior is observed in the storage unit between the two configurations. The order of classification, for both configurations and the four criteria, is the wind potential, the population and then the solar potential and the WT installation height. For both configurations, while the results are proportional to the wind and solar potential, they are inversely proportional to the population. As the population increases, demands increase, and therefore, a

larger initial amount of produced RES is intended to meet water and electricity needs before the excess is led to one of the storage technologies.

5.2.2   Between single and hybrid storage technologies

A corresponding sensitivity analysis is conducted based on the same key parameters between a single, WT/PV/DU/PHS, and a hybrid, WT/PV/DU/HPHS, storage configuration. Table 5-6 presents results for the WT/PV/DU/HPHS configuration and Figure 5-18 shows the corresponding graphical results.

The height of the wind turbines affects the wind speed that is exploited by the wind turbines and generally the speed measured at the hub height affects the produced wind energy. As shown in Fig 4-16 (a) and Fig, 4-18(a), an increase in the installation height of the wind turbines means higher wind energy production., therefore the cost of both energy and water is reduced, while EMCO2 quantities and contribution of the storage units are increased. Additionally, $LOLP_{hres}$ decreases as with more wind energy produced, more demands are expected to be met. For the same reason, PBP also decreases with the increase of WT installation height. While COE and COW are proportional to both models, in the case of LOLP, WT/PV/DU/HPHS is more affected by the changes in wind turbine installation. This is to be expected, as there is an additional storage unit, that of hydrogen. Also, as has been stated previously, all the demand for irrigation water is concentrated in the night hours and, as the remaining demands are reduced, the possible increase in wind energy production at night due to the installation of wind turbines at a greater height leads to the greater coverage of irrigation needs. This is more intense, especially when there is a second storage system, that of hydrogen, which acts as a backup. Additionally, the possible reduction in the total wind energy produced at night will lead to less coverage of the irrigation needs and if there is no second storage system from where uncovered energy can be exploited, the $LOLP_{ir}$ will increase more intensely, resulting in a more intense increase of the total $LOLP_{hres}$. Moreover, the comparison between WT/PV/DU/PHS and WT/PV/DU/PHS shows that the PHS has a different behavior than FC in changes of wind potential. Although the behavior of PHS is proportional to both increases and decreases in wind potential, the behavior of FC fluctuates. An increase in wind potential leads to a less intense increase in the FC contribution. This possibly happens as an increase in wind potential implies an increase in produced RES and therefore mode demands are covered. This means that a smaller amount of energy is sent to storage, so the second storage unit is used less. Such behavior is not observed by the changes in the solar potential, possibly because better wind speeds prevail on the island throughout the year compared to solar radiation.

Table 5-6 Sensitivity analysis results for WT/PV/DU/HPHS

| Criteria [WT/PV/DU/HPHS]	COE [€/kWh]	COE [€/m²]	EM_{CO_2} [tn/year]	PBP [years]	PHS [%]	FC [%]	$LOLP_{hres}$ [%]
Wind [-10%]	0.313	1.831	2114.18	11.69	16.11	3.61	27.35
Wind [+10%]	0.275	1.609	2445.84	10.28	18.66	4.38	16.55
Solar [-10%]	0.295	1.726	2253.83	10.98	16.76	3.87	22.95
Solar [+10%]	0.288	1.687	2337.88	10.75	18.50	4.18	19.86
Population [-10%]	0.294	1.720	2176.18	10.86	19.49	4.52	17.25
Population [+10%]	0.291	1.704	2400.62	10.96	15.75	3.70	25.29
WT height [-10%]	0.294	1.719	2274.88	10.96	17.52	3.95	22.07
WT height [+10%]	0.289	1.692	2318.74	10.79	17.82	4.06	20.64
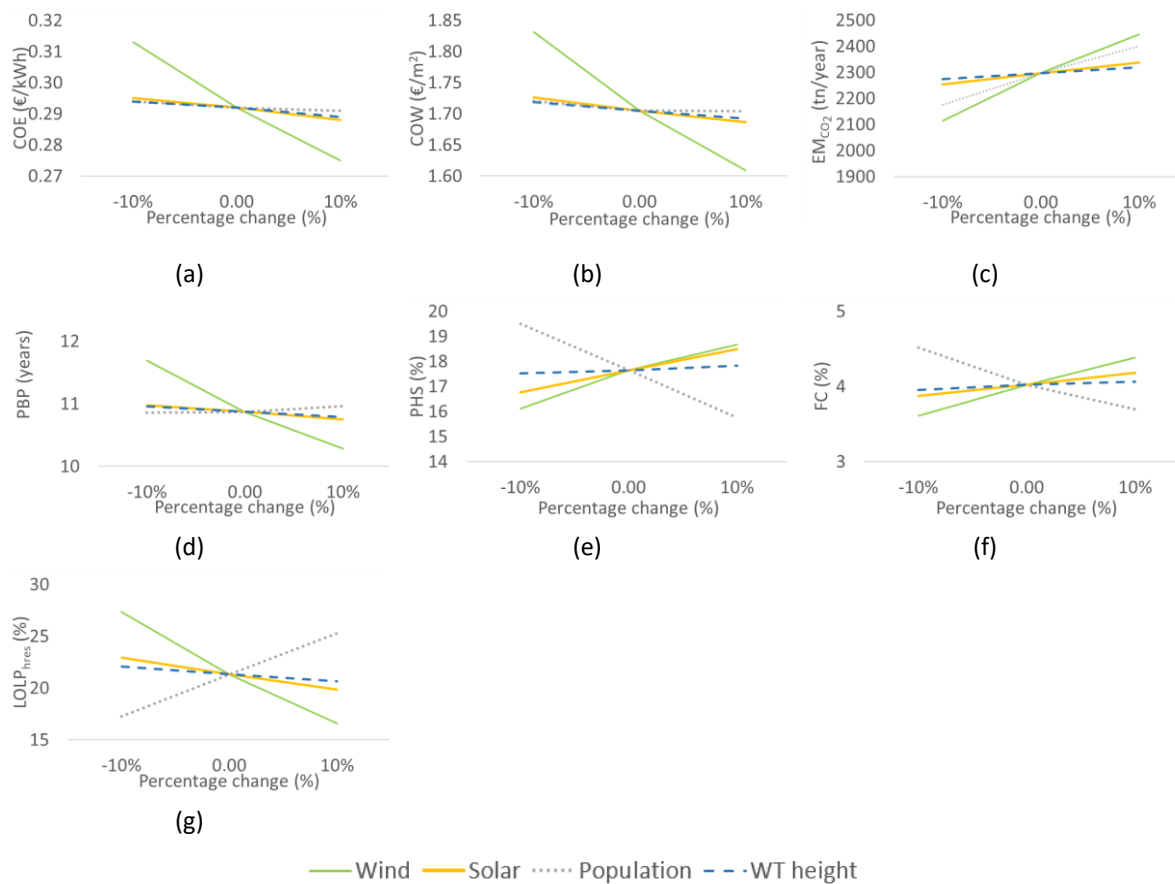
Figure 5-18 Sensitivity analysis graphical results for WT/PV/DU/HPHS

Also, variations in population and therefore the electrical and water demands, lead to a different behavior of COE and COW between simple and hybrid storage systems. Population changes are proportional to COE and COW changes for WT/PV/DU/PHS, however in WT/PV/DU/PHS changes in population are inversely proportional to COE and COW values. This behavior may be explained by the fact that the COE and COW depend on both the operation and maintenance costs and the energy produced by the HRES. And in the case of hybrid storage, the operation and maintenance costs are reduced and the energy produced is more due to the HRES's capability in storing more RES. Therefore, a better price is achieved in energy and desalinated water by the increase in demands. Finally, population variations lead to more intense changes in PBP and $LOLP_{hres}$ in the case of single compared to hybrid storage. However, if a comparison is made between WT/PV/DU/FC and WT/PV/DU/HPHS, it is observed that the $LOLP_{hres}$ changes are more intense in the second configuration, leading to the conclusion that the final choice of storage technology depends not only on the initial criteria of COE or COW or LOLP, but also changes in installation criteria, meteorological data and demand data must always be taken into account.

This chapter is based on the publication "M. Bertsiou, E. Baltas, Management of energy and water resources by minimizing the rejected renewable energy, Sustainable Energy Technologies and Assessments, Volume 52, 102002, 2022, https://doi.org/10.1016/j.seta.2022.102002M"

6.1   Methodology framework

In this section a methodology for estimating and minimizing the amount of rejected RES energy is presents and it is based to the work by Bertsiou and Baltas (2022b). The HRES has a wind PHS system with a 3.6 MW wind park, an 80,000 m^3 upper reservoir, a 1 MW pumping station, a 1.30 MW hydro turbine, and a 500 m^3/day desalination unit. Using 8760 data for one year of wind speeds, household consumption, domestic water and agricultural water demands, the HRES system is designed to fulfill water and electricity needs. Two scenarios are examined for the evaluation of the hybrid system. In the first scenario (case I), a portion of the energy generated by wind is supplied directly to the grid to meet its electricity needs, while the remaining energy is directed toward desalination and pumping. Domestic water desalination is given the highest priority. Any extra energy is used to pump water to the upper reservoir, with the remaining going toward desalinating irrigation water. A different plan is used in the second example (case II). The amount of wind energy produced is distributed into predefined percentages for desalination and pumping, while the remaining is provided straight to the system for electrical demands. Again, meeting domestic water supply demands is given the highest priority, with agriculture water supply needs coming second. No matter how much water is desalinated, it is assumed in both situations that the desalination reservoir has enough volume to store the desalinated water.

Using their own input data, any other isolated island that experiences a lack of energy or fresh water can easily adopt the proposed methodological framework. This will promote RES and lead to water independence because rejected RES will be assessed and further utilized depending on the direct penetration of wind energy into the system and the percentage of excess energy designated for desalination and pumping. Also, excess energy can be used to operate a second desalination plant, which will store additional desalinated water for later use. This desalinated water can be utilized for domestic and agricultural needs as well as the generation of green hydrogen, a new technology to replace conventional fuels and help combat global warming by reducing the overall quantity of CO_2 emissions to the atmosphere. The suggested framework can be used as a tool for planning by energy managers, decision-makers, and policy-makers to decide how to operate a hybrid system with the least amount of energy rejected.

Pumping water consumes a large amount of energy and wind energy technologies promise an alternative way to perform this operation without any energy cost. Also, such systems provide good reliability along with the outcome of optimum utilization of clean water (Poompavai & Kowsalya, 2019). The higher flexibility of small wind energy systems is prominent in these systems (Ram et al., 2017). Also, hydropower is the most important component of such systems, as it provides increased system efficiency as well as greater balance in energy supply (Mamassis et al., 2021). In addition, the implementation of energy storage systems achieves higher RES penetration and utilization, affects the total emissions of carbon dioxide (CO_2) to the atmosphere and minimizes the total amount of required water by the electricity generating facilities (Ogland-Hand et al., 2019). However, a percentage of produced wind energy cannot be utilized immediately, due to technical constraints (AL Ahmad & Sirjani, 2021) that are imposed by the LPS (Farrokhifar, 2016) and the limited size of the systems (Papaefthymiou & Papathanassiou, 2014), but neither can be stored, due to the volume of the upper reservoir and is being rejected. There are three sources of rejected renewable energy in an HRES. The first source depends on the percentage of wind energy that directly penetrates to the grid. This could be zero on days or hours when there is a lot of demand for electricity or low wind potential. However, is over zero and this excess energy is rejected when there is increased demand for electricity or high wind potential. The second source of rejected energy is associated with the pumping station and pump selection The second one is determined by the pumping station and pump selection. This energy is rejected if there is insufficient energy available for the pumps to function. The third source depends on the size of the upper reservoir. Despite the upper reservoir's size (Kaldellis et al., 2001) is based on the island's needs and the number of autonomy days, however, there will be days during the system's operation when excess pumped water must be rejected. This rejected water from the upper reservoir is converted into rejected energy. Energy storage technologies typically allow for two days of autonomy in an HRES (Bhandari et al., 2015).

After the data collection, the algorithm for the two operation schemes of the HRES is created and is analyzed in the following steps for each case. Figure 6-1 shows the algorithm for Case I is presented in, while Figure 6-2 shows the part of the algorithm that is being replaced for the second case. The dashed line in Figure 6-1 indicates this replacing part of the algorithm for the evaluation of Case II.

6.1.1 Rejected energy based on the direct penetration of wind energy

The flow chart of the algorithm for Case I is presented in Figure 6-1 and is followed for t=1-8760.

1. Based on the power curve of the installed wind turbines, the number of the installed WTs and the wind speed u_2 at hub height, the total amount of wind energy E_{wind} is calculated. It is supposed that 4 wind turbines of 900kW each.

2. Based on the percentage of direct penetration of wind energy in the network p_{dir}, unmet electricity needs D_{rem} are calculated.

If $(D_{tot} - p_{dir} \cdot E_{wind}) \geq 0$ then

$D_{rem} = D_{tot} - p_{dir} \cdot E_{wind}$ else

$D_{rem} = 0$, where D_{tot} the total amount of electricity needs in kWh.

3. Rejected energy due to the percentage of direct penetration of wind energy REJ_{dir} is calculated:

If $(p_{dir} \cdot E_{wind}) > D_{tot}$ then

$REJ_{dir} = p_{dir} \cdot E_{wind}$ else

$REJ_{dir} = 0$

4. The remaining energy for desalination and pumping is calculated:

$E_{rem} = (1 - p_{dir}) \cdot E_{wind}$

5. The desalination of the domestic water is the priority. After determining the energy required for the desalination of domestic water E_{desw}, the remaining energy needed to desalinate irrigation water E_{desir} is calculated:

$E_{desir} = E_{rem} - E_{desw}$,

where If $(D_w \cdot E_{RO}) \geq E_{rem}$ then

$E_{desw} = E_{rem}$ else

$E_{desw} = D_w \cdot E_{RO}$,

where D_w the total amount of desalinated domestic water.

6. After determining the energy needed to desalinate irrigation water E_{desir}, then remaining energy needed for the operation of the pumping station E_{pump} is determined:

$E_{pump} = E_{desw} - E_{desir}$,

where if $(D_{ir} \cdot E_{RO}) \geq E_{desir}$ then

$E_{desir} = E_{desw}$ else

$E_{desir} = D_{ir} \cdot E_{RO}$,

where D_{ir} the total needs of desalinated irrigation water.

7. The pumping station, which has four different pumps of varying capacities, is how E_{pump} is used. After the operation of the previous pump, it is checked whether the remaining energy E_{prem}^{i-1} after the operation of the previous pump is sufficient for the operation of the next pump and energy that can be utilized E_p^i is determined. This procedure is followed for each pump i.

If $E_{prem}^{i-1} \geq P_{pump}^i \cdot n_{pump}^i \cdot t$ then

$E_p^i = P_{pump}^i \cdot n_{pump}^i \cdot t$ else

$E_p^i = 0$

For the first pump (i=1), $E_{prem}^{i-1} = E_{pump}$

P_{pump}^i is the power and n_{pump}^i is the efficiency of each pump.

8. Rejected energy due to the pumping station REJ_{pump} is calculated after the operation of the last pump j:

$REJ_{pump} = E_{prem}^{i-1} - E_p^j$

9. In the end, the volume of the pumped water for each pump V_{pump}^i is calculated:

$V_{pump}^i = E_p^i \cdot n_{pump}^i / (\rho \cdot g \cdot H_{pump}^i)$

where ρ is water density in kg/m³, g is gravity acceleration in m/sec² and H_{pupmp} is the net head in m.

10. Total volume through pumping each time step t is:

$V_{tot}(t) = \sum_{i=1}^{j} V_{pump}^i(t) + V_{av}(t-1)$,

where V_{av} is the available volume in the upper tank after the operation of the turbine and the rejection of the exceeded volume in previous time step $t-1$ and is calculated in step 12.

11. After the operation of the turbine, it is checked whether the remaining water in the upper reservoir V_{up} exceeds the reservoir's capacity V_{cap} and rejected volume V_{rej} is calculated:

If $V_{up} \leq V_{cap}$ then

$V_{rej} = 0$ else

$V_{rej} = V_{up} - V_{cap}$

12. V_{av} depends on the volume of water required $V_{req}(t)$ at each time step t for the coverage of the electricity needs of t.

If $V_{req}(t) \leq V_{tot}(t) - V_{rej}(t)$ then

$V_{av}(t) = V_{tot}(t) - V_{rej}(t) - V_{req}(t)$ else

$V_{av}(t) = 0$

13. Rejected energy due to the reservoir REJ_{res} is calculated:

$REJ_{res} = \rho \cdot g \cdot H_{pump}^i \cdot n_{pump}^i \cdot V_{rej} / (3600 * 1000)$
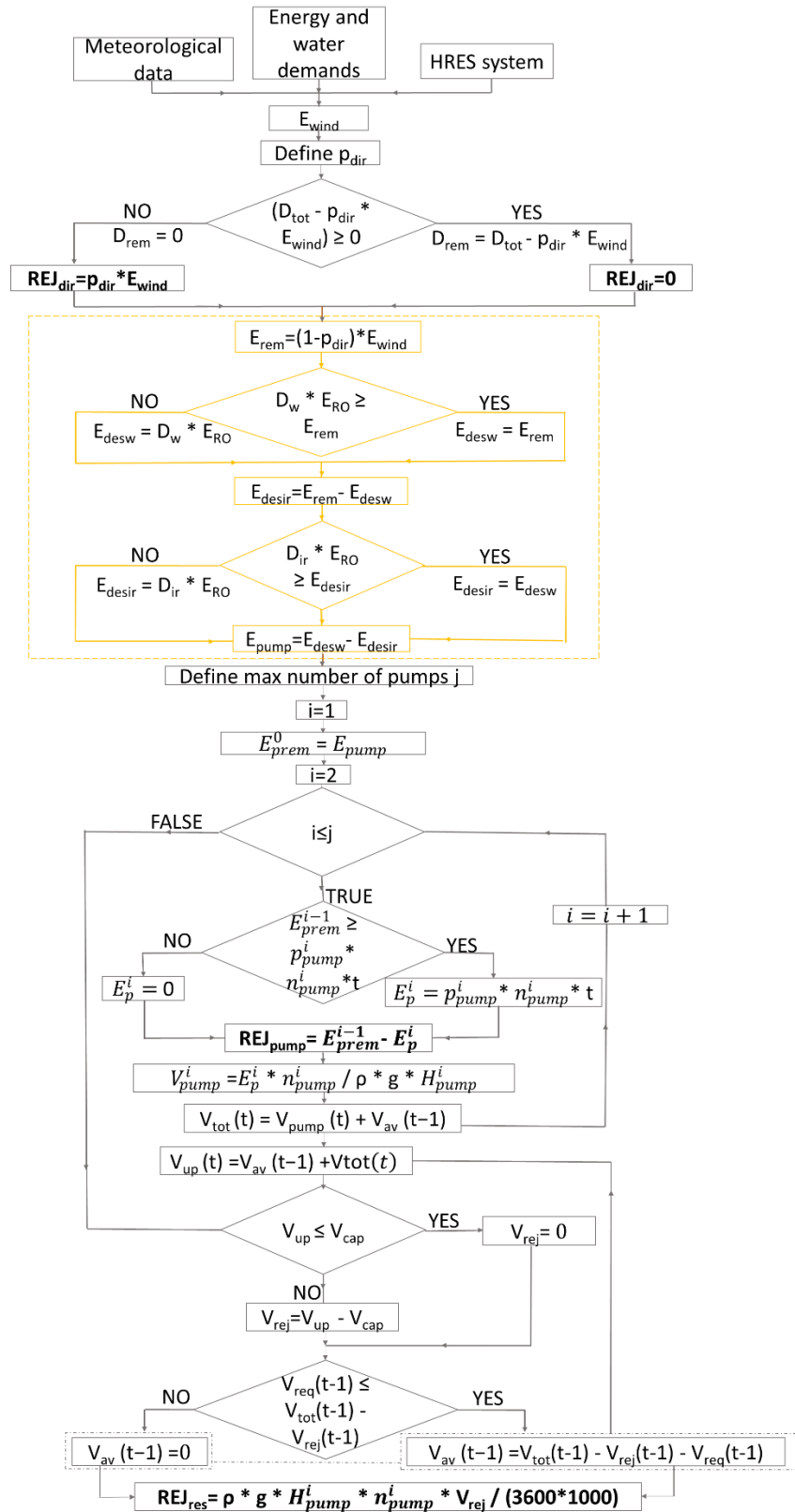
Figure 6-1 Flow chart of the algorithm for Case I

6.1.2 Rejected energy based on the percentage of energy set for desalination

The following procedures should be used in place of steps 4 through 6 in the second case, where the remaining percentage of energy that is not provided directly to the system for electrical demands is divided into predetermined percentages of energy for desalination and pumping. In Figure 6-2, the relating flowchart is depicted.
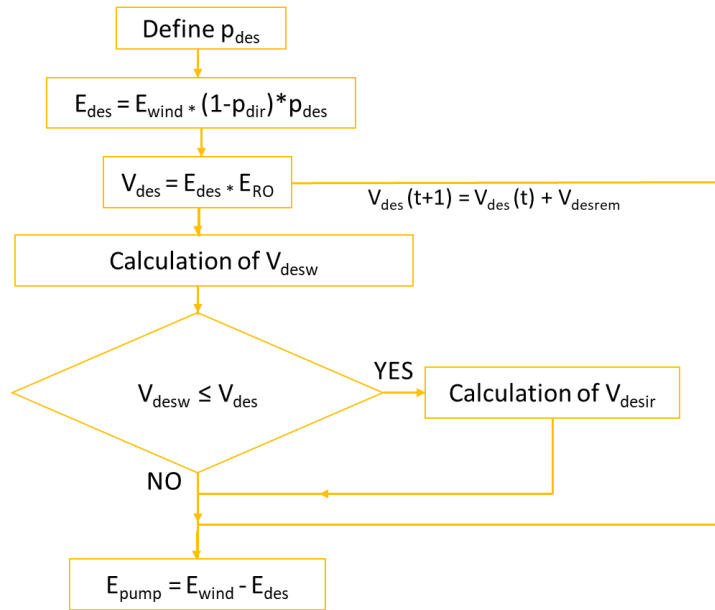

Figure 6-2 Flow chart of the algorithm for Case II

1. Energy for desalination E_{des} is:

   $E_{des} = [E_{wind}] \cdot (1 - p_{dir}) \cdot p_{des}$,

   where p_{des} is the percentage of energy set for desalination.

2. The volume of desalinated water is:

   $V_{des} = E_{des}/E_{RO}$

3. The desalination of domestic water is prioritized. Volume of desalinated domestic and irrigation water, V_{desw} and V_{desir} are estimated to determine whether the water supply demand is met. The remaining volume of desalinated water V_{desrem} is added in the volume of the subsequent step $t + 1$, if both domestic and irrigation water demands are covered

   $V_{des}(t + 1) = V_{des}(t) + V_{desrem}$

4. Energy for pumping E_{pump} is:

   $E_{pump} = E_{wind} - E_{des}$

5. Step 8 of the algorithm from section 6.1.1 continues after the energy for pumping has been calculated

- 120 -

6.2   Results

The dimensions of the pumping system, the upper tank, and the percentage of direct wind energy penetration in the grid have an important impact on the rejected energy from an HRES. The total rejected RES energy for both CASES (I and II) is $REJ_{tot} = REJ_{dir} + REJ_{pump} + REJ_{res}$, where REJ_{dir} is the amount of rejected energy as a result of the direct wind energy penetration, REJ_{pump} is the energy rejected based on the capacity of the pumping station, and REJ_{res} is the energy rejected due to the upper reservoir.

6.2.1   Case I – Rejected energy based on the direct penetration of wind energy
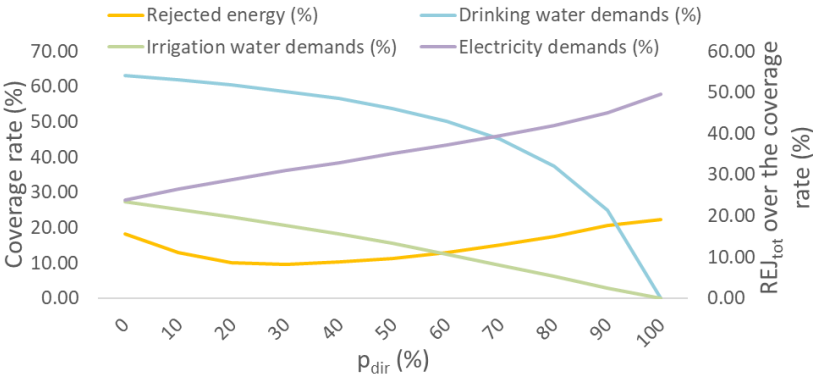
Figure 6-3 Coverage rate and REJ$_{tot}$ over the coverage rate related to p$_{dir}$ for Case I

In Figure 6-3, the percentage of direct energy to the grid can be selected based on the priority of the three demands that need to be fulfilled: domestic water, irrigation water, and electricity. If there is a higher demand for electricity, a different percentage of p_{dir} needs to be selected than if the priority is domestic or irrigation water. The trend of the electricity demand line is increasing, as p_{dir} is initially provided to fulfill electricity demand. On the other hand, water supply demand is prioritized over the energy produced by the hydro turbine, resulting in a downward trend compared to the increase of p_{dir}. If p_{dir} is set to 100%, irrigation needs will not be met, as it is the last priority in the proposed hybrid system. The proposed system's best performance seems to be at p_{dir} equal to 30%, resulting in the least amount of rejected energy. Figure 6-3 shows that a value of p_{dir} at 30% provides 60% fulfillment of domestic water, 21% fulfillment of irrigation water, and 31% fulfillment of household consumption of electricity. This performance indicates that the HRES is performing satisfactorily in relation to the fulfillment of the total demands.

The rejected energy per source (REJ_{dir}- REJ_{pump} -REJ_{res}) and the total rejected energy REJ_{tot} are both depicted in detail in Figure 6-4. For a variety of p_{dir} values, the rejected energy is minimized for

each source individually. REJ_{pump} increases by decreasing p_{dir} and is 0.00 for 100% p_{dir} and 76,526.42 for 90% p_{dir}. For p_dir values more than or equal to 50%, REJ_{res} is 0.00. When p_dir is less than 20%, REJ_{dir} is 0.00, and it increases as p_{dir} increases. However, for p_{dir} equal to 30%, the minimum value of REJ_{tot} is observed to be 196,652.35 kWh. As is to be expected, REJ_{dir} rises in tandem with p_{dir} because the more energy supplied directly to the grid, the more demands will be met until they are satisfied. Storage of energy is used to store excess wind energy. The downward trend of REJ_{pump} indicates that by increasing the energy given directly to the grid, less energy is left for the operation of the pumps in order to uplift water to the upper reservoir. This results in less wasted energy through the pumps.
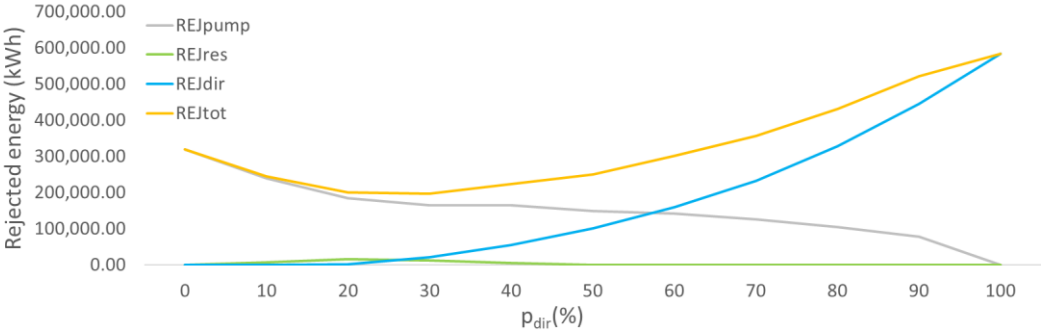

Figure 6-4 Rejected energy related to p_dir for Case I

To minimizing the REJ_{tot}, the rejected energy from each source is depicted in Figure 6-5 (a) when p_{dir} is set to 30 percent. Figure 6-5 (b) depicts a specific length of time in which a significant increase in REJ_{dir} and REJ_{res} is noticed.

The sudden increase in REJ_{dir} and REJ_{res} is the result of the low demand in September, Table 2-4, and the high wind potential at the same time, Figure 2-7 (b). Due to p_{dir} and the upper reservoir, the rejected energy appears to have reached its maximum capacity. In accordance with the wind potential and, consequently, the wind speed at the hub height of the wind turbines, REJ_{pump} seems to follow a constant waveform through the year, as it is depicted in Figure 6-5 (a).
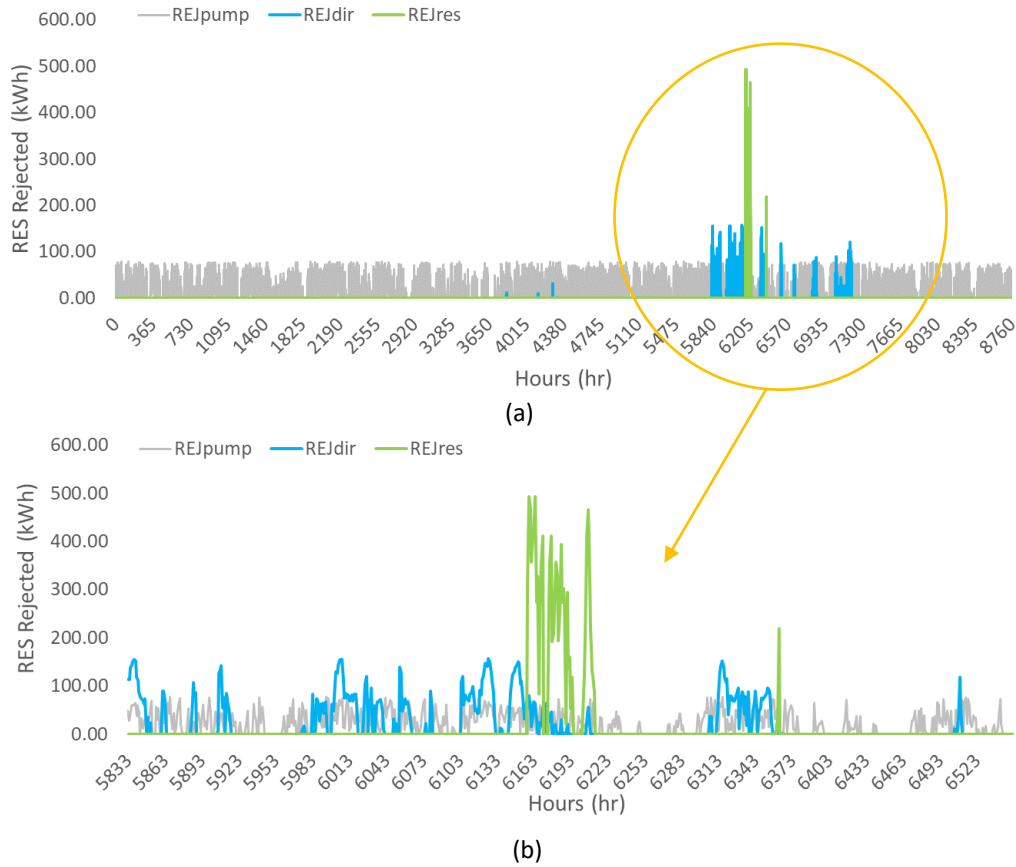
Figure 6-5 (a) Rejected energy by each source, (b) Detail

6.2.2   Case II – Rejected energy based on the percentage of energy set for desalination

In the second case, HRES's operational model is modified in accordance with the procedure in section 6.1.2. When p_{dir} is equal to 30%, REJ_{tot} is minimized, based on the findings of section 6.2.1. In this section, it is determined the amount of energy set aside for desalination, p_{des}, which yields the lowest possible value of REJ_{tot} for this case.

Figure 6-6 displays the minimizing of REJ_{tot} for p_{des} equal to 1 in conjunction with the examination of p_{des} and the coverage of the three demands (domestic water, irrigation water, and electricity). This indicates that there is no energy used for pumping and that the entire remaining portion of energy (70%) is used for desalination. As there is no potential for storing, this goes against the HRES's basic operating principle. Drinking and irrigation water demands are completely met for p_{des} between 1 and 0.9, whereas the least amount of electricity is available to meet demands. REJ_{tot} also has low values for these p_{des}. The proportion for which the fulfillment of domestic and irrigation demands is accomplished and energy is provided for energy household consumption is shown by the small decrease in REJ_{tot} for p_{des} ranging from 0.8 to 0.9. This also explains why the coverage of

electrical needs has been expanding gradually. As p_{des} declines, the availability of domestic and irrigation water falls because the energy needed for desalination is insufficient, while on the other hand, the fulfillment of the electricity demands grows.
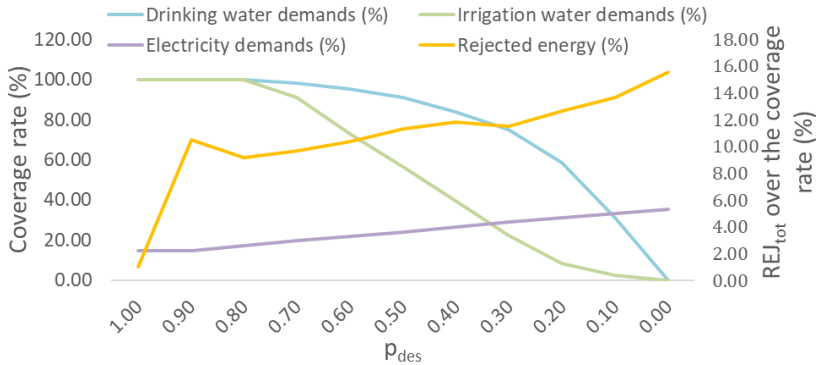

Figure 6-6 Coverage rate and REJtot over the coverage rate related to pdes for Case II

The overall rejected energy, REJ_{tot}, as well as REJ_{dir}, REJ_{pump}, and REJ_{res}, are presented in detail in Figure 6-7. Compared to REJ_{pump}, which is calculated zero when p_{des} is equal to 1, REJ_{res} and REJ_{dir} are low; however, REJ_{pump} steadily grows and maintains high values when p_{des} ranges from 0.9 to 0.

This signifies that if the desalination reservoir is large enough to fulfill all the consumptions, an effort to decrease the total rejected energy in this case, where a fixed percentage for desalination and pumping is established, results in a crucial decrease in meeting the electricity demands. Depending on the demand (desalinated water or electricity) that must be met in each project, it should always be decided whether to employ a fixed percentage for the desalination unit and the pumping station. Results from Figure 6-7 also show that, in relation to REJ_{tot}, the selection of the capacity of the pumping station is a critical decision in hybrid systems since it has the greatest impact on REJ_{tot} for a variety of p_{des}.
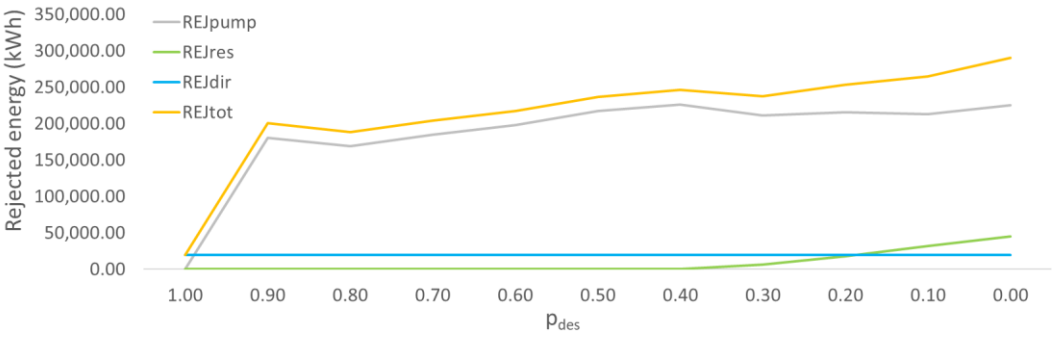

Figure 6-7 Rejected energy related to pdes for Case II

6.2.3   Produced and consumed energy during the operation of the HRES

When the HRES is operating, energy from the wind turbines is generated. This energy is split into direct network penetration $p_{dir} \cdot E_{wind}$, the remaining $E_{rem} = (1 - p_{dir}) \cdot E_{wind}$, as well as the produced hydro energy E_{hydro}. The energy that is produced and consumed, while the HRES is operating, is analyzed. The analysis only refers to Case I since, according to the former section's analysis, HRES performs better without a fixed proportion for desalination and pumping, concerning the total amount of rejected energy and the ability to fulfill both water and electricity consumptions. In this particular scheme, p_{dir} has been set at 30%, as it is demonstrated in section 6.2.1, because this is the value that yields the minimum amount of overall rejected energy.
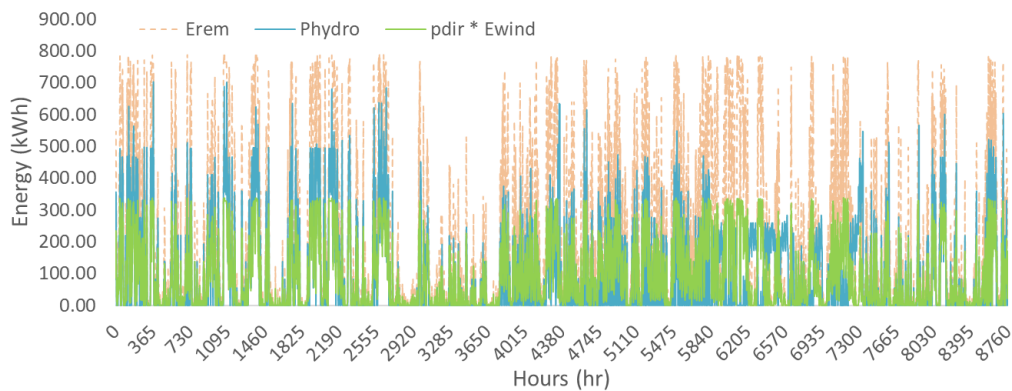

Figure 6-8 Produced energy from HRES

From the analysis of the wind speed u_2 at hub height z_2 data and the electricity demands data, it is evident that the produced hydro energy corresponds to the electricity demand, while the energy from the wind park, $E_{wind} = p_{dir} \cdot E_{wind} + (1 - p_{dir}) \cdot E_{wind}$, has the same waveform as the wind speed u_2 at hub height z_2, as shown in Figure 6-8. The primary way that HRES meets the electricity needs (beyond the initial 30% direct penetration of wind energy given in the system for electricity needs) is through the hydro turbine, as the generated wind energy covers the water needs, especially the domestic water needs, which are in priority. The beginning of the irrigation season and the additional energy needed to desalinate irrigation water cause a temporary fall in E_{rem} in May, however, the wind potential does not exhibit the corresponding period's substantial maximum wind speeds. As a result, E_{rem} decreases due to the decreased wind energy production and the rising demand.

Consumed energy is the combined amount of energy used for pumping E_{pump}, desalination for domestic water E_{desw} and desalination for irrigation water E_{desir}. These three distinct sources of consumption are depicted in Figure 6-9.

As would be expected, more energy is needed to meet the demand for irrigation water E_{desir} than for drinking water E_{desw} solely during the irrigation season. Apart from a few days in the spring months, during which both the wind potential and consumptions (water and electricity) show low values, both E_{desir} and E_{desw} follow the waveform of the respective demands, whereas E_{pump} continually increases its demand. Low wind potential results in less excess energy available to be utilized by the pumping station to store water, reducing therefore the amount of energy used by the pumps.
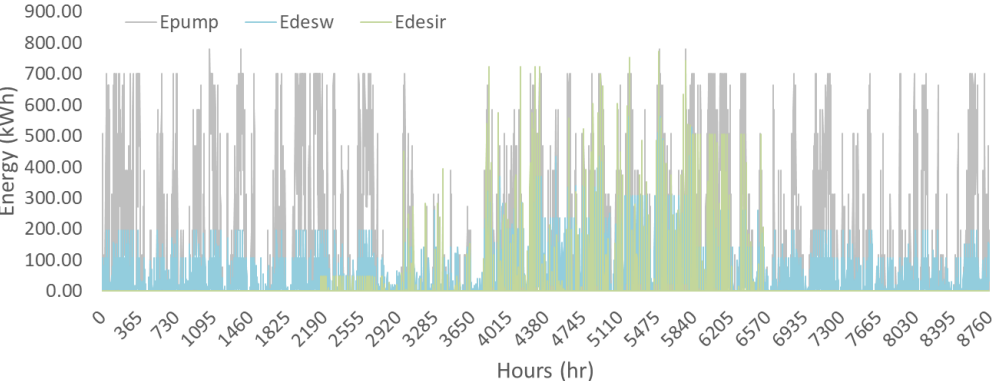

Figure 6-9 Consumed energy for demands coverage

Figure 6-8 and Figure 6-9 illustrate that the amount of hydroelectric energy generated is significantly less than the amount of energy needed for pumping. According to the findings, 1.5 units of energy are used for pumping for every unit of energy from the hydro turbine. The HRES is designed to store excess energy for periods of increased demand, which cannot be met by the direct penetration of wind energy and the only source of energy is the operation of the LPS and the use of conventional fuels. So, despite the more energy consumed by the pumps the use of them is preferable.

This research aims to develop a comprehensive approach for the integration of renewable energy sources in meeting energy and water needs in remote islands, by exploiting both their wind and potential, as well as different storage technologies for the storage of surplus renewable energy. The study area is Fournoi Korseon, an island in the North Aegean Sea. Firstly, an extensive presentation is demonstrated about renewable energy sources, the prevailing institutional framework in Greece and the EU's policy, hybrid renewable energy systems, different storage technologies and desalination technologies. Afterwards, the study area and the procession of the data used are presented. In Section 3 a methodology for the evaluation of eligible sites for the installation of wind turbines is developed, using a combination of MCDM and GIS for the design of a wind farm. In Section 4 energy management strategies are described based on single or hybrid storage methods, depending on the storage technologies of 7 different scenarios, resulting in the reliability analysis of each HRES and the estimation of economic and environmental indices, which are presented in Section 5. In Section 6, the methodology for calculating the rejected energy during the operation of an HRES is presented. The conclusions are summarized in the following paragraphs.

7.1   Optimal sitting of wind turbines based on different criteria

This thesis initially addresses the best location for wind turbines on the Greek island of Fournoi Korseon in the North Aegean. Greek islands have abundant wind potential, thus using wind turbines to supply their energy demands is receiving attention. Yet, the optimal location for installing wind turbines, combined with the existing legal framework, forms the basis for the utilization of high wind potential. An evaluation of possible locations for the installation of wind turbines using a set of proposed geomorphological, technical and spatial criteria, while considering environmental restrictions and the present legislation framework. Three major scenarios—the technical-oriented, the cultural-oriented, and the economic-oriented scenarios—are considered, with the combined use of MCDM and GIS and the estimation of the weights of the criteria. This analysis considers six factors: wind potential, altitude, and distances from the settlements, the road network, the mobile base stations and the archaeological sites. The AHP method is used to estimate the weights of the criteria for three scenarios to illustrate how they influence the final layout. In every scenario, the wind potential criterion takes priority because the wind turbines' capacity to generate even much energy as possible depends on having the maximum wind potential. Also, the three scenarios are executed while taking into account where the island's main settlement, Fournoi, is located. By adding

this additional restriction of retaining the minimum distance of Fournoi, energy losses through the cables are minimized. Finally, a sensitivity analysis is conducted for two criteria to see how a variation to any of them would impact the results.

Zone A, which is the same for each scenario, represents 27.9% of the island's total surface, indicating all the exclusion zones where wind turbines may not be installed. Zone E represents the most suitable locations and has the lowest values in the initial scenarios without the additional limitation of the distance from Fournoi; however, in the economic scenario, zone E has a higher value of 4%. Zone D, the zone that goes before Zone E, has high values, particularly in the economic-oriented scenario. The value of 54.1% suggests that more than half the island has sites that are suitable for installation with the values of the FS ranging from 0.50 to 0.75. Even though the altitude criterion is the fifth most important, the economic scenario has the majority of eligible locations. The scenario that prioritizes economic criteria seems to combine lower installation costs with a larger surface area with eligible sites. So, it can be predicted that ideal locations with significant wind potential can be combined with lower altitudes, reducing the installation cost and resulting in additional locations, at the same time, in the final zone E. Since it is preferable for such a project to be close to the settlement where there are the most residents, three additional acceptable maps are produced taking the proximity to Fournoi's main settlement into consideration as one more restriction. Also, the technical-oriented scenario, in this case, has the greatest number of suitable locations. Zone D, which in these supplementary scenarios represents the zone that demonstrates the most favorable locations, achieves a value of 10.48% in the technical scenario. Whereas the corresponding FS value for the initial technical scenario is 0.929, the maximum value of FS in these additional cases is 0.744 in the technical scenario. The technical scenario is then subjected to a sensitivity analysis for two different criteria to determine how a change in either one affects the new suitability maps. The first criterion is the wind potential, C_{wind} with the highest weight, and the second is the distance from the archaeological sites, C_{arch}, which has the lowest weight. The optimal locations are increasing as C_{wind} weight increases, whereas the optimal locations are decreasing as C_{arch} weight increases. It appears that the type of the selected criterion, rather than the weight, has a higher impact on new suitability maps.

7.2   Evaluation of single and hybrid storage technologies coupling with HRES

The framework for the simulation and assessment approach for a WT/PV system connected to a desalination station, and a PHS, a battery, or a hydrogen storage system is provided. Moreover, configurations using hybrid storage technologies are examined. Pumped hydro storage coupled with either batteries or an electrolyzer and a fuel cell. Three demands, household consumption, domestic water and irrigation water, are simultaneously met in order to compare alternative storage

technologies. For all configurations, results on the cost of energy, cost of water, payback period, loss of load probability, and eliminated CO2 quantities are estimated. These results also show the initial cost as well as the maintenance and operation costs. The simulations run at an hourly step using meteorological data (wind speed, solar radiation, temperature, precipitation, number of sunny days), demand data for household consumption, domestic and irrigation water needs, and data on the technical specifications of each subsystem, including wind turbines, photovoltaic modules, desalination units, pumping stations, hydro turbines, upper reservoirs, batteries, electrolyzers, fuel cells, and hydrogen tanks.

It has been shown that combinations of WTs and PVs produce improved results since they simultaneously utilize each area's wind and solar potential. In terms of using each storage technology, WT/PV/DU/PHS and WT/PV/DU/BT generally exhibit the same "behavior," however WT/PV/DU/PHS has lower energy and water costs as a result of its lower initial cost. This may result in considerably cheaper pricing for energy and desalinated water, especially considering that the upper reservoir may already be existing on the island. Yet, since it uses the LPS more often and has a shorter autonomous period, it produces more CO_2 overall. Moreover, LPS is used more in WT/PV/DU/FC because desalinating the water before it enters the electrolyzer to create hydrogen requires a significant amount of energy. The second storage appears to be more active in December, according to the analysis of supply and demand for the months of August and December. This could be explained by the fact that although the total amount of energy required increases in December compared to August, more excess energy is delivered to and used by the battery or the electrolyzer due to the greater wind potential.

For configurations consisting of both WTs and PVs, the monthly fulfillment of water supply is up to 87%; however, this percentage decreases for irrigation water, as would be predicted given that irrigation water is the final demand in the hierarchy of significance. In all configurations, there is complete coverage autonomy for October; however, for WT/PV/DU/PHS, WT/PV/DU/BT, WT/PV/DU/HPBS, and WT/PV/DU/HPHS, the autonomy extends to June and July for domestic water supply. Only the WT/PV/DU/FC scenario exhibits load losses in the domestic water supply during July. However, a larger coverage of domestic water demands is also seen in WT/PV/DU/HPHS, whereas WT/PV/DU/BT shows a greater coverage of domestic water needs when comparing the single storage technologies.

PHS, BT, and FC are three separate storage methods that produce energy. These systems often provide less energy than is required to power the pumps, charge the batteries, and activate the electrolyzer to create hydrogen. Yet, the goal of an HRES is to store energy produced by RES that cannot be used right away and use it during times of high demand when burning fossil fuels is the only other option. The comparison of WT/PV/DU/HPBS and WT/PV/DU/HPHS reveals a greater

contribution from FC in the case of hydrogen compared to batteries as well as a lower utilization of LPS. A potential explanation is that since secondary storage technologies, FC or BT, aren't used as frequently in hybrid storage, there's more energy lost during idle periods as a result of battery degradation. This relies on the battery's self-discharge rate, or. Higher water and energy costs are a result of the hybrid storage arrangements, with WT/PV/DU/HPHS being the greatest cost. However, because the decision must be taken in conjunction with the LOLP values, WT/PV/DU/HPHS exhibit lower LOLP values but also a shorter PBP. WT/PV/DU/HPHS exhibits better outcomes in terms of CO2 amounts and the Emissions Trading System penalty.

Additionally, a sensitivity analysis is conducted to determine the effects of population, wind and solar potential, and wind turbine installation height on all of the aforementioned indices as well as the contribution of each storage technology to the island's energy mix (pumped hydro storage, battery, and hydrogen). This analysis provides useful information about the strength of each factor's influence on the indices under consideration. The WT/PV/DU/PHS and WT/PV/DU/FC single storage technologies and the WT/PV/DU/PHS single and hybrid storage technologies are compared using sensitivity analysis. The relationship between the change in the starting value and each index is demonstrated by examining each parameter in the context of an increase and a decrease of 10%.

According to the results for single storage technologies, the WT/PV/DU/FC configuration is more sensitive to population fluctuations and is more sensitive to variations in wind potential and COE. The WT/PV/DU/FC arrangement is more susceptible to changes in wind speed, which has a higher effect on CO₂ emissions. Also, the population growth in both configurations causes an increase in EM_{CO_2}. It is also noteworthy that the contribution of the FC in the WT/PV/DU/FC configuration has a higher slope of the wind potential and population than the contribution of the PHS in the WT/PV/DU/PHS configuration. Moreover, the LPS operates less in WT/PV/DU/PHS than it does in WT/PV/DU/FC, and the LOLP$_{hres}$, which is more affected in WT/PV/DU/FC, exhibits the same pattern. The population, followed by the wind potential, the solar potential, and finally, the height of the WT installation, determine the classification for both configurations and the four criteria. Moreover, the results are inversely proportional to the population even though they are proportionate to the wind and solar potential.

While COE and COW are proportional to both models, according to the results of single and hybrid storage technologies, WT/PV/DU/HPHS is more affected by variations in the height of wind turbine installation in the case of LOLP. Also, a comparison of WT/PV/DU/PHS and WT/PV/DU/FC demonstrates that the PHS behaves differently from FC during changes in wind potential. The behavior of FC varies, whereas PHS is proportional to both rises and drops in wind potential. A smaller rise in the FC contribution results from an increase in wind potential. Changes in the solar potential do not reveal this tendency, probably as a result of the island experiencing more wind than solar

potential throughout the year. For WT/PV/DU/HPHS, population changes are negatively correlated with COE and COW values, but for WT/PV/DU/PHS, population changes are correlated with COE and COW changes. Finally, in the case of single storage compared to hybrid storage, population changes result in more significant changes in PBP and LOLP$_{hres}$. However, a comparison of WT/PV/DU/FC and WT/PV/DU/HPHS reveals that the LOLP$_{hres}$ changes are more pronounced in the second configuration. This observation leads to the conclusion that the final choice of storage technology depends not only on changes in installation criteria, meteorological data, and demand data but also on changes in the initial COE or COW, or LOLP criteria.

The benefits of coupling with a storage system and the significance of exploiting wind and solar potential in island energy systems are highlighted by the results of the proposed energy management solutions. They also offer details about the reliability of both storage technologies from the viewpoint of sensitivity and economic analysis. Any district that needs to export results on the performance of a hybrid renewable energy system is urged to utilize this simulation tool, by changing the input data relating to meteorological, demand, and sizing data. Through the water and energy independence of anhydrous islands, it also offers a dependable solution in the direction of environmental protection and adaptability to potential climate change. It provides the methodology to minimize the uncertainty in meeting water demand and expenditures, improving agricultural production, stimulating the cost-reduction of produced electricity, and promoting energy and water independence while promoting the penetration of renewable energy sources. The ability of local communities and/or ministries to choose the best configuration for a corresponding project in the area under their territory based on meteorological data, data on demand, and estimated values for energy, economic, and environmental indices constitutes the applicability of the results. Also, it is possible to evaluate a single storage system or a hybrid storage system in relation to the specific data of each island and in conjunction with wind turbines and solar modules. The configuration of the hybrid pumped hydrogen storage can also promote the use of renewable energy on small islands.

7.3   Rejected renewable energy during the operation of an HRES

Using the abundant solar and wind potential of the islands in Greece and managing water resources effectively can lead to energy and water independence, a decrease in the consumption of conventional fuels and a reduction in GHG. Wind energy generated can be applied to the grid directly or to the pumping station for the storage of seawater in the upper reservoir or to any other storage system for use when there is an energy deficit. Nevertheless, some of the generated renewable energy cannot be used immediately, cannot be stored and thus, is being rejected. Despite the fact that many studies are evaluating HRESs and concentrating on the installation, operation, reliability, or selection of the storage capacity, only a few studies address the rejected energy and the

simultaneous satisfaction of electrical demand and the domestic and irrigation supply in hourly time intervals. This study attempts to give a methodological framework for the estimation of the rejected energy of an HRES based on the amount of wind energy that enters the system directly and the amount of energy allocated to desalination and to pumping. Renewable energy that is rejected ends up in a dump. It is feasible to supply a system with additional storage technology, like a battery or hydrogen cells, after estimating this value. This rejected RES can be further stored in the second storage system and won't be lost. The grid system will become, thus, more secure and sustainable.

In order to evaluate the rejected energy at various operating scenarios, two separate scenarios are proposed depending on the potential for different uses of the HRES. Findings from case I are based on how much of the generated energy by the wind turbines is sent directly to the system (p_{dir}) for household consumption and how much is used in the desalination unit and the pumping station. In case II, a portion of the wind-generated energy is once more sent directly to the system for its electrical requirements, and results depend on the ratios of the remaining energy that are provided to the desalination unit and the pumping station. From case I, it is revealed that the system rejects the least amount of total energy over the length of one year when the direct percentage of wind energy, p_{dir}, is equal to 30%. Also, the suggested system's performance results in a 60% coverage of domestic water needs, a 21% coverage of agricultural water needs, and a 31% coverage of energy needs. Research results from case II demonstrate that allocating all excess energy to the desalination unit is the strategy that results in the least amount of rejected energy. Yet, compared to 31% of scenario I, a considerable decrease in meeting the electrical demands to 14% is seen in this case. On the other hand, compared to the corresponding results of case I, water demands are almost entirely satisfied. An analysis of the energy produced and used during the HRES's operation (WT/DU/PHS) reveals that 1.5 units of energy are used for pumping for every unit of hydro energy produced.

7.4   Directions for further research

However extensive the modeling of different renewable energy generation storage and management scenarios is, for gradual delignitization, carbon dioxide emission reduction and energy and water independence of remote and arid islands, inevitably crucial aspects will still be not thoroughly researched. Future perspectives of this research include the application of the integrated methodology to the remaining non-interconnected islands for the validation of the results. Further research is suggested in the direction of dimensioning optimization of the proposed configurations that have been examined, based on the reduction of the final price of water and energy, the increase of reliability for all three demands – household consumption, domestic and irrigation water – the reduction of rejected energy, the reduction of the payback time and the increase of the CO_2 that can be eliminated. Finally, another interesting area for relevant future research would be the

implementation of climate scenarios in order to examine all energy management strategies and different storage technologies in terms of reliability and rejected energy under the effects of climate change.

Acknowledgments

For all these years,

To my supervisor Professor Mr. Baltas Evangelos. For his trust, for the unique opportunity to work and study under his supervision and for his continuous and undivided guidance. Without his contribution, this PhD thesis would not only never have been completed but would not even have existed as an idea. To Professor Mr. Mamassis Nikolaos, for all his ideas and our constructive discussions. To Professor Mr. Karellas Sotirios for his contribution and suggestions in our meetings for the doctoral thesis. To the members of the Examination Board for guiding and evaluating my doctoral thesis, Professor Mr. Tsichrintzis Vassilios, Associate Professor Mr. Karpouzos Dimitrios, Professor Mr. Anagiotos Andreas and Professor Mrs. Kolokytha Elpida-Kleanthi.

To the people involved in providing data for the study area. Mr. Mytikas, engineer of the Municipality of Fournoi Korseon for his valuable information that helped us to have a complete view of the existing situation of the study area. Mrs. Spachi from DEDDIE Ag. Kirikou for the data on electricity consumption. Mrs. Vrontou from ELSTAT for the statistics she provided us. Mr. Lagouvardos, Mr. Vafiadis and Mr. Vougioukas, from the National Observatory of Athens for collecting and sending the meteorological data. Mr. Kontos from Marathondata for providing the ArcGIS software.

To the Hellenic Foundation for Research and Foundation for the 23-month fellowship grant for working unhindered on my PhD thesis and especially to Mrs. Koutsoulenti for our cooperation. To the Special Committee of NTUA and especially Mrs. Karagiozopoulou who dealt with the processing of my fellowship grant issues.

To Mrs. Skarlou administrative staff of NTUA for her unreserved help over the years has been invaluable even on matters outside her remit. To the colleagues I met and worked with in the Laboratory of Hydrology and Water Resources Development, Emilia, Elissavet, Yiorgos, Kostas and Apollon. To the students I met during the courses and to those with whom we collaborated on their diploma thesis; they taught me so much.

To everyone I've met over the years. As trivial as it sounds, we are all influenced by the people around us even if they are people we don't necessarily interact with for a long time. To my friends for being a support but especially for having good times. To Yiorgos, the master of rasters and pixels. To my friend Carmen who has been unwaveringly by my side for so many years.

To my parents for all the support and trust in my choices over the years and to my brother for his quiet strength.

To my partner and to our daughter. Dimitris, forever and for everything. Electra, my love has no limits.

References

Abdelshafy, A. M., Hassan, H., & Jurasz, J. (2018). Optimal design of a grid-connected desalination plant powered by renewable energy resources using a hybrid PSO–GWO approach. *Energy Conversion and Management*, *173*, 331–347. https://doi.org/10.1016/j.enconman.2018.07.083

Ainou, F. Z., Ali, M., & Sadiq, M. (2022). Green energy security assessment in Morocco: green finance as a step toward sustainable energy transition. *Environmental Science and Pollution Research*. https://doi.org/10.1007/s11356-022-19153-7

Ajiwiguna, T. A., Lee, G.-R., Lim, B.-J., Cho, S.-H., & Park, C.-D. (2021). Optimization of battery-less PV-RO system with seasonal water storage tank. *Desalination*, *503*, 114934. https://doi.org/10.1016/j.desal.2021.114934

Akter, H., Howlader, H. O. R., Nakadomari, A., Islam, Md. R., Saber, A. Y., & Senjyu, T. (2022). A Short Assessment of Renewable Energy for Optimal Sizing of 100% Renewable Energy Based Microgrids in Remote Islands of Developing Countries: A Case Study in Bangladesh. *Energies*, *15*(3), 1084. https://doi.org/10.3390/en15031084

AL Ahmad, A., & Sirjani, R. (2021). Optimal planning and operational strategy of energy storage systems in power transmission networks: An analysis of wind farms. *International Journal of Energy Research*, *45*(7), 11258–11283. https://doi.org/10.1002/er.6605

Aleluia, J., Tharakan, P., Chikkatur, A. P., Shrimali, G., & Chen, X. (2022). Accelerating a clean energy transition in Southeast Asia: Role of governments and public policy. *Renewable and Sustainable Energy Reviews*, *159*, 112226. https://doi.org/10.1016/j.rser.2022.112226

Ali, Y., Butt, M., sabir, M., Mumtaz, U., & Salman, A. (2018). Selection of suitable site in Pakistan for wind power plant installation using analytic hierarchy process (AHP). *Journal of Control and Decision*, *5*(2), 117–128. https://doi.org/10.1080/23307706.2017.1346490

Alkaisi, A., Mossad, R., & Sharifian-Barforoush, A. (2017). A Review of the Water Desalination Systems Integrated with Renewable Energy. *Energy Procedia*, *110*, 268–274. https://doi.org/10.1016/j.egypro.2017.03.138

Al-Karaghouli, A., & Kazmerski, L. L. (2013). Energy consumption and water production cost of conventional and renewable-energy-powered desalination processes. *Renewable and Sustainable Energy Reviews*, *24*, 343–356. https://doi.org/10.1016/j.rser.2012.12.064

Alkhalidi, A., Alqarra, K., Abdelkareem, M. A., & Olabi, A. G. (2022). Renewable energy curtailment practices in Jordan and proposed solutions. *International Journal of Thermofluids*, *16*, 100196. https://doi.org/10.1016/j.ijft.2022.100196

Allam, Z., Bibri, S. E., & Sharpe, S. A. (2022). The Rising Impacts of the COVID-19 Pandemic and the Russia–Ukraine War: Energy Transition, Climate Justice, Global Inequality, and Supply Chain Disruption. *Resources*, *11*(11), 99. https://doi.org/10.3390/resources11110099

Al-Shabeeb, A. R., Al-Adamat, R., & Mashagbah, A. (2016). AHP with GIS for a Preliminary Site Selection of Wind Turbines in the North West of Jordan. *International Journal of Geosciences*, *07*(10), 1208–1221. https://doi.org/10.4236/ijg.2016.710090

Al-Shammari, Z. W. J., Kother, S., Taha, I. A., Hayder, H. E., Hussam, M. A., Hadi, A., Azizan, M. M., & Rahman, A. S. F. (2021). *Green Micro-grid Based on PV/WT Hybrid System for Remote and Rural Population in Iraq: A Case Study* (pp. 1081–1093). https://doi.org/10.1007/978-981-16-0866-7_96

Al-Shetwi, A. Q. (2022). Sustainable development of renewable energy integrated power sector: Trends, environmental impacts, and recent challenges. *Science of The Total Environment*, *822*, 153645. https://doi.org/10.1016/j.scitotenv.2022.153645

Alturki, F. A., & Awwad, E. M. (2021). Sizing and Cost Minimization of Standalone Hybrid WT/PV/Biomass/Pump-Hydro Storage-Based Energy Systems. *Energies*, *14*(2), 489. https://doi.org/10.3390/en14020489

Alves, M. P., Gul, W., Cimini Junior, C. A., & Ha, S. K. (2022). A Review on Industrial Perspectives and Challenges on Material, Manufacturing, Design and Development of Compressed Hydrogen Storage Tanks for the Transportation Sector. *Energies*, *15*(14), 5152. https://doi.org/10.3390/en15145152

Antenna Construction Information Portal. (n.d.). Retrieved November 20, 2019, from https://keraies.eett.gr

Arabkoohsar, A., & Namib, H. (2021). Pumped hydropower storage. In *Mechanical Energy Storage Technologies* (pp. 73–100). Elsevier. https://doi.org/10.1016/B978-0-12-820023-0.00004-3

Balaras, K., Argyriou, A., & Karagiannis, F. (2006). *Conventional and un-conventional forms of energy*. Tekdotiki.

Baldinelli, A., Barelli, L., Bidini, G., Cinti, G., Di Michele, A., & Mondi, F. (2020). How to Power the Energy–Water Nexus: Coupling Desalination and Hydrogen Energy Storage in Mini-Grids with Reversible Solid Oxide Cells. *Processes*, *8*(11), 1494. https://doi.org/10.3390/pr8111494

Baltas, A. E., & Dervos, A. N. (2012). Special framework for the spatial planning & the sustainable development of renewable energy sources. *Renewable Energy*, *48*, 358–363. https://doi.org/10.1016/j.renene.2012.05.015

Bardis, G., Feloni, E., & Baltas, E. (2020). Simulation and Evaluation of a Hybrid Renewable Energy System for Supplying a Desalination Unit on the Island of Lipsi, Greece. *Advances in Sciences and Engineering*, *12*(1), 1–12. https://doi.org/10.32732/ase.2020.12.1.1

Baruah, A., Basu, M., & Amuley, D. (2021). Modeling of an autonomous hybrid renewable energy system for electrification of a township: A case study for Sikkim, India. *Renewable and Sustainable Energy Reviews*, *135*, 110158. https://doi.org/10.1016/j.rser.2020.110158

Bertsiou M, Feloni E, & Baltas E. (2017). Cost-benefit analysis for a Hybrid renewable energy system in Fournoi island. *Proceedings of the Sixth International Conference on Environmental Management, Engineering, Planning and Economics (CEMEPE 2017) and SECOTOX Conference*, 975–705.

Bertsiou, M., Feloni, E., Karpouzos, D., & Baltas, E. (2018). Water management and electricity output of a Hybrid Renewable Energy System (HRES) in Fournoi Island in Aegean Sea. *Renewable Energy*, *118*. https://doi.org/10.1016/j.renene.2017.11.078

Bertsiou, M. M., & Baltas, E. (2022a). Energy, Economic and Environmental Analysis of a Hybrid Power Plant for Electrification, and Drinking and Irrigation Water Supply. *Environmental Processes*, *9*(2). https://doi.org/10.1007/s40710-022-00575-x

Bertsiou, M. M., & Baltas, E. (2022b). Management of energy and water resources by minimizing the rejected renewable energy. *Sustainable Energy Technologies and Assessments*, *52*. https://doi.org/10.1016/j.seta.2022.102002

Bertsiou, M. M., & Baltas, E. (2022c). Power to Hydrogen and Power to Water Using Wind Energy. *Wind*, *2*(2), 305–324. https://doi.org/10.3390/wind2020017

Bertsiou, M. M., Theochari, A. P., & Baltas, E. (2021). Multi-criteria analysis and Geographic Information Systems methods for wind turbine siting in a North Aegean island. *Energy Science and Engineering*, *9*(1). https://doi.org/10.1002/ese3.809

Bhandari, B., Lee, K.-T., Lee, G.-Y., Cho, Y.-M., & Ahn, S.-H. (2015). Optimization of hybrid renewable energy power systems: A review. *International Journal of Precision Engineering and Manufacturing-Green Technology*, *2*(1), 99–112. https://doi.org/10.1007/s40684-015-0013-z

Bilgili, M., & Alphan, H. (2021). Visual Impact and Potential Visibility Assessment of Wind Turbines Installed in Turkey. *GAZI UNIVERSITY JOURNAL OF SCIENCE*. https://doi.org/10.35378/gujs.811568

Blakers, A., Stocks, M., Lu, B., & Cheng, C. (2021). A review of pumped hydro energy storage. *Progress in Energy*, *3*(2), 022003. https://doi.org/10.1088/2516-1083/abeb5b

Blaney HF, & Criddle WD. (1962). Determining consumptive use and irrigation water requirements (No. 1275). *Us Department of Agriculture*.

Borge-Diez, D., García-Moya, F. J., Cabrera-Santana, P., & Rosales-Asensio, E. (2021). Feasibility analysis of wind and solar powered desalination plants: An application to islands. *Science of The Total Environment*, *764*, 142878. https://doi.org/10.1016/j.scitotenv.2020.142878

Bouabdallah, A., Olivier, J. C., Bourguet, S., Machmoum, M., & Schaeffer, E. (2015). Safe sizing methodology applied to a standalone photovoltaic system. *Renewable Energy*, *80*, 266–274. https://doi.org/10.1016/j.renene.2015.02.007

Bouzounierakis, Katsigiannis, Fiorentzis, & Karapidakis. (2019). Effect of Hybrid Power Station Installation in the Operation of Insular Power Systems. *Inventions*, *4*(3), 38. https://doi.org/10.3390/inventions4030038

Bravi, M., & Basosi, R. (2014). Environmental impact of electricity from selected geothermal power plants in Italy. *Journal of Cleaner Production*, *66*, 301–308. https://doi.org/10.1016/j.jclepro.2013.11.015

Brenna, M., Corradi, A., Foiadelli, F., Longo, M., & Yaici, W. (2020). Numerical simulation analysis of the impact of photovoltaic systems and energy storage technologies on centralised generation: a case study for Australia. *International Journal of Energy and Environmental Engineering*, *11*(1), 9–31. https://doi.org/10.1007/s40095-019-00330-3

Brodny, J., & Tutak, M. (2023). Assessing the Energy and Climate Sustainability of European Union Member States: An MCDM-Based Approach. *Smart Cities*, *6*(1), 339–367. https://doi.org/10.3390/smartcities6010017

Bundschuh, J., Kaczmarczyk, M., Ghaffour, N., & Tomaszewska, B. (2021). State-of-the-art of renewable energy sources used in water desalination: Present and future prospects. *Desalination*, *508*, 115035. https://doi.org/10.1016/j.desal.2021.115035

Canales, F. A., Jurasz, J. K., Guezgouz, M., & Beluco, A. (2021). Cost-reliability analysis of hybrid pumped-battery storage for solar and wind energy integration in an island community. *Sustainable Energy Technologies and Assessments*, *44*, 101062. https://doi.org/10.1016/j.seta.2021.101062

Canbulat, S., Balci, K., Canbulat, O., & Bayram, I. S. (2021). Techno-Economic Analysis of On-Site Energy Storage Units to Mitigate Wind Energy Curtailment: A Case Study in Scotland. *Energies*, *14*(6), 1691. https://doi.org/10.3390/en14061691

Celik, E., Sacmaozu, G., & Irez, A. B. (2022). *Development of Carbon-Glass Fiber Reinforced Hybrid Composites: Applications in Offshore Wind Turbine Blades* (pp. 17–22). https://doi.org/10.1007/978-3-030-86741-6_4

Ceran, B., Mielcarek, A., Hassan, Q., Teneta, J., & Jaszczur, M. (2021). Aging effects on modelling and operation of a photovoltaic system with hydrogen storage. *Applied Energy*, *297*, 117161. https://doi.org/10.1016/j.apenergy.2021.117161

Cergibozan, R. (2022). Renewable energy sources as a solution for energy security risk: Empirical evidence from OECD countries. *Renewable Energy*, *183*, 617–626. https://doi.org/10.1016/j.renene.2021.11.056

Chien, F., Ajaz, T., Andlib, Z., Chau, K. Y., Ahmad, P., & Sharif, A. (2021). The role of technology innovation, renewable energy and globalization in reducing environmental degradation in Pakistan: A step towards sustainable environment. *Renewable Energy*, *177*, 308–317. https://doi.org/10.1016/j.renene.2021.05.101

Ciupageanu, D.-A., Barelli, L., Ottaviano, A., Pelosi, D., & Lazaroiu, G. (2019). Innovative power management of hybrid energy storage systems coupled to RES plants: The Simultaneous Perturbation Stochastic Approximation approach. *2019 IEEE PES Innovative Smart Grid Technologies Europe (ISGT-Europe)*, 1–5. https://doi.org/10.1109/ISGTEurope.2019.8905775

Collares-Pereira, M., & Rabl, A. (1979). The average distribution of solar radiation-correlations between diffuse and hemispherical and between daily and hourly insolation values. *Solar Energy*, *22*(2), 155–164. https://doi.org/10.1016/0038-092X(79)90100-2

CORINE Land Cover 2018. Land Cover Dataset for 2018. (n.d.). Retrieved August 4, 2020, from https://land.coper nicus.eu/pan-europ ean/corine-land-cover/ clc2018

Cotfas, D. T., & Cotfas, P. A. (2019). Multiconcept Methods to Enhance Photovoltaic System Efficiency. *International Journal of Photoenergy*, *2019*, 1–14. https://doi.org/10.1155/2019/1905041

Dalala, Z., Al-Omari, M., Al-Addous, M., Bdour, M., Al-Khasawneh, Y., & Alkasrawi, M. (2022). Increased renewable energy penetration in national electrical grids constraints and solutions. *Energy*, *246*, 123361. https://doi.org/10.1016/j.energy.2022.123361

Dambone Sessa, S., Tortella, A., Andriollo, M., & Benato, R. (2018). Li-Ion Battery-Flywheel Hybrid Storage System: Countering Battery Aging During a Grid Frequency Regulation Service. *Applied Sciences*, *8*(11), 2330. https://doi.org/10.3390/app8112330

Das, P., Das, B. K., Mustafi, N. N., & Sakir, Md. T. (2021). A review on pump-hydro storage for renewable and hybrid energy systems applications. *Energy Storage*, *3*(4). https://doi.org/10.1002/est2.223

Das, P., Das, B. K., Rahman, M., & Hassan, R. (2022). Evaluating the prospect of utilizing excess energy and creating employments from a hybrid energy system meeting electricity and freshwater demands using multi-objective evolutionary algorithms. *Energy*, *238*, 121860. https://doi.org/10.1016/j.energy.2021.121860

Dawood, F., Shafiullah, G., & Anda, M. (2020). Stand-Alone Microgrid with 100% Renewable Energy: A Case Study with Hybrid Solar PV-Battery-Hydrogen. *Sustainability*, *12*(5), 2047. https://doi.org/10.3390/su12052047

Dehghani, H., Vahidi, B., & Hosseinian, S. H. (2017). Wind farms participation in electricity markets considering uncertainties. *Renewable Energy*, *101*, 907–918. https://doi.org/10.1016/j.renene.2016.09.049

Dehghani-Sanij, A. R., Tharumalingam, E., Dusseault, M. B., & Fraser, R. (2019). Study of energy storage systems and environmental challenges of batteries. *Renewable and Sustainable Energy Reviews*, *104*, 192–208. https://doi.org/10.1016/j.rser.2019.01.023

Dhar, A., Naeth, M. A., Jennings, P. D., & Gamal El-Din, M. (2020). Perspectives on environmental impacts and a land reclamation strategy for solar and wind energy systems. *Science of The Total Environment*, *718*, 134602. https://doi.org/10.1016/j.scitotenv.2019.134602

Dhonde, M., Sahu, K., & Murty, V. V. S. (2022). The application of solar-driven technologies for the sustainable development of agriculture farming: a comprehensive review. *Reviews in Environmental Science and Bio/Technology*, *21*(1), 139–167. https://doi.org/10.1007/s11157-022-09611-6

Directive 2009/28/EC of the European Parliament and of the Council of 23 April 2009 on the promotion of the use of energy from renewable sources and amending and subsequently repealing Directives 2001/77/EC and 2003/30/EC. (2009). Official Journal of the European Union. L 140/16. . https://eur-lex.europa.eu/legal-content/EN/TXT/PDF/?uri=CELEX:32009L0028&from=EN

Directive (EU) 2018/2001 of the European Parliament and of the Council of 11 December 2018 on the promotion of the use of energy from renewable sources. (2018). Official Journal of the European Union. L 328/82.

Dong, C., Ji, D., Mustafa, F., & Khursheed, A. (2022). Impacts of COVID-19 pandemic on renewable energy production in China: transmission mechanism and policy implications. *Economic Research-Ekonomska Istraživanja*, *35*(1), 3857–3870. https://doi.org/10.1080/1331677X.2021.2005651

Dorber, M., Arvesen, A., Gernaat, D., & Verones, F. (2020). Controlling biodiversity impacts of future global hydropower reservoirs by strategic site selection. *Scientific Reports*, *10*(1), 21777. https://doi.org/10.1038/s41598-020-78444-6

Drobne, S., & Lisec, A. (2009). Multi-attribute Decision Analysis in GIS: Weighted Linear Combination and Ordered Weighted Averaging. *Informatica*, *33*(4), 459–473.

Eionet Report - ETC/CME 2019/8. European Topic Centre on Climate Change Mitigation and Energy. (2019). *Renewable energy in Europe. Recent growth and knock-on effects*. https://www. eionet.europa.eu/etcs/etc-cme/produ cts/etc-cme-repor ts/renew able-energy-in-europe-2019-recent-growth-and-knock-on-effects

Eisapour, A. H., Jafarpur, K., & Farjah, E. (2021). Feasibility study of a smart hybrid renewable energy system to supply the electricity and heat demand of Eram Campus, Shiraz University; simulation, optimization, and sensitivity analysis. *Energy Conversion and Management*, *248*, 114779. https://doi.org/10.1016/j.enconman.2021.114779

Elberry, A. M., Thakur, J., Santasalo-Aarnio, A., & Larmi, M. (2021). Large-scale compressed hydrogen storage as part of renewable electricity storage systems. *International Journal of Hydrogen Energy*, *46*(29), 15671–15690. https://doi.org/10.1016/j.ijhydene.2021.02.080

El-houari, H., Allouhi, A., Salameh, T., Kousksou., T., Jamil, A., & El Amrani, B. (2021). Energy, Economic, Environment (3E) analysis of WT-PV-Battery autonomous hybrid power plants in climatically varying regions. *Sustainable Energy Technologies and Assessments*, *43*, 100961. https://doi.org/10.1016/j.seta.2020.100961

Elmaadawy, K., Kotb, K. M., Elkadeem, M. R., Sharshir, S. W., Dán, A., Moawad, A., & Liu, B. (2020). Optimal sizing and techno-enviro-economic feasibility assessment of large-scale reverse osmosis desalination powered with hybrid renewable energy sources. *Energy Conversion and Management*, *224*, 113377. https://doi.org/10.1016/j.enconman.2020.113377

Eltamaly, A. M., Ali, E., Bumazza, M., Mulyono, S., & Yasin, M. (2021). Optimal Design of Hybrid Renewable Energy System for a Reverse Osmosis Desalination System in Arar, Saudi Arabia. *Arabian Journal for Science and Engineering*, *46*(10), 9879–9897. https://doi.org/10.1007/s13369-021-05645-0

Ember, Daily Carbon Prices. (n.d.). Retrieved December 8, 2022, from https://ember-climate.org/data/data-tools/carbon-price-viewer/

ENERCON Product Overview. (n.d.). Retrieved May 3, 2022, from https://www.enercon.de/fileadmin/Redakteur/Medien-Portal/broschueren/ pdf/en/ENERCON_Produkt_en_06_2015.pdf

Energy for the Future: Renewable Sources of Energy: White Paper for a Community Strategy and Action Plan. (1997).

Esan, O. C., Shi, X., Pan, Z., Huo, X., An, L., & Zhao, T. S. (2020). Modeling and Simulation of Flow Batteries. *Advanced Energy Materials*, 2000758. https://doi.org/10.1002/aenm.202000758

Escamilla, A., Sánchez, D., & García-Rodríguez, L. (2022). Assessment of power-to-power renewable energy storage based on the smart integration of hydrogen and micro gas turbine technologies. *International Journal of Hydrogen Energy*, *47*(40), 17505–17525. https://doi.org/10.1016/j.ijhydene.2022.03.238

Esmaeilion, F. (2020). Hybrid renewable energy systems for desalination. *Applied Water Science*, *10*(3), 84. https://doi.org/10.1007/s13201-020-1168-5

EUNICE. (2023). *Details of TILOS Project*. https://eunice-group.com/projects/tilos-project/

European Environment Agency. (n.d.). *Trends and projections in Europe 2021*. Retrieved March 7, 2023, from https://www.eea.europa.eu/highlights/eu-achieves-20-20-20

European Environment Agency. (2020). *Greenhouse Gas Emission Intensity of Electricity Generation by Country*. https:// www. eea. europa. eu/ data- and- maps/ daviz/ co2- emiss ion- inten sity- 9/# tab- googl echar tid_ googl echar tid_ googl echar tid_ chart_ 1111

Farh, H. M. H., Al-Shamma'a, A. A., Al-Shaalan, A. M., Alkuhayli, A., Noman, A. M., & Kandil, T. (2022). Technical and Economic Evaluation for Off-Grid Hybrid Renewable Energy System Using Novel Bonobo Optimizer. *Sustainability*, *14*(3), 1533. https://doi.org/10.3390/su14031533

Farrokhifar, M. (2016). Optimal operation of energy storage devices with RESs to improve efficiency of distribution grids; technical and economical assessment. *International Journal of Electrical Power & Energy Systems*, *74*, 153–161. https://doi.org/10.1016/j.ijepes.2015.07.029

Ferreira, J. H. I., & Camacho, J. R. (2017). Prospects of Small Hydropower Technology. In *Renewable Hydropower Technologies*. InTech. https://doi.org/10.5772/66532

Filotis, Database for the Natural Environment of Greece. (n.d.). Retrieved May 31, 2022, from https://filotis.itia.ntua.gr

Finnegan, W., Jiang, Y., Dumergue, N., Davies, P., & Goggins, J. (2021). Investigation and Validation of Numerical Models for Composite Wind Turbine Blades. *Journal of Marine Science and Engineering*, *9*(5), 525. https://doi.org/10.3390/jmse9050525

Fiorentzis, K., Katsigiannis, Y., & Karapidakis, E. (2020). Full-Scale Implementation of RES and Storage in an Island Energy System. *Inventions*, *5*(4), 52. https://doi.org/10.3390/inventions5040052

Fiorillo, D., Kapelan, Z., Xenochristou, M., De Paola, F., & Giugni, M. (2021). Assessing the Impact of Climate Change on Future Water Demand using Weather Data. *Water Resources Management*, *35*(5), 1449–1462. https://doi.org/10.1007/s11269-021-02789-4

Fornarelli, R., Shahnia, F., Anda, M., Bahri, P. A., & Ho, G. (2018). Selecting an economically suitable and sustainable solution for a renewable energy-powered water desalination system: A rural Australian case study. *Desalination*, *435*, 128–139. https://doi.org/10.1016/j.desal.2017.11.008

GEODATA. Open data accessible to everyone. . (n.d.). Retrieved November 20, 2019, from https://geoda ta.gov. gr/datas et/aioli kos-khart es-tes-elladas

Geofabrik. OpenStreetMap Data. (n.d.). Retrieved November 20, 2019, from http://downl oad.geofa brik.de/ europ e/greece.html

Geoportal Map of Regulatory Authority for Energy (RAE) . (n.d.). Retrieved May 31, 2022, from https://geo.rae.gr/

Ghenai, C., Salameh, T., & Merabet, A. (2020). Technico-economic analysis of off grid solar PV/Fuel cell energy system for residential community in desert region. *International Journal of Hydrogen Energy*, *45*(20), 11460–11470. https://doi.org/10.1016/j.ijhydene.2018.05.110

Giamalaki, M., & Tsoutsos, T. (2019). Sustainable siting of solar power installations in Mediterranean using a GIS/AHP approach. *Renewable Energy*, *141*, 64–75. https://doi.org/10.1016/j.renene.2019.03.100

Gkiokas, G., Lagos, D., Korres, G., & Hatziargyriou, N. D. (2022). A hardware in the loop testbed for adaptive protection of non-inteconnected island systems with high RES penetration. *2022 International Conference on Smart Grid Synchronized Measurements and Analytics (SGSMA)*, 1–7. https://doi.org/10.1109/SGSMA51733.2022.9805999

Gude, V. G. (2016). Desalination and sustainability – An appraisal and current perspective. *Water Research*, *89*, 87–106. https://doi.org/10.1016/j.watres.2015.11.012

Guezgouz, M., Jurasz, J., Bekkouche, B., Ma, T., Javed, M. S., & Kies, A. (2019). Optimal hybrid pumped hydro-battery storage scheme for off-grid renewable energy systems. *Energy Conversion and Management*, *199*, 112046. https://doi.org/10.1016/j.enconman.2019.112046

Hamanah, W. M., Abido, M. A., & Alhems, L. M. (2020). Optimum Sizing of Hybrid PV, Wind, Battery and Diesel System Using Lightning Search Algorithm. *Arabian Journal for Science and Engineering*, *45*(3), 1871–1883. https://doi.org/10.1007/s13369-019-04292-w

Hausmann, J. N., Schlögl, R., Menezes, P. W., & Driess, M. (2021). Is direct seawater splitting economically meaningful? *Energy & Environmental Science*, *14*(7), 3679–3685. https://doi.org/10.1039/D0EE03659E

He, Y., Guo, S., Zhou, J., Wu, F., Huang, J., & Pei, H. (2021). The quantitative techno-economic comparisons and multi-objective capacity optimization of wind-photovoltaic hybrid power system considering different energy storage technologies. *Energy Conversion and Management*, *229*, 113779. https://doi.org/10.1016/j.enconman.2020.113779

He, Y., Li, X., Huang, P., & Wang, J. (2022). Exploring the Road toward Environmental Sustainability: Natural Resources, Renewable Energy Consumption, Economic Growth, and Greenhouse Gas Emissions. *Sustainability*, *14*(3), 1579. https://doi.org/10.3390/su14031579

Heffron, R. J., Körner, M.-F., Schöpf, M., Wagner, J., & Weibelzahl, M. (2021). The role of flexibility in the light of the COVID-19 pandemic and beyond: Contributing to a sustainable and resilient energy future in Europe. *Renewable and Sustainable Energy Reviews*, *140*, 110743. https://doi.org/10.1016/j.rser.2021.110743

Hellenic Network of Solar Energy 2002-2012. (n.d.). Retrieved June 9, 2022, from http://atmosphere-upatras.gr/solarmaps

Hellenic Statistical Authority . (n.d.). Retrieved November 16, 2020, from https://www.statistics.gr/en/home/

Herrera-León, S., Lucay, F., Kraslawski, A., Cisternas, L. A., & Gálvez, E. D. (2018). Optimization Approach to Designing Water Supply Systems in Non-Coastal Areas Suffering from Water Scarcity. *Water Resources Management*, *32*(7), 2457–2473. https://doi.org/10.1007/s11269-018-1939-z

Hinokuma, T., Farzaneh, H., & Shaqour, A. (2021). Techno-Economic Analysis of a Fuzzy Logic Control Based Hybrid Renewable Energy System to Power a University Campus in Japan. *Energies*, *14*(7), 1960. https://doi.org/10.3390/en14071960

Hoffstaedt, J. P., Truijen, D. P. K., Fahlbeck, J., Gans, L. H. A., Qudaih, M., Laguna, A. J., De Kooning, J. D. M., Stockman, K., Nilsson, H., Storli, P.-T., Engel, B., Marence, M., & Bricker, J. D. (2022). Low-head pumped hydro storage: A review of applicable technologies for design, grid integration, control and modelling. *Renewable and Sustainable Energy Reviews*, *158*, 112119. https://doi.org/10.1016/j.rser.2022.112119

Hunt, J. D., Zakeri, B., Lopes, R., Barbosa, P. S. F., Nascimento, A., Castro, N. J. de, Brandão, R., Schneider, P. S., & Wada, Y. (2020). Existing and new arrangements of pumped-hydro storage plants. *Renewable and Sustainable Energy Reviews*, *129*, 109914. https://doi.org/10.1016/j.rser.2020.109914

International Energy Agency. (2021). *IEA Energy Atlas*. https://www.iea.org/countries/greece

Ioannidis, R., & Koutsoyiannis, D. (2020). A review of land use, visibility and public perception of renewable energy in the context of landscape impact. *Applied Energy*, *276*, 115367. https://doi.org/10.1016/j.apenergy.2020.115367

IRENA. (2020). *Renewable Capacity Statistics 2020* . www.irena.org/publications/2020/Mar/Renewable-Capacity-Statistics-2020

Ishaq, H., Dincer, I., & Crawford, C. (2022). A review on hydrogen production and utilization: Challenges and opportunities. *International Journal of Hydrogen Energy*, *47*(62), 26238–26264. https://doi.org/10.1016/j.ijhydene.2021.11.149

Islam, M. S., Das, B. K., Das, P., & Rahaman, M. H. (2021). Techno-economic optimization of a zero emission energy system for a coastal community in Newfoundland, Canada. *Energy*, *220*, 119709. https://doi.org/10.1016/j.energy.2020.119709

Izadi, A., Shahafve, M., Ahmadi, P., & Javani, N. (2022). Transient simulation and techno-economic assessment of a near-zero energy building using a hydrogen storage system and different backup fuels. *International Journal of Hydrogen Energy*, *47*(74), 31927–31940. https://doi.org/10.1016/j.ijhydene.2022.06.033

Janota, L., Surovezhko, A., & Igissenov, A. (2022). Comprehensive evaluation of the planned development of intermittent renewable sources within the EU. *Energy Reports*, *8*, 214–220. https://doi.org/10.1016/j.egyr.2022.01.093

Javed, Ashfaq, Singh, Hussain, & Ustun. (2019). Design and Performance Analysis of a Stand-alone PV System with Hybrid Energy Storage for Rural India. *Electronics*, *8*(9), 952. https://doi.org/10.3390/electronics8090952

Javed, M. S., Ma, T., Jurasz, J., & Mikulik, J. (2021). A hybrid method for scenario-based techno-economic-environmental analysis of off-grid renewable energy systems. *Renewable and Sustainable Energy Reviews*, *139*, 110725. https://doi.org/10.1016/j.rser.2021.110725

Jouttijärvi, S., Lobaccaro, G., Kamppinen, A., & Miettunen, K. (2022). Benefits of bifacial solar cells combined with low voltage power grids at high latitudes. *Renewable and Sustainable Energy Reviews*, *161*, 112354. https://doi.org/10.1016/j.rser.2022.112354

Jurasz, J., Ceran, B., & Orłowska, A. (2020). Component degradation in small-scale off-grid PV-battery systems operation in terms of reliability, environmental impact and economic performance. *Sustainable Energy Technologies and Assessments*, *38*, 100647. https://doi.org/10.1016/j.seta.2020.100647

Kakoulaki, G., Kougias, I., Taylor, N., Dolci, F., Moya, J., & Jäger-Waldau, A. (2021). Green hydrogen in Europe – A regional assessment: Substituting existing production with electrolysis powered by

renewables. *Energy Conversion and Management*, *228*, 113649. https://doi.org/10.1016/j.enconman.2020.113649

Kakoulas, D. A., Golfinopoulos, S. K., Koumparou, D., & Alexakis, D. E. (2022). The Effectiveness of Rainwater Harvesting Infrastructure in a Mediterranean Island. *Water*, *14*(5), 716. https://doi.org/10.3390/w14050716

Kaldellis, J. K. (2020). *Hybrid Wind Energy Solutions Including Energy Storage* (pp. 103–129). https://doi.org/10.1007/978-3-030-26446-8_7

Kaldellis, J. K. (2021). Supporting the Clean Electrification for Remote Islands: The Case of the Greek Tilos Island. *Energies*, *14*(5), 1336. https://doi.org/10.3390/en14051336

Kaldellis, J. K., Kavadias, K., & Christinakis, E. (2001). Evaluation of the wind–hydro energy solution for remote islands. *Energy Conversion and Management*, *42*(9), 1105–1120. https://doi.org/10.1016/S0196-8904(00)00125-4

Kaldellis, J. K., & Zafirakis, D. (2020). Prospects and challenges for clean energy in European Islands.The TILOS paradigm. *Renewable Energy*, *145*, 2489–2502. https://doi.org/10.1016/j.renene.2019.08.014

Kalogirou, S. A. (2018). Introduction to Renewable Energy Powered Desalination. In *Renewable Energy Powered Desalination Handbook* (pp. 3–46). Elsevier. https://doi.org/10.1016/B978-0-12-815244-7.00001-5

Kapsali, M., & Anagnostopoulos, J. S. (2017). Investigating the role of local pumped-hydro energy storage in interconnected island grids with high wind power generation. *Renewable Energy*, *114*, 614–628. https://doi.org/10.1016/j.renene.2017.07.014

Karami, N., Moubayed, N., & Outbib, R. (2017). General review and classification of different MPPT Techniques. *Renewable and Sustainable Energy Reviews*, *68*, 1–18. https://doi.org/10.1016/j.rser.2016.09.132

Katsaprakakis, D. Al., Dakanali, I., Condaxakis, C., & Christakis, D. G. (2019). Comparing electricity storage technologies for small insular grids. *Applied Energy*, *251*, 113332. https://doi.org/10.1016/j.apenergy.2019.113332

Katsaprakakis, D. Al., Proka, A., Zafirakis, D., Damasiotis, M., Kotsampopoulos, P., Hatziargyriou, N., Dakanali, E., Arnaoutakis, G., & Xevgenos, D. (2022). Greek Islands' Energy Transition: From Lighthouse Projects to the Emergence of Energy Communities. *Energies*, *15*(16), 5996. https://doi.org/10.3390/en15165996

Katsivelakis, M., Bargiotas, D., Daskalopulu, A., Panapakidis, I. P., & Tsoukalas, L. (2021). Techno-Economic Analysis of a Stand-Alone Hybrid System: Application in Donoussa Island, Greece. *Energies*, *14*(7), 1868. https://doi.org/10.3390/en14071868

Kazem, H. A., Al-Badi, H. A. S., Al Busaidi, A. S., & Chaichan, M. T. (2017). Optimum design and evaluation of hybrid solar/wind/diesel power system for Masirah Island. *Environment, Development and Sustainability*, *19*(5), 1761–1778. https://doi.org/10.1007/s10668-016-9828-1

Kazem, H. A., Chaichan, M. T., Al-Waeli, A. H. A., & Sopian, K. (2020). A review of dust accumulation and cleaning methods for solar photovoltaic systems. *Journal of Cleaner Production*, *276*, 123187. https://doi.org/10.1016/j.jclepro.2020.123187

Kefif, N., Melzi, B., Hashemian, M., Assad, M. E. H., & Hoseinzadeh, S. (2022). Feasibility and optimal operation of micro energy hybrid system (hydro/wind) in the rural valley region. *International Journal of Low-Carbon Technologies*, *17*, 58–68. https://doi.org/10.1093/ijlct/ctab081

Khalili, T., Bidram, A., Nojavan, S., & Jermsittiparsert, K. (2020). Selection of Cost-Effective and Energy-Efficient Storages with Respect to Uncertain Nature of Renewable Energy Sources and Variations of Demands. In *Integration of Clean and Sustainable Energy Resources and Storage in Multi-Generation Systems* (pp. 15–27). Springer International Publishing. https://doi.org/10.1007/978-3-030-42420-6_2

Khan, I., Zakari, A., Zhang, J., Dagar, V., & Singh, S. (2022). A study of trilemma energy balance, clean energy transitions, and economic expansion in the midst of environmental sustainability: New insights from three trilemma leadership. *Energy*, *248*, 123619. https://doi.org/10.1016/j.energy.2022.123619

Khan, M. Z. A., Khan, H. A., & Aziz, M. (2022). Harvesting Energy from Ocean: Technologies and Perspectives. *Energies*, *15*(9), 3456. https://doi.org/10.3390/en15093456

Kotsifakis, K., Kourtis, I., Feloni, E., & Baltas, E. (2020). *Assessment of Rain Harvesting and RES Desalination for Meeting Water Needs in an Island in Greece* (pp. 59–62). https://doi.org/10.1007/978-3-030-13068-8_14

Kourtis, I. M., Kotsifakis, K. G., Feloni, E. G., & Baltas, E. A. (2019). Sustainable Water Resources Management in Small Greek Islands under Changing Climate. *Water*, *11*(8), 1694. https://doi.org/10.3390/w11081694

Krishan, O., & Suhag, S. (2019). An updated review of energy storage systems: Classification and applications in distributed generation power systems incorporating renewable energy

resources. *International Journal of Energy Research*, *43*(12), 6171–6210. https://doi.org/10.1002/er.4285

Krupnik, S., Wagner, A., Vincent, O., Rudek, T. J., Wade, R., Mišík, M., Akerboom, S., Foulds, C., Smith Stegen, K., Adem, Ç., Batel, S., Rabitz, F., Certomà, C., Chodkowska-Miszczuk, J., Denac, M., Dokupilová, D., Leiren, M. D., Ignatieva, M. F., Gabaldón-Estevan, D., … von Wirth, T. (2022). Beyond technology: A research agenda for social sciences and humanities research on renewable energy in Europe. *Energy Research & Social Science*, *89*, 102536. https://doi.org/10.1016/j.erss.2022.102536

Lagouvardos, K., Kotroni, V., Bezes, A., Koletsis, I., Kopania, T., Lykoudis, S., Mazarakis, N., Papagiannaki, K., & Vougioukas, S. (2017). The automatic weather stations NOANN network of the National Observatory of Athens: operation and database. *Geoscience Data Journal*, *4*(1), 4–16. https://doi.org/10.1002/gdj3.44

Lagouvardou, S., & Psaraftis, H. N. (2022). Implications of the EU Emissions Trading System (ETS) on European container routes: A carbon leakage case study. *Maritime Transport Research*, *3*, 100059. https://doi.org/10.1016/j.martra.2022.100059

Lata-García, J., Jurado, F., Fernández-Ramírez, L. M., & Sánchez-Sainz, H. (2018). Optimal hydrokinetic turbine location and techno-economic analysis of a hybrid system based on photovoltaic/hydrokinetic/hydrogen/battery. *Energy*, *159*, 611–620. https://doi.org/10.1016/j.energy.2018.06.183

Law 3851/2010: 'Accelerating the development of Renewable Energy Sources to deal with climate change and other regulations addressing issues under the authority of the Ministry of Environment, Energy and Climate Change.' (2010). Official Gazette Α ́ 85/04.06.2010.

Leonhardt, R., Noble, B., Poelzer, G., Fitzpatrick, P., Belcher, K., & Holdmann, G. (2022). Advancing local energy transitions: A global review of government instruments supporting community energy. *Energy Research & Social Science*, *83*, 102350. https://doi.org/10.1016/j.erss.2021.102350

Li, F.-F., & Qiu, J. (2016). Multi-objective optimization for integrated hydro–photovoltaic power system. *Applied Energy*, *167*, 377–384. https://doi.org/10.1016/j.apenergy.2015.09.018

Lin, S., Ma, T., & Shahzad Javed, M. (2020). Prefeasibility study of a distributed photovoltaic system with pumped hydro storage for residential buildings. *Energy Conversion and Management*, *222*, 113199. https://doi.org/10.1016/j.enconman.2020.113199

Liu, H., Khan, I., Zakari, A., & Alharthi, M. (2022). Roles of trilemma in the world energy sector and transition towards sustainable energy: A study of economic growth and the environment. *Energy Policy*, *170*, 113238. https://doi.org/10.1016/j.enpol.2022.113238

López González, D. M., & Garcia Rendon, J. (2022). Opportunities and challenges of mainstreaming distributed energy resources towards the transition to more efficient and resilient energy markets. *Renewable and Sustainable Energy Reviews*, *157*, 112018. https://doi.org/10.1016/j.rser.2021.112018

Ma, T., & Javed, M. S. (2019). Integrated sizing of hybrid PV-wind-battery system for remote island considering the saturation of each renewable energy resource. *Energy Conversion and Management*, *182*, 178–190. https://doi.org/10.1016/j.enconman.2018.12.059

Madaleno, M., Dogan, E., & Taskin, D. (2022). A step forward on sustainability: The nexus of environmental responsibility, green technology, clean energy and green finance. *Energy Economics*, *109*, 105945. https://doi.org/10.1016/j.eneco.2022.105945

Maisanam, A. K. S., Biswas, A., & Sharma, K. K. (2021). Integrated socio-environmental and techno-economic factors for designing and sizing of a sustainable hybrid renewable energy system. *Energy Conversion and Management*, *247*, 114709. https://doi.org/10.1016/j.enconman.2021.114709

Malczewski, J. (1999). *GIS and Multicriteria Decision Analysis*. John Wiley & Sons.

Malczewski, J. (2004). GIS-based land-use suitability analysis: a critical overview. *Progress in Planning*, *62*(1), 3–65. https://doi.org/10.1016/j.progress.2003.09.002

Malczewski, J. (2006). GIS-based multicriteria decision analysis: a survey of the literature. *International Journal of Geographical Information Science*, *20*(7), 703–726. https://doi.org/10.1080/13658810600661508

Mamassis, N., Efstratiadis, A., Dimitriadis, P., Iliopoulou, T., Ioannidis, R., & Koutsoyiannis, D. (2021). Water and Energy. In *Handbook of Water Resources Management: Discourses, Concepts and Examples* (pp. 619–657). Springer International Publishing. https://doi.org/10.1007/978-3-030-60147-8_20

Maqsood, J., Farooque, A. A., Abbas, F., Esau, T., Wang, X., Acharya, B., & Afzaal, H. (2022). Application of Artificial Neural Networks to Project Reference Evapotranspiration Under Climate Change Scenarios. *Water Resources Management*, *36*(3), 835–851. https://doi.org/10.1007/s11269-021-02997-y

Marocco, P., Ferrero, D., Lanzini, A., & Santarelli, M. (2022). The role of hydrogen in the optimal design of off-grid hybrid renewable energy systems. *Journal of Energy Storage*, *46*, 103893. https://doi.org/10.1016/j.est.2021.103893

Martínez-Huerta, M. V., & Lázaro, M. J. (2017). Electrocatalysts for low temperature fuel cells. *Catalysis Today*, *285*, 3–12. https://doi.org/10.1016/j.cattod.2017.02.015

Mavromatakis, F., Makrides, G., Georghiou, G., Pothrakis, A., Franghiadakis, Y., Drakakis, E., & Koudoumas, E. (2010). Modeling the photovoltaic potential of a site. *Renewable Energy*, *35*(7), 1387–1390. https://doi.org/10.1016/j.renene.2009.11.010

Monforti Ferrario, A., Bartolini, A., Segura Manzano, F., Vivas, F. J., Comodi, G., McPhail, S. J., & Andujar, J. M. (2021). A model-based parametric and optimal sizing of a battery/hydrogen storage of a real hybrid microgrid supplying a residential load: Towards island operation. *Advances in Applied Energy*, *3*, 100048. https://doi.org/10.1016/j.adapen.2021.100048

Myronidis, D., & Nikolaos, T. (2021). Changes in climatic patterns and tourism and their concomitant effect on drinking water transfers into the region of South Aegean, Greece. *Stochastic Environmental Research and Risk Assessment*, *35*(9), 1725–1739. https://doi.org/10.1007/s00477-021-02015-y

Nasir, M. H., Wen, J., Nassani, A. A., Haffar, M., Igharo, A. E., Musibau, H. O., & Waqas, M. (2022). Energy Security and Energy Poverty in Emerging Economies: A Step Towards Sustainable Energy Efficiency. *Frontiers in Energy Research*, *10*. https://doi.org/10.3389/fenrg.2022.834614

Nassar, Y. F., Abdunnabi, M. J., Sbeta, M. N., Hafez, A. A., Amer, K. A., Ahmed, A. Y., & Belgasim, B. (2021). Dynamic analysis and sizing optimization of a pumped hydroelectric storage-integrated hybrid PV/Wind system: A case study. *Energy Conversion and Management*, *229*, 113744. https://doi.org/10.1016/j.enconman.2020.113744

Navarro Barrio, R., Sola, I., Blanco-Murillo, F., del-Pilar-Ruso, Y., Fernández-Torquemada, Y., & Sánchez-Lizaso, J. L. (2021). Application of salinity thresholds in Spanish brine discharge regulations: Energetic and environmental implications. *Desalination*, *501*, 114901. https://doi.org/10.1016/j.desal.2020.114901

Nazir, M. S., Mahdi, A. J., Bilal, M., Sohail, H. M., Ali, N., & Iqbal, H. M. N. (2019). Environmental impact and pollution-related challenges of renewable wind energy paradigm – A review. *Science of The Total Environment*, *683*, 436–444. https://doi.org/10.1016/j.scitotenv.2019.05.274

Nik, V. M., Perera, A. T. D., & Chen, D. (2021). Towards climate resilient urban energy systems: a review. *National Science Review*, *8*(3). https://doi.org/10.1093/nsr/nwaa134

Nikas-Nasioulis, I., Bertsiou, M. M., & Baltas, E. (2022). Investigation of Energy, Water, and Electromobility Through the Development of a Hybrid Renewable Energy System on the Island of Kos. *WSEAS TRANSACTIONS ON ENVIRONMENT AND DEVELOPMENT*, *18*, 543–554. https://doi.org/10.37394/232015.2022.18.53

Nikitidou, E., Kazantzidis, A., Tzoumanikas, P., Salamalikis, V., & Bais, A. F. (2015). Retrieval of surface solar irradiance, based on satellite-derived cloud information, in Greece. *Energy*, *90*, 776–783. https://doi.org/10.1016/j.energy.2015.07.103

Nirmal Mukundan, C. M., Jayaprakash, P., Subramaniam, U., & Almakhles, D. J. (2020). Binary Hybrid Multilevel Inverter-Based Grid Integrated Solar Energy Conversion System With Damped SOGI Control. *IEEE Access*, *8*, 37214–37228. https://doi.org/10.1109/ACCESS.2020.2974773

Notton, G., Lazarov, V., & Stoyanov, L. (2010). Optimal sizing of a grid-connected PV system for various PV module technologies and inclinations, inverter efficiency characteristics and locations. *Renewable Energy*, *35*(2), 541–554. https://doi.org/10.1016/j.renene.2009.07.013

Notton, G., Mistrushi, D., Stoyanov, L., & Berberi, P. (2017). Operation of a photovoltaic-wind plant with a hydro pumping-storage for electricity peak-shaving in an island context. *Solar Energy*, *157*, 20–34. https://doi.org/10.1016/j.solener.2017.08.016

Nouri, N., Balali, F., Nasiri, A., Seifoddini, H., & Otieno, W. (2019). Water withdrawal and consumption reduction for electrical energy generation systems. *Applied Energy*, *248*, 196–206. https://doi.org/10.1016/j.apenergy.2019.04.023

Nunez, S., Arets, E., Alkemade, R., Verwer, C., & Leemans, R. (2019). Assessing the impacts of climate change on biodiversity: is below 2 °C enough? *Climatic Change*, *154*(3–4), 351–365. https://doi.org/10.1007/s10584-019-02420-x

Official Gazette 15. (1991). *Characterization of area Agios Georgios in Fournoi Ikarias as an archaeological site* (Issue B).

Official Gazette 25. (1993). *Characterization of area Petrokopi in Fournoi Ikarias as an archaeological site* (Issue B).

Official Gazette 85. (2010). *Acceleration of the development of Renewable Energy Sources for dealing with climate crisis and other provisions within the competence of the Ministry of Environment, Energy and Climate Change* (Issue A).

Official Gazette 1031. (1996). *Characterization of Ikaria areas as archaeological sites* (Issue B).

Official Gazette 2464. (2008). *Adoption of a specific spatial planning framework and sustainable development for renewable energy and its environmental impact strategic study* (Issue B).

Ogland-Hand, J. D., Bielicki, J. M., Wang, Y., Adams, B. M., Buscheck, T. A., & Saar, M. O. (2019). The value of bulk energy storage for reducing CO2 emissions and water requirements from regional electricity systems. *Energy Conversion and Management*, *181*, 674–685. https://doi.org/10.1016/j.enconman.2018.12.019

Ökten, K., & Kurşun, B. (2022). Thermo-economic assessment of a thermally integrated pumped thermal energy storage (TI-PTES) system combined with an absorption refrigeration cycle driven by low-grade heat source. *Journal of Energy Storage*, *51*, 104486. https://doi.org/10.1016/j.est.2022.104486

Olabi, A. G., & Abdelkareem, M. A. (2022). Renewable energy and climate change. *Renewable and Sustainable Energy Reviews*, *158*, 112111. https://doi.org/10.1016/j.rser.2022.112111

Olabi, A. G., Wilberforce, T., Elsaid, K., Salameh, T., Sayed, E. T., Husain, K. S., & Abdelkareem, M. A. (2021). Selection Guidelines for Wind Energy Technologies. *Energies*, *14*(11), 3244. https://doi.org/10.3390/en14113244

Panagopoulos, A. (2021). Water-energy nexus: desalination technologies and renewable energy sources. *Environmental Science and Pollution Research*, *28*(17), 21009–21022. https://doi.org/10.1007/s11356-021-13332-8

Papaefthymiou, S. V., & Papathanassiou, S. A. (2014). Optimum sizing of wind-pumped-storage hybrid power stations in island systems. *Renewable Energy*, *64*, 187–196. https://doi.org/10.1016/j.renene.2013.10.047

Papapostolou, C. M., Kondili, E. M., Zafirakis, D. P., & Tzanes, G. T. (2020). Sustainable water supply systems for the islands: The integration with the energy problem. *Renewable Energy*, *146*, 2577–2588. https://doi.org/10.1016/j.renene.2019.07.130

Paris Agreement. FCCC/CP/2015/L.9/Rev.1. UNFCCC secretariat. (2016). https://unfccc.int/process-and-meetings/the-paris-agreement/the-paris-agreement

Phan, & Lai. (2019). Control Strategy of a Hybrid Renewable Energy System Based on Reinforcement Learning Approach for an Isolated Microgrid. *Applied Sciences*, *9*(19), 4001. https://doi.org/10.3390/app9194001

Poompavai, T., & Kowsalya, M. (2019). Control and energy management strategies applied for solar photovoltaic and wind energy fed water pumping system: A review. *Renewable and Sustainable Energy Reviews*, *107*, 108–122. https://doi.org/10.1016/j.rser.2019.02.023

Potashnikov, V., Golub, A., Brody, M., & Lugovoy, O. (2022). Decarbonizing Russia: Leapfrogging from Fossil Fuel to Hydrogen. *Energies*, *15*(3), 683. https://doi.org/10.3390/en15030683

PPC Renewables. (2023). *Naeras: The Hybrid Power Plant of Ikaria*. https://ppcr.gr/el/announcements/news/335-naeras-yvridiko-ergo-ikarias

Psiloglou, B. E., Giannakopoulos, C., Majithia, S., & Petrakis, M. (2009). Factors affecting electricity demand in Athens, Greece and London, UK: A comparative assessment. *Energy*, *34*(11), 1855–1863. https://doi.org/10.1016/j.energy.2009.07.033

Public power Corporation. (n.d.). Retrieved January 9, 2023, from https://www.dei.gr/el/gia-to-spiti/revma/g1-g1n/

Pugsley, A., Zacharopoulos, A., Mondol, J. D., & Smyth, M. (2018). Solar Desalination Potential Around the World. In *Renewable Energy Powered Desalination Handbook* (pp. 47–90). Elsevier. https://doi.org/10.1016/B978-0-12-815244-7.00002-7

Pujari, H. K., & Rudramoorthy, M. (2021). Optimal design and techno-economic analysis of a hybrid grid-independent renewable energy system for a rural community. *International Transactions on Electrical Energy Systems*, *31*(9). https://doi.org/10.1002/2050-7038.13007

Qi, X., Wang, J., Królczyk, G., Gardoni, P., & Li, Z. (2022). Sustainability analysis of a hybrid renewable power system with battery storage for islands application. *Journal of Energy Storage*, *50*, 104682. https://doi.org/10.1016/j.est.2022.104682

Rahman, A., Farrok, O., & Haque, M. M. (2022). Environmental impact of renewable energy source based electrical power plants: Solar, wind, hydroelectric, biomass, geothermal, tidal, ocean, and osmotic. *Renewable and Sustainable Energy Reviews*, *161*, 112279. https://doi.org/10.1016/j.rser.2022.112279

Ram, J. P., Rajasekar, N., & Miyatake, M. (2017). Design and overview of maximum power point tracking techniques in wind and solar photovoltaic systems: A review. *Renewable and Sustainable Energy Reviews*, *73*, 1138–1159. https://doi.org/10.1016/j.rser.2017.02.009

Rehman, S., & Khan, S. A. (2017). Multi-Criteria Wind Turbine Selection using Weighted Sum Approach. *International Journal of Advanced Computer Science and Applications*, *8*(6), 128–132.

Ren, J., & Ren, X. (2018). Sustainability ranking of energy storage technologies under uncertainties. *Journal of Cleaner Production*, *170*, 1387–1398. https://doi.org/10.1016/j.jclepro.2017.09.229

Rezaei, M., Mostafaeipour, A., Jafari, N., Naghdi-Khozani, N., & Moftakharzadeh, A. (2020). Wind and solar energy utilization for seawater desalination and hydrogen production in the coastal areas of southern Iran. *Journal of Engineering, Design and Technology*, *18*(6), 1951–1969. https://doi.org/10.1108/JEDT-06-2019-0154

Rezaei, M., Naghdi-Khozani, N., & Jafari, N. (2020). Wind energy utilization for hydrogen production in an underdeveloped country: An economic investigation. *Renewable Energy*, *147*, 1044–1057. https://doi.org/10.1016/j.renene.2019.09.079

Rievaj, V., Gaňa, J., & Synák, F. (2019). Is hydrogen the fuel of the future? *Transportation Research Procedia*, *40*, 469–474. https://doi.org/10.1016/j.trpro.2019.07.068

Ritchie, H., Roser, M., & Rosado, P. (2022). *"Energy". Published online at OurWorldInData.org*. https://ourworldindata.org/energy

Robinius, M., Raje, T., Nykamp, S., Rott, T., Müller, M., Grube, T., Katzenbach, B., Küppers, S., & Stolten, D. (2018). Power-to-Gas: Electrolyzers as an alternative to network expansion – An example from a distribution system operator. *Applied Energy*, *210*, 182–197. https://doi.org/10.1016/j.apenergy.2017.10.117

Rokicki, T., Jadczak, R., Kucharski, A., Bórawski, P., Bełdycka-Bórawska, A., Szeberényi, A., & Perkowska, A. (2022). Changes in Energy Consumption and Energy Intensity in EU Countries as a Result of the COVID-19 Pandemic by Sector and Area Economy. *Energies*, *15*(17), 6243. https://doi.org/10.3390/en15176243

Saaty, T. L. (1977). A scaling method for priorities in hierarchical structures. *Journal of Mathematical Psychology*, *15*(3), 234–281. https://doi.org/10.1016/0022-2496(77)90033-5

Sacchi, R., Bauer, C., Cox, B., & Mutel, C. (2022). When, where and how can the electrification of passenger cars reduce greenhouse gas emissions? *Renewable and Sustainable Energy Reviews*, *162*, 112475. https://doi.org/10.1016/j.rser.2022.112475

San Marchi, C., Hecht, E. S., Ekoto, I. W., Groth, K. M., LaFleur, C., Somerday, B. P., Mukundan, R., Rockward, T., Keller, J., & James, C. W. (2017). Overview of the DOE hydrogen safety, codes and standards program, part 3: Advances in research and development to enhance the scientific basis for hydrogen regulations, codes and standards. *International Journal of Hydrogen Energy*, *42*(11), 7263–7274. https://doi.org/10.1016/j.ijhydene.2016.07.014

Sánchez, A., Zhang, Q., Martín, M., & Vega, P. (2022). Towards a new renewable power system using energy storage: An economic and social analysis. *Energy Conversion and Management*, *252*, 115056. https://doi.org/10.1016/j.enconman.2021.115056

Sargentis, G.-F., Ioannidis, R., Iliopoulou, T., Dimitriadis, P., & Koutsoyiannis, D. (2021). Landscape Planning of Infrastructure through Focus Points' Clustering Analysis. Case Study: Plastiras Artificial Lake (Greece). *Infrastructures*, *6*(1), 12. https://doi.org/10.3390/infrastructures6010012

Sarris, D., Bertsiou, M. M., & Baltas, E. (2019). Evaluation of a Hybrid Renewable Energy System (HRES) in Patmos Island. *International Journal of Renewable Energy Sources*, *4*, 40–47.

Sato, M., Rafaty, R., Calel, R., & Grubb, M. (2022). Allocation, allocation, allocation! The political economy of the development of the European Union Emissions Trading System. *WIREs Climate Change*, *13*(5). https://doi.org/10.1002/wcc.796

Schrotenboer, A. H., Veenstra, A. A. T., uit het Broek, M. A. J., & Ursavas, E. (2022). A Green Hydrogen Energy System: Optimal control strategies for integrated hydrogen storage and power generation with wind energy. *Renewable and Sustainable Energy Reviews*, *168*, 112744. https://doi.org/10.1016/j.rser.2022.112744

Seedahmed, M. M. A., Ramli, M. A. M., Bouchekara, H. R. E. H., Shahriar, M. S., Milyani, A. H., & Rawa, M. (2022). A techno-economic analysis of a hybrid energy system for the electrification of a remote cluster in western Saudi Arabia. *Alexandria Engineering Journal*, *61*(7), 5183–5202. https://doi.org/10.1016/j.aej.2021.10.041

Setas Lopes, A., Castro, R., & Silva, C. S. (2020). Design of water pumped storage systems: A sensitivity and scenario analysis for island microgrids. *Sustainable Energy Technologies and Assessments*, *42*, 100847. https://doi.org/10.1016/j.seta.2020.100847

Simanullang, M., & Prost, L. (2022). Nanomaterials for on-board solid-state hydrogen storage applications. *International Journal of Hydrogen Energy*, *47*(69), 29808–29846. https://doi.org/10.1016/j.ijhydene.2022.06.301

Simão, M., & Ramos, H. (2020). Hybrid Pumped Hydro Storage Energy Solutions towards Wind and PV Integration: Improvement on Flexibility, Reliability and Energy Costs. *Water*, *12*(9), 2457. https://doi.org/10.3390/w12092457

Skroufouta, S., & Baltas, E. (2021). Investigation of hybrid renewable energy system (HRES) for covering energy and water needs on the Island of Karpathos in Aegean Sea. *Renewable Energy*, *173*, 141–150. https://doi.org/10.1016/j.renene.2021.03.113

Smart & Sustainable Island. (2023). *Astypalea: The first smart & sustainable Mediterranean Island*. https://smartastypalea.gov.gr/?lang=el%29

Spiller, M., Müller, C., Mulholland, Z., Louizidou, P., Küpper, F. C., Knosala, K., & Stenzel, P. (2022). Reducing Carbon Emissions from the Tourist Accommodation Sector on Non-Interconnected Islands: A Case Study of a Medium-Sized Hotel in Rhodes, Greece. *Energies*, *15*(10), 3801. https://doi.org/10.3390/en15103801

Stoyanov, L., Bachev, I., Zarkov, Z., Lazarov, V., & Notton, G. (2021). Multivariate Analysis of a Wind–PV-Based Water Pumping Hybrid System for Irrigation Purposes. *Energies*, *14*(11), 3231. https://doi.org/10.3390/en14113231

Subramanian, S., Sankaralingam, C., Elavarasan, R. M., Vijayaraghavan, R. R., Raju, K., & Mihet-Popa, L. (2021). An Evaluation on Wind Energy Potential Using Multi-Objective Optimization Based Non-Dominated Sorting Genetic Algorithm III. *Sustainability*, *13*(1), 410. https://doi.org/10.3390/su13010410

Sultan, H. M., Menesy, A. S., Kamel, S., Korashy, A., Almohaimeed, S. A., & Abdel-Akher, M. (2021). An improved artificial ecosystem optimization algorithm for optimal configuration of a hybrid PV/WT/FC energy system. *Alexandria Engineering Journal*, *60*(1), 1001–1025. https://doi.org/10.1016/j.aej.2020.10.027

Sürer, M. G., & Arat, H. T. (2022). Advancements and current technologies on hydrogen fuel cell applications for marine vehicles. *International Journal of Hydrogen Energy*, *47*(45), 19865–19875. https://doi.org/10.1016/j.ijhydene.2021.12.251

Swanson, A. C., & Bohlman, S. (2021). Cumulative Impacts of Land Cover Change and Dams on the Land–Water Interface of the Tocantins River. *Frontiers in Environmental Science*, *9*. https://doi.org/10.3389/fenvs.2021.662904

Syafii, S., Wati, W., & Fahreza, R. (2021). Techno-economic-enviro optimization analysis of diesel/PV/wind with pumped hydro storage for Mentawai Island microgrid. *Bulletin of Electrical Engineering and Informatics*, *10*(5), 2396–2404. https://doi.org/10.11591/eei.v10i5.3167

Thimmaraju, M., Sreepada, D., Babu, G. S., Dasari, B. K., Velpula, S. K., & Vallepu, N. (2018). Desalination of Water. In *Desalination and Water Treatment*. InTech. https://doi.org/10.5772/intechopen.78659

Tian, J., Yu, L., Xue, R., Zhuang, S., & Shan, Y. (2022). Global low-carbon energy transition in the post-COVID-19 era. *Applied Energy*, *307*, 118205. https://doi.org/10.1016/j.apenergy.2021.118205

Triantafyllou, P., Koroneos, C., Kondili, E., Kollas, P., Zafirakis, D., Ktenidis, P., & Kaldellis, J. K. (2021). Optimum green energy solution to address the remote islands' water-energy nexus: the case study of Nisyros island. *Heliyon*, *7*(9), e07838. https://doi.org/10.1016/j.heliyon.2021.e07838

Turan, İ., & Uyar, T. S. (2022). *Transition Period to Renewable Energy Usage: Turkey Case* (pp. 375–394). https://doi.org/10.1007/978-3-031-05125-8_16

Van Sark, W. G. J. H. M., Van der Velde, H. C., Coelingh, J. P., & Bierbooms, W. A. A. M. (2019). Do we really need rotor equivalent wind speed? *Wind Energy*, *22*(6), 745–763. https://doi.org/10.1002/we.2319

Vazaios, E. (1987). *Applications of Solar Energy* (Third). Paraskinio.

Voogd, H. (1983). *Evaluation for Urban and Regional Planning*.

Vourdoubas, J. (2022). Study about Water-energy Nexus in the Island of Crete, Greece. In *Novel Perspectives of Engineering Research Vol. 8* (pp. 134–146). Book Publisher International (a part of SCIENCEDOMAIN International). https://doi.org/10.9734/bpi/rtcams/v8/15569D

Wang, C., Raza, S. A., Adebayo, T. S., Yi, S., & Shah, M. I. (2023). The roles of hydro, nuclear and biomass energy towards carbon neutrality target in China: A policy-based analysis. *Energy*, *262*, 125303. https://doi.org/10.1016/j.energy.2022.125303

Wichelns, D. (2017). The water-energy-food nexus: Is the increasing attention warranted, from either a research or policy perspective? *Environmental Science & Policy*, *69*, 113–123. https://doi.org/10.1016/j.envsci.2016.12.018

Xia, J., Xu, G., Guo, P., Peng, H., Zhang, X., Wang, Y., & Zhang, W. (2018). Tempo-Spatial Analysis of Water Quality in the Three Gorges Reservoir, China, after its 175-m Experimental Impoundment. *Water Resources Management*, *32*(9), 2937–2954. https://doi.org/10.1007/s11269-018-1918-4

Xu, D., Acker, T., & Zhang, X. (2019). Size optimization of a hybrid PV/wind/diesel/battery power system for reverse osmosis desalination. *Journal of Water Reuse and Desalination*, *9*(4), 405–422. https://doi.org/10.2166/wrd.2019.019

Xu, X., Hu, W., Cao, D., Huang, Q., Chen, C., & Chen, Z. (2020). Optimized sizing of a standalone PV-wind-hydropower station with pumped-storage installation hybrid energy system. *Renewable Energy*, *147*, 1418–1431. https://doi.org/10.1016/j.renene.2019.09.099

Yang, Z., Wu, Y., Zhang, Z., Li, H., Li, X., Egorov, R. I., Strizhak, P. A., & Gao, X. (2019). Recent advances in co-thermochemical conversions of biomass with fossil fuels focusing on the synergistic effects. *Renewable and Sustainable Energy Reviews*, *103*, 384–398. https://doi.org/10.1016/j.rser.2018.12.047

Yanxing, Z., Maoqiong, G., Yuan, Z., Xueqiang, D., & Jun, S. (2019). Thermodynamics analysis of hydrogen storage based on compressed gaseous hydrogen, liquid hydrogen and cryo-compressed hydrogen. *International Journal of Hydrogen Energy*, *44*(31), 16833–16840. https://doi.org/10.1016/j.ijhydene.2019.04.207

Yu, M., Wang, K., & Vredenburg, H. (2021). Insights into low-carbon hydrogen production methods: Green, blue and aqua hydrogen. *International Journal of Hydrogen Energy*, *46*(41), 21261–21273. https://doi.org/10.1016/j.ijhydene.2021.04.016

Yue, M., Lambert, H., Pahon, E., Roche, R., Jemei, S., & Hissel, D. (2021). Hydrogen energy systems: A critical review of technologies, applications, trends and challenges. *Renewable and Sustainable Energy Reviews*, *146*, 111180. https://doi.org/10.1016/j.rser.2021.111180

Zafeirakou, A., Karavi, A., Katsoulea, A., Zorpas, A., & Papamichael, I. (2022). Water resources management in the framework of the circular economy for touristic areas in the Mediterranean: case study of Sifnos Island in Greece. *Euro-Mediterranean Journal for Environmental Integration*, *7*(3), 347–360. https://doi.org/10.1007/s41207-022-00319-1

Zakeri, B., Paulavets, K., Barreto-Gomez, L., Echeverri, L. G., Pachauri, S., Boza-Kiss, B., Zimm, C., Rogelj, J., Creutzig, F., Ürge-Vorsatz, D., Victor, D. G., Bazilian, M. D., Fritz, S., Gielen, D., McCollum, D. L., Srivastava, L., Hunt, J. D., & Pouya, S. (2022). Pandemic, War, and Global Energy Transitions. *Energies*, *15*(17), 6114. https://doi.org/10.3390/en15176114

Zhang, C., Wei, Y.-L., Cao, P.-F., & Lin, M.-C. (2018). Energy storage system: Current studies on batteries and power condition system. *Renewable and Sustainable Energy Reviews*, *82*, 3091–3106. https://doi.org/10.1016/j.rser.2017.10.030

Appendices

Appendix A – Abbreviations

Appendix B – List of Figures

Appendix C – List of Tables

Appendix D – Extended Summary in Greek (Εκτεταμένη περίληψη)

Appendix E – Complete List of Publications

AHP	analytic hierarchy process	OPEX	operational expenditure
BT	battery storage	PBP	payback period
CAPEX	capital expenditure	PHS	pumped hydro storage system
COE	cost of energy	PPC	public power corporation
COP21	21st conference of parties	PV	photovoltaic module
COW	cost of water	RES	renewable energy sources
DU	desalination unit	RRF	recovery and resilience facility
EC	european commission	UNFCCC	united nations framework convention on climate change
EEA	european environment agency	WEN	water energy nexus
EL	electrolyzer	WT	wind turbine
ETS	emissions trading system		
FC	fuel cell		
GHG	greenhouse gas emissions		
GIS	geographic information systems		
HPBS	hybrid pumped battery storage system		
HPHS	hybrid pumped hydrogen storage system		
HRES	hybrid renewable energy system		
IEA	international energy agency		
IRENA	international renewable energy agency		
LCOE	levelized cost of energy		
LOLP	loss of load probability		
LPS	local power station		
MCDM	multi criteria decision making		
NDCs	nationally determined contributions		
NNIs	non-interconnected islands		

1. Εισαγωγή

Οι ανανεώσιμες πηγές ενέργειας (ΑΠΕ) αποτελούν την κύρια προτεραιότητα για την Ευρωπαϊκή Ένωση (ΕΕ), όπως αποδεικνύεται από το θεσμικό πλαίσιο που εισήχθη τις τελευταίες δεκαετίες και οδηγεί στην αυξανόμενη διείσδυση των ΑΠΕ στο ενεργειακό ισοζύγιο παγκοσμίως με τη μετάβαση από τα ορυκτά καύσιμα και στη μείωση των εκπομπών αερίων του θερμοκηπίου. Οι εφαρμογές ΑΠΕ, για την κάλυψη των παγκόσμιων αναγκών σε ηλεκτρική ενέργεια, καθοδηγείται και από την κλιματική αλλαγή. Ο στόχος των ΑΠΕ για το 2030 έχει οριστεί στο 32% της ακαθάριστης τελικής κατανάλωσης, σε 32,5% αύξηση για την ενεργειακή απόδοση και ελάχιστη μείωση της τάξης των 40% στις εκπομπές αερίων του θερμοκηπίου, βάσει της Οδηγίας για τις ΑΠΕ 2018/2001/ΕΕ.

Οι στόχοι της ΕΕ για το κλίμα και την ενέργεια έχουν σημαντικό αντίκτυπο στις ενεργειακές και κλιματικές πολιτικές των κρατών μελών της, ενθαρρύνοντας τις επενδύσεις σε ΑΠΕ και σε μέτρα ενεργειακής απόδοσης. Η Ελλάδα, ως μέλος της ΕΕ, συμμετέχει στην πρωτοβουλία για την ενίσχυση του μεριδίου των ΑΠΕ στο ενεργειακό ισοζύγιο και έχει θέσει τους δικούς της στόχους για αύξηση του μεριδίου των ΑΠΕ στην τελική κατανάλωση ενέργειας και κατανάλωσης ηλεκτρικής ενέργειας έως το 2030.

Η Συμφωνία του Παρισιού για την Κλιματική Αλλαγή είναι μια διεθνής συμφωνία που εγκρίθηκε το 2015 από τη Σύμβαση Πλαίσιο των Ηνωμένων Εθνών για την Κλιματική Αλλαγή για τον περιορισμό της υπερθέρμανσης του πλανήτη πολύ κάτω από τους 2°C πάνω από τα προβιομηχανικά επίπεδα και τη συνέχιση των προσπαθειών για περιορισμό της αύξησης της θερμοκρασίας στους 1,5°C. Η συμφωνία στοχεύει να ενισχύσει την ικανότητα των χωρών να αντιμετωπίζουν τις επιπτώσεις της κλιματικής αλλαγής, να αυξήσει την ανθεκτικότητα των οικοσυστημάτων και να διευκολύνει τη μετάβαση σε οικονομίες χαμηλών εκπομπών άνθρακα. Η Συμφωνία του Παρισιού ορίζει μια σειρά διατάξεων και μηχανισμών για την προώθηση της διεθνούς συνεργασίας και συνεργασίας, συμπεριλαμβανομένης της υποβολής τεχνικών εκθέσεων (Nationally Determined Contributions, NDCs) που περιγράφουν τις προσπάθειες κάθε χώρας να μειώσει τις εκπομπές αερίων του θερμοκηπίου και να προσαρμοστεί στις επιπτώσεις της κλιματικής αλλαγής. Καθιερώνει επίσης ένα σύστημα διαφάνειας, αναγνωρίζοντας την ανάγκη υποστήριξης των αναπτυσσόμενων χωρών για να εφαρμόσουν τους στόχους τους τους και να προσαρμοστούν στις επιπτώσεις της κλιματικής αλλαγής.

Η μετάβαση στις ΑΠΕ προσφέρει πολλά οφέλη, συμπεριλαμβανομένης της μείωσης των εκπομπών αερίων του θερμοκηπίου, που συμβάλλουν στην κλιματική αλλαγή και έχουν αρνητικές επιπτώσεις στην ανθρώπινη υγεία και το περιβάλλον. Επιπλέον, οι ΑΠΕ μπορούν να μειώσουν το κόστος της

ενέργειας, να αυξήσουν την ενεργειακή ασφάλεια βασιζόμενες σε τοπικές, βιώσιμες πηγές ενέργειας, να δημιουργήσουν θέσεις εργασίας και να τονώσουν την οικονομική ανάπτυξη. Σύμφωνα με την Έκθεση Eionet, από το 2005 έως το 2018, οι ευρωπαϊκές χώρες αύξησαν την ισχύ τους από ΑΠΕ από 180 GW σε 465 GW. Το 2019, οι ανανεώσιμες τεχνολογίες αντιπροσώπευαν περίπου το 11% της παγκόσμιας πρωτογενούς ενέργειας. Παρά τις προκλήσεις όπως η ανάγκη δημιουργίας υποδομών και η προσαρμογή σε εναλλακτικές πηγές ενέργειας, τα οφέλη των ΑΠΕ καθιστούν τη μετάβαση αυτή απαραίτητη. Η στοχαστική φύση των ΑΠΕ, όπως η ηλιακή και η αιολική ενέργεια, καθιστά δύσκολη την πρόβλεψη και τη διαχείριση του ενεργειακού ισοζυγίου, απαιτώντας νέες προσεγγίσεις στη διαχείριση και αποθήκευση της περίσσειας ενέργειας. Τέλος, η μετάβαση στις ΑΠΕ χρειάζεται να συνδυαστεί με σημαντική κρατική, οικονομική και κοινωνική υποστήριξη, καθώς πολλές χώρες και βιομηχανίες εξακολουθούν να εξαρτώνται σε μεγάλο βαθμό από τα ορυκτά καύσιμα και η μετάβαση στις ΑΠΕ απαιτεί αλλαγές πολιτικής, επενδύσεις και κρατική υποστήριξη.

Η πανδημία COVID-19 έχει προκαλέσει σημαντική μείωση της ζήτησης ενέργειας σε όλους τους τομείς, οδηγώντας σε υπερπροσφορά ενέργειας και μειωμένες επενδύσεις σε νέα ενεργειακά έργα. Ωστόσο, έχει επίσης επιταχύνει την ενεργειακή μετάβαση και έχει εγείρει ερωτήματα σχετικά με την ανθεκτικότητα των ενεργειακών συστημάτων σε κρίσεις, υπογραμμίζοντας την ανάγκη για εναλλακτικές πηγές και συστήματα ενέργειας. Ο Μηχανισμός Ανάκαμψης και Ανθεκτικότητας (RRF) είναι ένα ταμείο που ιδρύθηκε από την ΕΕ για να υποστηρίξει τα κράτη μέλη στην ανάκαμψή τους από τις οικονομικές και κοινωνικές επιπτώσεις της πανδημίας COVID-19 και η Ελλάδα έχει λάβει χρηματοδότηση για τη στήριξη της μετάβασης της χώρας σε χαμηλή κατανάλωση άνθρακα, βελτίωση της ενεργειακής απόδοσης και ανάπτυξη παραγωγής πράσινου υδρογόνου μέσω ΑΠΕ. Ο πόλεμος στην Ουκρανία είχε επίσης σοβαρό αντίκτυπο στον ενεργειακό τομέα της χώρας, επηρεάζοντας τόσο την παραγωγή όσο και τη διανομή της ενέργειας, με σημαντικές επιπτώσεις όπως καταστροφές σε ενεργειακές υποδομές, διακοπές στον εφοδιασμό άνθρακα, εξάρτηση από το ρωσικό αέριο και μειωμένες εξαγωγές ηλεκτρικής ενέργειας.

Η αυξανόμενη διείσδυση των ΑΠΕ στο ενεργειακό ισοζύγιο έχει οδηγήσει σε νέες προκλήσεις για την εξισορρόπηση της προσφοράς και της ζήτησης. Η στοχαστική φύση της αιολικής και της ηλιακής ενέργειας και η εξάρτηση από διάφορους κλιματικούς παράγοντες, καθιστούν δύσκολη την πρόβλεψη της διαθεσιμότητας ενέργειας και την κάλυψη της άμεσης ζήτησης ηλεκτρικής ενέργειας. Η λύση σε αυτό το πρόβλημα είναι η χρήση υβριδικών συστημάτων ανανεώσιμων πηγών ενέργειας (ΥΒΣ), τα οποία συνδυάζουν τουλάχιστον μία μορφή ΑΠΕ και τουλάχιστον μία μορφή τεχνολογίας αποθήκευσης ενέργειας για την αποθήκευση πλεονάζουσας ανανεώσιμης ενέργειας που δεν μπορεί να χρησιμοποιηθεί άμεσα. Τα ΥΒΣ συμβάλλουν στη μείωση των εκπομπών αερίων του θερμοκηπίου και στην ενεργειακή ανεξαρτησία μειώνοντας τη λειτουργία των τοπικών σταθμών παραγωγής, ειδικά σε απομακρυσμένες περιοχές όπως είναι τα ελληνικά νησιά. Στο Σχήμα 1 φαίνεται η παροχή

ΑΠΕ από έργα αιολικά, ηλιακά και αντλησιοταμίευσης, για την Ελλάδα και για χρονική περίοδο από το 1990 έως το 2021.

Παροχή ανανεώσιμων πηγών ενέργειας ανά πηγή, Ελλάδα 1990-2021
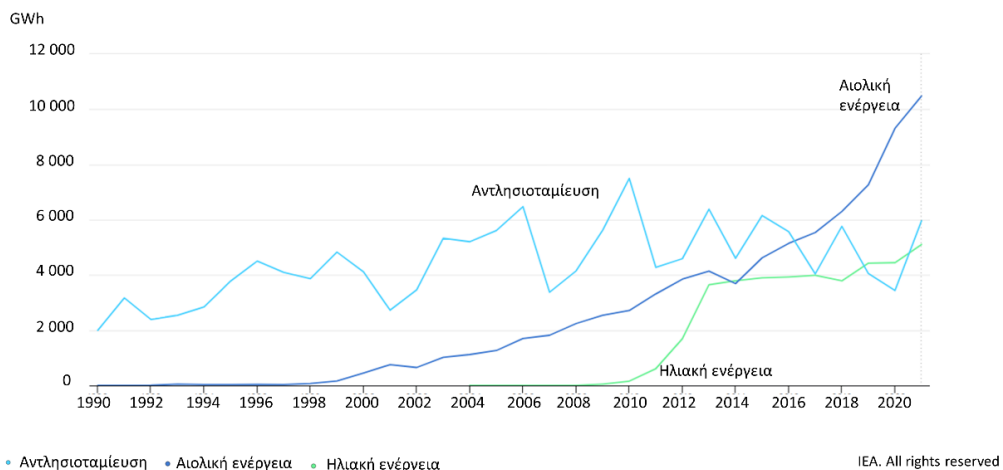
Σχήμα 1 Παροχή ανανεώσιμων πηγών ενέργειας ανά πηγή, Ελλάδα 1990-2021 (International Energy Agency, 2021)

Το πρώτο ΥΒΣ στην Ελλάδα βρίσκεται στην Ικαρία και αποτελείται από αιολικό πάρκο, υδροηλεκτρικούς σταθμούς, δεξαμενές νερού, αντλιοστάσια και κέντρα ελέγχου ενέργειας και διανομής φορτίου. Το δεύτερο ΥΒΣ βρίσκεται στην Τήλο και περιλαμβάνει μία ανεμογεννήτρια, έναν φωτοβολταϊκό σταθμό, σύστημα αποθήκευσης μπαταριών και φορτιστή ηλεκτροκίνητων οχημάτων. Τέλος, ένα ΥΒΣ στην Αστυπάλαια θα είναι έτοιμο προς λειτουργία έως το τέλος του 2023, με στόχο να καλύψει έως και το 50% της συνολικής ενεργειακής ζήτησης του νησιού και το 100% των αναγκών φόρτισης ηλεκτρικών οχημάτων, και ο σκοπός είναι να επεκταθεί για να καλύψει περισσότερο από το 80% της συνολικής ενέργειας του νησιού μέχρι το τέλος του 2026. Τα έργα αυτά συμβάλλουν στη μείωση των εκπομπών CO_2, στην προστασία του περιβάλλοντος, στην ενίσχυση της ενεργειακής επάρκειας, στη μείωση του ενεργειακού κόστους, στον περιορισμό της εξάρτησης από τα συμβατικά καύσιμα, στη βελτίωση της ενεργειακής ασφάλειας και στην αναβάθμιση του τουρισμού στο νησί.

Η χρήση συστημάτων αποθήκευσης ενέργειας σε συνδυασμό με συστήματα ΑΠΕ ενισχύουν την αξιοπιστία και την αποδοτικότητα του δικτύου, ενώ μειώνουν την υψηλού κόστους παραγωγή ηλεκτρικής ενέργειας, ειδικά σε μη διασυνδεδεμένα νησιά (ΜΔΝ) που τροφοδοτούνται από συμβατικά καύσιμα. Τα συστήματα αποθήκευσης ενέργειας επιτρέπουν την συνεχή ικανοποίηση της ζήτησης αποθηκεύοντας ενέργεια σε περιόδους χαμηλής ζήτησης και χρησιμοποιώντας την αποθηκευμένη ενέργεια όταν η ζήτηση είναι υψηλή. Η ενσωμάτωση υδροηλεκτρικών έργων αντλησιοταμίεσης, μπαταριών και αποθήκευσης παραγωγής υδρογόνου με ΑΠΕ είναι ένα ταχέως αναπτυσσόμενο πεδίο έρευνας.
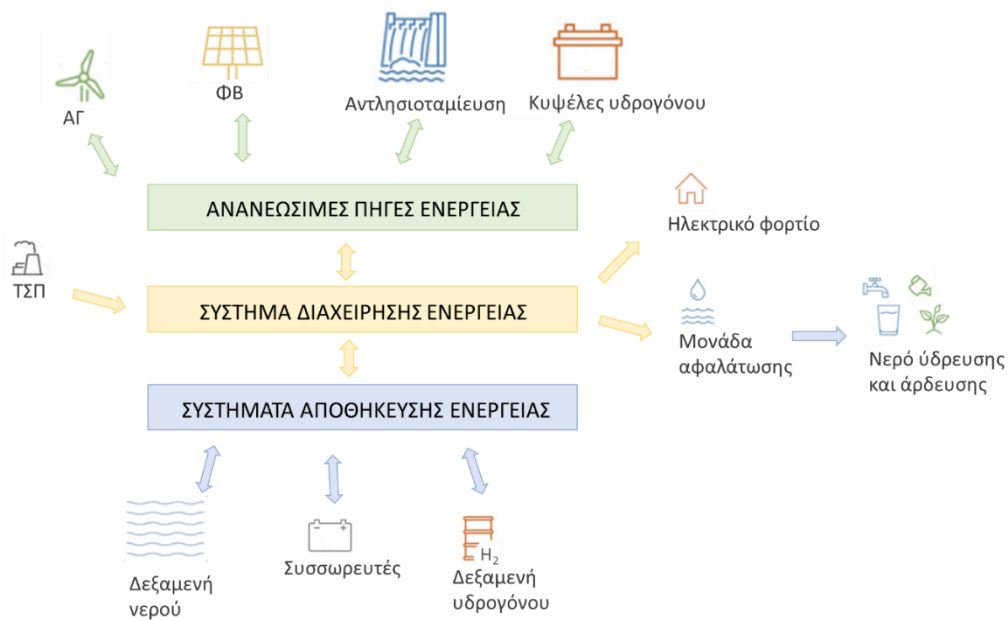
Σχήμα 2 Υβριδικά συστήματα ανανεώσιμων πηγών ενέργειας

Η τεχνολογία της αντλησιοταμίευσης είναι μια από τις πιο ευρέως χρησιμοποιούμενες τεχνολογίες αποθήκευσης ενέργειας, η οποία περιλαμβάνει την άντληση νερού από μια χαμηλότερη δεξαμενή σε μια υψηλότερη δεξαμενή όταν υπάρχει πλεόνασμα ΑΠΕ. Όταν υπάρχει έλλειμμα ενέργειας, το νερό ρέει πίσω στην κάτω δεξαμενή μέσω ενός υδροστροβίλου. Τέτοια έργα έχουν ενεργειακή απόδοση έως και 85%, καθιστώντας τα μια από τις πιο αποδοτικές τεχνολογίες αποθήκευσης ενέργειας που είναι διαθέσιμες και έχει χαρακτηριστεί ως η πιο βιώσιμη τεχνολογία αποθήκευσης. Ωστόσο, απαιτείται υψηλό κόστος κεφαλαίου, μεγάλος χώρος εγκατάστασης και πρόσβαση σε κατάλληλο έδαφος. Αρκετές μελέτες έχουν διερευνήσει την ενσωμάτωση της αντλησιοταμίευσης σε συστήματα ΑΠΕ οδηγούν σε βιώσιμη παροχή ηλεκτρικής ενέργειας και πολλές μελέτες έχουν διεξαχθεί σχετικά με αυτή την ενσωμάτωση. Τα αποτελέσματα δείχνουν ότι οι ΑΠΕ σε συνδυασμό με την αντλησιοταμίευση είναι μια οικονομικά ανταγωνιστική και αξιόπιστη εναλλακτική λύση για αστικές και αγροτικές περιοχές με υψηλές δυνατότητες για ΑΠΕ.

Οι μπαταρίες είναι μια επίσης ευρέως χρησιμοποιούμενη τεχνολογία αποθήκευσης ενέργειας που αποθηκεύει ενέργεια σε χημική μορφή και την απελευθερώνει ως ηλεκτρική ενέργεια όταν χρειάζεται. Προσφέρουν ευελιξία για ένα ευρύ φάσμα εφαρμογών και μπορούν εύκολα να κλιμακωθούν για να καλύψουν διαφορετικές ανάγκες, καθιστώντας τα αποτελεσματικά για εφαρμογές μικρής και μεγάλης κλίμακας. Έχουν διεξαχθεί πολλές μελέτες για τη σύζευξη ΥΒΣ με μπαταρίες με στόχο τη βελτιστοποίηση της διαμόρφωσης του συστήματος, το χαμηλό κόστος ενέργειας, την ελαχιστοποίηση εκπομπών θερμοκηπίου και τα αποτελέσματα δείχνουν ότι η χρήση

μπαταριών μπορούν να βελτιώσουν τη σταθερότητα του συστήματος, να αυξήσουν τη διείσδυση των ΑΠΕ, να μειώσουν το κόστος καυσίμων και τις εκπομπές CO_2.

Η ανάπτυξη συστημάτων αποθήκευσης υδρογόνου σε ΥΒΣ έχει γίνει ιδιαίτερα δημοφιλές ερευνητικό θέμα τα τελευταία χρόνια. Το υδρογόνο μπορεί να παραχθεί χρησιμοποιώντας περίσσεια ενέργειας από ΑΠΕ μέσω ηλεκτρόλυσης αφαλατωμένου νερού και να αποθηκευτεί για μελλοντική χρήση, παρέχοντας μια ευέλικτη τεχνολογία αποθήκευσης ενέργειας. Η παραγωγή υδρογόνου με χρήση μόνο ΑΠΕ μπορεί να παράγει πράσινο υδρογόνο, μια εντελώς καθαρή και βιώσιμη τεχνολογία αποθήκευσης ενέργειας. Έχουν δημοσιευτεί διάφορες μελέτες, στις οποίες εφαρμόζονται λύσεις αποθήκευσης υδρογόνου για ΥΒΣ. Αυτές οι μελέτες προτείνουν διαφορετικούς σχεδιασμούς ΥΒΣ, αναλύουν την οικονομική τους βιωσιμότητα και τον περιβαλλοντικό αντίκτυπό τους.

Αρκετές ερευνητικές μελέτες έχουν συγκρίνει διαφορετικές τεχνολογίες αποθήκευσης που συνδέονται με ΥΒΣ για διάφορες εφαρμογές, συμπεριλαμβανομένων απομακρυσμένων νησιωτικών κοινοτήτων. Οι μελέτες καταλήγουν ότι τα συστήματα αντλησιοταμίευσης είναι πιο οικονομικά και φιλικά προς το περιβάλλον από τις τεχνολογίες αποθήκευσης μπαταριών, ενώ οι τεχνολογίες αποθήκευσης μπαταριών προσφέρουν σημαντικά οφέλη για εφαρμογές μικρής κλίμακας. Η ενοποίηση των τεχνολογιών αποθήκευσης ενέργειας με ΑΠΕ είναι ένα κρίσιμο θέμα για την επίτευξη βιώσιμης και αξιόπιστης ενέργειας. Επίσης, πολλές φορές να απαιτείται ένας συνδυασμός τεχνολογιών αποθήκευσης για να διασφαλιστεί η μέγιστη αξιοπιστία παροχής ενέργειας από ΑΠΕ, χωρίς να γίνεται απόρριψη ενέργειας. Η υβριδική αποθήκευση είναι μια προσέγγιση για να ξεπεραστεί η πρόκληση της διακοπτόμενης παραγωγής ενέργειας από ΑΠΕ, όπου η πλεονάζουσα ενέργεια μπορεί να αποθηκευτεί σε ένα δεύτερο αποθηκευτικό μέσο διαφορετικής τεχνολογία. Πολλές μελέτες σχετικά με υβριδικά συστήματα αποθήκευσης έχουν δημοσιευθεί υποδηλώνοντας τα οφέλη των υβριδικών έναντι των απλών συστημάτων αποθήκευσης Ωστόσο, το κόστος ενός ΥΒΣ είναι σημαντικό και η οικονομική του σκοπιμότητα εξαρτάται από την τοπική ενεργειακή ζήτηση και τη διαθεσιμότητα φυσικών πόρων.

Ταυτόχρονα, η έλλειψη πόσιμου νερού στα ελληνικά νησιά είναι ένα σημαντικό πρόβλημα. Η χρήση εμφιαλωμένου νερού αυξάνεται ανταποκρινόμενη στην ανάγκη για πόσιμο νερό, γεγονός που αυξάνει το κόστος ζωής. Η μεταφορά πόσιμου νερού στα νησιά από την ηπειρωτική χώρα κοστίζει μεταξύ 7 και 12 ευρώ ανά κυβικό μέτρο. Επιπλέον, προβλήματα με την ποσότητα και την ποιότητα των υπόγειων υδάτων προκύπτουν ως αποτέλεσμα των πολυάριθμων, ιδιωτικών γεωτρήσεων που έχουν ανοίξει για αρδευτικούς σκοπούς. Προκειμένου να υποστηριχθεί η μετάβαση στις ΑΠΕ και να μετριαστούν οι επιπτώσεις της κλιματικής αλλαγής, ένα ΥΒΣ και μια μονάδα αφαλάτωσης μπορούν να συνδυαστούν για να παρέχουν σημαντικές οικιακές παροχές νερού για κατοίκους και τουρίστες, καθώς και νερό για γεωργικές και βιομηχανικές χρήσεις. Η αφαλάτωση απαιτεί σημαντική ποσότητα

ενέργειας και η χρήση ορυκτών καυσίμων για την τροφοδοσία των μονάδων αφαλάτωσης μπορεί να συμβάλει στην παραγωγή εκπομπών του θερμοκηπίου. Ο συνδυασμός της αφαλάτωσης με συστήματα ΑΠΕ, ωστόσο, μπορεί να συμβάλει στη μείωση του αποτυπώματος άνθρακα της αφαλάτωσης και να την καταστήσει πιο βιώσιμη. Ειδικά στην περίπτωση των ελληνικών νησιών, η σύζευξη ΥΒΣ με μια μονάδα αφαλάτωσης μπορεί να χρησιμοποιήσει αιολική και ηλιακή ενέργεια, καθώς και το άφθονο θαλασσινό νερό που περιβάλλει κάθε νησί, για να διαχειριστεί τις ελλείψεις σε ενέργεια και νερό. Η αφαλάτωση του θαλασσινού νερού μπορεί να εγγυηθεί την παροχή νερού σε νησιά με περιορισμένους υδάτινους πόρους. Επιπλέον, η χρήση τεχνολογιών που βασίζονται στις ΑΠΕ για οικιακές και γεωργικές εφαρμογές βελτιώνει την ασφάλεια της παροχής νερού και την ανεξαρτησία από τα ορυκτά καύσιμα, ενώ παρέχει επίσης την ευκαιρία να βελτιωθεί ο δεσμός Νερού-Ενέργειας (Water Energy Nexus, NEX), την αλληλεξάρτηση μεταξύ νερού και ενέργειας, ένα θέμα που έχει προσελκύσει περισσότερο ενδιαφέρον από τους τομείς της έρευνας και της πολιτικής.

Η αφαλάτωση είναι η διαδικασία αφαίρεσης αλατιού και άλλων ορυκτών από το θαλασσινό νερό ή το υφάλμυρο νερό για να καταστεί κατάλληλο για ανθρώπινη κατανάλωση ή γεωργική χρήση. Υπάρχουν δύο βασικές μέθοδοι αφαλάτωσης: η θερμική και με τη χρήση μεμβρανών. Η πιο κοινή μορφή αφαλάτωσης είναι η αντίστροφη ώσμωση (ΑΩ), η οποία χρησιμοποιεί υψηλή πίεση για να πιέσει το θαλασσινό νερό μέσα από μια μεμβράνη και σε μια δεξαμενή συλλογής. Μονάδες αφαλάτωσης με βάση τις μεμβράνες επί του παρόντος αντισταθμίζουν περίπου το 70% όλων των εγκαταστάσεων. Σήμερα, το 63% της αγοράς αφαλάτωσης αντιστοιχεί στην αφαλάτωση με αντίστροφη όσμωση. Επίσης, σε σύγκριση με τις θερμικές τεχνολογίες αφαλάτωσης, οι μονάδες ΑΩ έχουν 25% χαμηλότερο κόστος κεφαλαίου. Οι μονάδες αφαλάτωσης μπορούν επίσης να χρησιμοποιηθούν για την παροχή αφαλατωμένου νερού για ηλεκτρόλυση στην παραγωγή πράσινου υδρογόνου από ΑΠΕ. Η ανάγκη για αφαλατωμένο νερό άρδευσης αναμένεται επίσης να καλύψει τις αρδευτικές ανάγκες της περιοχής πέρα από τη ζήτηση για οικιακό νερό. Μεταξύ όλων των τεχνολογιών αφαλάτωσης που μπορούν να χρησιμοποιηθούν σε συνδυασμό με ΑΠΕ, η ΑΩ είναι η κύρια τεχνική αφαλάτωσης επειδή χρησιμοποιεί συγκριτικά λιγότερη ενέργεια και έχει χαμηλό σχετικό κόστος. Η ΑΩ αντιστοιχεί σήμερα στο 51 % της συνολικής χρήσης τεχνολογιών αφαλάτωσης που βασίζονται σε ΑΠΕ. Η κατανάλωση ενέργειας για ένα σύστημα ΑΩ ποικίλλει από 3,7 και 8 kWh/m³ και επηρεάζεται τόσο από την ποιότητα του νερού όσο και από το μέγεθος της μονάδας αφαλάτωσης. Η υψηλότερη κατανάλωση ενέργειας σχετίζεται με την αυξημένη αλατότητα του νερού και τα μικρότερα μεγέθη των μονάδων αφαλάτωσης.

Η συμβολή αυτής της διατριβής στο ερευνητικό πεδίο συνίσταται στην ανάπτυξη ενός ολοκληρωμένου μεθοδολογικού πλαισίου για τη χωροθέτηση ανεμογεννητριών, στην ανάπτυξη στρατηγικών ενεργειακής διαχείρισης των ΥΒΣ που συνδέουν διαφορετικές τεχνολογίες αποθήκευσης, απλές ή υβριδικές, με ταυτόχρονη κάλυψη ενεργειακών και υδατικών απαιτήσεων και του μεθοδολογικού πλαισίου για την εκτίμηση της απορριφθείσας ανανεώσιμης ενέργειας από

ένα ΥΒΣ. Τα κύρια ερευνητικά σημεία αυτής της διατριβής μπορούν να συνοψιστούν στα ακόλουθα σημεία.

Α. Παρουσιάζεται η μεθοδολογία για την αξιολόγηση πιθανών θέσεων εγκατάστασης ανεμογεννητριών, χρησιμοποιώντας διαφορετικά σενάρια και πραγματοποιώντας ανάλυση ευαισθησίας. Λαμβάνεται υπόψη τόσο οι παράμετροι των περιβαλλοντικών περιορισμών όσο και το ισχύον νομοθετικό πλαίσιο για τη χωροθέτηση ενός αιολικού πάρκου. Διερευνώνται επίσης σενάρια εγκατάστασης αιολικού πάρκου πιο κοντά στους οικισμούς με σκοπό τις μικρότερες δυνατές απώλειες ενέργειας λόγω μεταφοράς ρεύματος μέσω καλωδίων. Η μεθοδολογία και τα αποτελέσματα αναλύονται στο Κεφάλαιο 3, ενώ τα συμπεράσματα παρουσιάζονται στην ενότητα 7.1.

Β. Παρουσιάζεται η αξιολόγηση των ΥΒΣ που χρησιμοποιούν ανεμογεννήτριες και φωτοβολταϊκές μονάδες, καθώς και σύζευξη με μονάδα αφαλάτωσης, συνδυάζοντας διαφορετικές τεχνολογίες αποθήκευσης για την αποθήκευση της πλεονάζουσας ανανεώσιμης ενέργειας. Η έρευνα αυτή επικεντρώνεται στη σύγκριση διαφορετικών συστημάτων αποθήκευσης, παρέχοντας τις αντίστοιχες λεπτομερείς στρατηγικές διαχείρισης ενέργειας για απλή ή υβριδική αποθήκευση με την ταυτόχρονη παροχή ενέργειας για οικιακή και αρδευτική κατανάλωση, με βάση ενεργειακά, οικονομικά και περιβαλλοντικά κριτήρια. Η μεθοδολογία χρησιμοποιεί γεωγραφικά, μετεωρολογικά δεδομένα, δεδομένα πληθυσμού και ζήτησης (νερό, ενέργεια), οδηγώντας σε συμπεράσματα σχετικά με τη λειτουργία και την αξιοπιστία τέτοιων έργων. Η έρευνα προσπαθεί να απαντήσει ποια διαμόρφωση είναι πιο αποτελεσματική στην κάλυψη των απαιτήσεων ενέργειας και νερού, οδηγώντας στην αποφυγή της έναρξης λειτουργίας των ρυπογόνων τοπικών σταθμών παραγωγής ηλεκτρικής ενέργειας. Πώς επηρεάζει κάθε διαμόρφωση το κόστος ενέργειας, το κόστος του αφαλατωμένου νερού, την πιθανότητα απώλειας φορτίου, την περίοδο απόσβεσης και τη μείωση των εκπομπών CO_2; Πώς επηρεάζουν τα αποτελέσματα οι αλλαγές σε μετεωρολογικούς, δημογραφικούς παράγοντες και παράγοντες εγκατάστασης;

Γ. Παρέχεται το μεθοδολογικό πλαίσιο για την εκτίμηση και ελαχιστοποίηση της απορριφθείσας ανανεώσιμης ενέργειας μέσω ΥΒΣ. Η ποσότητα της απορριφθείσας ενέργειας επιχειρείται να υπολογιστεί με βάση το ποσοστό άμεσης διείσδυσης της αιολικής ενέργειας στο σύστημα και το ποσοστό ενέργειας που έχει οριστεί για αφαλάτωση έναντι άντλησης. Η ελαχιστοποίηση της απορριφθείσας ενέργειας θα οδηγήσει σε ένα πιο αξιόπιστο και βιώσιμο σύστημα. Θα έχει επίσης ως αποτέλεσμα την προώθηση των ΑΠΕ, που αποτελεί προτεραιότητα παγκοσμίως, στη μείωση της κατανάλωσης ορυκτών καυσίμων και στην ενεργειακή και υδατική ανεξαρτησία. Με βάση τα αποτελέσματα προσδιορίζεται το βέλτιστο άμεσο ποσοστό ανανεώσιμης ενέργειας στο σύστημα. Η μεθοδολογία και τα αποτελέσματα αναλύονται στο Κεφάλαιο 6, ενώ τα συμπεράσματα παρουσιάζονται στην ενότητα 7.3.

Στην Ενότητα 1 της παρούσας διατριβής γίνεται η παρουσίαση των ΑΠΕ, του θεσμικού πλαισίου που επικρατεί, η ανάλυση των ΥΒΣ, των διαφορετικών τεχνολογιών αποθήκευσης και των μεθόδων αφαλάτωσης. Τέλος, παρουσιάζεται ο στόχος, τα κίνητρα, η δομή και η συμβολή αυτής της έρευνας. Στην Ενότητα 2 παρουσιάζεται η περιοχή μελέτης και η επεξεργασία των δεδομένων. Η ενότητα 3 παρουσιάζει την μεθοδολογία χωροθέτησης των ΑΓ μαζί με τα αποτελέσματα για τρία σενάρια με διαφορετικούς συνδυασμούς κριτηρίων και την πραγματοποίηση ανάλυσης ευαισθησίας. Στην ενότητα 4 παρουσιάζεται η μεθοδολογία για τη μοντελοποίηση κάθε στοιχείου του ΥΒΣ, οι διάφορες διαμορφώσεις ΑΠΕ και τεχνολογιών αποθήκευσης, οι στρατηγικές διαχείρισης ενέργειας και τέλος η μεθοδολογία για την οικονομική και περιβαλλοντική ανάλυση. Στην Ενότητα 5 παρουσιάζονται τα αντίστοιχα αποτελέσματα για κάθε διαμόρφωση ΥΒΣ και η μεταξύ τους σύγκριση μαζί με ανάλυση ευαισθησίας για συγκεκριμένα δεδομένα εισαγωγής. Στην Ενότητα 6, παρουσιάζεται η μεθοδολογία για τον υπολογισμό της απορριφθείσας ενέργειας από ένα ΥΒΣ. Με βάση τα αποτελέσματα προσδιορίζεται το βέλτιστο άμεσο ποσοστό ανανεώσιμης ενέργειας στο σύστημα. Στην Ενότητα 7, παρουσιάζονται τα συμπεράσματα και προτάσεις για μελλοντική έρευνα. Στο τέλος, βρίσκονται οι Ευχαριστίες και η λίστα των Παραπομπών, καθώς και τα Παραρτήματα σχετικά με τις συντομογραφίες, τον κατάλογο των σχημάτων και των πινάκων, η εκτενής περίληψη στα ελληνικά και ο πλήρης κατάλογος των δημοσιεύσεων που σχετίζονται με αυτή τη διατριβή.

2. Περιοχή μελέτης

Το σύμπλεγμα των Φούρνων Κορσεών βρίσκεται στο Αιγαίο Πέλαγος, νοτιοδυτικά της Σάμου και ανατολικά της Ικαρίας στην Ελλάδα. Το μεγαλύτερο νησί είναι οι Φούρνοι Κορσεών, με έκταση 30,5 τ. χλμ. και πληθυσμό 1400 κατοίκους. Το κλίμα στους Φούρνους Κορσεών είναι μεσογειακό, με ήπιους χειμώνες και παρατεταμένα ξηρά και ζεστά καλοκαίρια. Η σημερινή κατάσταση της αγροτικής παραγωγής και του τουρισμού στο νησί περιορίζεται σε λίγες ελιές και αμπέλια για ιδιωτική χρήση. Το νησί διαθέτει 27 καταγεγραμμένα καταλύματα και 10 εστιατόρια, με την τουριστική περίοδο αιχμής να είναι τον Αύγουστο. Τα τελευταία χρόνια η τουριστική περίοδος έχει επεκταθεί από τον Μάιο έως τον Σεπτέμβριο. Το σύστημα ύδρευσης του νησιού περιλαμβάνει μονάδα αφαλάτωσης και φυσική πηγή πόσιμου νερού. Το νησί συνδέεται με το κοντινό νησί της Σάμου για τις ενεργειακές του ανάγκες, με αποτέλεσμα περιστασιακές διακοπές ρεύματος σε περιόδους υψηλής ζήτησης. Ωστόσο, το νησί έχει υψηλό αιολικό και ηλιακό δυναμικό που παραμένει αναξιοποίητο. Αυτή τη στιγμή αξιολογούνται δύο πιθανές θέσεις για αιολικά πάρκα, ενώ ένα έργο υβριδικής ενέργειας έχει άδεια παραγωγής και αναμένει άδεια λειτουργίας. Μια άλλη αίτηση υβριδικού έργου στα νότια του νησιού έχει απορριφθεί. Ολόκληρο το νησί των Φούρνων στην Ελλάδα ανήκει στον βιότοπο Natura, σύμφωνα με τη βάση δεδομένων Filotis. Το νησί έχει

πολλά ιστορικά μνημεία όπως η Ακρόπολη, ο Αρχαίος οικισμός Καμάρι, το Αρχαίο Λατομείο στο Πετροκόπιο και ο Σαρκοφάγος.

Οι οικιακές ανάγκες σε νερό παρέχονται από την Τεχνική Υπηρεσία του νησιού και είναι ίσες με περίπου 91.500 κ.μ. ετησίως. Χρησιμοποιώντας τη μέθοδο Blaney-Criddle υπολογίζεται η εξατμισοδιαπνοή η οποία αντικατοπτρίζει τις απαιτήσεις σε νερό άρδευσης. Η αρδευτική περίοδος εκτείνεται από τον Απρίλιο έως τον Σεπτέμβριο και η αφαλάτωση για άρδευση υπολογίζεται μόνο για αυτούς τους μήνες. Οι συνολικές απαιτήσεις σε νερό άρδευσης είναι ίσες με περίπου 102.000 κ.μ. ετησίως.

Στον Πίνακα 1 παρουσιάζονται οι μηνιαίες ενεργειακές απαιτήσεις για αφαλάτωση οικιακού και αρδευτικού νερού, καθώς και οι ενεργειακές απαιτήσεις για την οικιακή κατανάλωση (ηλεκτρικό φορτίο). Στοιχεία σχετικά με το ηλεκτρικό φορτίο παρέχονται από τη Δημόσια Επιχείρηση Ηλεκτρισμού (ΔΕΗ).

Πίνακας 1 Παροχή ανανεώσιμων πηγών ενέργειας ανά πηγή, Ελλάδα 1990-2021 (International Energy Agency, 2021)

Μήνας	Οικιακό νερό (kWh)	Νερό άρδευσης (kWh)	Οικιακή κατανάλωση (kWh)	Συνολική κατανάλωση (kWh)
Ιανουάριος	31,590	0	665,446	697,036
Φεβρουάριος	31,590	0	601,048	632,638
Μάρτιος	31,590	0	665,446	697,036
Απρίλιος	31,590	5,778	495,990	533,358
Μάιος	42,120	117,192	296,050	455,362
Ιούνιος	59,670	151,177	286,500	497,347
Ιούλιος	70,200	170,315	434,000	674,515
Αύγουστος	91,260	153,850	504,835	749,945
Σεπτέμβριος	42,120	60,788	162,840	265,748
Οκτώβριος	31,590	0	168,268	199,858
Νοέμβριος	31,590	0	325,680	357,270
Δεκέμβριος	31,590	0	665,446	697,036
ΣΥΝΟΛΟ	**526,500**	**659,100**	**5,271,549**	**6,457,149**

Το νησί έχει υψηλό αιολικό και ηλιακό δυναμικό. Στοιχεία για την ταχύτητα του ανέμου, τη θερμοκρασία και τη βροχόπτωση λαμβάνονται από τον μετεωρολογικό σταθμό Φούρνων Κορσεών του Εθνικού Αστεροσκοπείου Αθηνών. Επίσης, στοιχεία για την ηλιακή ακτινοβολία λαμβάνονται από τον μετεωρολογικό σταθμό της Σάμου, καθώς στο σταθμό των Φούρνων δεν υπάρχουν μετρήσεις ηλιακής ακτινοβολίας. Για τον υπολογισμό της ενέργειας από το ΦΒ χρησιμοποιείται η ολική ηλιακή ακτινοβολία στο κεκλιμένο επίπεδο H_T, η οποία υπολογίζεται με βάση την ηλιακή απόκλιση $δ$, την ωριαία γωνία δύσης του ηλίου $ω_{ss}$, την γεωμετρική παράμετρο για τη μέση μέρα

του μήνα R_b, το γεωγραφικό πλάτος φ, την κλίση επιφάνειας αναφοράς β, τον λόγο μέσης διάχυσης ακτινοβολίας H_d, προς την αντίστοιχη μέση ολική σε οριζόντιο επίπεδο H και τον μέσο μηνιαίο δείκτη αιθριότητας k_t.
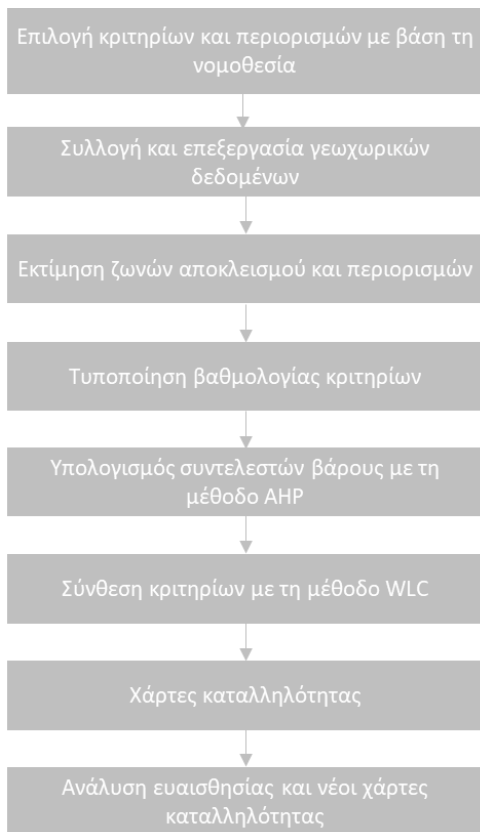
3. Χωροθέτηση ανεμογεννητριών

Η μεθοδολογία για την αξιολόγηση των επιλέξιμων χώρων για την εγκατάσταση ΑΓ είναι ένας συνδυασμός Πολυκριτηριακής Λήψης Αποφάσεων (MCDM) και Συστημάτων Γεωγραφικών Πληροφοριών (GIS) για τον σχεδιασμό αιολικού πάρκου στην περιοχή μελέτης. Βασίζεται σε γεωμορφολογικά, τεχνικά και χωρικά κριτήρια, σύμφωνα με το ισχύον νομοθετικό πλαίσιο. Η ιδέα πίσω από αυτή τη στρατηγική είναι να προσφέρει μια ευέλικτη δομή λήψης αποφάσεων που παρουσιάζει διάφορα σενάρια, επιτρέποντας στην επιλογή της σειρά σπουδαιότητας των κριτηρίων που ταιριάζει στις ιδιαιτερότητές της εκάστοτε περιοχής. Στόχος είναι η παροχή μιας εξατομικευμένης προσέγγισης που να ανταποκρίνεται στις μοναδικές ανάγκες κάθε ενδιαφερόμενου. Τα βάρη των κριτηρίων εκτιμώνται με την εφαρμογή της Διαδικασίας Αναλυτικής Ιεραρχίας (AHP) για να καταδειχθεί ο αντίκτυπός τους στον τελικό σχεδιασμό. Τα κριτήρια που επιλέγονται για αξιολόγηση είναι το κριτήριο του αιολικού δυναμικού C_{wind}, του υψομέτρου C_{alt}, της απόστασης από τους οικισμούς C_{setl}, της απόστασης από το οδικό δίκτυο C_{road}, της απόστασης από σταθμούς κινητής τηλεφωνίας C_{tele} και τέλος της απόστασης από αρχαιολογικούς χώρους C_{arch}. Η μεθοδολογία που ακολουθήθηκε για την τυποποίηση των κριτηρίων και την επιβολή περιορισμών απεικονίζεται στον Πίνακα 2.

Πίνακας 2 Κριτήρια εγκατάστασης ανεμογεννητριών

Κριτήριο	Περιορισμοί
C_{wind}	Ταχύτητες ανέμου > 2 m/sec
C_{alt}	Υψηλά υψόμετρα συνεπάγονται υψηλό αιολικό δυναμικό
C_{setl}	Απόσταση από τα όρια > 500 m
C_{road}	Απόσταση < 10,000 m
C_{tele}	Απόσταση > 200 m
C_{arch}	Απόσταση > 500 m

Η μεθοδολογία GIS-MCDM που ακολουθείται για την χωροθέτηση των ανεμογεννητριών παρουσιάζεται στο Σχήμα 3.

Σχήμα 3 Μεθοδολογία GIS-MCDM για χωροθέτηση ανεμογεννητριών

Η μελέτη εξετάζει τρία διαφορετικά σενάρια, το καθένα εστιάζοντας σε διαφορετικά κριτήρια που θα οδηγήσουν στο καλύτερο αποτέλεσμα για την χωροθέτηση, λαμβάνοντας υπόψη το αιολικό δυναμικό ως προτεραιότητα σε όλα τα σενάρια. Το τεχνικό σενάριο (Σενάριο 1) δίνει προτεραιότητα στα κριτήρια που θα οδηγήσουν στην καλύτερη απόδοση της ανεμογεννήτριας. Αυτά τα κριτήρια είναι το αιολικό δυναμικό και κριτήρια που σχετίζονται με οικισμούς και δρόμους για να διασφαλιστεί ότι δεν επηρεάζεται η μεταφορά ηλεκτρικής ενέργειας μέσω καλωδίων. Το δεύτερο είναι το πολιτιστικό σενάριο (Σενάριο 2), που δίνει μεγαλύτερη βαρύτητα στην απόσταση από τους αρχαιολογικούς χώρους. Τέλος, στο οικονομικό σενάριο (Σενάριο 3), η εστίαση είναι στο χαμηλότερο κόστος του έργου, το οποίο έχει ως αποτέλεσμα την αποφυγή μεγάλων υψομέτρων, αν και προτεραιότητα εξακολουθεί να είναι το υψηλό αιολικό δυναμικό και η προτίμηση για τοποθεσίες κοντά σε οδικά δίκτυα ή υπάρχοντα τηλεπικοινωνιακούς σταθμούς, προκειμένου να αποφευχθούν περαιτέρω έργα, όπως η εκσκαφή δρόμου.

Δημιουργούνται τρεις επιπλέον χάρτες καταλληλότητας προσθέτοντας τον περιορισμό της εγγύτητας με τον κύριο οικισμό των Φούρνων Κορσεών, που έχει τους περισσότερους κατοίκους και τις υψηλότερες ενεργειακές απαιτήσεις. Η συνεκτίμηση των κριτηρίων της απόστασης από τον κύριο οικισμό και η εγκατάσταση των ανεμογεννητριών κοντά σε αυτή την περιοχή με αυξημένες

ενεργειακές ανάγκες, οδηγεί στη μείωση των ενεργειακών απωλειών κατά τη μετάδοση μέσω απομακρυσμένων περιοχών.

Για την αξιολόγηση της ευαισθησίας των αποτελεσμάτων, πραγματοποιείται ανάλυση ευαισθησίας στα βάρη δύο κριτηρίων, συγκεκριμένα C_{wind} και C_{arch} του πρώτου σεναρίου. Η ανάλυση εξετάζει τα αποτελέσματα των αλλαγών ±5% και ±10% στις προτεινόμενες τιμές για αυτά τα κριτήρια. Τέλος, παράγονται νέοι χάρτες καταλληλότητας και τελικές βαθμολογίες με βάση τα ενημερωμένα βάρη.

Η πρώτη κατηγορία (Ζώνη Α) είναι η μηδενική ζώνη και αντιστοιχεί σε περιοχές όπου δεν επιτρέπεται η εγκατάσταση ΑΓ. Η ζώνη αυτή καλύπτει το 27,9% της συνολικής έκτασης του νησιού και παραμένει ίδια για κάθε σενάριο, καθώς δείχνει τις εξαιρούμενες περιοχές του νησιού για εγκατάσταση ανεμογεννητριών σύμφωνα με την κείμενη νομοθεσία. Οι υπόλοιπες τέσσερις κατηγορίες (Ζώνη Β, C, D και E) ταξινομούνται με βάση τις τελικές βαθμολογίες (FS) έως 0,25, 0,50, 0,75 και τη μέγιστη τιμή που μπορεί να φτάσει κάθε FS. Στο Σενάριο 1 η ζώνη Γ είναι η μεγαλύτερη ζώνη και καλύπτει περίπου το 41% του νησιού και ακολουθεί η ζώνη Δ με ποσοστό 26,9%. Η καλύτερη ζώνη για εγκατάσταση είναι η ζώνη Ε, η οποία καλύπτει το 1,7% της έκτασης του νησιού και έχει μέγιστη τιμή FS περίπου 0,91. Στο Σενάριο 2 η ζώνη Β αντιστοιχεί στο 7,9% της περιοχής του νησιού, ενώ η ζώνη Γ καλύπτει το 51,4% του νησιού. Η ζώνη Δ αντιστοιχεί στο 12,5% της συνολικής έκτασης του νησιού και η ζώνη Ε έχει τη χαμηλότερη κάλυψη μόλις 0,3%, που είναι η πιο ευνοϊκή κατηγορία για εγκατάσταση. Η μέγιστη τιμή FS για αυτό το σενάριο είναι περίπου 0,84, η οποία είναι χαμηλότερη από την αντίστοιχη τιμή του πρώτου σεναρίου, υποδεικνύοντας ότι οι πολιτιστικοί περιορισμοί έχουν αρνητικό αντίκτυπο στο FS για αυτό το νησί. Στο Σενάριο 3 η ζώνη Β καλύπτει μόνο το 0,2%, η ζώνη Γ καλύπτει το 13,8%, η ζώνη Δ καλύπτει το 54,1% και η ζώνη Ε καλύπτει το 4% της συνολικής έκτασης του νησιού. Η υψηλότερη τιμή του FS είναι 0,93, που είναι υψηλότερη από τις αντίστοιχες τιμές του πρώτου και του δεύτερου σεναρίου.

Η μελέτη περιλαμβάνει επίσης τρεις επιπλέον χάρτες καταλληλότητας, λαμβάνοντας υπόψη τον περιορισμό της γειτνίασης με τον κύριο οικισμό των Φούρνων. Η εγκατάσταση αιολικού πάρκου προτιμάται να βρίσκεται κοντά στην περιοχή με τους περισσότερους κατοίκους και τις υψηλότερες ενεργειακές απαιτήσεις. Περιορίζοντας την απόσταση από τον κύριο οικισμό, μειώνονται οι απώλειες ενέργειας λόγω μετάδοσης από απομακρυσμένες περιοχές. Σε αυτό το σενάριο, το ποσοστό της Ζώνης Α παραμένει το ίδιο με τα σενάρια που εξετάστηκαν προηγουμένως και καλύπτει το 27,9% της συνολικής νησιωτικής έκτασης. Ωστόσο, οι πρόσθετοι χάρτες καταλληλότητας έχουν μόνο τρεις ζώνες, με τη ζώνη Β να έχει τιμές FS έως 0,25, τη ζώνη C έως 0,5 και τη ζώνη D έως τις υψηλότερες δυνατές τιμές FS που μπορούν να επιτευχθούν.

Οι χάρτες καταλληλότητας για τα σενάρια 1, 2 και 3 φαίνονται στο Σχήμα 4 (α), (β), (γ) αντίστοιχα. Σε αυτά τα τρία πρόσθετα σενάρια, απεικονίζονται μόνο τέσσερις ζώνες καθώς η τιμή FS δεν υπερβαίνει το 0,744, το οποίο είναι χαμηλότερο από την αντίστοιχη τιμή για τα αρχικά σενάρια,

όπου το FS είναι έως 0,929. Αυτό συμβαίνει λόγω της εισαγωγής ενός πρόσθετου περιορισμού, με αποτέλεσμα χαμηλότερες τιμές FS. Για το πρώτο σενάριο, πάνω από το 69% της νησιωτικής έκτασης κατανέμεται στις ζώνες Β και Γ, ενώ για τα σενάρια 2 και 3 τα αντίστοιχα ποσοστά είναι 71% και 61%, αντίστοιχα. Η Ζώνη Δ αντιστοιχεί στο 1,81% στο πρώτο σενάριο, στο 0,19% στο δεύτερο και στο 10,48% στο τρίτο.
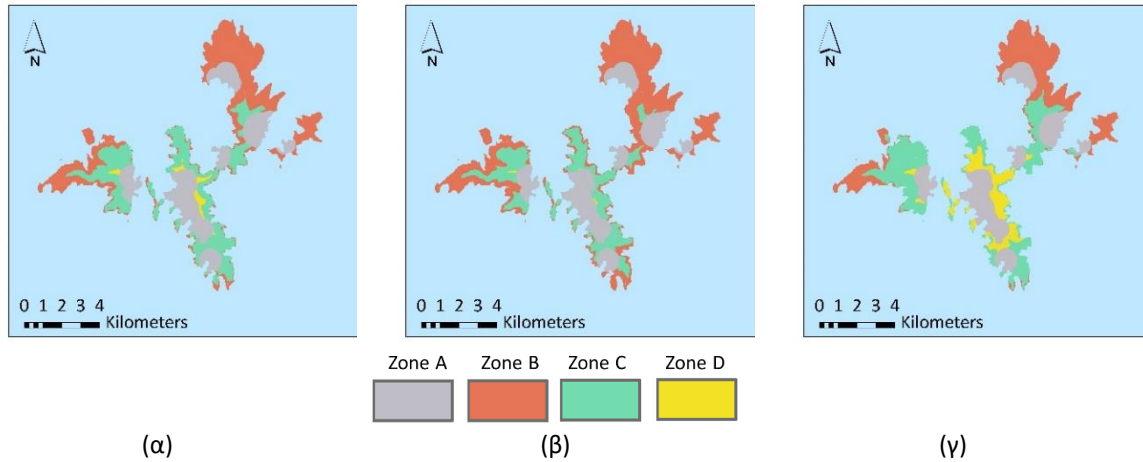
Σχήμα 4 Χάρτες καταλληλότητας με βάση την απόσταση από τον οικισμό των Φούρνων (α) Σενάριο 1, (β) Σενάριο 2, (γ) Σενάριο 3

4. Στρατηγικές Διαχείρισης Ενέργειας και Οικονομική και Περιβαλλοντική Ανάλυση

Σε αυτή τη διατριβή, παρουσιάζεται η αξιολόγηση και σύγκριση των αποτελεσμάτων διαφορετικών σεναρίων σύζευξης ΥΒΣ με διαφορετικές ΑΠΕ και διαφορετικές τεχνολογίες αποθήκευσης. Στα διαφορετικά σενάρια των ΥΒΣ γίνεται σύζευξη μίας ή περισσοτέρων ΑΠΕ ενώ, ανάλογα με το εξεταζόμενο σενάριο, ενσωματώνεται απλή ή υβριδική αποθήκευση για την περίσσεια ενέργειας. Χρησιμοποιούνται ανεμογεννήτριες, φωτοβολταϊκά, μονάδα αφαλάτωσης, αντλησιοταμίευση, συσσωρευτές και αποθήκευση υδρογόνου.

Η ισχύς που αποδίδουν οι ανεμογεννήτριες P_{WT} υπολογίζεται από την καμπύλη ισχύος και περιγράφεται με την Εξίσωση 1.

$$\begin{cases} \text{if } u(t) < u_{cut-in} \text{ then } P_{WT}(t) = 0 \\ \text{if } u_{cut-in} < u(t) < u_{rated} \text{ then } P_{WT}(t) = \text{according to the wind speed and the power curve} \\ \text{if } u_{rated} \leq u(t) < u_{cut-out} \text{ then } P_{WT}(t) = P_{WT}^{max} \\ \text{if } u(t) \geq u_{cut-out}(t) \text{ then } P_{WT}(t) = 0 \end{cases}$$

Εξίσωση 1

όπου u_{cut-in} η ταχύτητα εισόδου (m/sec), $u_{cut-out}$ η ταχύτητα εξόδου (m/sec), u_{rated} η ονομαστική ταχύτητα (m/sec) και P_{WT}^{max} η μέγιστη ισχύς (kW) που μπορεί να αποδώσει η ανεμογεννήτρια.

Επίσης η ισχύς P_{PV} που αποδίδουν τα φωτοβολταϊκά δίνεται από την Εξίσωση 2.

$$P_{PV}(t) = P_{STC} \cdot \frac{G_t(t)}{G_{STC}} \cdot PR_{PV} \cdot PR_{inv} \cdot PR_{grid} \cdot PR_T(t)$$

Εξίσωση 2

όπου P_{STC} η μέγιστη χωρητικότητα σε κανονικές συνθήκες λειτουργίας (W/m²), $G_t(t)$ η ηλιακή ακτινοβολία σε κεκλιμένο επίπεδο (W/m²), PR_{PV} ο συντελεστής απόδοσης του ΦΒ (%), PR_{inv} ο συντελεστής απόδοσης του αντιστροφέα (%), PR_{grid} ο συντελεστής απόδοσης του δικτύου (%) και $PR_T(t)$ ο συντελεστής απόδοσης της κυψελίδας (%)

Στην αντλησιοταμίευση η δεξαμενή του νερού υπόκεινται στον περιορισμό ότι δεν μπορεί η στάθμη να είναι κάτω από το 10% της συνολικής χωρητικότητας, ενώ η ποσότητα του νερού που μπορεί να αντληθεί στην άνω δεξαμενή V_p υπολογίζεται από την Εξίσωση 3.

$$V_p = \frac{E_{sur} \cdot PR_p}{\rho \cdot g \cdot H}$$

Εξίσωση 3

όπου ρ η πυκνότητα του νερού (kg/m³), g η επιτάχυνση της βαρύτητας (m/sec²), H το μανομετρικό (m), PR_p ο συντελεστής απόδοσης του αντλητικού σταθμού (%) και E_{sur} η περίσσεια ενέργεια που δίνεται για άντληση (kWh).

Παρομοίως για την μπαταρία η χωρητικότητα δεν μπορεί να είναι μικρότερη από την ελάχιστη κατάσταση φόρτισης του συσσωρευτή SOC_{min}, ενώ η χωρητικότητα του υπολογίζεται από την Εξίσωση 4.

$$C_{bat} = \frac{P_L \cdot d_A}{PR_{bat} \cdot PR_{inv} \cdot DOD}$$

Εξίσωση 4

όπου P_L η μέση ημερήσια κατανάλωση (kWh/day), d_A οι μέρες της αυτονομίας, PR_{bat} ο συντελεστής απόδοσης της μπαταρίας (%), PR_{inv} ο συντελεστής απόδοσης του αντιστροφέα (%) και DOD το βάθος εκφόρτισης της μπαταρίας (%).

Τέλος η ποσότητα του υδρογόνου H_2 σε κιλά που παράγεται όταν υπάρχει περίσσεια ενέργειας E_{sur} δίνεται από την Εξίσωση 5.

$$H_2 = E_{sur} \cdot PR_{el} / 37.8$$

Εξίσωση 5

όπου PR_{el} ο συντελεστής απόδοσης του ηλεκτρολύτη (%),

ενώ η ενέργεια που παράγεται από την κυψέλη υδρογόνου E_{FC} δίνεται από την Εξίσωση 6.

$$E_{FC} = H_2 \cdot PR_{FC} \cdot 37.8$$

Εξίσωση 6

όπου PR_{FC} ο συντελεστής απόδοσης της κυψέλης υδρογόνου (%).

Τέλος για την παραγωγή 1 kg υδρογόνου απαιτούνται 9 kg αφαλατωμένου νερού και η δεξαμενή αποθήκευσης του υδρογόνου υπόκεινται στον περιορισμό ότι δεν μπορεί η στάθμη να είναι κάτω από το 10% της συνολικής χωρητικότητας.

Τα σενάρια που εξετάζονται φαίνονται στον Πίνακα 3.

Πίνακας 3 Διαμορφώσεις συστημάτων ΑΠΕ

Διαμόρφωση	1	2	3	4	5	6	7
Ανεμογεννήτριες (WT)	✓	✓	✓	✓	✓	✓	✓
Φωτοβολταϊκά (PV)			✓	✓	✓	✓	✓
Μον. αφαλάτωσης (DU)		✓	✓	✓	✓	✓	✓
Αντλησιοταμίευση (PHS)	✓	✓	✓			✓	✓
Συσσωρευτές (BT)				✓		✓	
Αποθ. υδρογόνου (FC)					✓		✓

5. Ενεργειακά, Οικονομικά και Περιβαλλοντικά Αποτελέσματα

Ενδεικτικά στο Σχήμα 5 παρουσιάζονται οι διάφορες πηγές ενέργειας που συμμετέχουν ετησίως στο ενεργειακό μείγμα του νησιού για τα Σενάρια 2 έως 7, τα οποία όλα διαθέτουν μονάδα αφαλάτωσης σε σχέση με το Σενάριο 1 που χρησιμοποιείται αποκλειστικά για κάλυψη ενεργειακών αναγκών και όχι αναγκών αφαλάτωσης. Στο WT/DU/PHS, η συνολική συνεισφορά από τα WT είναι μικρότερη από ό,τι στις υπόλοιπες διαμορφώσεις όπου το ενεργειακό μείγμα περιλαμβάνει ενέργεια από φωτοβολταϊκά. Η συμβολή των ΑΓ και των ΦΒ είναι η ίδια, καθώς η επιλογή της τεχνολογίας αποθήκευσης δεν επηρεάζει τη διείσδυση των ΑΠΕ στο ΥΒΣ, ενώ η συμβολή του συστήματος αποθήκευσης και του ΤΣΠ (LPS) παρουσιάζει σημαντική διαφορά. Η διαμόρφωση με την ελάχιστη χρήση του ΤΣΠ είναι η WT/PV/DU/HPHS, που σημαίνει αρχικά ότι η υβριδική αποθήκευση ξεπερνά τα τελικά αποτελέσματα και ότι η χρήση υδρογόνου ως δεύτερη μονάδα αποθήκευσης, σε σύγκριση με τις μπαταρίες, έχει ως αποτέλεσμα μειωμένη χρήση συμβατικών καυσίμων. Αυτό είναι εντυπωσιακό, παρόλο που η παραγωγή υδρογόνου απαιτεί την κατανάλωση περισσότερης ενέργειας για την αφαλάτωση του νερού στον ηλεκτρολύτη. Παρατηρείται διακύμανση στη συμβολή της αντλησιοταμίευσης και της μπαταρίας σε σύγκριση με το σύστημα αποθήκευσης υδρογόνου. Αν και τα τρία συστήματα αποθήκευσης έχουν διαστασιολογηθεί σύμφωνα με δύο ημέρες αυτονομίας, το PHS και το ΒΤ ικανοποιούν περίπου το 21% της συνολικής ζήτησης, ενώ το FC ικανοποιεί το 17% της συνολικής ζήτησης, γεγονός που δείχνει ότι το FC συμμετέχει λιγότερο στο ενεργειακό ισοζύγιο και αυξάνει τη χρήση του ΤΣΠ. Στη συνέχεια, μεταξύ των διαμορφώσεων με απλή αποθήκευση, η αντλούμενη αποθήκευση δίνει καλύτερα αποτελέσματα σχετικά με τη χρήση ΤΣΠ στο 21,77%, ενώ η μέγιστη χρήση ΤΣΠ παρατηρείται στην ενιαία αποθήκευση με σύστημα υδρογόνου. Στο WT/PV/DU/FC, αυτή η κατανάλωση ενέργειας για αφαλάτωση νερού γίνεται εμφανής, στερώντας

την κάλυψη των ενεργειακών αναγκών του νησιού, είτε πρόκειται για ενεργειακές ανάγκες για αφαλάτωση οικιακού και αρδευτικού νερού είτε για ενεργειακές ανάγκες για οικιακή κατανάλωση. Επίσης, η χρήση του ΤΣΠ είναι παρόμοια τόσο στην απλή αποθήκευση μπαταρίας όσο και στην υβριδική αποθήκευση μπαταρίας, επομένως η σύγκριση θα πρέπει να γίνει παρακάτω με τις τελικές τιμές ενέργειας και νερού που προκύπτουν.

(α)

(β)

(γ)

(δ)

(ε)

(στ)
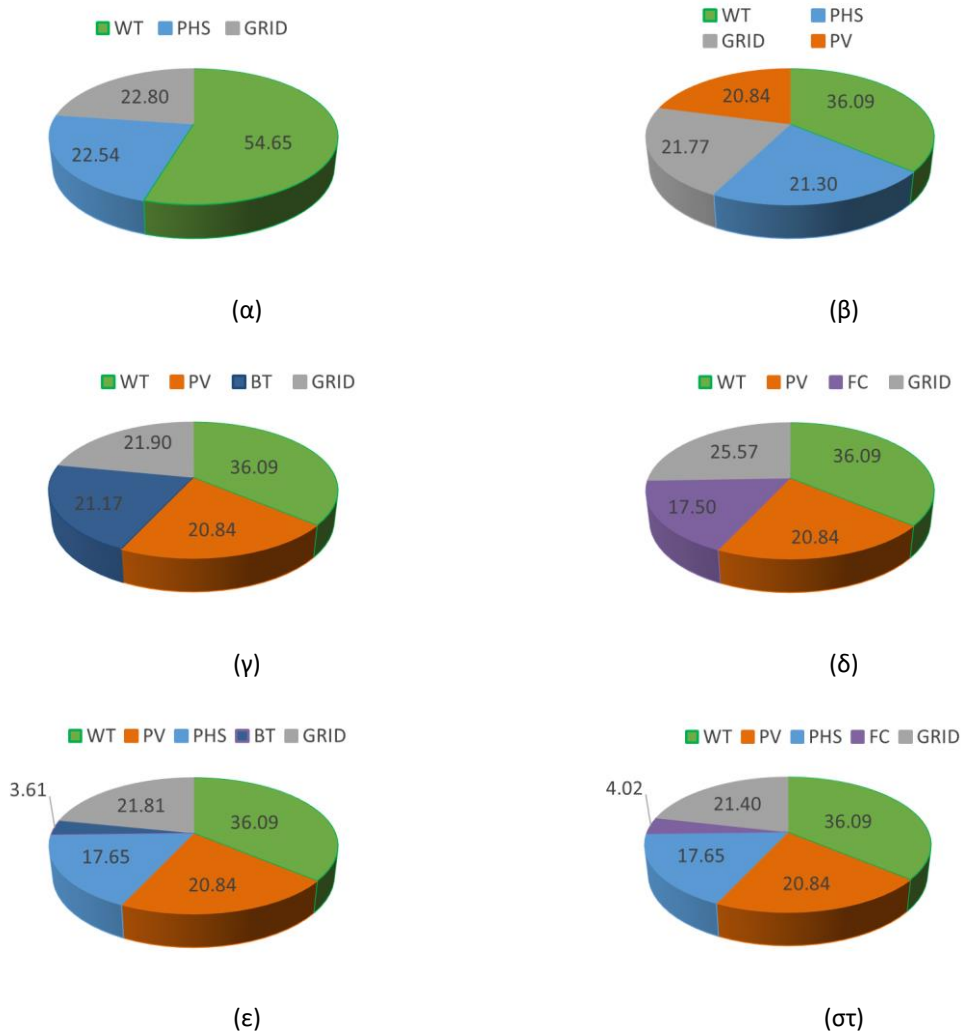
Σχήμα 5 Καταναλώσεις από διαφορετικές πηγές ενέργειας: (α) WT/DU/PHS; (β) WT/PV/DU/PHS; (γ) WT/PV/DU/BT; (δ) WT/PV/DU/FC; (ε) WT/PV/DU/HPBS; (στ) WT/PV/DU/HPHS

Η ενέργεια που παράγεται από τις τρεις διαφορετικές τεχνολογίες αποθήκευσης, PHS, BT και FC, ακολουθεί ένα παρόμοιο μοτίβο στην προσπάθεια των συστημάτων να εκπληρώσουν τις ενεργειακές απαιτήσεις, όπως φαίνεται στο Σχήμα 6. Επιπλέον, αποδεικνύεται ότι η ενέργεια που παράγεται από τα συστήματα PHS, BT και FC είναι συνήθως χαμηλότερη από την ενέργεια που απαιτείται για τη λειτουργία των αντλιών, τη φόρτιση των μπαταριών και τη λειτουργία του

ηλεκτρολύτη για την παραγωγή υδρογόνου. Ακόμα κι έτσι, η ιδέα πίσω από ένα ΥΒΣ είναι η αποθήκευση παραγόμενης ενέργειας από ΑΠΕ που δεν μπορεί να χρησιμοποιηθεί άμεσα και η χρήση της σε περιόδους υψηλής ζήτησης όπου η εκκίνηση του ΤΣΠ και κατά συνέπεια η χρήση ορυκτών καυσίμων είναι η εναλλακτική λύση. Η διαφορετική συμπεριφορά των τεχνολογιών αποθήκευσης PHS, BT και FC, όπως φαίνεται στο Σχήμα 5, μπορεί να εξηγηθεί από το γεγονός ότι η ενέργεια που χρειάζεται ο ηλεκτρολύτης για την παραγωγή υδρογόνου περιλαμβάνει επίσης την ενέργεια που απαιτείται για την αφαλάτωση του νερού που χρησιμοποιείται. Για την αποθήκευση υδρογόνου, η συνεισφορά του ΤΣΠ αυξάνεται καθ' όλη τη διάρκεια του έτους. Η ενέργεια που χρησιμοποιείται για την άντληση και τη φόρτιση των μπαταριών φαίνεται να είναι μεγαλύτερη από την ενέργεια που καταναλώνεται κατά την αφαλάτωση στο WT/PV/DU/FC. Ωστόσο, στη σύγκριση μεταξύ των δύο διαμορφώσεων με υβριδική αποθήκευση, παρατηρείται μεγαλύτερη συνεισφορά του υδρογόνου σε σχέση με την μπαταρία, άρα και μειωμένη χρήση του ΤΣΠ στην περίπτωση του υδρογόνου σε σύγκριση με τις μπαταρίες. Μια πιθανή εξήγηση είναι ότι στην υβριδική αποθήκευση γίνεται όλο και λιγότερο συχνή χρήση της δευτερεύουσας τεχνολογίας αποθήκευσης, υδρογόνου ή μπαταρίας, επομένως ο χρόνος αδράνειας της μπαταρίας οδηγεί σε μεγαλύτερες απώλειες λόγω της φυσικής εκφόρτισης της μπαταρίας και εξαρτάται από τον ρυθμό αυτοεκφόρτισης σ, της μπαταρίας.
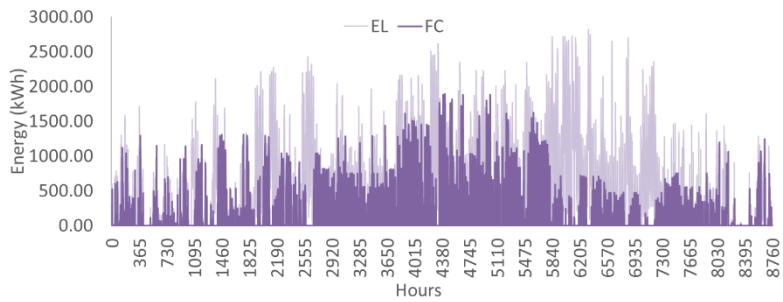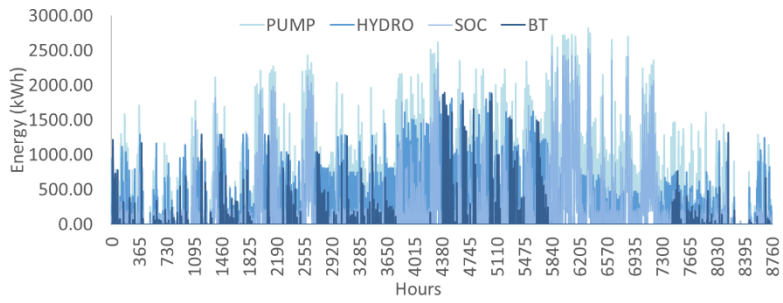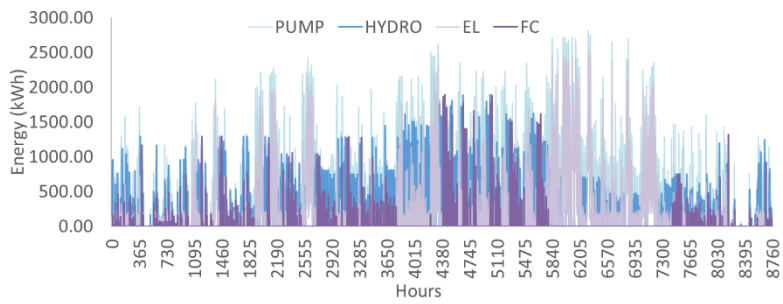

(α)

(β)

(γ)

(δ)

(ε)

(στ)
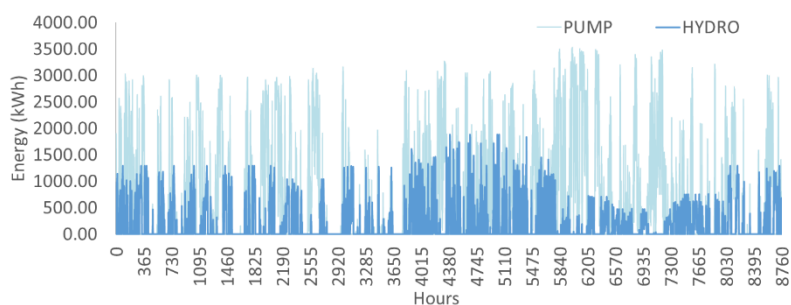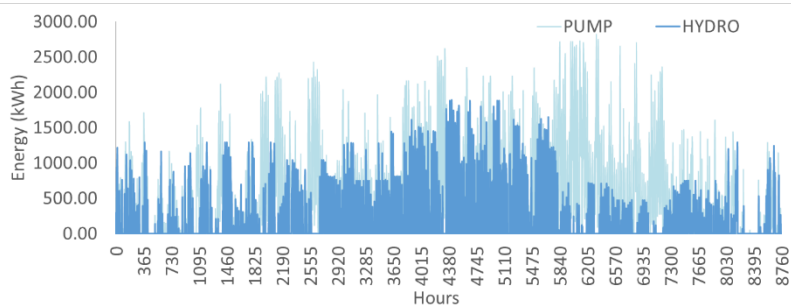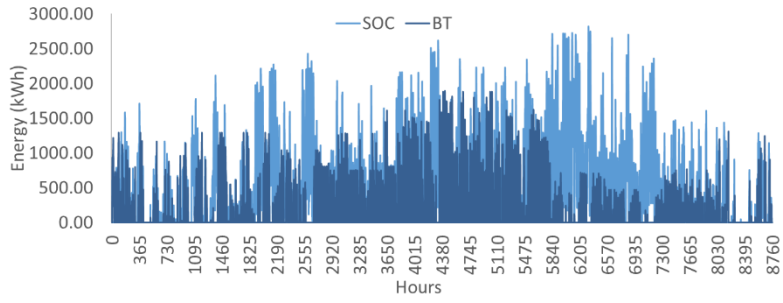
Σχήμα 6 Επίπεδα αποθήκευσης: (α) WT/DU/PHS; (β) WT/PV/DU/PHS; (γ) WT/PV/DU/BT; (δ) WT/PV/DU/FC; (ε) WT/PV/DU/HPBS; (στ) WT/PV/DU/HPHS

Οι συγκρίσεις μεταξύ τεχνολογιών απλής αποθήκευσης, Πίνακας 4, δείχνουν ότι η αντλησιοταμίεση έχει χαμηλότερο αρχικό κόστος (*Initial cost*), ωστόσο, το κόστος λειτουργίας και συντήρησης (*O&M cost*) μειώνεται στην περίπτωση αποθήκευσης υδρογόνου. Επίσης, μεταξύ WT/DU/PHS και WT/PV/DU/PHS, η δεύτερη διαμόρφωση έχει χαμηλότερο κόστος O&M. Παρατηρείται λοιπόν ότι με την εισαγωγή ΦΒ έναντι ΑΓ, το κόστος μειώνεται σημαντικά, πράγμα που σημαίνει ότι η περαιτέρω αντικατάσταση του ΦΒ μπορεί επίσης να οδηγήσει σε χαμηλότερες τιμές ενέργειας και νερού. Άρα, η σύγκριση εξαρτάται και από την πιθανότητα απώλειας φορτίου (LOLP) κάθε ΥΒΣ. Επίσης, το υψηλότερο αρχικό κόστος φαίνεται στην περίπτωση του συστήματος αποθήκευσης μπαταρίας. Όλα τα παραπάνω συνυπολογίζονται στις τελικές τιμές ενέργειας (COE) και νερού (COW). Η χαμηλότερη τιμή παρατηρείται στο WT/PV/DU/PHS, ακολουθούμενο από το WT/PV/DU/FC, το WT/DU/PHS και τέλος το WT/PV/DU/BT. Κατά συνέπεια, ακολουθείται η ίδια σειρά για την περίοδο απόσβεσης (PBP). Ωστόσο, οι χαμηλότερες τιμές LOLP παρατηρούνται στο WT/PV/DU/PHS και οι μέγιστες στο WT/PV/DU/FC, καταλήγοντας στο συμπέρασμα ότι στην απλή αποθήκευση η διαμόρφωση WT/PV/DU/PHS είναι συνολικά ανώτερη. Η διαμόρφωση, η οποία αποτελείται μόνο από WT δίνει καλύτερα αποτελέσματα όσον αφορά τις ποσότητες CO_2 και την ποινή από το Σύστημα Εμπορίας Δικαιωμάτων Εκπομπών, παρόλο που ο συντελεστής εκπομπής των ηλιακών τεχνολογιών είναι υψηλότερος σε σύγκριση με τις τεχνολογίες αιολικής ενέργειας. Αυτό συμβαίνει γιατί η συμβολή της αντίστοιχης τεχνολογίας αποθήκευσης είναι επίσης σημαντική στο τελικό ενεργειακό μείγμα.

Πίνακας 4 Ενεργειακή, οικονομική και περιβαλλοντική ανάλυση για συστήματα απλής αποθήκευσης

Παράμετρος	WT/DU/PHS	WT/PV/DU/PHS	WT/PV/DU/BT	WT/PV/DU/FC
Initial cost [€]	16,652,335	16,690,685	24,937,252	22,510,192
O&M cost [€]	735,035	513,534	508,261	299,102
COE [€/kWh]	0.262	0.215	0.281	0.241
COW [€/m³]	1.532	1.257	1.643	1.408
$LOLP_{hres}$ [%]	22.79	21.74	21.90	25.57
$LOLP_{el}$ [%]	23.73	23.08	23.25	26.51
$LOLP_d$ [%]	13.49	8.47	8.61	10.93
$LOLP_{ir}$ [%]	22.80	21.81	21.95	20.95
PBP [years]	13.59	11.18	14.26	12.05
EM_{CO_2} [tn/year]	2,323.56	2,286.37	2,282.54	2.175.48
$EM_{CO_2}\ price$ [€]	206,634.42	203,326.79	202,986.69	193.465.41

Οι συγκρίσεις μεταξύ υβριδικών τεχνολογιών αποθήκευσης, Πίνακας 5, δείχνουν χαμηλότερο αρχικό κόστος σε WT/PV/DU/HPBS, αλλά χαμηλότερο κόστος συντήρησης σε WT/PV/DU/HPHS. Τέλος, όσον αφορά το COE και το COW, οι χαμηλότερες τιμές επιτυγχάνονται όταν οι μπαταρίες συνδυάζονται

με αντλησιοταμίευση. Ωστόσο, καθώς η επιλογή πρέπει να γίνει σε συνδυασμό με τις τιμές LOLP, παρατηρούνται χαμηλότερες τιμές LOLP αλλά και μικρότερη PBP στην υβριδική διαμόρφωση που αποτελείται από αντλησιοταμίευση και τεχνολογία αποθήκευσης υδρογόνου. Όσον αφορά τις ποσότητες CO_2 και την ποινή από το Σύστημα Εμπορίας Δικαιωμάτων Εκπομπών, το WT/PV/DU/HPHS παρουσιάζει καλύτερα αποτελέσματα. Μεταξύ απλής και υβριδικής αποθήκευσης, οι χαμηλότερες τιμές LOLP δίνονται από την υβριδική αποθήκευση, ωστόσο, οι τιμές ενέργειας και νερού είναι συγκριτικά υψηλότερες από ό,τι στις επιλογές απλής αποθήκευσης.

Πινακας 5 Ενεργειακή, οικονομική και περιβαλλοντική ανάλυση για συστήματα υβριδικής αποθήκευσης

| Παράμετρος	WT/PV/DU/HPBS	WT/PV/DU/HPHS
$Initial\ cost$ [€]	23,083,058	28,378,818
$O\&M\ cost$ [€]	525,898	423,220
COE [€/kWh]	0.267	0.292
COW [€/m³]	1.561	1.705
$LOLP_{hres}$ [%]	21.74	21.33
$LOLP_{el}$ [%]	23.02	22.66
$LOLP_{d}$ [%]	8.50	8.11
$LOLP_{ir}$ [%]	22.32	21.47
PBP [years]	13.77	10.87
EM_{CO_2} [tn/year]	2,285.26	2,297.24
$EM_{CO_2}\ price$ [€]	203,227.94	204,293.25

6. Απορριφθείσα Ανανεώσιμη Ενέργεια

Στην ενότητα αυτή παρουσιάζεται μια μεθοδολογία εκτίμησης και ελαχιστοποίησης της ποσότητας της απορριφθείσας ενέργειας ΑΠΕ Εξετάζονται δύο σενάρια για την αξιολόγηση του υβριδικού συστήματος. Στο πρώτο σενάριο (περίπτωση Ι), ένα μέρος της ενέργειας που παράγεται από τον άνεμο παρέχεται απευθείας στο δίκτυο για να καλύψει τις ανάγκες του σε ηλεκτρική ενέργεια, p_{dir}, ενώ η υπόλοιπη ενέργεια κατευθύνεται προς την αφαλάτωση και την άντληση. Η αφαλάτωση του νερού ύδρευσης είναι σε προτεραιότητα. Οποιαδήποτε επιπλέον ενέργεια χρησιμοποιείται για την άντληση νερού στην επάνω δεξαμενή, με την υπόλοιπη να πηγαίνει προς την αφαλάτωση του νερού άρδευσης. Στο δεύτερο σενάριο η ποσότητα της παραγόμενης αιολικής ενέργειας κατανέμεται σε προκαθορισμένα ποσοστά για αφαλάτωση και άντληση, ενώ η υπόλοιπη παρέχεται απευθείας στο σύστημα για ηλεκτρικές απαιτήσεις. Και πάλι, η κάλυψη των αναγκών παροχής νερού ύδρευσης είναι σε προτεραιότητα. Υπάρχουν τρεις πηγές απορριφθείσας ανανεώσιμης ενέργειας σε ένα ΥΒΣ. Η πρώτη πηγή εξαρτάται από το ποσοστό της αιολικής ενέργειας που διεισδύει άμεσα στο δίκτυο. Αυτό θα μπορούσε να είναι μηδενικό τις ημέρες ή ώρες που υπάρχει μεγάλη ζήτηση για ηλεκτρική ενέργεια ή χαμηλό αιολικό δυναμικό. Η δεύτερη πηγή ενέργειας που απορρίπτεται σχετίζεται με το

αντλιοστάσιο και την επιλογή των αντλιών. Αυτή η ενέργεια απορρίπτεται εάν δεν υπάρχει επαρκής διαθέσιμη ενέργεια για τη λειτουργία των αντλιών. Η τρίτη πηγή εξαρτάται από το μέγεθος της άνω δεξαμενής. Παρά το γεγονός ότι το μέγεθος της ανώτερης δεξαμενής βασίζεται στις ανάγκες του νησιού και στον αριθμό των ημερών αυτονομίας, ωστόσο, θα υπάρξουν ημέρες κατά τη λειτουργία του συστήματος που θα πρέπει να απορριφθεί το αντλούμενο νερό. Αυτό το νερό που απορρίπτεται από την επάνω δεξαμενή μετατρέπεται σε απορριφθείσα ενέργεια. Στα Σχήματα 7 και 8 παρουσιάζονται τα αποτελέσματα για το Σενάριο 1 σχετικά με το ποσοστό κάλυψης των αναγκών και την απορριφθείσα ενέργεια με βάση το p_{dir}, καθώς και την απορριφθείσα ενέργεια ανά «πηγή» με βάση το p_{dir} αντίστοιχα. Παρατηρείται ότι η ελαχιστοποίηση της συνολικής απορριφθείσας ενέργειας επιτυγχάνεται για p_{dir} ίσο με 30%, ενώ η ικανοποίηση της κάθε ανάγκης επιτυγχάνεται σε διαφορετικά ποσοστά για κάθε ανάγκη.
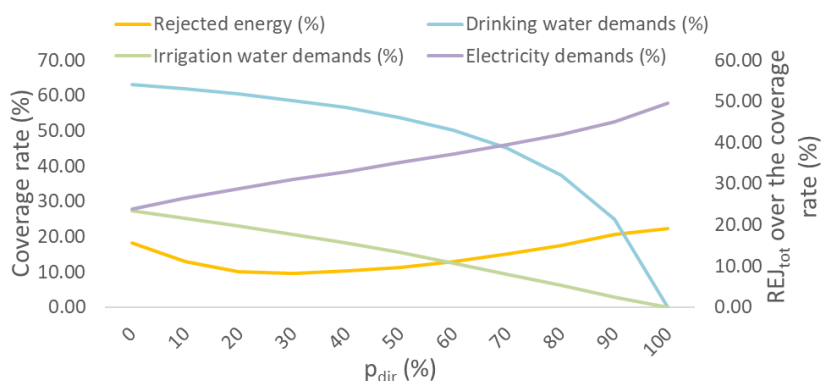
Σχήμα 7 Ποσοστό κάλυψης αναγκών και συνολικά απορριφθείσα ενέργεια με βάση το pdir για το Σενάριο 1
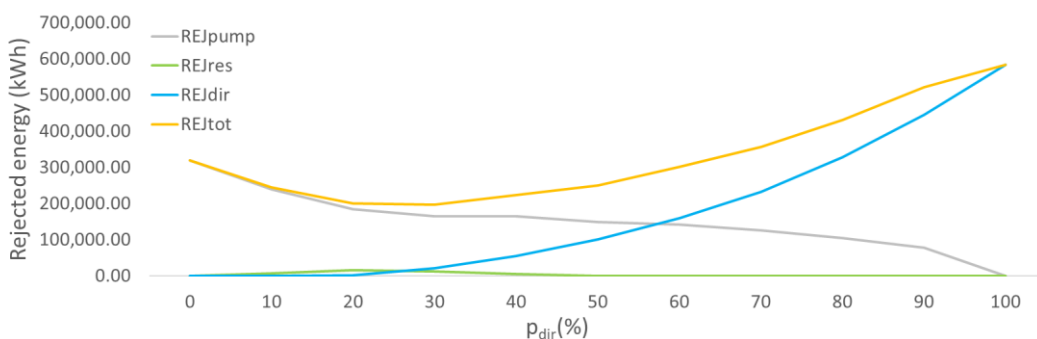
Σχήμα 8 Απορριφθείσα ενέργεια ανά «πηγή» με βάση το pdir για το Σενάριο 1

7. Συμπεράσματα και Μελλοντική Έρευνα

Αυτή η διατριβή αρχικά πραγματεύεται την χωροθέτηση ΑΓ στο ελληνικό νησί των Φούρνων Κορσεών στο Βόρειο Αιγαίο. Η βέλτιστη χωροθέτηση για την εγκατάσταση ανεμογεννητριών, σε συνδυασμό με το υπάρχον νομικό πλαίσιο, αποτελεί τη βάση για την αξιοποίηση του υψηλού αιολικού δυναμικού. Η αξιολόγηση πιθανών θέσεων εγκατάστασης ανεμογεννητριών γίνεται με

χρήση του συνόλου των προτεινόμενων γεωμορφολογικών, τεχνικών και χωρικών κριτηρίων, λαμβάνοντας υπόψη τους περιβαλλοντικούς περιορισμούς και το ισχύον νομοθετικό πλαίσιο. Τρία κύρια σενάρια — το τεχνικό, το πολιτισμικό και το οικονομικό προσανατολισμό — εξετάζονται, με τη συνδυασμένη χρήση MCDM και GIS και την εκτίμηση της βαρύτητας των κριτηρίων. Αυτή η ανάλυση λαμβάνει υπόψη έξι παράγοντες: αιολικό δυναμικό, υψόμετρο και αποστάσεις από τους οικισμούς, το οδικό δίκτυο, τους κινητούς σταθμούς βάσης και τους αρχαιολογικούς χώρους. Η μέθοδος AHP χρησιμοποιείται για την εκτίμηση των βαρών των κριτηρίων για τρία σενάρια για να δείξει πώς επηρεάζουν την τελική διάταξη. Σε κάθε σενάριο, το κριτήριο του αιολικού δυναμικού έχει προτεραιότητα, επειδή η ικανότητα των ανεμογεννητριών να παράγουν όσο το δυνατόν περισσότερη ενέργεια εξαρτάται από το μέγιστο αιολικό δυναμικό. Επίσης, τα τρία σενάρια εκτελούνται ενώ λαμβάνεται υπόψη που βρίσκεται ο κύριος οικισμός του νησιού, οι Φούρνοι. Προσθέτοντας αυτόν τον επιπλέον περιορισμό διατήρησης της ελάχιστης απόστασης των Φούρνων, ελαχιστοποιούνται οι απώλειες ενέργειας μέσω των καλωδίων. Τέλος, διεξάγεται μια ανάλυση ευαισθησίας για δύο κριτήρια προκειμένου να παρατηρηθεί πώς μια παραλλαγή σε οποιοδήποτε από αυτά επηρεάζει τα αποτελέσματα.

Η ζώνη Α, η οποία είναι ίδια για κάθε σενάριο, αντιπροσωπεύει το 27,9% της συνολικής επιφάνειας του νησιού, υποδεικνύοντας όλες τις ζώνες αποκλεισμού όπου ενδέχεται να μην εγκατασταθούν ανεμογεννήτριες. Η ζώνη Ε αντιπροσωπεύει τις καταλληλότερες τοποθεσίες και έχει τις χαμηλότερες τιμές στα αρχικά σενάρια χωρίς τον πρόσθετο περιορισμό της απόστασης από τους Φούρνους. Ωστόσο, στο οικονομικό σενάριο, η ζώνη Ε έχει υψηλότερη τιμή 4%. Η ζώνη Δ, η ζώνη που προηγείται της Ζώνης Ε, έχει υψηλές αξίες, ιδιαίτερα στο οικονομικό σενάριο. Η τιμή του 54,1% υποδηλώνει ότι πάνω από το μισό νησί έχει τοποθεσίες που είναι κατάλληλες για εγκατάσταση με τις τιμές του FS να κυμαίνονται από 0,50 έως 0,75. Παρόλο που το κριτήριο υψομέτρου είναι το πέμπτο πιο σημαντικό, το οικονομικό σενάριο έχει την πλειοψηφία των επιλέξιμων τοποθεσιών. Το σενάριο που δίνει προτεραιότητα στα οικονομικά κριτήρια φαίνεται να συνδυάζει χαμηλότερο κόστος εγκατάστασης με μεγαλύτερη επιφάνεια με επιλέξιμες τοποθεσίες. Έτσι, μπορεί να προβλεφθεί ότι ιδανικές τοποθεσίες με σημαντικό αιολικό δυναμικό μπορούν να συνδυαστούν με χαμηλότερα υψόμετρα, μειώνοντας το κόστος εγκατάστασης και καταλήγοντας σε επιπλέον θέσεις, ταυτόχρονα, στην τελική ζώνη Ε. Δεδομένου ότι είναι προτιμότερο για ένα τέτοιο έργο να κοντά στον οικισμό όπου υπάρχουν οι περισσότεροι κάτοικοι, παράγονται τρεις επιπλέον αποδεκτοί χάρτες λαμβάνοντας υπόψη την εγγύτητα στον κύριο οικισμό των Φούρνων ως έναν ακόμη περιορισμό. Επίσης, το τεχνικό σενάριο, σε αυτή την περίπτωση, έχει τον μεγαλύτερο αριθμό κατάλληλων τοποθεσιών. Η ζώνη Δ, η οποία σε αυτά τα συμπληρωματικά σενάρια αντιπροσωπεύει τη ζώνη που εμφανίζει τις πιο ευνοϊκές τοποθεσίες, επιτυγχάνει μια τιμή 10,48% στο τεχνικό σενάριο. Ενώ η αντίστοιχη τιμή FS για το αρχικό τεχνικό σενάριο είναι 0,929, η μέγιστη τιμή FS σε αυτές τις πρόσθετες περιπτώσεις είναι 0,744 στο τεχνικό σενάριο. Στη συνέχεια, το τεχνικό σενάριο

υποβάλλεται σε ανάλυση ευαισθησίας για δύο διαφορετικά κριτήρια για να προσδιοριστεί πώς μια αλλαγή σε ένα από τα δύο επηρεάζει τους νέους χάρτες καταλληλότητας. Το πρώτο κριτήριο είναι το αιολικό δυναμικό, το C_{wind} με το μεγαλύτερο βάρος και το δεύτερο η απόσταση από τους αρχαιολογικούς χώρους, το C_{arch}, που έχει το μικρότερο βάρος. Οι βέλτιστες θέσεις αυξάνονται όσο αυξάνεται το βάρος του C_{wind}, ενώ οι βέλτιστες θέσεις μειώνονται καθώς αυξάνεται το βάρος του C_{arch}. Φαίνεται ότι ο τύπος του επιλεγμένου κριτηρίου, παρά το βάρος, έχει μεγαλύτερο αντίκτυπο στους νέους χάρτες καταλληλότητας.

Εν συνεχεία, παρέχεται το πλαίσιο για την προσομοίωση και αξιολόγηση διαφορετικών διαμορφώσεων μεταξύ ΑΠΕ και τεχνολογιών αποθήκευσης. Επιπλέον, εξετάζονται διαμορφώσεις που χρησιμοποιούν υβριδικές τεχνολογίες αποθήκευσης. Ο σκοπός είναι η ικανοποίηση ταυτόχρονα των αναγκών σε νερό ύδρευσης και άρδευση, καθώς και των απαιτήσεων κατανάλωσης ηλεκτρικού ρεύματος. Για όλα τα εξεταζόμενα σενάρια εκτιμώνται τα αποτελέσματα σχετικά με το κόστος ενέργειας, το κόστος του νερού, την περίοδο απόσβεσης, την πιθανότητα απώλειας φορτίου και τις ποσότητες CO2 που έχουν εξαλειφθεί. Τα αποτελέσματα δείχνουν επίσης το αρχικό κόστος καθώς και το κόστος συντήρησης και λειτουργίας. Οι προσομοιώσεις είναι ωριαίες χρησιμοποιώντας μετεωρολογικά δεδομένα (ταχύτητα ανέμου, ηλιακή ακτινοβολία, θερμοκρασία, βροχόπτωση, αριθμός ηλιόλουστων ημερών), δεδομένα ζήτησης για ηλεκτρική κατανάλωση και νερό ύδρευσης και άρδευσης και δεδομένα τεχνικών προδιαγραφών κάθε υποσυστήματος, συμπεριλαμβανομένων ΑΓ, ΦΒ, μονάδας αφαλάτωσης, αντλητικής μονάδας, υδροστροβίλου, δεξαμενών, μπαταριών, ηλεκτρολυτών, κυψελών υδρογόνου και δεξαμενών υδρογόνου. Αποδεικνύεται ότι ο συνδυασμός ΑΓ και ΦΒ οδηγεί σε καλύτερα αποτελέσματα, καθώς αξιοποιείται ταυτόχρονα το αιολικό και ηλιακό δυναμικό κάθε περιοχής. Όσον αφορά τη χρήση κάθε τεχνολογίας αποθήκευσης, η χρήση αντλησιοταμίευσης ή μπαταρίας παρουσιάζει γενικά την ίδια «συμπεριφορά», ωστόσο το η χρήση αντλησιοταμίευσης έχει χαμηλότερο κόστος ενέργειας και νερού ως αποτέλεσμα του χαμηλότερου αρχικού κόστους. Αυτό μπορεί να οδηγήσει σε σημαντικά φθηνότερες τιμές για την ενέργεια και το αφαλατωμένο νερό, ειδικά αν ληφθεί υπόψη ότι η άνω δεξαμενή αποθήκευσης νερού μπορεί να υφίσταται από πριν στο νησί. Ωστόσο, δεδομένου ότι χρησιμοποιείται περισσότερο ο τοπικός σταθμός παραγωγής (ΤΣΠ), λόγω μικρότερης περιόδου αυτόνομης λειτουργίας του ΥΒΣ, εκπέμπονται περισσότερα CO_2 συνολικά. Επιπλέον, ο ΤΣΠ χρησιμοποιείται περισσότερο στο σύστημα με αποθήκευση υδρογόνου επειδή απαιτείται αφαλάτωση του νερού πριν την ηλεκτρόλυση και αυτό απαιτεί σημαντική ποσότητα ενέργειας. Η υβριδική αποθήκευση φαίνεται να είναι πιο ενεργή τον Δεκέμβριο, σύμφωνα με την ανάλυση προσφοράς και ζήτησης για τους μήνες Αύγουστο και Δεκέμβριο. Αυτό μπορεί να εξηγηθεί από το γεγονός ότι, αν και η συνολική ποσότητα ενέργειας που απαιτείται αυξάνεται τον Δεκέμβριο σε σύγκριση με τον Αύγουστο, περισσότερη πλεονάζουσα ενέργεια παραδίδεται και χρησιμοποιείται από την μπαταρία ή τον ηλεκτρολύτη λόγω του μεγαλύτερου αιολικού δυναμικού. Για διαμορφώσεις που αποτελούνται από ΑΓ και ΦΒ, η

μηνιαία παροχή νερού είναι έως και 87%. Ωστόσο, το ποσοστό αυτό μειώνεται για το νερό άρδευσης, όπως θα προβλεπόταν δεδομένου ότι το νερό άρδευσης είναι η τελική ζήτηση στην ιεραρχία της ζήτησης. Σε όλα τα σενάρια υπάρχει πλήρης αυτονομία κάλυψης για τον Οκτώβριο. Ωστόσο, για τα σενάρια με αντλησιοταμίευση, μπαταρία, καθώς και στα δύο υβριδικά σενάρια αποθήκευσης (αντλησιοταμίευση-μπαταρία και αντλησιοταμίευση-υδρογόνο) η αυτονομία επεκτείνεται έως τον Ιούνιο και τον Ιούλιο για την παροχή νερού ύδρευσης. Μόνο το σενάριο με την αποθήκευση μέσω υδρογόνου παρουσιάζει απώλειες φορτίου στο νερό ύδρευσης κατά τη διάρκεια του Ιουλίου. Ωστόσο, μεγαλύτερη κάλυψη των αναγκών για νερό ύδρευσης παρατηρείται στο υβριδικό έργο αντλησιοταμίευσης-υδρογόνου και στην αποθήκευση με μπαταρία. Η σύγκριση μεταξύ των υβριδικών συστημάτων αποθήκευσης δείχνει μεγαλύτερη συμβολή από το υδρογόνο σε σύγκριση με τις μπαταρίες, καθώς και χαμηλότερη χρήση του ΤΣΠ. Μια πιθανή εξήγηση είναι ότι εφόσον οι τεχνολογίες δευτερεύουσας αποθήκευσης, υδρογόνο και μπαταρίες, δεν χρησιμοποιούνται τόσο συχνά κατά την υβριδική αποθήκευση, χάνεται περισσότερη ενέργεια κατά τις περιόδους αδράνειας ως αποτέλεσμα της αποφόρτισης της μπαταρίας. Το υψηλότερο κόστος νερού και ενέργειας είναι αποτέλεσμα των υβριδικών ρυθμίσεων αποθήκευσης, με το σύστημα αντλησιοταμίευσης-υδρογόνου να έχει το μεγαλύτερο κόστος. Ωστόσο, επειδή η απόφαση πρέπει να ληφθεί σε συνδυασμό με πιθανότητα απώλειας φορτίου, το σύστημα αντλησιοταμίευσης-υδρογόνου εμφανίζει χαμηλότερες τιμές πιθανότητας απώλειας φορτίου αλλά και μικρότερη περίοδο απόσβεσης.

Η ανάλυση ευαισθησίας για τον προσδιορισμό των επιπτώσεων του πληθυσμού, του αιολικού και ηλιακού δυναμικού και του ύψους εγκατάστασης των ανεμογεννητριών στα αποτελέσματα γίνεται ανάμεσα στην αντλησιοταμίευση και την αποθήκευση υδρογόνου καθώς και μεταξύ αντλησιοταμίευσης και της υβριδικής αντλησιοταμίευσης-υδρογόνου. Σύμφωνα με τα αποτελέσματα για τεχνολογίες απλής αποθήκευσης, η αντλησιοταμίευση είναι πιο ευαίσθητη στις διακυμάνσεις του πληθυσμού, στις διακυμάνσεις του αιολικού δυναμικού και της τιμής της ενέργειας. Η αποθήκευση υδρογόνου είναι πιο ευαίσθητη σε αλλαγές στην ταχύτητα του ανέμου και στις εκπομπές CO_2. Ο πληθυσμός, ακολουθούμενος από το αιολικό δυναμικό, το ηλιακό δυναμικό και, τέλος, το ύψος της εγκατάστασης WT, καθορίζουν την σειρά ταξινόμησης των κριτηρίων και για τις δύο διαμορφώσεις. Γενικότερα η συμπεριφορά του κάθε σεναρίου οδηγεί στο συμπέρασμα ότι η τελική επιλογή της τεχνολογίας αποθήκευσης εξαρτάται όχι μόνο από αλλαγές στα κριτήρια εγκατάστασης, μετεωρολογικά δεδομένα και δεδομένα ζήτησης αλλά και από αλλαγές στα αρχικά κριτήρια, τιμής ενέργειας ή νερού και πιθανότητα απώλειας φορτίου.

Προκειμένου να αξιολογηθεί η απορριφθείσα ενέργεια σε διάφορα σενάρια λειτουργίας, προτείνονται δύο ξεχωριστά σενάρια ανάλογα με τις δυνατότητες για διαφορετικές χρήσεις του ΥΒΣ. Τα ευρήματα από την περίπτωση I βασίζονται στο ποσοστό από την παραγόμενη αιολική ενέργεια που αποστέλλεται απευθείας στο σύστημα (p_{dir}) για οικιακή κατανάλωση και το ποσοστό που

χρησιμοποιείται στη μονάδα αφαλάτωσης και στο αντλιοστάσιο. Στην περίπτωση ΙΙ, ένα μέρος της παραγόμενης αιολικής ενέργειας αποστέλλεται πάλι απευθείας στο σύστημα για τις ηλεκτρικές του ανάγκες και τα αποτελέσματα εξαρτώνται από τον λόγο της ενέργειας που παρέχεται στη μονάδα αφαλάτωσης σε σχέση με το αντλιοστάσιο. Από την περίπτωση Ι, αποκαλύπτεται ότι το σύστημα απορρίπτει την ελάχιστη ποσότητα συνολικής ενέργειας κατά τη διάρκεια ενός έτους όταν το άμεσο ποσοστό αιολικής ενέργειας, p_{dir}, είναι ίσο με 30%. Επίσης, η απόδοση του προτεινόμενου συστήματος έχει ως αποτέλεσμα την κάλυψη 60% των αναγκών σε νερό ύδρευσης, 21% κάλυψης των αναγκών σε νερό άρδευσης και 31% των ενεργειακών αναγκών. Τα αποτελέσματα της έρευνας από την περίπτωση ΙΙ καταδεικνύουν ότι η κατανομή όλης της πλεονάζουσας ενέργειας στη μονάδα αφαλάτωσης είναι η στρατηγική που οδηγεί στη μικρότερη ποσότητα ενέργειας που απορρίπτεται. Ωστόσο, σε σύγκριση με το 31% του σεναρίου Ι, παρατηρείται σημαντική μείωση στην κάλυψη των ενεργειακών απαιτήσεων στο 14% σε αυτή την περίπτωση. Από την άλλη πλευρά, σε σύγκριση με τα αντίστοιχα αποτελέσματα της περίπτωσης Ι, οι απαιτήσεις σε νερό ικανοποιούνται σχεδόν πλήρως. Μια ανάλυση της ενέργειας που παράγεται και καταναλώνεται κατά τη λειτουργία ενός ΥΒΣ, που αποτελείται από ανεμογεννήτριες, μονάδα αφαλάτωσης και μονάδα αντλησιοταμίευσης αποκαλύπτει ότι 1,5 μονάδες ενέργειας χρησιμοποιούνται για άντληση για κάθε μονάδα υδροηλεκτρικής ενέργειας που παράγεται.

Οι μελλοντικές προοπτικές αυτής της έρευνας περιλαμβάνουν χωροθέτηση ΑΓ λαμβάνοντας υπόψιν και τις απαιτούμενες αποστάσεις που πρέπει να τηρούνται μεταξύ τους και την εξαγωγή αποτελεσμάτων αξιοπιστίας των ΥΒΣ με βάση τους διαφορετικούς συνδυασμούς ΑΠΕ και τεχνολογιών αποθήκευσης που μελετήθηκαν στο πλαίσιο της παρούσας διδακτορικής διατριβής. Ένας άλλος ενδιαφέρον τομέας για σχετική μελλοντική έρευνα θα ήταν η εφαρμογή κλιματικών σεναρίων προκειμένου να εξεταστούν όλες οι στρατηγικές διαχείρισης ενέργειας και οι διαφορετικές τεχνολογίες αποθήκευσης όσον αφορά την αξιοπιστία και την απόρριψη ενέργειας υπό τις επιπτώσεις της κλιματικής αλλαγής. Τέλος, προτείνεται περαιτέρω έρευνα προς την κατεύθυνση της βέλτιστης διαστασιολόγησης των προτεινόμενων σεναρίων, με κριτήριο τη μείωση της τελικής τιμής του νερού και της ενέργειας, την αύξηση της αξιοπιστίας, τη μείωση της απορριφθείσας ενέργειας και τη μείωση του χρόνου απόσβεσης.

Publications in Scientific Journals

M. Bertsiou, E. Baltas, Power to hydrogen and power to water using wind energy, Wind, 2(2), 305-324, 2022, https://doi.org/10.3390/wind2020017

M. Bertsiou, E. Baltas, Energy, economic and environmental analysis of a hybrid power plant for electrification and drinking and irrigation water supply, Environmental Processes, 9(2), 1-28, 2022, https://doi.org/10.1007/s40710-022-00575-x

I. Nikas-Nasioulis, **M. Bertsiou**, E. Baltas, Investigation of energy, water, and electromobility through the development of a hybrid renewable energy system on the island of Kos, WSEAS Transactions on Environment and Development, Volume 18, May 2022, Pages 543-554, https://doi.org/10.37394/232015.2022.18.53

M. Bertsiou, E. Baltas, Management of energy and water resources by minimizing the rejected renewable energy, Sustainable Energy Technologies and Assessments, Volume 52, 102002, 2022, https://doi.org/10.1016/j.seta.2022.102002M

M. Bertsiou, A.P. Theochari, E. Baltas, Multi-criteria analysis and GIS methods for wind turbine siting in a North Aegean island, Energy Science & Engineering, Volume 9, January 2021, Pages 4-18, https://doi:10.1002/ese3.809

D. Sarris, **M. Bertsiou**, E. Baltas, Evaluation of a Hybrid Renewable Energy System (HRES) in Patmos Island, International Journal of Renewable Energy Sources, Volume 4, 2019, 40-47

M. Bertsiou, E. Feloni, D. Karpouzos, E. Baltas, Water management and electricity output of a Hybrid Renewable Energy System (HRES) in Fournoi island in Aegean Sea, Renewable Energy, Volume 118, April 2018, Pages 790–798, https://doi:10.1016/j.renene.2017.11.078

Fully evaluated conference publications

M. Bertsiou, E. Baltas, Evaluation of a Hybrid Renewable Energy System for the Supply of a Desalination Unit for Handling Salinization, Protection and Restoration of the Environment XVI, Kalamata, Greece, July 5-8, 2022

M. Bertsiou, E. Baltas, Pump Hydro Storage and Comparison of Wind and Solar Energy Integration for Water Independence of Isolated Systems, 15th Panhellenic Conference of the Hellenic Hydrotechnical Union, Thessaloniki, Greece, June 2-3, 2022

A.F. Papathanasiou, **M. Bertsiou**, E. Baltas, Evaluation of an HRES using pumped-storage or hydrogen storage for water demands in Skyros island, 15th Panhellenic Conference of the Hellenic Hydrotechnical Union, Thessaloniki, Greece, June 2-3, 2022

M. Bertsiou, E. Baltas, Development of a Methodology of Hybrid Systems for Covering Water Demand on Dry Islands, International Conference on Natural Science and Environment (ICNSE), Prague, Czech Republic, November 21-22, 2019

M. Bertsiou, E. Feloni, E. Baltas, Cost-benefit analysis for a Hybrid renewable energy system in Fournoi island, Proceedings of the Sixth International Conference on Environmental Management, Engineering, Planning & Economics, Thessaloniki, Greece, June 25-30, 2017, 697-705

Presentation in Conferences

K. Kafasis, E. Baltas, **M. Bertsiou,** Dimensioning of Hybrid System with Desalination Units and capability of recovery and utilization of brine for Amorgos Island, 2nd World Conference on Sustainability, Energy and Environment, Berlin, Germany, December 9-11, 2022

A.F. Papathanasiou, **M. Bertsiou**, E. Baltas, Evaluation of an HRES using pumped-storage or hydrogen storage for water and energy demands in Skyros island, 7th IAHR Europe Congress, Athens, Greece, September 7-9, 2022

D. Sarris, **M. Bertsiou**, E. Baltas, Evaluation of a Hybrid Renewable Energy System (HRES) in Patmos Island, 8th International Conference on Energy Systems, Environment, Entrepreneurship and Innovation (ICESEEI '19), London, UK, February 23-25, 2019

M. Bertsiou, E. Baltas, Development, Application, Methodology of Hybrid Systems for Covering Water Demand on Islands, Challenges for the Islands in the era of the Circular Economy, Chania, Greece, September 20-22, 2018

M. Detsika, E. Feloni, **M. Bertsiou**, E. Baltas, Development of a GIS-assisted multi-criteria approach for the proper location of wind farms in Florina region, 26th ArcGIS users Annual Meeting, Athens, Greece, May 10-11, 2018

P. Misiris, E. Feloni, **M. Bertsiou**, D. Karpouzos, E. Baltas, Assessment of a Hybrid Renewable Energy System (HRES) in a small island in Greece, 4th International Conference on Energy, Sustainability and Climate Change, Santorini, Greece, June 12-14, 2017

M. Bertsiou, E. Feloni, E. Baltas, Evaluation of a Hybrid System for Renewable Energy in a Small Island in Greece, 19th International Conference on Energy, Ecological and Environmental Engineering, London, United Kingdom, January 19-20, 2017